JAERI-Research
2004-026

CRITICALITY AND DOPPLER REACTIVITY WORTH UNCERTAINTY DUE TO RESOLVED RESONANCE PARAMETER ERRORS —FORMULA FOR SENSITIVITY ANALYSIS—

February 2005

Atsushi ZUKERAN*, Tsuneo NAKAGAWA, Keiichi SHIBATA,
Makoto ISHIKAWA* and Tetsushi HINO*

日本原子力研究所
Japan Atomic Energy Research Institute

本レポートは，日本原子力研究所が不定期に公刊している研究報告書です。
入手の問合わせは，日本原子力研究所研究情報部研究情報課（〒319－1195 茨城県那珂郡東海村）あて，お申し越しください。なお，このほかに財団法人原子力弘済会資料センター（〒319－1195　茨城県那珂郡東海村日本原子力研究所内）で複写による実費頒布をおこなっております。

This report is issued irregularly.
Inquiries about availability of the reports should be addressed to Research Information Division, Department of Intellectual Resources, Japan Atomic Energy Research Institute, Tokai-mura, Naka-gun, Ibaraki-ken 〒319－1195, Japan.

編集兼発行　日本原子力研究所

Criticality and Doppler Reactivity Worth Uncertainty Due to Resolved Resonance Parameter Errors — Formula for Sensitivity Analysis —

Atsushi ZUKERAN[*1], Tsuneo NAKAGAWA, Keiichi SHIBATA,
Makoto ISHIKAWA[*2] and Tetsushi HINO[*1]

Department of Nuclear Energy System
Tokai Research Establishment
Japan Atomic Energy Research Institute
Tokai-mura, Naka-gun, Ibaraki-ken

(Received November 15, 2004)

Uncertainties of reactivities due to those of resolved resonance parameters are evaluated by so-called" direct k-difference method". Then, effective cross section of an individual isotope and reaction type is described in terms of infinitely diluted cross section $\sigma_{\infty xik}$ and resonance self-shielding factor f^{k}_{xi} (x: reaction, i: isotope, k: sequence number of resonance) as a function of resonance parameters, and reactivity is evaluated from the neutron balance using the effective cross section and neutron flux. Consequently, reactivity uncertainties such as effective multiplication factor can be estimated by the sensitivity coefficients of the infinitely diluted cross section and resonance self-shielding factor to the changes of resonance parameters of interest. In the present work, the uncertainties of the resolved resonance parameters for the evaluated nuclear data file JENDL-3.2 were estimated on the basis of Breit-Wigner Multi-level formula. For the Reich-Moore resonance parameters complied in the library, the uncertainties equivalent to the Breit-Wigner resonance parameters are estimated. The resonance self-shielding factor based on NR-approximation is analytically described. Reactivity uncertainty evaluation method for the effective multiplication factor k_{eff}, temperature coefficient α, Doppler reactivity worth ρ is developed by means of the sensitivity coefficient against the resonance parameter. Final uncertainties of the reactivities are estimated by means of error propagation law using the level-wise uncertainties. Preliminary uncertainty evaluation of Doppler reactivity worth due to the uncertainties of resolved resonance parameters results about 4% at the temperature 728 K for large sodium-cooled fast breeder reactor.

Keywords: Criticality, Doppler Reactivity, Resonance Parameter, Uncertainty Evaluation

---

This report is the detailed documentation of an article entitled "Doppler Reactivity Worth Uncertainties due to Resolved Resonance Parameter Errors", Proc. Int. Conf. on Nuclear Data for Science and Technology, Oct. 7 – 12, 2001, Tsukuba, Japan, published as Journal of Nuclear Science and Technology, Supplement 2, pp.1097–1100 (Aug. 2002). Publication of this report has been permitted by Atomic Energy Society of Japan.

*1 Power & Industrial Systems R & D Laboratory, Hitachi, Ltd.
*2 Japan Nuclear Cycle Development Institute (JNC)

分離共鳴パラメータの誤差が臨界性とドップラー反応度に及ぼす不確かさ
— 感度解析用計算式の導出 —

日本原子力研究所東海研究所エネルギーシステム研究部
瑞慶覧　篤[*1]・中川　庸雄・柴田　恵一・石川　真[*2]・日野　哲士[*1]

（2004 年 11 月 15 日受理）

分離共鳴パラメータの不確かさによる反応度の不確かさを、所謂「直接 k_{eff} 一差分法」で評価する。そこで、共鳴パラメータの関数として、個々の核種の実効断面積を無限希釈断面積 $\sigma_{\infty xik}$ と共鳴自己遮蔽因子 f^{*}_{xi}（x:反応、i:同位体、k:共鳴レベルの番号）の項で表し、反応度はこれらの実効断面積と体系の中性子束を用いて中性子バランスから求める。従って、実効増倍率等の反応度の不確かさは着目している共鳴パラーメータの変化に対する無限希釈断面積と共鳴自己遮蔽因子の共鳴パラメータの変化に対する感度係数を用いて評価する事が出来る。本研究では、評価済核データファイル JENDL-3.2 に格納されている分離共鳴パラメータの不確かさは Breit-Wigner 多準位公式を用いて推定した。このファイルに格納されている Reich-Moore 形式の共鳴パラメータに対する不確かさは Breit-Wigner 多準位公式に等価な共鳴パラメータの不確かさとして求めた。NR 近似に基づく共鳴自己遮蔽因子を解析式で表した。実効増倍率 k_{eff}、温度係数α、ドップラー反応度ρに対する共鳴パラメータの感度係数から反応度の不確かさを評価する手法を開発した。分離共鳴パラメータの不確かさによる反応度の最終的な不確かさを個々の共鳴レベルの寄与に対する不確かさをもとに、誤差伝播則で全共鳴レベルに対する値を評価した。予備的な評価によると、共鳴パラメータの不確かさに基づくナトリウム冷却大型高速炉のドップラー反応度の不確かさは、728 K で、約 4%であった。

本報告書は、2001 年につくば市で開催された核データ国際会議に発表した論文「ドップラー反応度価値の分離共鳴パラメータの誤差に起因する不確かさの評価」(Journal of Nuclear Science and Technology, Supplement 2, 1097 – 1100 (Aug.2002)) の定式化等に関する詳細報告である。なお、(社) 日本原子力学会から著作権上の許諾を得ている。

東海研究所：〒319–1195 茨城県那珂郡東海村白方白根 2–4
*1 ㈱日立製作所電力・電機開発研究所
*2 核燃料サイクル開発機構

Contents

目　次

Notation

i	:	Isotope identification No.
A_i	:	Mass number of isotope i
N_i	:	Atom density of isotope i $(atom \cdot cm^{-3})$
E	:	Incident neutron energy (eV)
x	:	Nuclear reaction indicator
k	:	Sequence No. of resonance
T	:	Temperature in Kelvin (K)
k	:	Wave number
p	:	Nuclear reaction whose parameter is changed
g	:	Energy group number
E_{ik}	:	k-th resonance energy of isotope i
g_{ik}	:	Spin statistical weight
Δ_{ik}	:	Doppler width of the k-th resonance of isotope i (eV)
κ_{Blz}	:	Boltzmann constant $(eV \cdot K^{-1})$
$\sigma^k_{eff\,xi}$	:	Effective cross section for reaction x of isotope i and resonance k
Σ_{pi}	:	Macro-scopic potential scattering cross section (cm^{-1})
$\Gamma_{n\,ik}$	:	Neutron width (eV)
$\Gamma_{\gamma\,ik}$	:	Capture width (eV)
$\Gamma_{f\,ik}$	:	Fission width (eV)
Γ_{ik}	:	Total width (eV)
$\Gamma(x)$	:	Γ function
$\sigma_{\gamma\,ik}$	:	Microscopic Neutron capture cross section $(barn)$
$\sigma_{f\,ik}$	:	Microscopic Fission cross section $(barn)$
$\sigma_{t\,ik}$	:	Microscopic Total cross section $(barn)$
$\sigma_{0\,ik}$	:	Total Resonance peak cross section $(barn)$
$\sigma_{p\,ik}$	:	Potential scattering cross section of isotope i and resonance k (barn)
$\sigma_{back\,i}$ or σ_0	:	Potential scattering cross section per resonance atom (barn), σ_0 used for plotting for simplicity.
ψ	:	Doppler symmetric function
χ	:	Doppler asymmetric function
ϕ^g	:	Neutron spectrum of group g $(n/cm^2 \cdot s)$
$W-table$	:	W-table
$w(z)$	:	Complex W-function
S^R_{xik}	:	Sensitivity coefficient of reactor parameter R to resolved resonance parameter Γ_x of isotope i and resonance level k
I_{xik}	:	Resonance integral for reaction x of isotope i and resonance level k $(barn)$
f^k_{xi}	:	Resonance self-shielding factor for reaction x of isotope i and resonance level k
β_{ik}	:	β-value defined by $\frac{\sigma_{pi}+\sigma_{back\,i}}{\sigma_{0\,ik}}$
λ^*	:	DeBroglie wave length of neutron (cm)

This is a blank page.

1 Introduction

Uncertainty of Doppler reactivity worth has been evaluated from the sample Doppler experiments made on critical assemblies such as in ZPPR and from limited whole core Doppler experiment made on SEFOR. The uncertainty of about 30% [1] (3σ) due to the nuclear data and the calculational method is estimated for large sodium cooled fast breeder reactor[2]. In such uncertainty evaluation, the reactivity worth is estimated from k_{eff}'s or perturbation theory and then individual contribution of resonance level is masked by averaging procedure for multi-group cross section. The contribution from the resonance parameters can be estimated from some limited benchmark analyses based on the direct k-difference or perturbation theory where some resonance parameters are artificially changed. Such a direct method, however, cannot be applied for whole resonance parameters of interest because of a huge amount of resonances in practice. The present work is motivated from such a circumstance.

Considering the resonance effect to the reactor characteristics, uncertainties of resonance parameters mainly reflects the reactor characteristics such as criticality k_{eff} through the resonance self-shielding factor (f-factor) and infinitely diluted cross section. The f-factor, however, is an indirect quantity of the resonance parameters because the shielding effect arises from the depression of neutron flux ϕ due to resonance absorption while the flux ϕ itself is a function of the resonance parameters of all isotopes of interest. In addition to this indirect effect, a huge amount of the resolved resonance parameters, about 3000×2 (fission and capture reactions) resonances of the whole resonant materials employed in a reactor, gives a practical difficulty to directly estimate the uncertainty by about 3000×2 times flux calculations. Consequently, development of uncertainty evaluation method is requested from reactor design and cross section adjustment[3].

The reactivity worth can be expressed by the perturbation theory as well as the difference of the two k_{eff}'s between the perturbed core by the change of resonance parameter and the reference core. The perturbation theory requires the real and adjoint fluxes but the direct k-difference method uses only real flux. In other word, the sensitivity study based on perturbation theory requires an extra study on adjoint flux as a function of admixture of cross sections mainly contributed from fuel isotopes, but direct k-difference method does not need such an extra work. As far as the uncertainty evaluation, the direct k-difference method is preferred to the perturbation theory of the accurate neutron flux is given. On the other hand, uncertainty of the reactor characteristics can be expressed as the statistical summation of uncertainty components come from constituent isotopes and the uncertainties of their resonance parameters. Then, the uncertainty component can be described by the sensitivity coefficients that are essentially perturbation effects in a sense that only net effects are withdrawn. Therefore, sensitivity coefficient method based on direct k-difference method is adopted in this work.

In the present work, Breit-Wigner multi-level formula is used. For recently evaluated nuclear data files such as JENDL-3.2[4] and ENDF/B-VI[5], Reich-Moore formula for resolved resonance is adopted for mainly fuel and structure material. It has an inverse matrix in the cross section formula and thus its sensitivity coefficient formula against resonance parameter may be too complicated to be out of analytical approach. However, the Breit-Wigner type well do as far as the uncertainty evaluation since the peak cross sections based on both formula are nearly equal. The sensitivity to the resonance parameter can be satisfactorily expressed by Breit-Wigner formula.

Uncertainties of the resolved resonance parameters are estimated for the evaluated nuclear data library JENDL-3.2. For the Reich-Moore parameters, uncertainties equivalent to Breit-Wigner parameters are estimated.

In Section 2, current status of the uncertainties of resolved resonance parameters are briefly reviewed. Section 3 is devoted to the basic definition of the k_{eff} and Doppler reactivity worth based on the direct k-difference method. Treatments of the non-resonant cross sections are re-

marked. In the Section 4, Doppler-broadening functions as a basic quantities to estimate the effective cross sections are extensively studied where analytical expressions for Doppler broadening functions and resonance self-shielding factor are emphasized. In the section 5, the resonance self-shielding factor for individual resonance is shown together with its partial derivative with respect to basic variables. In the last half of this section the basic formula of resonance self-shielding factor in multi-group theory is discussed. In the Section 6, analytical formula for sensitivity analyses are described for the k_{eff}, temperature coefficient α and Doppler reactivity worth ρ. In Section 7, some typical results of numerical analyses are shown. The overall and detailed numerical analyses will be reported as a separate document where the uncertainties of resolved resonance parameters and final uncertainties of reactivity, especially Doppler reactivity worth, are emphasized.

In this work, algebraic calculations and graphics were carried out by using Maple Computer Algebra System[7, 8].

2 Uncertainty of Resolved Resonance Parameter

Neutron resonance effect in the nuclear engineering can be typically observed as the Doppler reactivity effect through the change of resonance self-shielding factor as function of temperature and the potential scattering cross section per resonance absorber. Usually, main resonant materials in a nuclear reactor and their number of resonances are about 260 resonances for ^{235}U, 1602 (s-wave=473,p-wave=1129) for ^{238}U, 1015(s-wave) for ^{239}Pu, 205(s-wave) for^{240}Pu and 127(s-,p- and d-waves) for ^{56}Fe, respectively. Therefore, in the nuclear engineering about total 3600 at least resonances are considered and processed by resonance calculation code such as $NJOY$[12] and MC^2-2[13]. In order to evaluate the reactivity uncertainty due to the uncertainties of resolved resonance parameters, these resonances have to be simultaneously considered.

Reich-Moore Formula is adopted in the recent evaluated nuclear data files such as JENDL-3.2 and ENDF/B-IV for main nuclear fuel elements and structure materials. In this work, however, equivalent resonance parameters and their uncertainties were evaluated by T. Nakagawa and K. Shibata[6]. In general, the uncertainties of resonance parameters themselves based on experimental and/or analytical evaluation could not be definitely determined because they are multidimensional function of resonance energy and resonance widths, and these parameters are correlated with one another, as found in the area analysis to determine the resonance parameters from experimental data. Therefore, considering the ambiguity of the resonance parameter uncertainties, the simpler Breit-Wigner multi-level formula is enough.

The uncertainties of the resolved resonance parameters of the typical fuel elements mainly contributing the Doppler reactivity worth are shown in **Fig. 1** to **14**. In order to convert the Reich-Moore parameters with two fission widths, namely Γ_{f1} and Γ_{f2}, to the Breit-Wigner's single fission width and to estimate its uncertainties are approximated by

$$\overline{\Gamma_f} = \sqrt{{\Gamma_{f1}}^2+{\Gamma_{f2}}^2} \tag{1}$$

$$\frac{\overline{\delta\Gamma_f}}{\overline{\Gamma_f}} = \sqrt{\left\{\frac{\Gamma_{f1}^2}{\Gamma_{f1}^2+\Gamma_{f2}^2}\right\}\cdot\left(\frac{\delta\Gamma_{f1}}{\Gamma_{f1}}\right)^2+\left\{\frac{\Gamma_{f2}^2}{\Gamma_{f1}^2+\Gamma_{f2}^2}\right\}\cdot\left(\frac{\delta\Gamma_{f2}}{\Gamma_{f2}}\right)^2} \tag{2}$$

2.1 Uncertainty of ^{238}U Resolved Resonance Parameter

The number of resolved resonances of ^{238}U is 1602 as a whole; i.e., 473 s-wave resoances as shown in **Fig. 1** and 1129 p-wave resonances in **Fig. 4**. The errors of these resonance energies

are very small and the absolute error of 0.1 % are assigned for all levels whose errors are not available in the document for evaluation and/or measurement.

The uncertainties of ^{238}U s-wave neutron widths are smaller than about 15 % except 13 resonances as shown in **Fig. 2**. In this case, the 15 % is seemed to be assumed as a mean uncertainty. The largest uncertainty of about 42 % is assigned for 1005.2 eV resonance. For the p-wave, significantly large uncertainties $\simeq$ 100% exist around resonance energy 6000 eV as shown in **Fig. 5** where assumed uncertainty is about 15 %. Excluding these larger 6 resonances, the uncertainties are smaller than about 40 %.

Mean radiation width for the ^{238}U s-wave neutron are 23 meV and almost of all (1602) resonances are assigned by this mean value except about 17 resonances as shown in **Fig. 3**. The largest uncertainty of 45 % exists in the 145.66 eV resonance and larger ones can be found below 1600 eV. Above this energy, however, the constant uncertainties of about 5 % are assigned to the mean radiation width as shown by a horizontal line.

2.2 Uncertainty of ^{239}Pu Resolved Resonance Parameter

The uncertainties of ^{239}Pu resonance energies are also significantly small in comparison with those of other resonance parameters, but they are enhanced above 1000 eV as shown in **Fig. 7** although the maximum uncertainty is about 0.16 % around 1700 eV. Below 1000 eV, the resonance energy uncertainties are assumed to be about 0.005 %.

The uncertainties of ^{239}Pu s-wave neutron widths are scattered around the mean value of 10%, i.e., $10 \pm 10\%$ as shown in Fig. 12.

However, the uncertainties of s-wave radiation widths are assigned to a limited levels as shown in **Fig. 9** whose maximum value is about 20%. The mean uncertainty of 15% is assigned to the other levels.

The uncertainties of fission widths for s-wave neutron are shown in **Fig. 10** for ^{239}Pu, and the maximum uncertainty of 20 % is the same to that of radiation width as shown in **9**. The mean uncertainty of 15% is assigned to ^{239}Pu fission and capture resonances.

2.3 Uncertainty of ^{240}Pu Resolved Resonance Parameter

The uncertainties of resonance energies for ^{240}Pu are also small, whose magnitudes are less than 0.18 % assigned to the first resonance at $Er = 1.05$ eV as shown in **Fig. 11**. Below 600 eV, the uncertainties are seemed to be slightly enhanced.

The uncertainties of ^{240}Pu s-wave neutron widths are smaller than about 60 % except 3 resonances as shown in **Fig. 12**. The first 2 resonances with significantly larger uncertainties are located in the subthreshold fission indicating in the **Fig. 18** but the third one has no correspondence.

The uncertainties of radiation widths of ^{240}Pu are assigned below about 800 eV and above it a mean value of 30% are adopted as shown in **Fig. 13**. Evaluated uncertainties are seemed to be smaller than about 13% except most of levels assigned by mean uncertainty.

Fission width uncertainties of ^{240}Pu are shown in **Fig. 14**, whose maximum uncertainty is about 100 %. The larger fission widths of ^{239}Pu and ^{240}Pu are seemed to be governed by subthreshold fission and some grouping structure of resonances exist around the subthreshold fission levels having extremely larger fission widths. Typical and famous structure observed by Migneco and Theobald[9] can be found in the case of ^{240}Pu as shown in **Fig. 18** and similar structure can be also found in ^{239}Pu fission in **Fig. 17**. The magnitudes of these larger fission widths are greater than the ^{238}U radiation width of about 23 meV. Such a large fission width significantly enlarges the total resonance width which gives extremely large Doppler width

because of $\Delta \propto \frac{\Gamma}{\sqrt{T}}$(T: temperature) and then some problems arise in the numerical analysis of resonance self-shielding factor as discussed in Section 6.

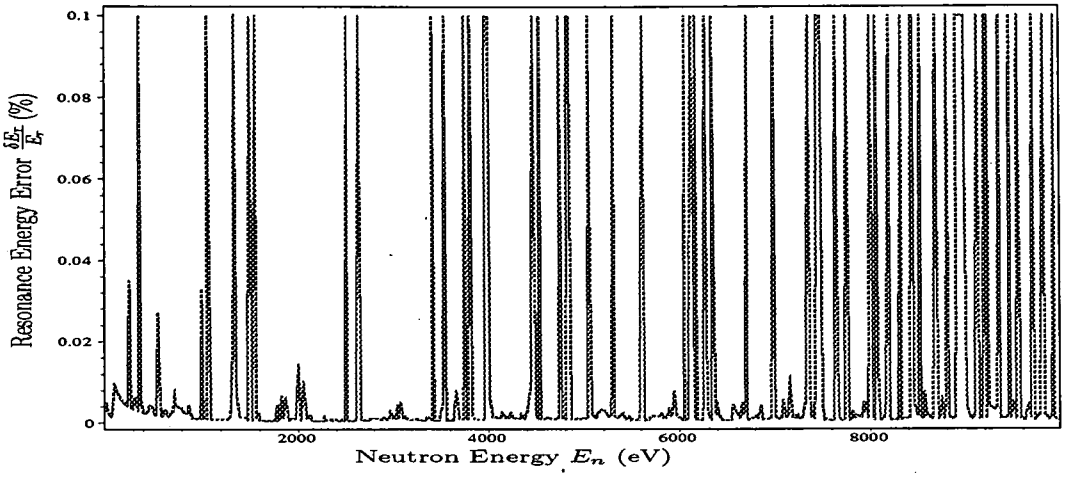

Figure 1: Uncertainty of S-wave Resonance Energy $\frac{\delta Er}{Er}$ of ^{238}U

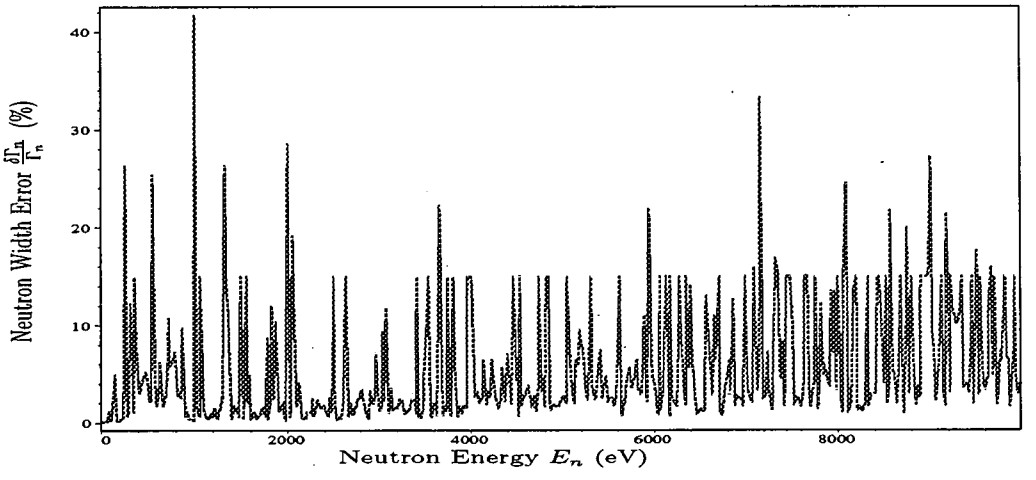

Figure 2: Uncertainty of S-wave Neutron Width $\frac{\delta\Gamma_n}{\Gamma_n}$ of ^{238}U

3 Criticality and Doppler Reactivity

Reactivity worth can be obtained as the difference of effective multiplication factors k_{eff}'s, so-called "direct k_{eff} difference method", between two systems of interest. As long as the accuracy of k_{eff} calculation is guaranteed, the direct k_{eff} difference method is preferred in a sense that the k_{eff} can be described by neutron balance in terms of only real fluxes.

In the neutron balance equation, the k_{eff} is defined by the ratio of the neutron production rate to the effective neutron absorption rates including the neutron leakage i.e.,

$$k_{eff} = \frac{< \nu\Sigma_f\phi >}{< \Sigma_f\phi > + < \Sigma_\gamma\phi > + L}, \tag{3}$$

$$= k_\infty \cdot \frac{1}{1 + L^\star}, \tag{4}$$

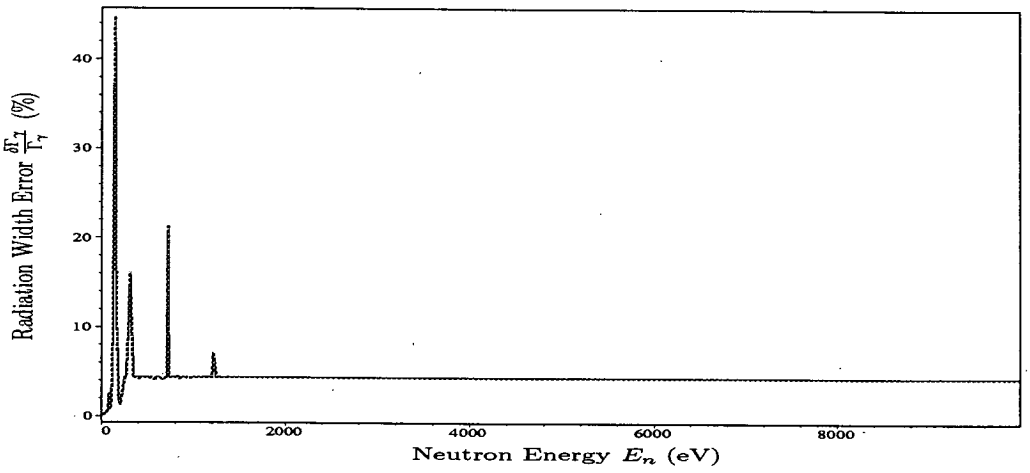

Figure 3: Uncertainty of S-wave Radiation Width $\frac{\delta\Gamma_\gamma}{\Gamma_\gamma}$ of ^{238}U

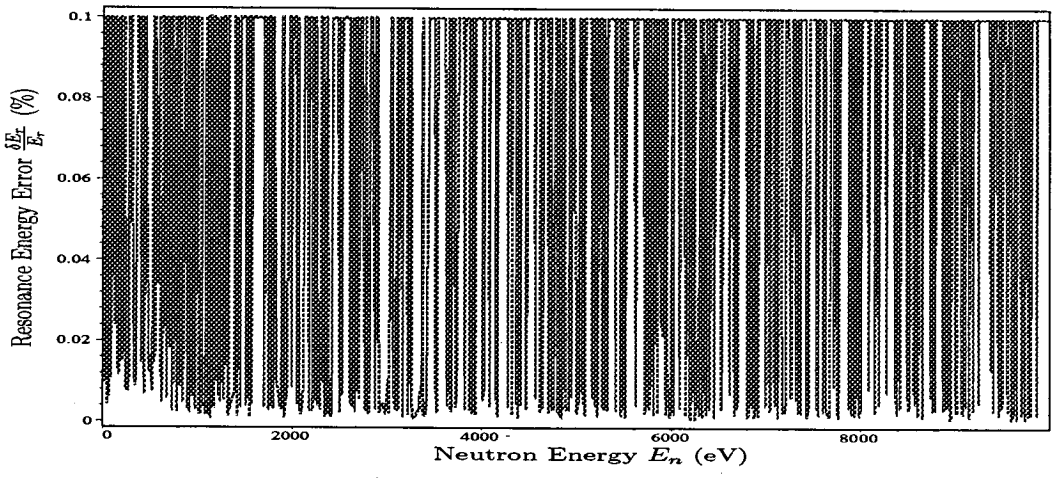

Figure 4: Uncertainty of P-wave Resonance Energy $\frac{\delta Er}{Er}$ of ^{238}U

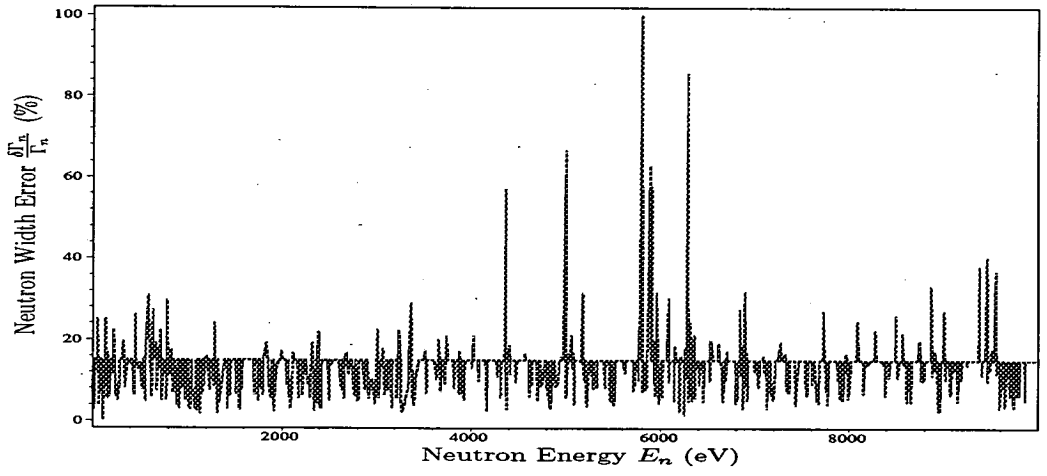

Figure 5: Uncertainty of P-wave Neutron Width $\frac{\delta\Gamma_n}{\Gamma_n}$ of ^{238}U

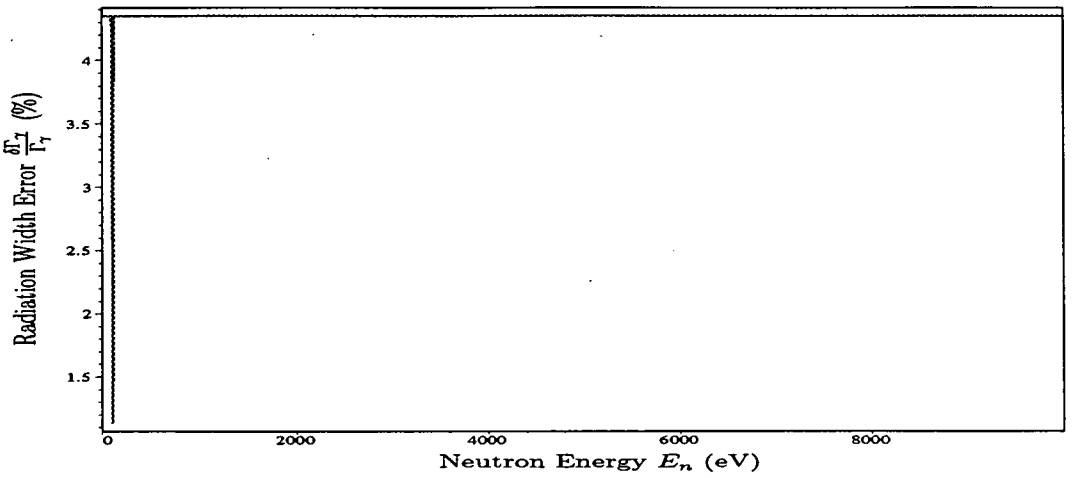

Figure 6: Uncertainty of P-wave Radiation Width $\frac{\delta\Gamma_\gamma}{\Gamma_\gamma}$ of ^{238}U

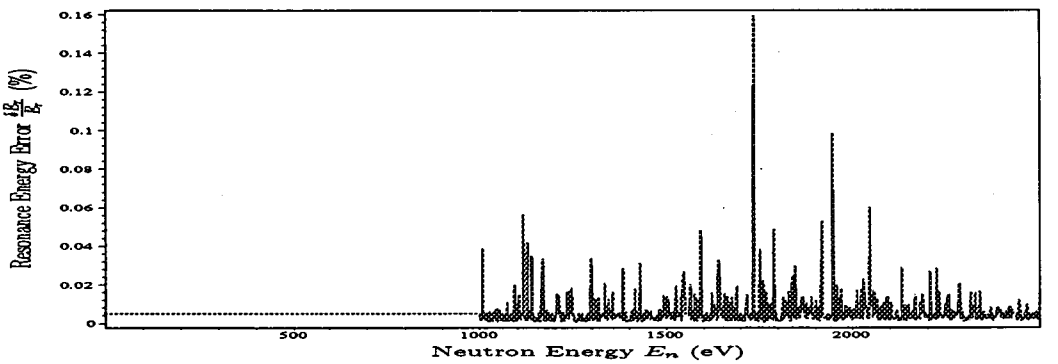

Figure 7: Uncertainty of S-wave Resonance Energy $\frac{\delta Er}{Er}$ of ^{239}Pu

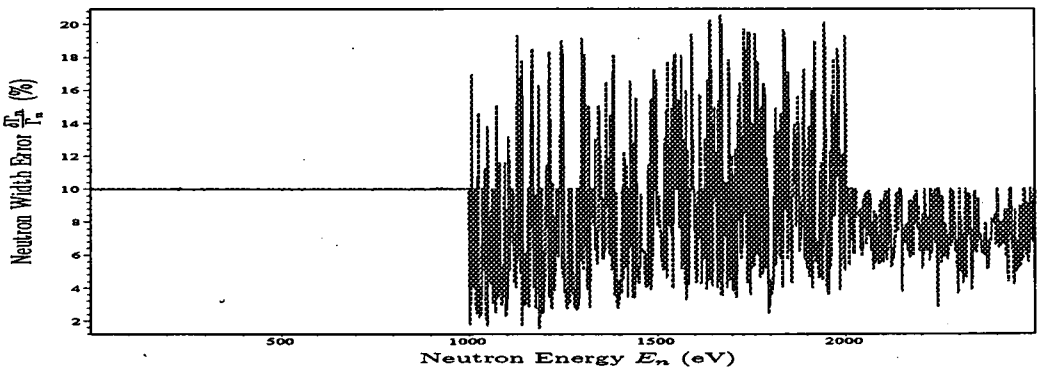

Figure 8: Uncertainty of S-wave Neutron Width $\frac{\delta\Gamma_n}{\Gamma_n}$ of ^{239}Pu

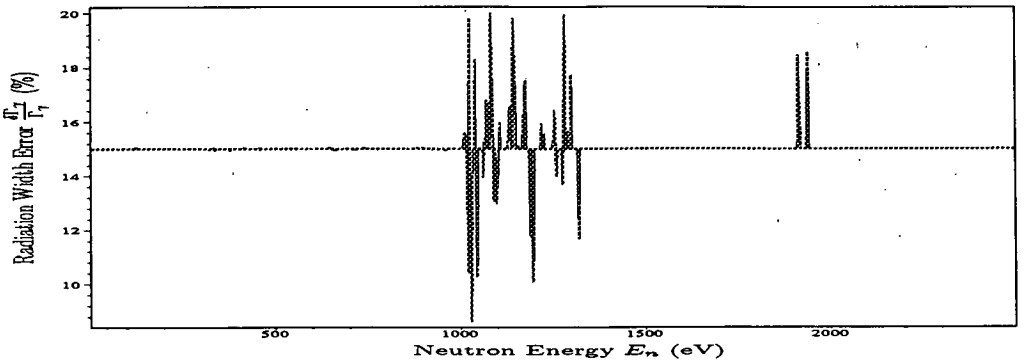

Figure 9: Uncertainty of S-wave Radiation Width $\frac{\delta\Gamma_\gamma}{\Gamma_\gamma}$ of ^{239}PU

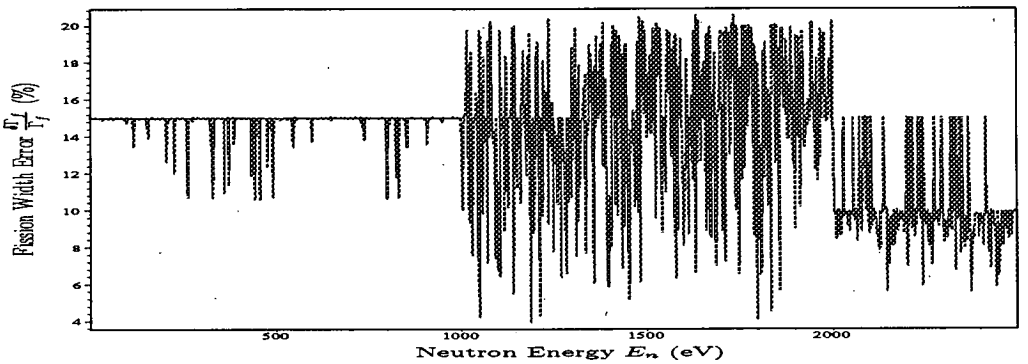

Figure 10: Uncertainty of S-wave Fission Width $\frac{\delta\Gamma_f}{\Gamma_f}$ of ^{239}Pu

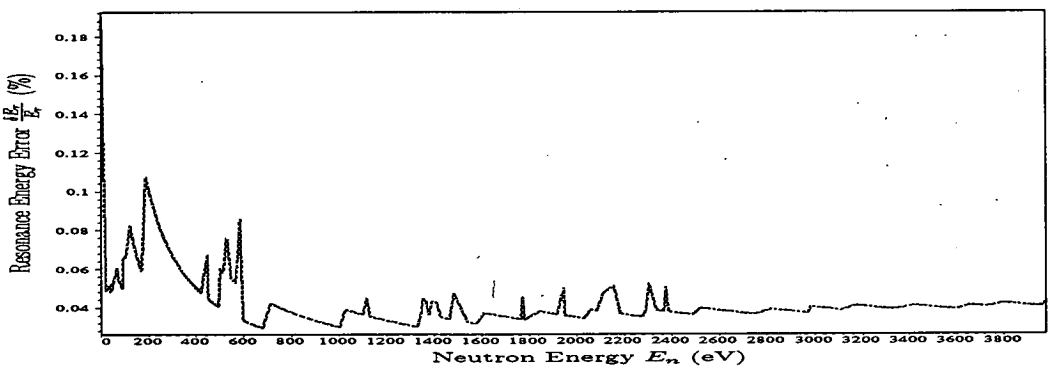

Figure 11: Uncertainty of S-wave Resonance Energy $\frac{\delta Er}{Er}$ of ^{240}Pu

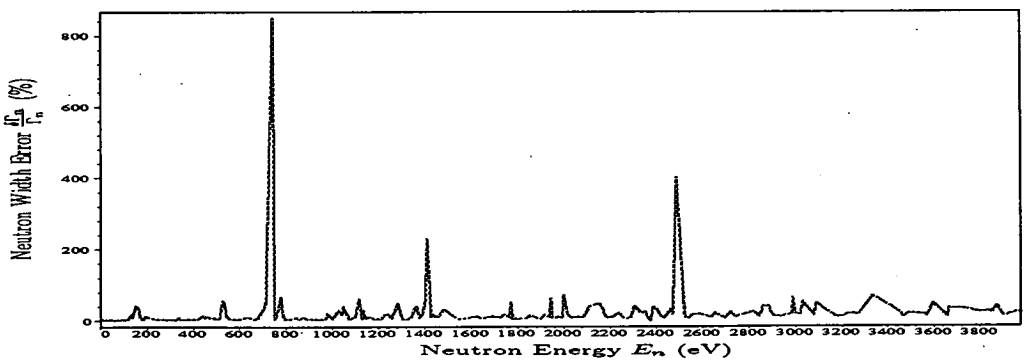

Figure 12: Uncertainty of S-wave Neutron Width $\frac{\delta\Gamma_n}{\Gamma_n}$ of ^{240}Pu

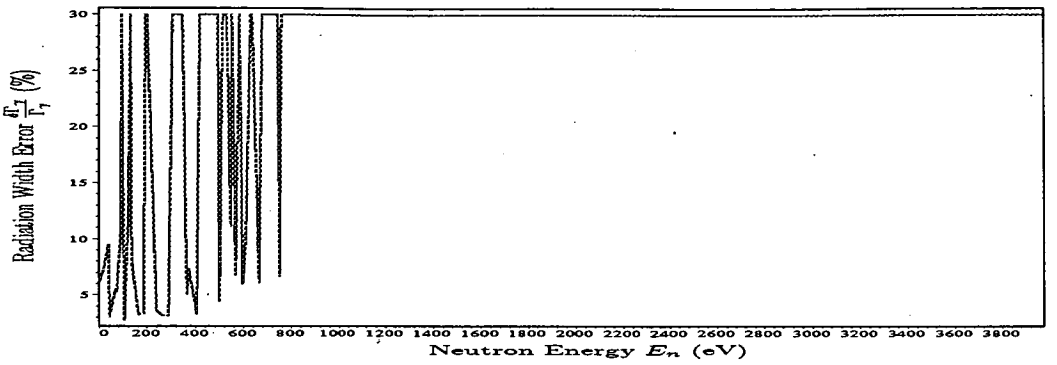

Figure 13: Uncertainty of S-wave Radiation Width $\frac{\delta\Gamma_\gamma}{\Gamma_\gamma}$ of ^{240}PU

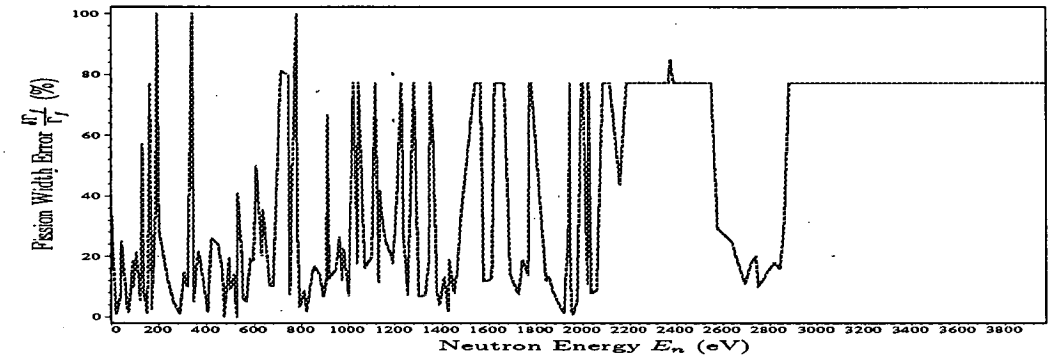

Figure 14: Uncertainty of S-wave Fission Width $\frac{\delta\Gamma_f}{\Gamma_f}$ of ^{240}Pu

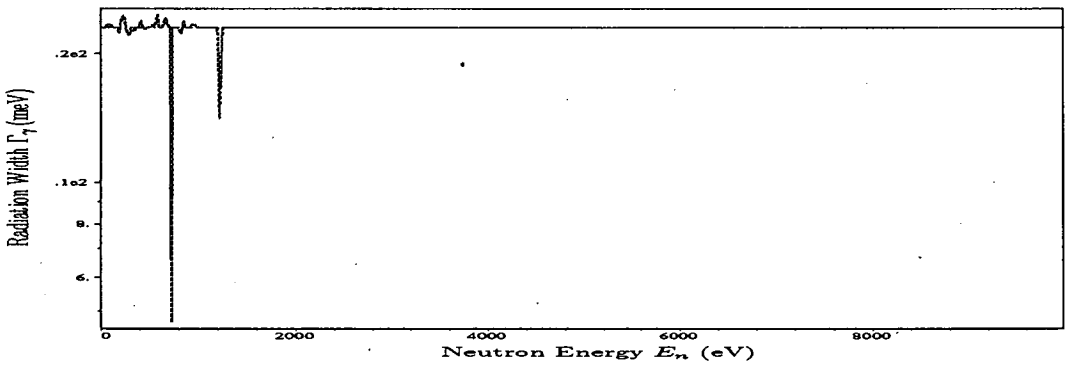

Figure 15: S-wave Radiation Width Γ_γ of ^{238}U

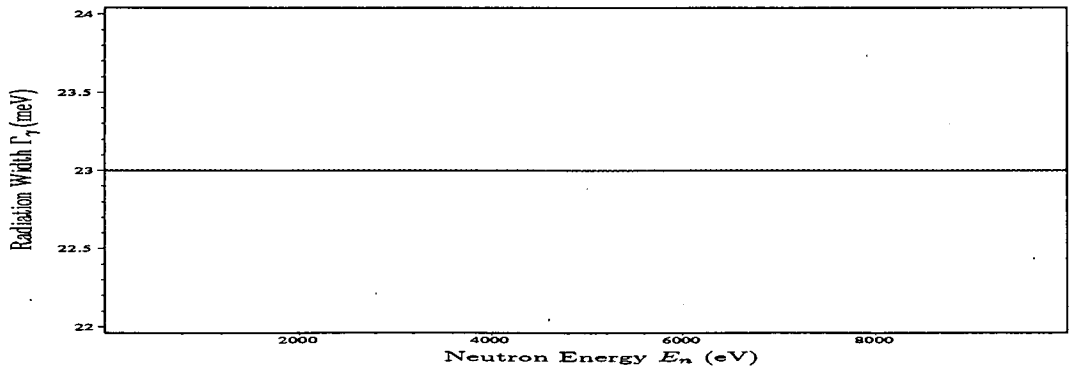

Figure 16: P-wave Radiation Width Γ_γ of ^{238}U

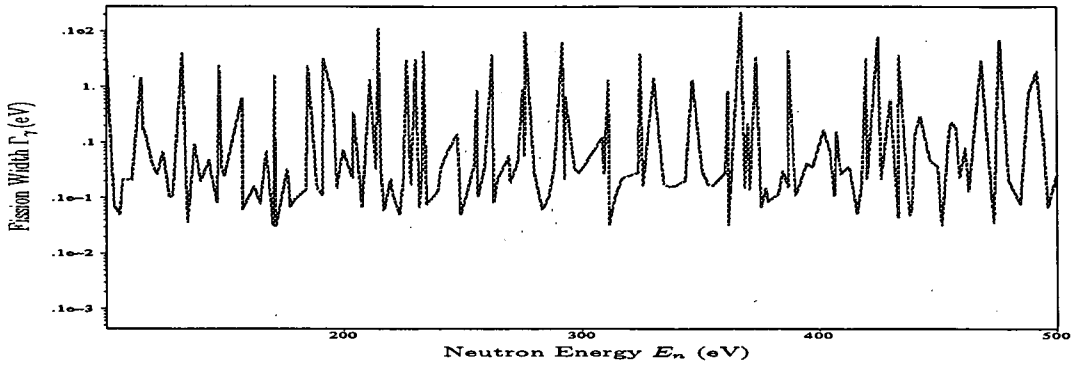

Figure 17: S-wave Fission Width Γ_f of ^{239}Pu RpFig:P9S48

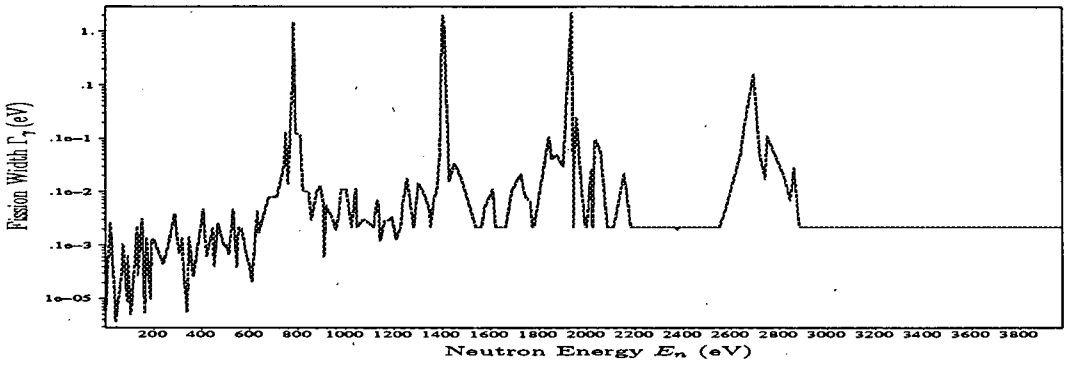

Figure 18: S-wave fission Width Γ_f of ^{240}Pu

$$< \cdots > \;=\; \int_{dV}\int_{dE} \cdots \tag{5}$$

dV : Volume element,

dE : Neutron energy interval,

where suffixes f and γ mean the fission and neutron capture reactions respectively, and blakets $< .. >$ means the space-energy integration of macroscopic reaction rates. The k-infinite, denoted by k_∞, and effective neutron leakage $L^\star$ can be defined by reaction rates as shown below,

$$k_\infty \;=\; \frac{< \nu\Sigma_f\phi >}{< \Sigma_f\phi > + < \Sigma_\gamma\phi >}, \tag{6}$$

$$\;=\; \frac{< \nu\Sigma_f\phi >^{Res} + < \nu\Sigma_f\phi >^{Non-Res}}{< \Sigma_f\phi >^{Tot} + < \Sigma_\gamma\phi >^{Tot}}, \tag{7}$$

$$L^\star \;=\; \frac{L}{< \Sigma_f\phi >^{Tot} + < \Sigma_\gamma\phi >^{Tot}}. \tag{8}$$

While, total reaction rate for overall energy range denoted by superscript "Tot" is the sum of resonance part for individual resonance contribution and non-resonant parts in the higher energy region above the top of resolved resonance or the top of unresolved resonance. In this work, the unresolved resonance is treated as the non-resonant part since the present sensitivity study is focused on the resolved resonance. The sensitivity analysis will be extended to the unresolved resonance in near future. The explicit expression of the total reaction rates is as follow,

$$< \nu\Sigma_f\phi >^{Tot} = \sum_i N_i \int_E \nu_i(E)\sigma_{fi}(E)\phi(E)dE, \quad (9)$$

$$= < \nu\Sigma_f\phi >^{Res} + < \nu\Sigma_f\phi >^{Non-Res}, \quad (10)$$

$$< \Sigma_f\phi >^{Tot} = \sum_i N_i \int_E \sigma_{fi}(E)\phi(E)dE, \quad (11)$$

$$= < \Sigma_f\phi >^{Res} + < \Sigma_f\phi >^{Non-Res}, \quad (12)$$

$$< \Sigma_\gamma\phi >^{Tot} = \sum_i N_i \int_E \sigma_{\gamma i}(E)\phi(E)dE, \quad (13)$$

$$= < \Sigma_\gamma\phi >^{Res} + < \Sigma_\gamma\phi >^{Non-Res}, \quad (14)$$

where

$< \nu\Sigma_f\phi >^{Res}$: Resolved resonance part of neutron production,
$< \nu\Sigma_f\phi >^{Non-Res}$: Non-resonant part of neutron production,
$< \Sigma_\gamma\phi >^{Res}$: Resolved resonance part of (n,γ) reaction,
$< \Sigma_\gamma\phi >^{Non-Res}$: Non-resonant part of (n,γ) reaction including structure and moderator materials,

and suffix i means the isotope, and the volume integral is omitted here for simplicity and the energy integration limit is up to the top (highest energy) of resolved resonance for the resonance part.

The critical leakage term L^{crit} and the critical $\nu - value$ to hold the system to be critical can be related to the k_∞ as

$$L^{\star crit} = k_\infty - 1, \quad (15)$$

$$\nu^{crit} = \left(1 + \frac{< \Sigma_\gamma\phi >^{Tot}}{< \Sigma_f\phi >^{Tot}}\right) \cdot (1 + L^\star). \quad (16)$$

In the present work, the criticality search is performed by adjusting the constant factor to be multiplied by the reference ν-value with a reference effective multi-group cross sections giving nearly critical system.

The Doppler reactivity worth ρ is defined by the direct k-difference as

$$\rho = \frac{1}{k'_{eff}} - \frac{1}{k_{eff}} = \frac{k_{eff} - k'_{eff}}{k_{eff}k'_{eff}}, \quad (17)$$

where k'_{eff} and k_{eff} mean the effective multiplication factors of high temperature system and reference (low temperature) systems, respectively, which are functions of micro-scopic cross sections as shown by Eqs. (9), (11) and (13). These cross sections, $\sigma_{fi}(E)$ and $\sigma_{\gamma i}(E)$, have to be prepared by considering the resonance self-shielding effects as functions of potential scattering cross section per resonance absorber and reactor temperature as discussed below.

4 Resonance Self-Shielding Factor

4.1 Effective Cross Section

Effective cross section σ_{effx} for isotope i and reaction x at temperature T is defined by a flux weighted average cross section as shown below;

$$\sigma^g_{effx}(T) = \frac{\int_{E_0}^{E_1} \sigma(E,T)\phi(E,T)dE}{\int_{E_0}^{E_1} \phi(E,T)dE}, \tag{18}$$

where E means the neutron energy, E_0 and E_1 are energy boundaries of a broad groups, and $\phi(E)$ indicates the neutron flux. Consequently, the σ^g_{effx} can be obtained from the microscopic cross section based on nuclear data including resonance parameters as far as the neutron flux is available. Usually, fine or super-fine group flux obtained by neutron spectrum calculation code such as MC^2-2[13] is used. The flux depression effects due to resonance to the effective cross section σ^g_{effx} is taken into account by NR(Narrow resonance) approximation as,

$$\phi_i(E,T) \simeq \frac{1}{E\cdot\Sigma_{ti}(E,T)}, \tag{19}$$

$$\Sigma_{ti}(E,T) = \sum_{i=1}^{n} N_i\sigma_{ti}(E,T), \tag{20}$$

and then the effective cross section for a single ultra-fine group k becomes the following simple form,

$$\sigma^g_{effxik}(T) = \frac{\int_{E_0}^{E_1} \frac{\sigma_{xik}(E,T)dE}{E\cdot\Sigma_{tik}(E,T)}}{\int_{E_0}^{E_1} \frac{1}{E\cdot\Sigma_{tik}(E,T)}dE} \tag{21}$$

$$\simeq \frac{\Sigma_{pi}}{\Delta u^k}\int_{E_0}^{E_1} \frac{\sigma_{xik}(E,T))}{E\cdot\Sigma_{tik}(E,T)}dE, \tag{22}$$

where macroscopic potential scattering cross section Σ_{pi} and lethargy width Δu^k are introduced together with the macroscopic total cross section Σ_{tik}. The $\sigma_{xik}(E,T)$ is the resonant cross section for a reaction x of the i-th isotope at neutron energy E. For instance, the Breit-Wigner form for the resonant cross section at $T=0$ (K) is,

$$\sigma_{\gamma ik}(E) = \frac{\pi}{\mathrm{k}^2}\cdot\frac{g\Gamma_{nik}\Gamma_{\gamma ik}}{(E-E_{ik})^2+(\Gamma_{tik}/2)^2}, \tag{23}$$

where,

k	:	Wave number $= 2.19685\cdot10^{-3}\left[\frac{A_i}{A_i+1}\right]\sqrt{E}$,
E_{ik}	:	Resonance energy of i-th isotope and k-th resonance (eV),
g_{ik}	=	$\frac{2J+1}{2(2I+1)}$: spin statistical weight,
I	:	Target spin,
J	:	The spin of compound nucleus,
Γ_{nik}	:	Neutron width (eV),
Γ_{tik}	:	Total width (eV).

For an arbitrary temperature, the partial cross sections such as radiative capture cross section

can be expressed by taking into account the Doppler broadening effects expressed by symmetric function ψ and asymmetric function χ as shown below,

$$\sigma_{\gamma ik}(E,T) = \sigma_{0ik}(E)\cdot\frac{\Gamma_{\gamma ik}}{\Gamma_{ik}}\cdot\psi(E,T), \tag{24}$$

$$\sigma_{fik}(E,T) = \sigma_{0ik}(E)\cdot\frac{\Gamma_{fik}}{\Gamma_{ik}}\cdot\psi(E,T), \tag{25}$$

$$\sigma_{tik}(E,T) = \sigma_{0ik}(E)\cdot\psi(E,T)+a_{pik}\cdot\chi(E,T)+\sigma_{pi}, \tag{26}$$

where the Doppler broadening function can be expressed in terms of dimensionless energy x and relative resonance width θ to Doppler width as,

$$\psi(x_{ik},\theta_{ik}) = \frac{\theta_{ik}}{\sqrt{4\cdot\pi}}\int_{-\infty}^{+\infty}\frac{exp[-\frac{\theta_{ik}^2}{4}\cdot(x_{ik}-y)^2]}{1+y^2}dy, \tag{27}$$

$$\chi(x_{ik},\theta_{ik}) = \frac{\theta_{ik}}{\sqrt{4\cdot\pi}}\int_{-\infty}^{+\infty}\frac{2y\cdot exp[-\frac{\theta_{ik}^2}{4}\cdot(x_{ik}-y)^2]}{1+y^2}dy, \tag{28}$$

$$\sigma_{oik} = \frac{cnst}{|E_{ik}|}\cdot\left[\frac{A_i+1}{A_i}\right]^2\cdot\frac{g\Gamma_{noik}}{\Gamma_{ik}}, \tag{29}$$

$$cnst = 2.6039953\times10^6, \tag{30}$$

$$a_{pik} = \left[\frac{g\Gamma_{n0\,ik}\,\sigma_{pi}}{\Gamma_{ik}\,\sigma_{0ik}}\right]^{1/2}, \tag{31}$$

($\Gamma_{n0\,ik}$: Neutron width at a resonance position) ,

$$\theta_{ik} = \frac{\Gamma_{ik}}{\Delta_{ik}}, \tag{32}$$

$$\Delta_{ik} = \sqrt{\frac{4\kappa_{Blz}TE_{ik}}{A_i}}, \tag{33}$$

$$x_{ik} = \frac{2(E-E_{ik})}{\Gamma_{ik}}, \tag{34}$$

A_i : Mass number of an isotope i,
T : Temperature in Kelvin (K),
Δ_{ik} : Doppler width (eV),
σ_{pi} : Potential scattering cross section (barn),
κ_{Blz} $=8.6171\cdot10^{-5}$ (eV/K) : Boltzmann constant.

The Doppler widths Δ_{ik}'s as functions of temperature are shown in **Figs. 19** and **20** for ^{238}U resonance at $Er = 6.67$ eV and for ^{239}Pu resonance at $E_r = 214.56$ eV, respectively. The latter ^{239}Pu resonance is shown as an example of "wide resonance" with total width of $\Gamma = 11.22\,eV$ due to large fission width $\Gamma_f = 11.17\,eV$, where suffix xik is omitted for simplicity. The Δ_{ik}-value of ^{238}U is in general small, at most about 220 meV at temperature $T = 5000$

K because of the smaller total width, on the other side, that of ^{239}Pu is also small except larger total width whose Δik-value exceeds 1 eV as shown in Fig. 20 than 1 eV because of the larger resonance energy.

The relative resonance widths to the Doppler width, θ_{ik}'s, are shown in **Figs. 21** and

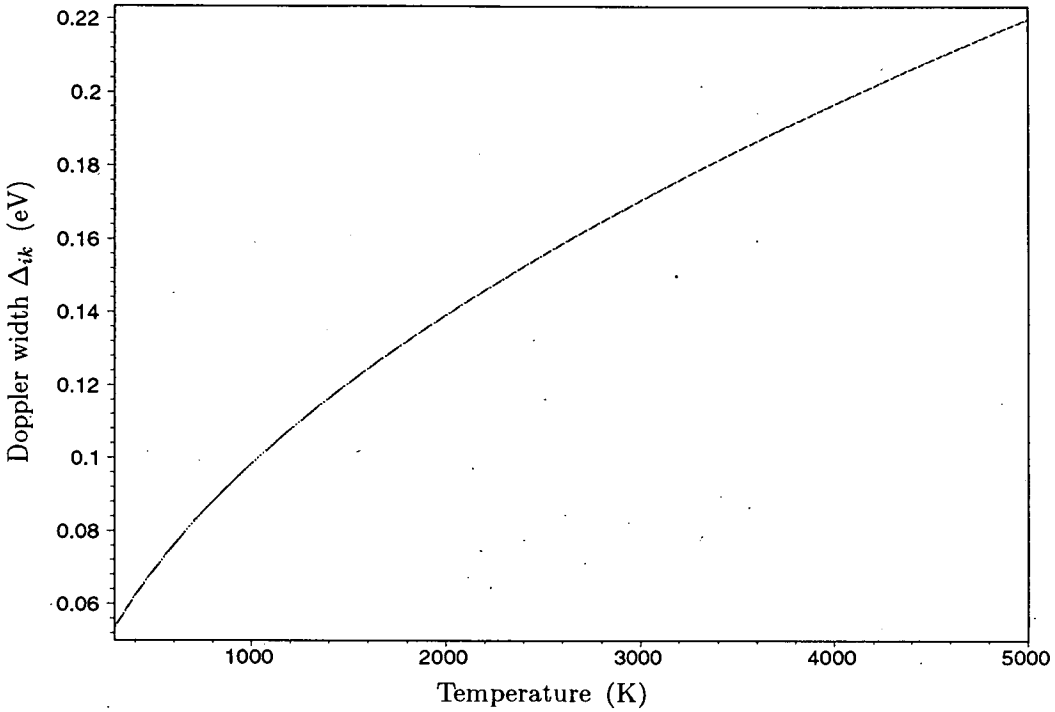

Figure 19: Doppler width Δ_{ik} (eV) of ^{238}U 6.67 eV Resonance with total width $\Gamma_{ik} = 24.89$ meV as Function of Temperature. This resonance is cited as a typical case with relatively narrow total width.

20 for ^{238}U narrow resonance and ^{239}Pu wide resonance with $\Gamma = 11.22$ eV at $E_r = 214.56$ eV mentioned above, respectively. The θ-values are smaller than unity for ^{238}U narrow resonance but greater than 36 for the ^{239}Pu wide resonance due to the larger fission width of $\Gamma_f = 11.17$ eV. The θ function as temperature has the maximum value at the lowest temperature of interest since it is proportional to the inverse temperature as well as the total width Γ as expected from the θ definition Eq. (32). It is a severer problems that the larger θ-values of wide resonance tends to induce an overflow error in the numerical evaluation of ψ and χ functions.

Such a wide fission width was observed for ^{240}Pu subthreshold fission by Migneco and Thebald[9] and was introduced in terms of the states associated with the second minimum of the potential energy surface as a function of deformation in nuclear fission. Typical example can be found in the ^{239}Pu and ^{240}Pu evaluated resonance parameters in JENDL-3.2[4] as shown in **Figs. 17** and **18**, respectively.

Typical example of Doppler broadened cross section as a function of neutron energy and temperature is shown in **Fig. 23** for the ^{240}Pu 1.05 eV resonance. The Doppler broadened ^{240}Pu capture cross section is strongly coupled with the $1/v$ thermal cross section because the resonance energy 1.05 eV is in the thermal neutron energy range. At extremely high temperature of 3.6×10^6 K close to the innermost temperature of the solar, the resonance peak cross section is reduced to about $\frac{1}{25}$ of that at the room temperature.

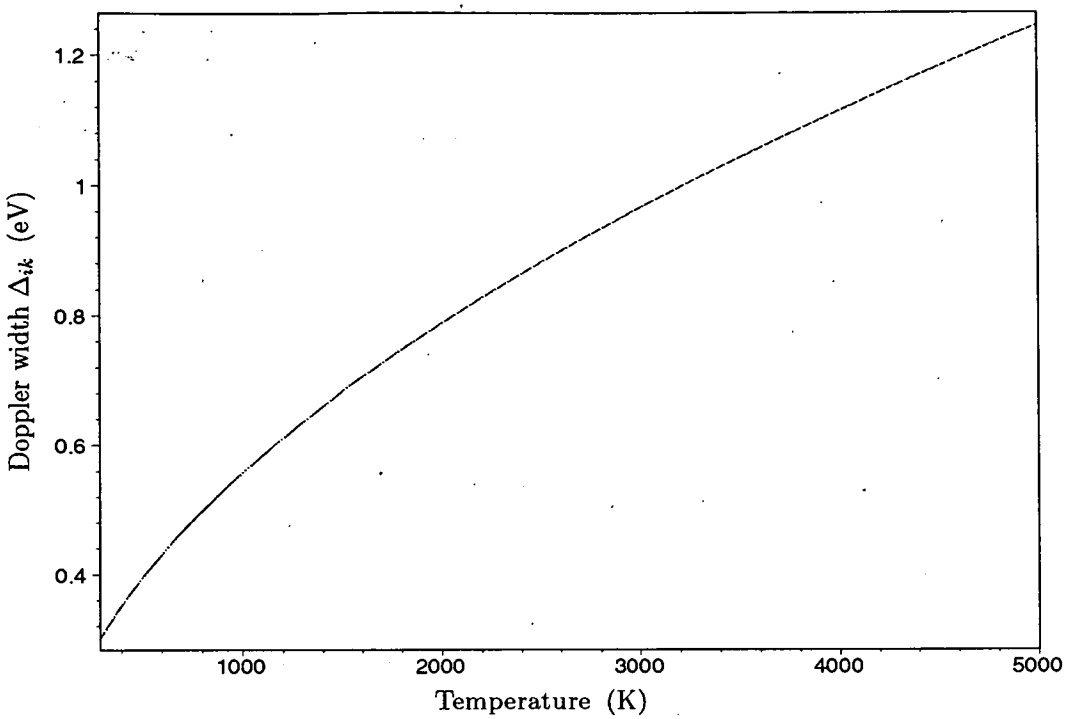

Figure 20: Doppler width Δ_{ik} (eV) of ^{239}Pu 214.56 eV Resonance total width $\Gamma_{ik} = 11.22$ eV as Function of Temperature. This resonance is shown as an example of wide resonance with extremely large resonance width.

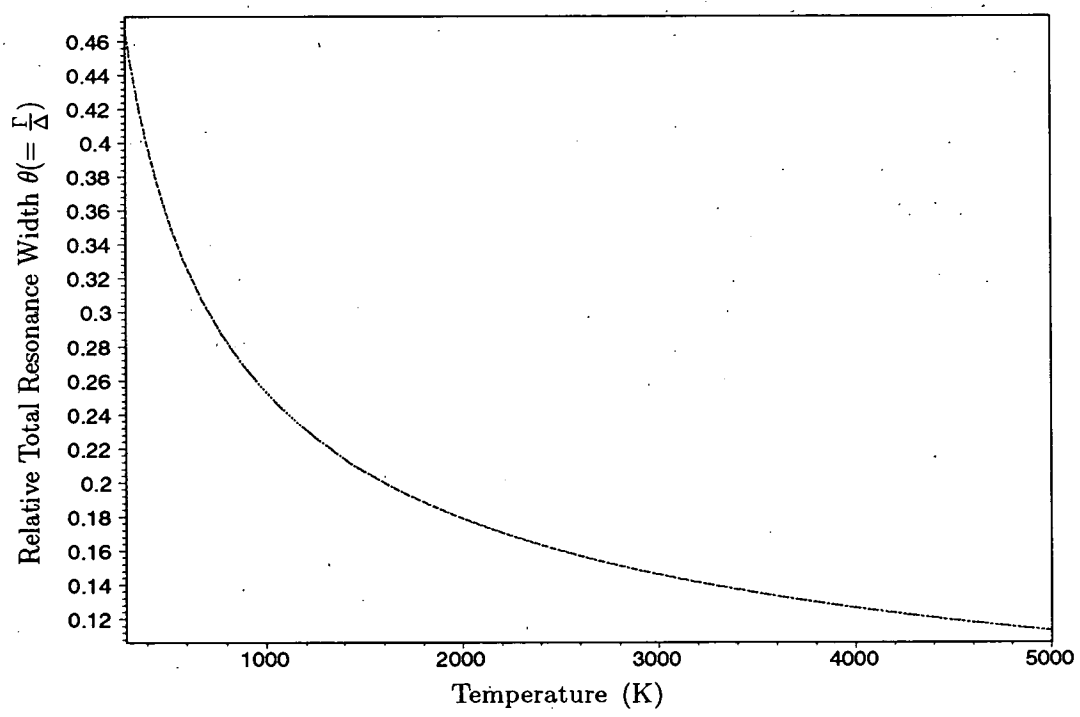

Figure 21: Relative total resonance width $\theta(=\frac{\Gamma}{\Delta})$ of ^{238}U 6.67 eV Resonance as Function of Temperature. This resonance level is adopted as an example of "Narrow Resonance".

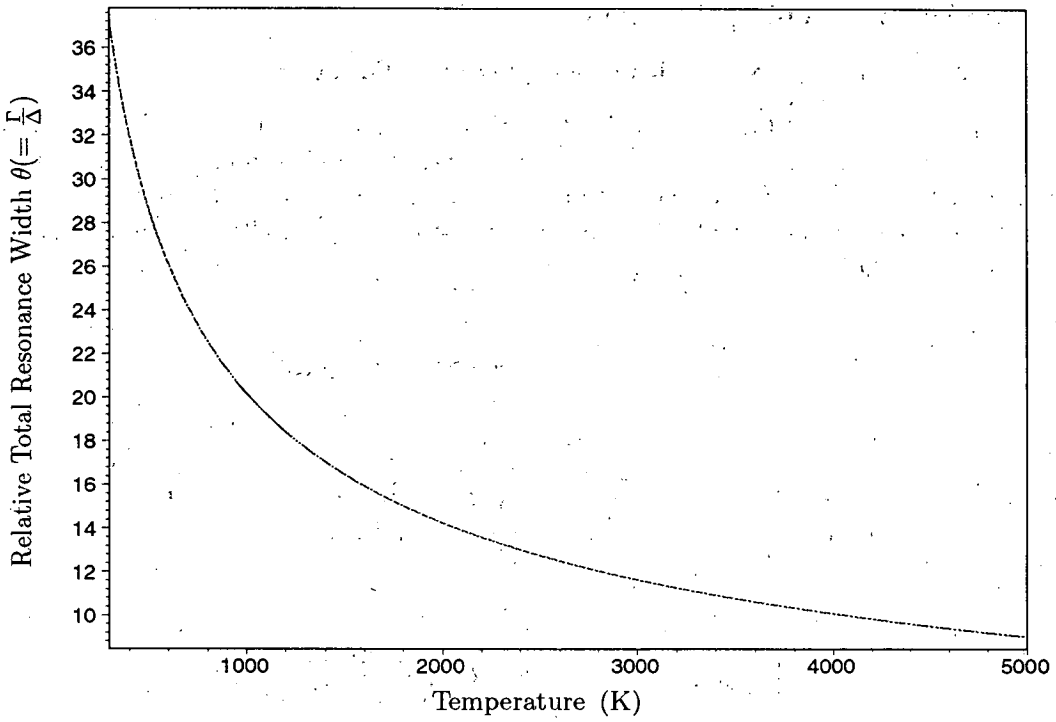

Figure 22: Relative total resonance width $\theta(=\frac{\Gamma}{\Delta})$ of ^{239}Pu 214.65 eV Resonance as Function of Temperature. This resonance level is adopted as an example of "Wide Resonance".

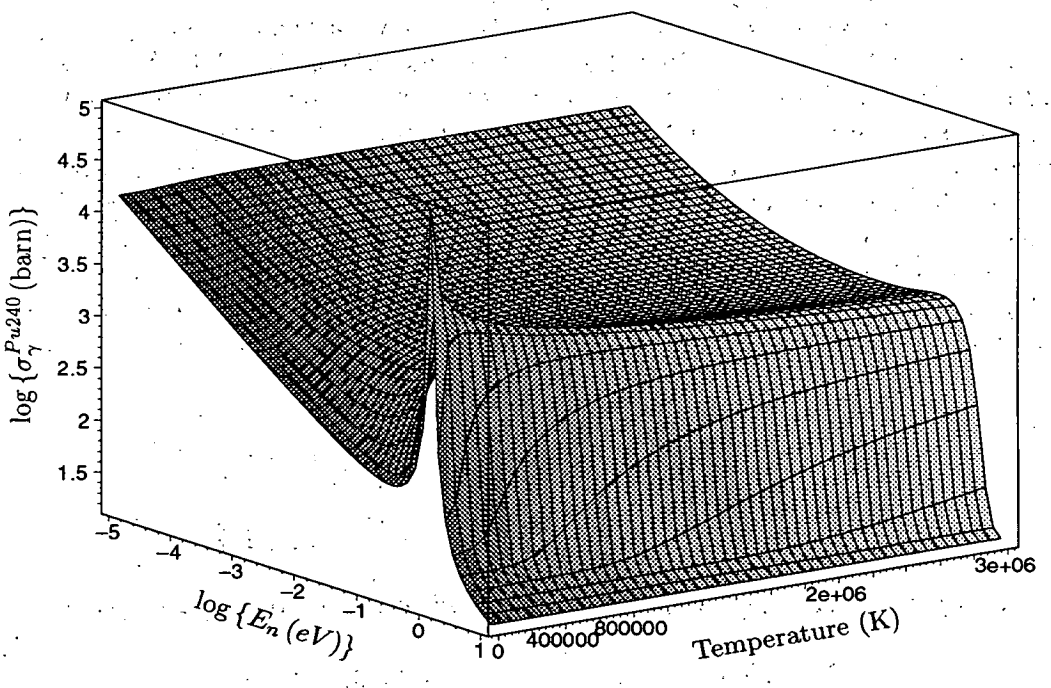

Figure 23: Capture Cross Section of ^{240}Pu 1.05 eV Resonance as a Function of Neutron Energy E_n and Temperature T. The $1/v$-term in the thermal region is superimposed.

4.2 Doppler Broadening Function

4.2.1 ψ and χ Functions based on Complex $w(z)$ Function

The Doppler broadening functions defined by Eqs. (27) and (28) have the integrations over infinite range of dimensionless energy x and consequently numerical integration by using Gaussian integration formula is not effective from accuracy point of view. Usually, complex $w(\mathbf{z})$ function is used and its numerical table, so-called "W-table", is installed in many calculational codes. The $w(\mathbf{z})$ function is defined by,

$$w(\mathbf{z}) = w(u,v) = exp(-\mathbf{z}^2) \cdot erfc(-i\mathbf{z}), \tag{35}$$

$$\mathbf{z} = u + iv. \tag{36}$$

Then, the Doppler broadening functions ψ and χ can be expressed by its real and imaginary parts as shown below and whose arguments are function of θ and x variables defined by Eq. (32) and (34)

$$\psi(x_{ik},\theta_{ik}) = \frac{\theta_{ik}\sqrt{\pi}}{2} \cdot \Re w\left(\frac{\theta_{ik}x_{ik}}{2}, \frac{\theta_{ik}}{2}\right), \tag{37}$$

$$\chi_i(x_{ik},\theta_{ik}) = \theta_{ik}\sqrt{\pi} \cdot \Im w\left(\frac{\theta_{ik}x_{ik}}{2}, \frac{\theta_{ik}}{2}\right). \tag{38}$$

The symmetric Doppler broadening function $\psi(u,v)$ and asymmetric one $\chi(u,v)$ are shown in **Figs. 24** and **25** as functions of u and v. As shown in Eqs.(37) and (38), the variable v is the function of u, i.e., $u = v \cdot x$, and thus small bump can be found below $v \simeq 0.1$.

The symmetric Doppler broadening function $\psi(En,T)$ and asymmetric one $\chi(E_n,T)$ defined by Eqs.(39) and (40) are shown in **Figs. 26** and **27** as functions of E_n and T. As well known, the $\psi(E_n,T)$ function has a peak at the resonance position and decreasing as the energy E_n apart from the resonance energy E_r. While, the $\chi(E_n,T)$ function is the asymmetric with respect to the resonance energy E_r and tends to be vanishing at the both wings. Consequently, the total cross section has a dip in front of the resonance energy because it has a composite function of the ψ and χ as shown in Eq. (26). The dip arises from the behavior of asymmetric function χ characterizing the interference between the potential and resonance scatterings.

By using the power series expansion of error-function, the $w(\mathbf{z})$-function can be completely separated into real and imaginary parts, and resultant analytical formula for ψ and χ are shown below;

$$\psi(x,\theta) = \sqrt{\pi}\frac{\theta}{2}\,\Re\left[e^{-\left\{\frac{\theta}{2}(x+i)\right\}^2}\left[1 + erf\left\{i\cdot\frac{\theta}{2}(x+i)\right\}\right]\right], \tag{39}$$

$$\chi(x,\theta) = \sqrt{\pi}\,\theta\,\Im\left[e^{-\left\{\frac{\theta x}{2}(x+i)\right\}^2}\left[1 + erf\left\{i\cdot\frac{\theta}{2}(x+i)\right\}\right]\right]. \tag{40}$$

These Doppler broadening functions can be related to the complex $w(\mathbf{z})$-function as,

$$2\,\psi\left(\frac{u}{v}, 2v\right) + i\cdot\chi\left(\frac{u}{v}, 2v\right) = 2\sqrt{\pi}\,v\,\mathbf{w}(u,v), \quad (i=\sqrt{-1}), \tag{41}$$

where

$$u = \frac{1}{2}\cdot\theta x, \quad v = \frac{1}{2}\cdot\theta, \quad \text{inversely} \quad x = \frac{u}{v}, \qquad \theta = 2v, \tag{42}$$

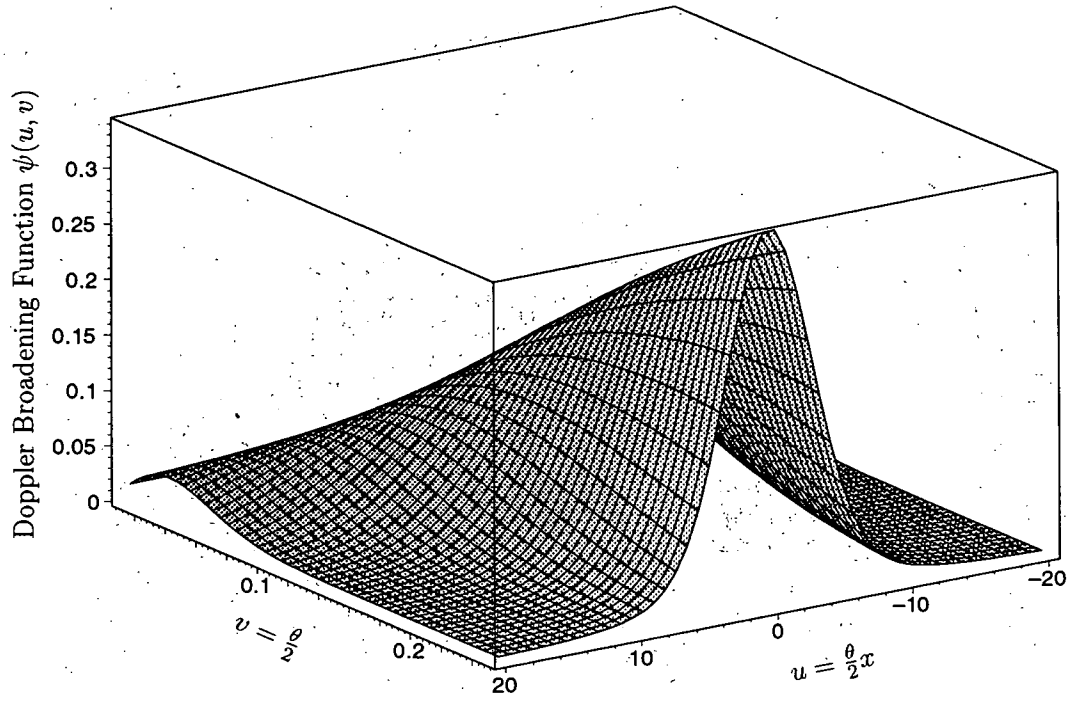

Figure 24: Exact Symmetric Doppler Broadening Function $\psi(u,v)$ as a Function of $u=\frac{\theta}{2}\cdot x$ and $v=\frac{\theta}{2}$. The Doppler broadening function $\psi(u,v)$ expressed by the real part of complex w(z)-function is shown on the $u-v$ plane and $u=0$ is the resonance position.

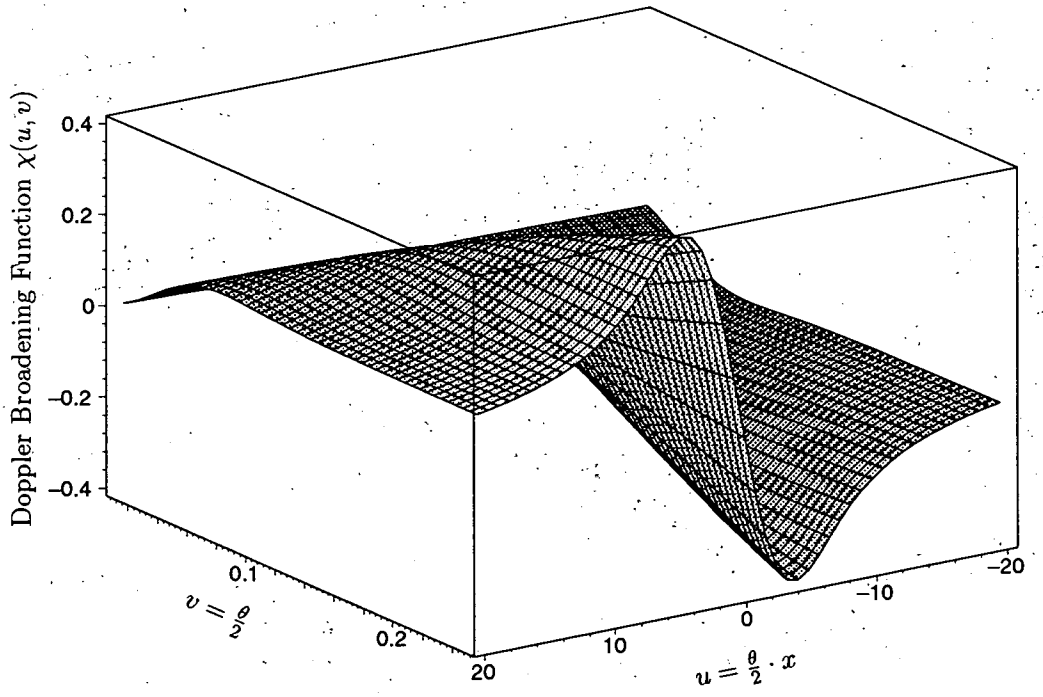

Figure 25: Exact Asymmetric Doppler Broadening Function $\chi(u,v)$ as a Function of $u=\frac{\theta}{2}\cdot x$ and $v=\frac{\theta}{2}$. The Doppler broadening function $\chi(u,v)$ expressed by the imaginary part of complex w(z)-function is shown on the $u-v$ plane and $u=0$ is the resonance position..

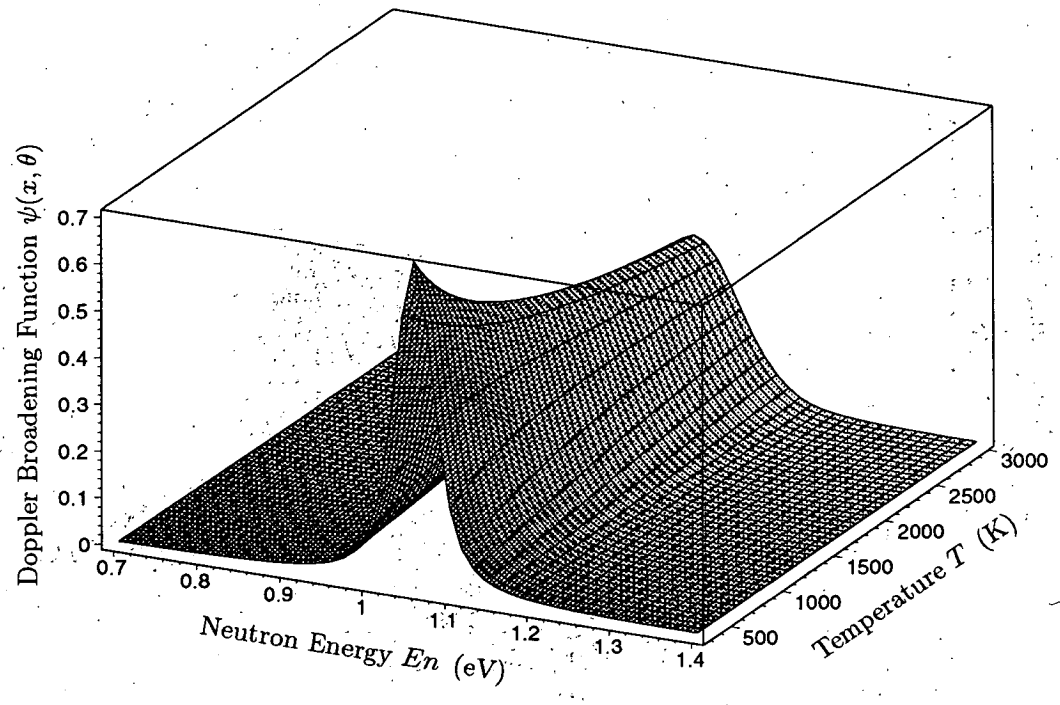

Figure 26: Exact Symmetric Doppler Broadening Function $\psi(x,\theta)$ for ^{240}Pu 1.05 eV Resonance as a Function of Neutron Energy E_n and Temperature T. The Doppler broadening function $\psi(x,\theta)$ expressed by the real part of complex w(z)-function, Eq.(39), is shown on the $E_n - T$ plane.

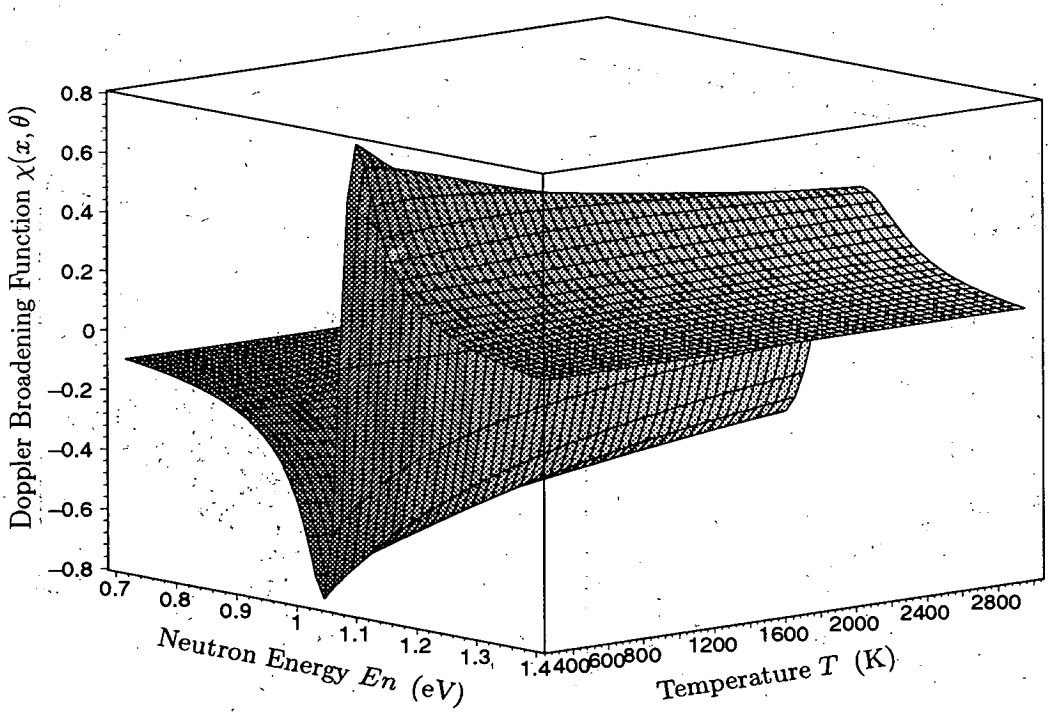

Figure 27: Exact Asymmetric Doppler Broadening Function $\chi(x,\theta)$ for ^{240}Pu 1.05 eV Resonance as a Function of Neutron Energy E_n and Temperature T. The Doppler broadening function $\chi(u,v)$ expressed by the imaginary part of complex w(z)-function, Eq.(40), is shown on the $E_n - T$ plane.

and thus the left-hand side of Eq. (41) is the same to $2\psi(x,\theta)+i\chi(x,\theta)$.

For wide resonance such as ^{239}Pu's resonance at 214.65 eV with the fission width $\Gamma_f = 11.17$ eV, numerical calculation of $w(\mathbf{z})$ function takes overflow because of large $\theta(=\frac{\Gamma}{\Delta})$. In this case, an asymptotic approximation for $w(\mathbf{z})$ function can be adopted, i.e.,

$$w(\mathbf{z}) = \frac{1}{\sqrt{\pi}} \cdot \frac{i}{\mathbf{z}} \qquad (\text{ for large } \Gamma). \tag{43}$$

This approximation gives the same result to so-called "Natural Line Width" based on "Low Temperature Model", since the large Γ is equivalent to the low temperature as expected from the θ definition Eqs. (32) with (33). As long as this approximation adopted, Doppler broadening functions as well as the broadened cross sections do not depend on the temperature as shown in **Fig. 28**.

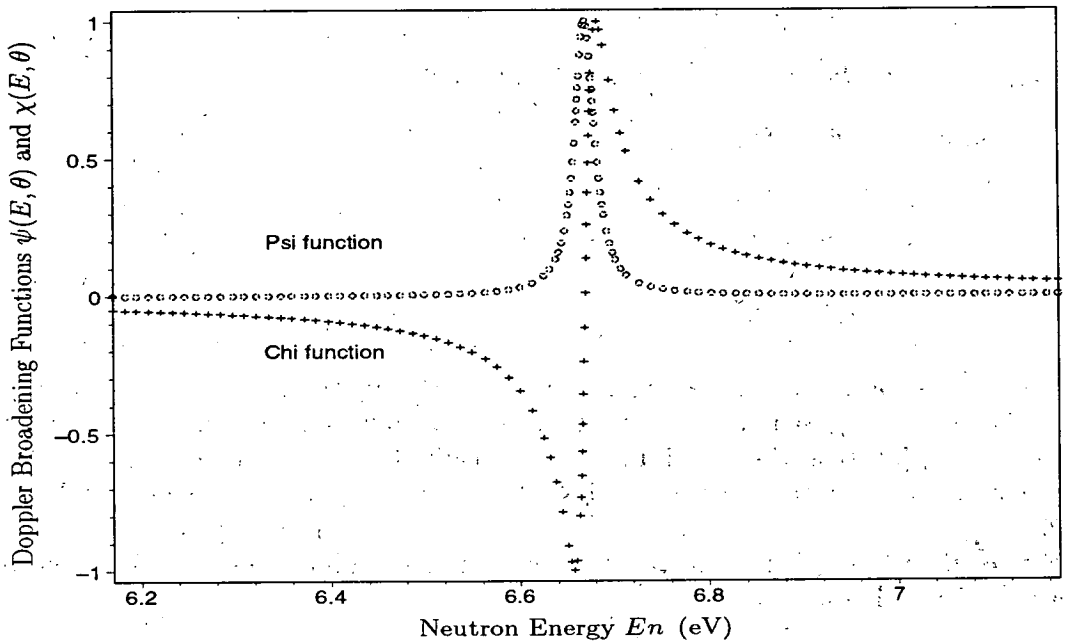

Figure 28: Asymptotic Doppler Broadening Functions $\psi(E,\theta)$ and $\chi(E,\theta)$ for ^{238}U 6.67 eV Resonance based on $w(z) \simeq \frac{1}{\sqrt{\pi}} \cdot \frac{i}{z}$. The asymptotic functions do not depend on the temperature variable T through the $\theta \propto \frac{1}{\sqrt{T}}$, so-called "Natural Line Width".

4.2.2 ψ and χ Functions based on Infinite Series Expansion

The complex w-function defined by Eq. (35) can be also separated into an exponential and *error*-function terms as;

$$\begin{aligned} w(\mathbf{z}) &= exp(-\mathbf{z}^2) \cdot [1 - erf(-i \cdot \mathbf{z})], & (44) \\ &= exp\Big\{-(u^2 - v^2)\Big\} \cdot [cos(2\,uv) - i \cdot sin(2\,uv)] \\ &\times \; [1 - erf\,\{-i \cdot (u + i \cdot v)\}], & (45) \end{aligned}$$

since

$$-\mathbf{z}^2 = -(u^2 - v^2) - i \cdot 2uv. \tag{46}$$

Therefore, the $w(\mathbf{z})$ function can be completely separated into real and imaginary parts if the error function erf can be separated. According to H. E. Salzer[10], the complex error function can be expanded into the infinite series as,

$$erf(u^\dagger + iv^\dagger) = E_{re} + i \cdot E_{im}, \tag{47}$$

$$E_{re} = erf(u^\dagger) + \frac{e^{-u^{\dagger 2}}}{\pi}\left[\frac{1-\cos(2\,u^\dagger v^\dagger)}{2u^\dagger} + 2\sum_{n=1}^{nmax}\frac{e^{\frac{1}{4}n^2}}{n^2+4\,u^{\dagger 2}}\cdot f_n(u^\dagger, v^\dagger)\right], \tag{48}$$

$$E_{im} = \frac{e^{-u^{\dagger 2}}}{\pi}\left[\frac{\sin(2\,u^\dagger v^\dagger)}{2u^\dagger} + 2\sum_{n=1}^{nmax}\frac{e^{\frac{1}{4}n^2}}{n^2+4\,u^{\dagger 2}}\cdot g_n(u^\dagger, v^\dagger)\right], \tag{49}$$

$$f_n(u^\dagger, v^\dagger) = 2u^\dagger - 2u^\dagger\cdot\cosh(nv^\dagger)\cos(2u^\dagger v^\dagger) + n\sinh(nv^\dagger)\sin(2u^\dagger v^\dagger), \tag{50}$$

$$g_n(u^\dagger, v^\dagger) = 2u^\dagger\cdot\cosh(nv^\dagger)\sin(2u^\dagger v^\dagger) + n\sinh(nv^\dagger)\cos(2u^\dagger v^\dagger), \tag{51}$$

where $u^\dagger$ and $v^\dagger$ are defined by

$$u^\dagger + i\cdot v^\dagger = -i\cdot(u + i\cdot v), \tag{52}$$

$$u^\dagger = v = \frac{1}{2}\theta, \qquad v^\dagger = -u = -\frac{1}{2}\theta x. \tag{53}$$

The truncation error ϵ of this series expansion is $\epsilon \simeq 10^{-16}|erf(u+iv)|$ for $nmax = \infty$. The numerical test in the present work results that $nmax$ is about 10 around $x = 0$, but for the wings of ψ and χ functions the magnitude of $nmax$ had to be extended up to about 40. Typical examples of ψ and χ functions based on this infinite series expansion are shown in **Figs. 29** and **30**.

Finally, the ψ and χ functions can be expressed in terms of real functional functions based on power series as shown below,

$$\psi(x,\theta) = \frac{\sqrt{\pi}}{2}\theta\, e^{-\{(\frac{\theta}{2})^2(x^2-1)\}}\left[cos\left(\frac{1}{2}\theta^2 x\right)\cdot\left\{1 - erf\left(\frac{\theta}{2}\right) - F_n(x,\theta)\right\} + sin\left(\frac{1}{2}\theta^2 x\right)\cdot G_n(x,\theta)\right], \tag{54}$$

$$\chi(x,\theta) = -\sqrt{\pi}\,\theta\, e^{-\{(\frac{\theta}{2})^2(x^2-1)\}}\left[sin\left(\frac{1}{2}\theta^2 x\right)\cdot\left\{1 - erf\left(\frac{\theta}{2}\right) - F_n(x,\theta)\right\} - cos\left(\frac{1}{2}\theta^2 x\right)\cdot G_n(x,\theta)\right], \tag{55}$$

where the power series $F_n(x,\theta)$ and $G_n(x,\theta)$ are expressed in terms of auxiliary functions $f_n(x,\theta)$ and $g_n(x,\theta)$ defined by Eqs. (50) and (51) as shown below,

$$F_n(x,\theta) = \frac{1}{\pi}\cdot e^{-(\frac{\theta}{2})^2}\left[\frac{1-cos\left(\frac{1}{2}\theta^2 x\right)}{\theta} + 2\sum_{n=1}^{nmax}\frac{e^{-\frac{1}{4}n^2}}{n^2+\theta^2}\cdot f_n(x,\theta)\right], \tag{56}$$

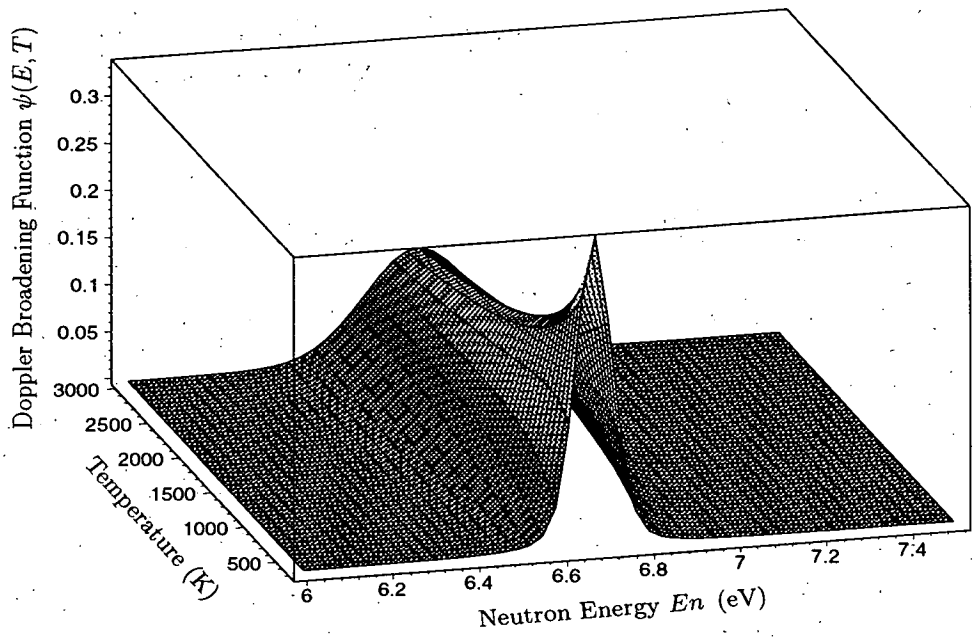

Figure 29: Symmetric Doppler Broadening Function $\phi(E,T)$ for ^{238}U 6.67 eV Resonance based on an Infinite Series Expansion as shown by Eq.(55).

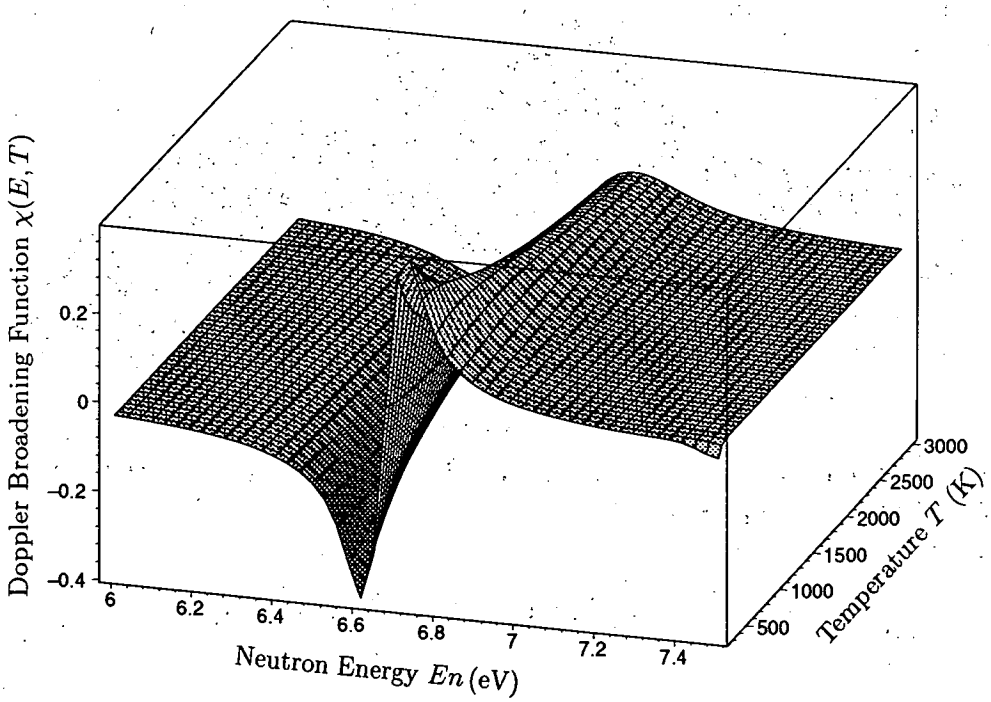

Figure 30: Asymmetric Doppler Broadening Function $\chi(E,T)$ for ^{238}U 6.67 eV Resonance based on an Infinite Series Expansion as shown by Eq.(55). In the low temperature region, the convergency is not good as shown in the slightly downward slope around (7.4 eV, 500 K).

$$G_n(x,\theta) = \frac{1}{\pi}\cdot e^{-\left(\frac{\theta}{2}\right)^2}\left[\frac{sin\left(\frac{1}{2}\theta^2 x\right)}{\theta} - 2\sum_{n=1}^{nmax}\frac{e^{-\frac{1}{4}n^2}}{n^2+\theta^2}\cdot g_n(x,\theta)\right], \quad (57)$$

with

$$f_n(x,\theta) = \theta - \theta\cdot\cosh\left\{\frac{n}{2}\cdot\theta x\right\}\cos\left\{\frac{1}{2}\cdot\theta^2 x\right\} + n\cdot\sinh\left\{\frac{n}{2}\cdot\theta x\right\}\sin\left\{\frac{1}{2}\cdot\theta^2 x\right\}, \quad (58)$$

$$g_n(x,\theta) = -\theta\cdot\cosh\left\{\frac{n}{2}\cdot\theta x\right\}\sin\left\{\frac{1}{2}\cdot\theta^2 x\right\} - n\cdot\sinh\left\{\frac{n}{2}\cdot\theta x\right\}\cos\left\{\frac{1}{2}\cdot\theta^2 x\right\}. \quad (59)$$

Predominant part of ψ is the $\theta \times exponential \times cos \times (1 - error\ function)$ terms while in χ is $\theta \times exponential \times sin \times (1 - error\ function)$ terms, respectively, and the F_n and G_n terms are minor correction terms as shown in **Figs. 32** for ψ and in **Figs. 34** for χ. At the high temperature limit whose θ-value is nearly equal to 0, $\psi(x,\theta)$ can be approximated by $F_{exp}(x,\theta)$

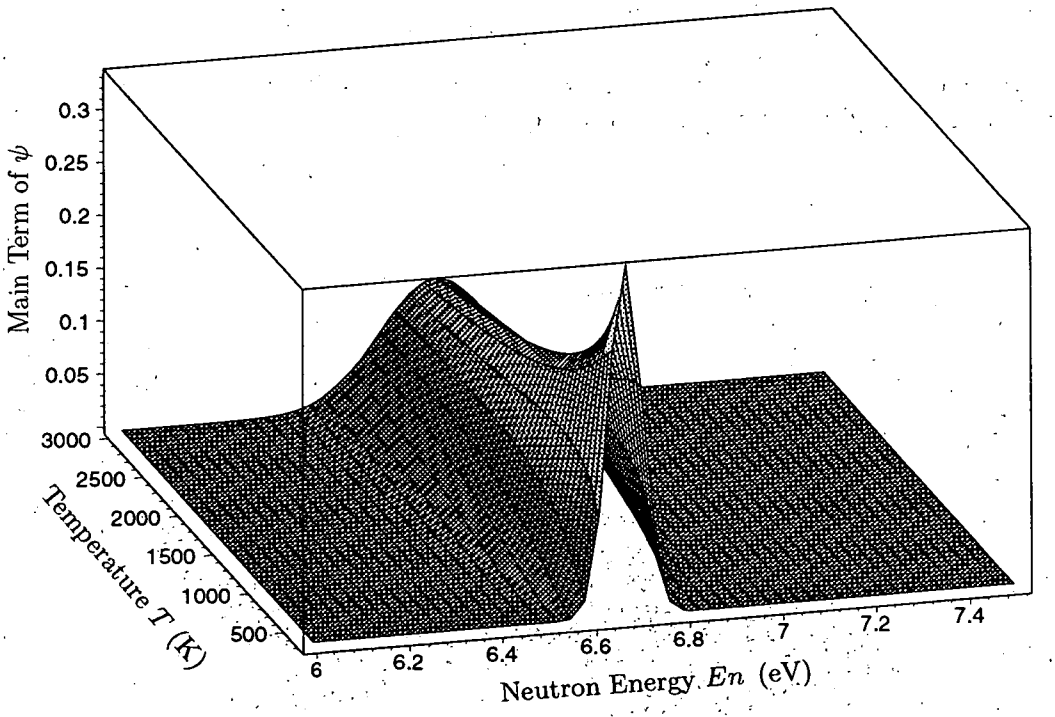

Figure 31: The Main Term of Eq. Eq.(55) without F_n of ψ Function for ^{238}U 6.67 eV Resonance : $\psi \simeq \frac{\sqrt{\pi}}{2}\theta e^{-\left\{\left(\frac{\theta}{2}\right)^2(x^2-1)\right\}} cos\left(\frac{1}{2}\theta^2 x\right)\cdot\left\{1 - erf\left(\frac{\theta}{2}\right)\right\}$

$$F_{exp}(x,\theta) = \frac{\sqrt{\pi}}{2}\theta\cdot e^{-\left(\frac{\theta}{2}\right)^2(x^2-1)}\cos\left\{\frac{1}{2}\theta^2 x\right\}\left\{1 - erf\left(\frac{\theta}{2}\right)\right\} \quad (60)$$

$$F_{exp}(0,\theta) = \frac{\sqrt{\pi}}{2}\theta\cdot e^{+\left(\frac{\theta}{2}\right)^2} erfc\left(\frac{\theta}{2}\right), (\text{at a resonance position, } x=0) \quad (61)$$

$$\simeq \frac{\sqrt{\pi}}{2}\theta\cdot e^{+\left(\frac{\theta}{2}\right)^2}, (\text{for small } \theta \text{ at a resonance position, } x=0) \quad (62)$$

which is the same form to the ψ-function derived from the original definition of ψ-function for the small θ value (high temperature) as shown in the Section 4.2.4(a).

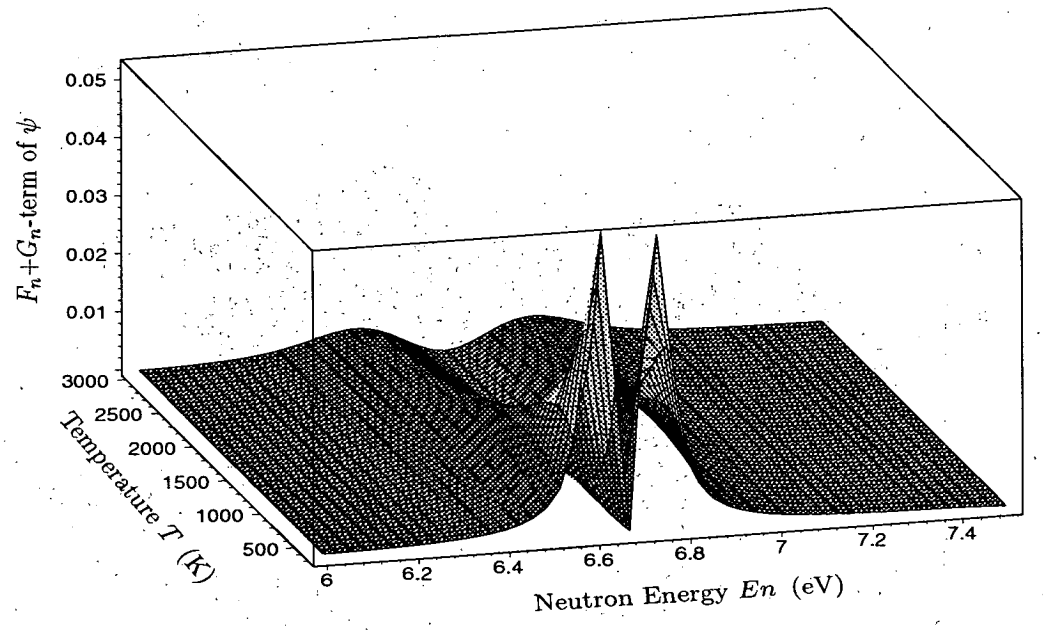

Figure 32: The F_n and G_n Terms without Error Function of ψ Function: $\psi \simeq \frac{\sqrt{\pi}}{2}\,\theta\, e^{-\left\{(\frac{\theta}{2})^2(x^2-1)\right\}}\left[cos\left(\frac{1}{2}\theta^2\, x\right)\cdot F_n + sin\left(\frac{1}{2}\theta^2\, x\right)\cdot G_n\right]$

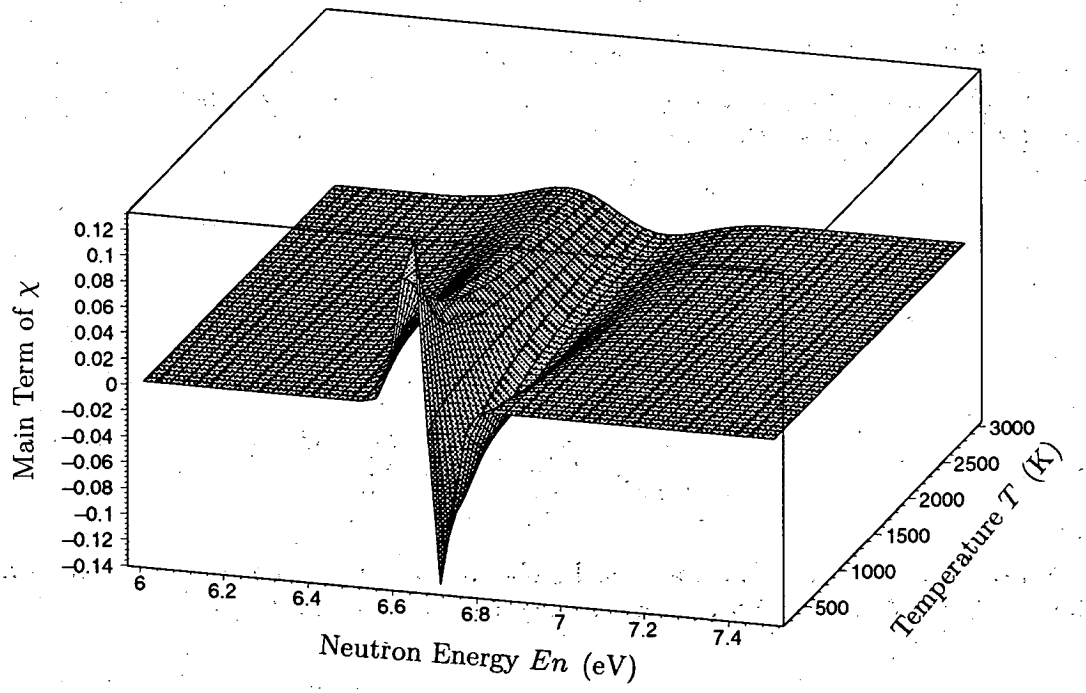

Figure 33: Main Term of χ Function: $\chi \simeq -\sqrt{\pi}\,\theta\, e^{-\left\{(\frac{\theta}{2})^2(x^2-1)\right\}} sin\left(\frac{1}{2}\theta^2\, x\right)\cdot\left\{1 - erf\left(\frac{\theta}{2}\right)\right\}$

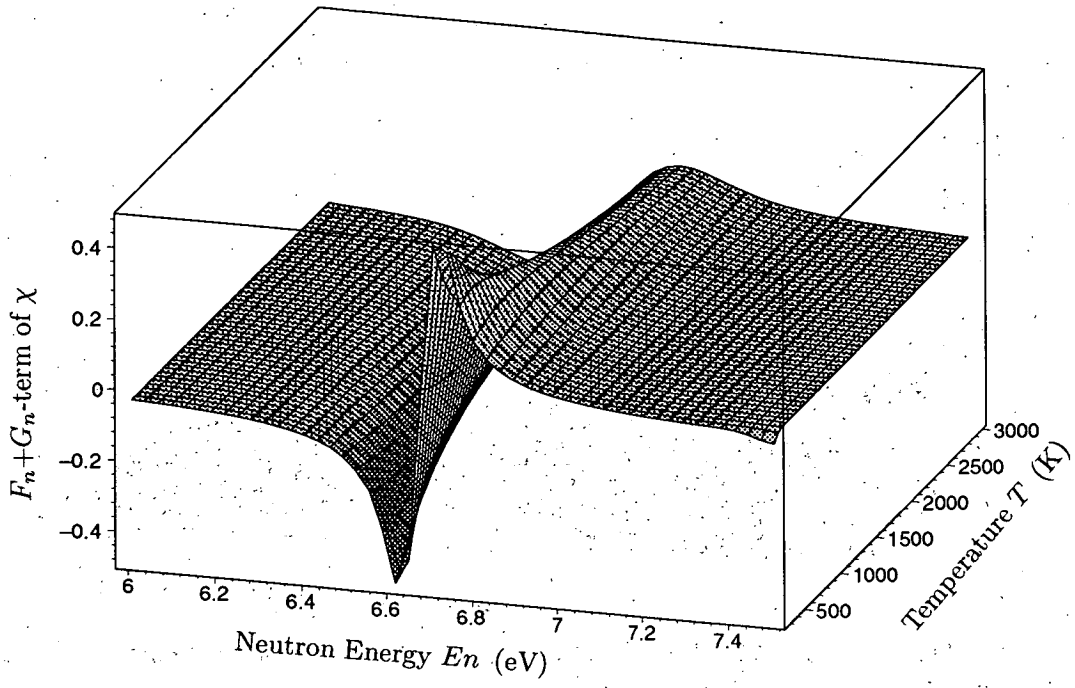

Figure 34: The F_n and G_n Terms without Error Function of χ Function: $\chi \simeq -\sqrt{\pi}\,\theta\, e^{-\{(\frac{\theta}{2})^2(x^2-1)\}}\left[sin\left(\frac{1}{2}\theta^2\, x\right)\cdot F_n + cos\left(\frac{1}{2}\theta^2\, x\right)\cdot G_n\right]$. In the low temperature region, the convergency is not good as shown in the slightly downward slope around (7.4 eV, 500 K).

4.2.3 ψ and χ Functions based on Hermite Polynomial

The $w(\mathbf{z})$ function introduced as Eq. (35) can be expressed by an infinite series expansion based on Hermite polynomials[11] as

$$w(\mathbf{z}) = \frac{i}{\pi}\cdot\int_{-\infty}^{+\infty}\frac{e^{-t^2}}{z-t}, dt \tag{63}$$

$$= \frac{1}{\pi}\lim_{n\to\infty}\sum_{n=1}^{n^*} H_k^{(n)}\frac{i}{z-x_k^{(n)}}, \tag{64}$$

$$= \frac{1}{\pi}\lim_{n\to\infty}\sum_{n=1}^{n} H_k^{(n)}\frac{v+i\cdot\left\{u-x_k^{(n)}\right\}}{\left\{u-x_k^{(n)}\right\}^2+v^2}. \tag{65}$$

Consequently, ψ and χ functions can be obtained as an infinite series in relative to the definitions Eqs. (37) and (38) based on the $w(\mathbf{z})$ function as shown below,

$$\psi(E,\theta) = \frac{1}{\sqrt{\pi}}\lim_{n\to\infty}\sum_{k=1}^{n} H_k^{(n)}\frac{\left(\frac{\theta}{2}\right)^2}{\left\{\left(\frac{\theta}{2}\right)\cdot x_{ir}-x_k^{(n)}\right\}^2+\left(\frac{\theta}{2}\right)^2}, \tag{66}$$

$$\chi(E,\theta) = \frac{2}{\sqrt{\pi}}\lim_{n\to\infty}\sum_{k=1}^{n} H_k^{(n)}\frac{\left(\frac{\theta}{2}\right)\cdot\left\{\left(\frac{\theta}{2}\right)\cdot x_{ir}-x_k^{(n)}\right\}}{\left\{\left(\frac{\theta}{2}\right)\cdot x_{ir}-x_k^{(n)}\right\}^2+\left(\frac{\theta}{2}\right)^2}, \tag{67}$$

where the k-th zero-point $x_k^{(n)}$ of n-th order of Hermit polynomial $H^n(x)$ and its weight $H_k^{(n)}$ are found in Table 25.10 of [11].

Convergences of ψ and χ functions are not so good for small θ-value at high temperature but for large θ-value at low temperature the convergences are significantly improved as shown in **Figs. 35** and **37**. Therefore, these expressions Eqs. (66) and (67) can be used an alternative expressions for the natural line width as discussed in the following 4.2.4(b), which are much milder functions of temperature as shown in **Figs. 36** and **38**.

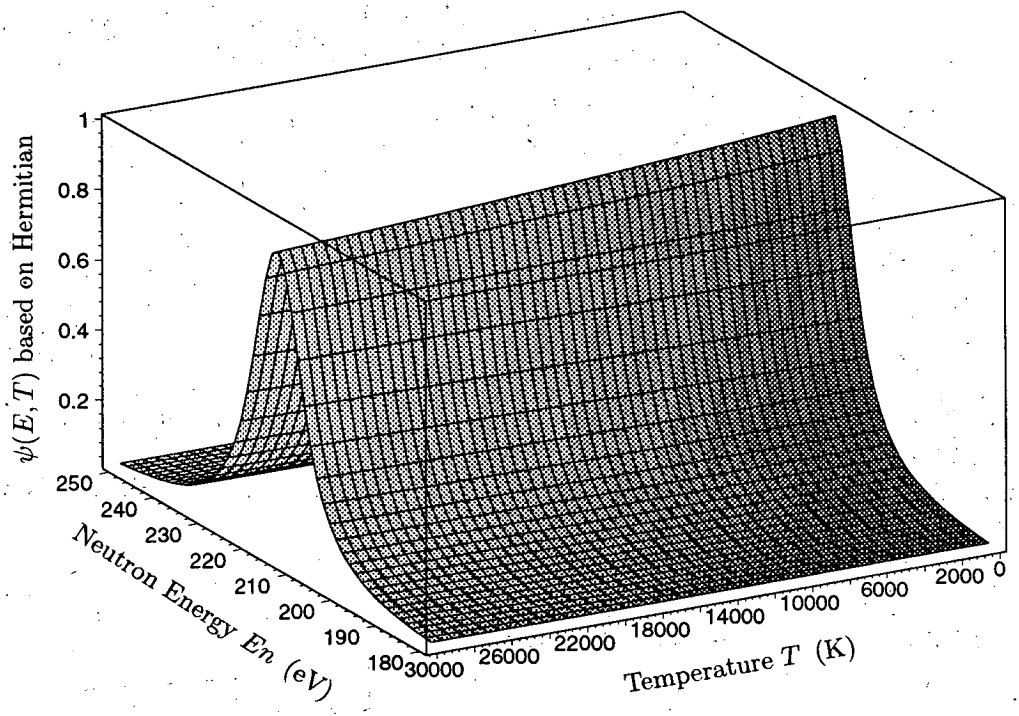

Figure 35: Symmetric Doppler Broadening Function $\psi(E,T)$ for ^{239}Pu 214.56 eV Resonance based on Hermite Expansion. The first order approximation ($k=1$) of Hermite polynomial Eq.(66) is used. The temperature dependence is shown by $\theta(T)$ while the "natural line width" approximation does not have the temperature dependence.

4.2.4 ψ and χ Functions for Special Cases

(a): High Temperature Approximation

The ψ and χ functions for the high temperature with $\lim_{T\to\infty}\theta(T)=0$ can be obtained as the limiting case of the Eqs. (54) and (55) as

$$\psi(x,\theta) = \frac{\sqrt{\pi}}{2}\theta\, e^{-\{(\frac{\theta}{2})^2(x^2-1)\}}\cdot erfc\left(\frac{\theta}{2}\right), \tag{68}$$

$$\simeq \frac{\sqrt{\pi}}{2}\theta\, e^{-\{(\frac{\theta}{2})^2(x^2-1)\}}, \tag{69}$$

$$\simeq \frac{\sqrt{\pi}}{2}\theta\, e^{-\{(\frac{\theta}{2}\cdot x)^2\}} \qquad \text{(because } \theta\simeq 0 \text{ and } exp\{(\theta/2)^2\}\simeq 1\text{)}, \tag{70}$$

$$\chi(x,\theta) \simeq 0.0, \tag{71}$$

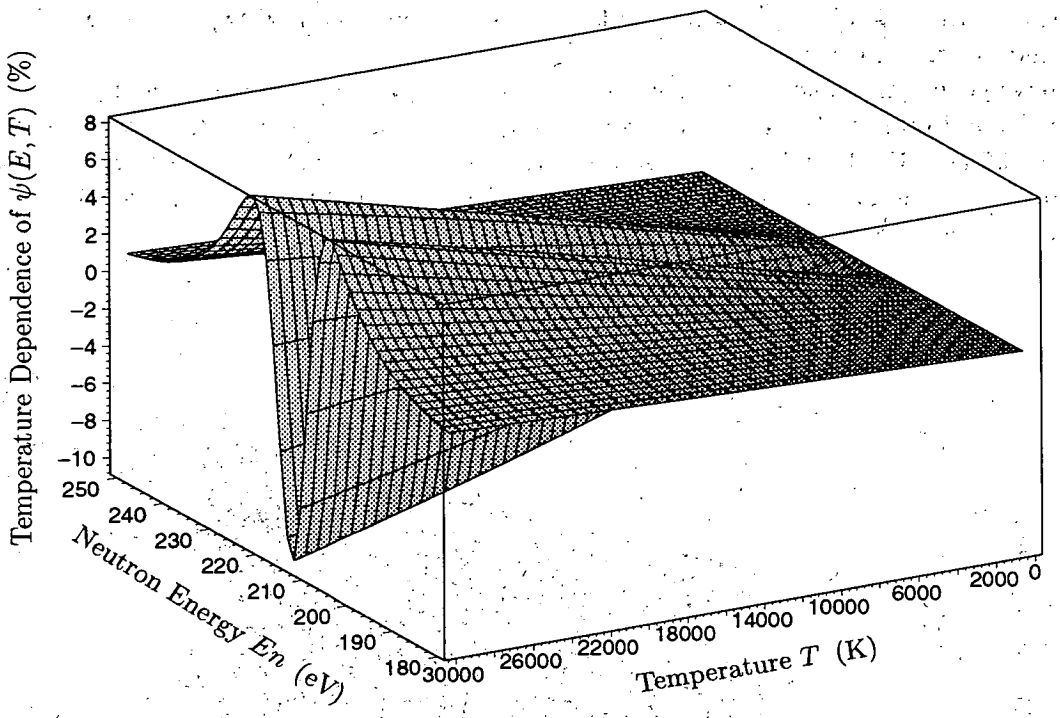

Figure 36: Temperature Dependence of Symmetric Doppler Broadening Function $\psi(E,T)$ for ^{239}Pu 214.56 eV Resonance based on Hermite Expansion. Relative deviation to the reference temperature 273 K is shown in percent. The first order approximation ($k = 1$) of Hermite polynomial Eq.(67) is also used.

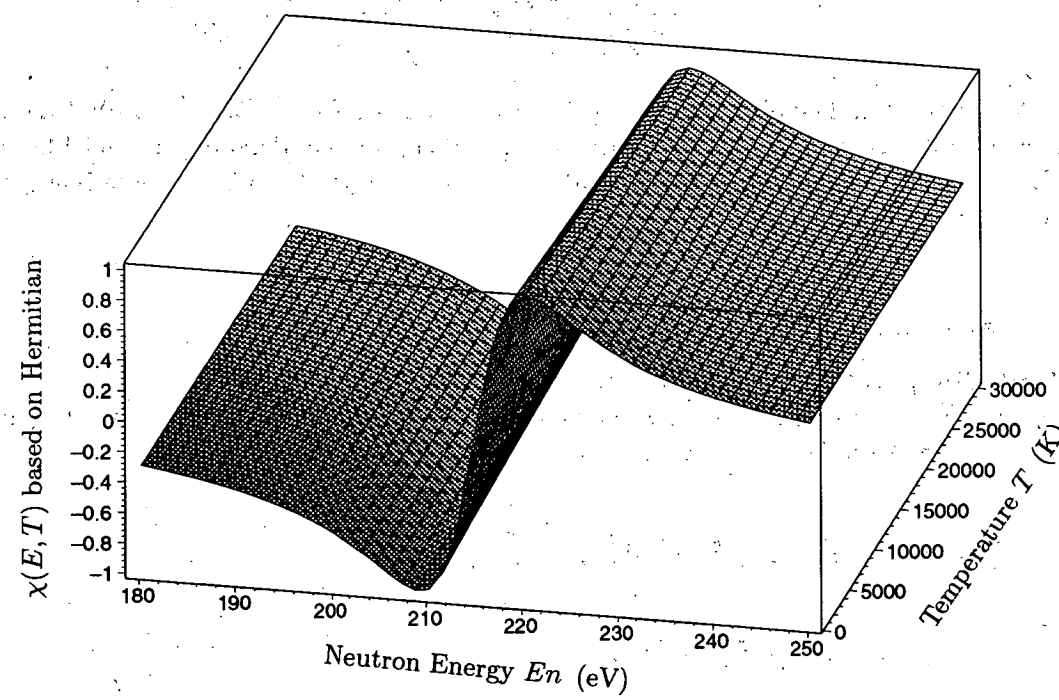

Figure 37: Asymmetric Doppler Broadening Function $\chi(E,T)$ for ^{239}Pu 214.56 eV Resonance based on Hermite Expansion.

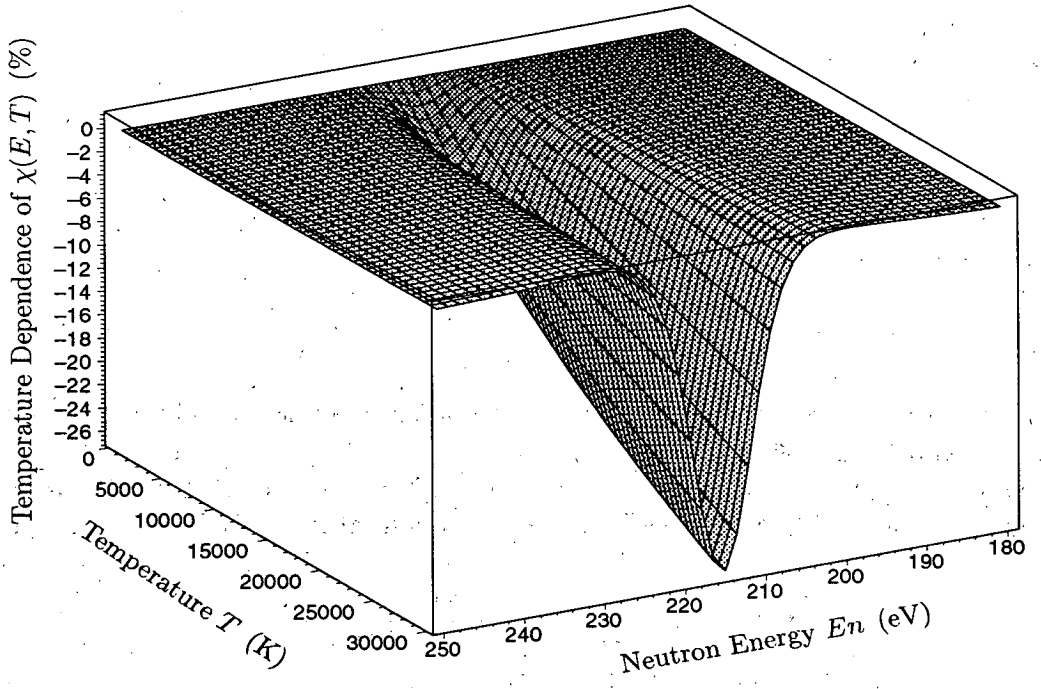

Figure 38: Temperature Dependence of Asymmetric Doppler Broadening Function $\chi(E,T)$ for ^{239}Pu 214.56 eV Resonance based on Hermite Expansion. Relative deviation to the reference temperature 273 K is shown in percent.

The temperature and energy dependencies of approximated function were shown in **Figs. 29** and **30**. The functional value of symmetric Doppler broadening function ψ tends to zero as temperature increasing towards infinity, while, the asymmetric function χ is automatically vanishing due to its inherent relation to ψ as,

$$\chi(x,\theta) = 2x \cdot \psi(x,\theta,) + \left(\frac{2}{\theta}\right)^2 \frac{\partial\psi}{\partial x}, \tag{72}$$

$$= 2 \cdot (x-x) \cdot \psi = 0. \tag{73}$$

Therefore, at present work, null-χ function is used so as to keep consistency between ψ and χ functions when the high temperature approximation is applied to the formulation of resonance self-shielding factor in Section 5.2.

(b): Low Temperature Approximation– Natural Line Width

Inversely, for an extremely low temperature, the argument of the exponential function of the ψ definition Eq. (27) becomes significantly large and the exponential function can be approximated by δ-function. Then, the ψ-function tends to a natural line shape as;

$$\psi(x,\theta) \simeq Rnorm \cdot \frac{\theta}{\sqrt{\pi}} \int_{-\infty}^{\infty} \frac{\delta(x-y)}{1+y^2} dy, \tag{74}$$

$$= Rnorm \cdot \frac{\theta}{\sqrt{\pi}} \frac{1}{1+x^2} \tag{75}$$

$$= \frac{1}{1+x^2}, \tag{76}$$

$$\chi(x,\theta) \simeq Rnorm \cdot \frac{\theta}{\sqrt{\pi}} \int_{-\infty}^{\infty} \frac{2y\delta(x-y)}{1+y^2} dy, \tag{77}$$

$$= Rnorm \cdot \frac{\theta}{\sqrt{\pi}} \frac{2x}{1+x^2}, \tag{78}$$

$$= \frac{2x}{1+x^2}, \tag{79}$$

where $Rnorm$ was introduced to satisfy the integration condition for ψ to be $\int \psi(x,\theta)dx = \pi$, and this condition results $Rnorm = \frac{\sqrt{\pi}}{\theta}$.

The same results can be obtained from the ψ and χ formula based on the Hermite polynomials Eqs. (66) and (67) by taking the first order of Hermite polynomials $n = 1$ for simplicity.

$$\psi(x,\theta) \simeq \frac{1}{\sqrt{\pi}} H_1^{(1)} \frac{1}{\left\{x - \frac{2}{\theta} \cdot x_1^{(1)}\right\}^2 + 1}, \tag{80}$$

$$\simeq \frac{1}{x^2+1} \quad \text{(for large } \theta\text{-value)}, \tag{81}$$

$$\chi(E,\theta) \simeq \frac{2x}{x^2+1} \quad \text{(for large } \theta\text{-value)}, \tag{82}$$

where the θ-value at low temperature was assumed to be significantly large and the second term in the $\{\ldots\}$ of denominator of Eq. (80) can be assumed to be 0, and it was used that the weight of the first order Hermit polynomials is $\sqrt{\pi}$. As previously remarked in "High Temperature Model" in the bottom of Section 4.2.4(a), "Low Temperature" is equivalent to the large (wide) resonance width.

In ordinary computer code such as MC^2-2[13], the ψ and χ functions are defined by Eqs. (37) and (38) using the "W-table" installed in the code. In the present work, however, in order to take precise temperature dependence and smoothly trends against the changes of resonance parameters, an analytical derivation of the sensitivity coefficient formula are preferred to the numerical approach. As shown in Section 5.2, final form of resonance self-shielding factor and its sensitivity coefficients are functions of ψ-value at the resonance position and then accurate ψ, and χ functional values based on the exact formula Eqs. (37) and (38) are needed.

(c): ψ and χ at a Resonance Position

For the present work, the resonance self-shielding factor in Section 5.2 is expressed by analytical function using only this $\psi(0,\sqrt{2}\theta)$-value as the resulted from analytical integrations of $\psi^m\chi^n$ (m,n:integers) terms. Therefore, only precise $\psi(0,\sqrt{2}\theta)$-values are requested as will be shown in Eqs. (120) to (128).

At a resonance energy, the functions $\psi(0,\theta)$ and $\chi(0,\theta)$ based on the high temperature approximations, Eqs. (68) and (71), become a simple analytical and null functions, respectively, as shown below,

$$\psi(0,\theta) = \frac{\sqrt{\pi}}{2} \cdot \theta \cdot exp\left\{\left(\frac{\theta}{2}\right)^2\right\} erfc\left\{\frac{\theta}{2}\right\}, \tag{83}$$

$$\chi(0,\theta) = 0.0. \tag{84}$$

While, the $\psi(E,\theta)$-function at an extremely high temperature ($\theta = \frac{\Gamma}{\Delta_{ik}} << 1$) can be expressed by an exponential function as shown by Eq. (70),

$$\psi(E,\theta) = \frac{\sqrt{\pi}}{2}\theta \cdot exp\left[-\left(\frac{\theta}{2}\right)^2\left\{\frac{2(E-E_r)}{\Gamma}\right\}^2\right], \tag{85}$$

$$\chi(E,\theta) = 0.0. \tag{86}$$

The "High Temperature Approximation" in the present work is used for small θ-value because of $\theta \propto \frac{\Gamma}{\sqrt{T}}$, which is equivalent to narrow resonance with small Γ-value.

As long as considering the limited cases with larger θ, the $\psi(0,\theta)$ function can be approximated by the following infinite series,

$$\psi_0^h(\zeta) = 1 + \sum_{n=1}^{\infty} \frac{(-1)^n \cdot 2^n \Gamma(n+\frac{1}{2})}{\sqrt{\pi} \cdot \theta^{2n}}. \tag{87}$$

As shown in **Fig. 39**, in the low temperature region (large θ) this model is consistent with the exact expression defined by the complex function but in the high temperature (small θ) region the sharply decreasing trend is found. That is, an extended use of this $\psi_0^h(\zeta)$ function to the higher temperature region is impossible. Finally, in present work, the numerical table based on the exact ψ_0 function defined by the complex $w(\mathbf{z})$-function is used for the resultant formula of sensitivity coefficient, since an exact temperature gradient of the f-factor is needed in order to estimate the Doppler sensitivity coefficients and so on.

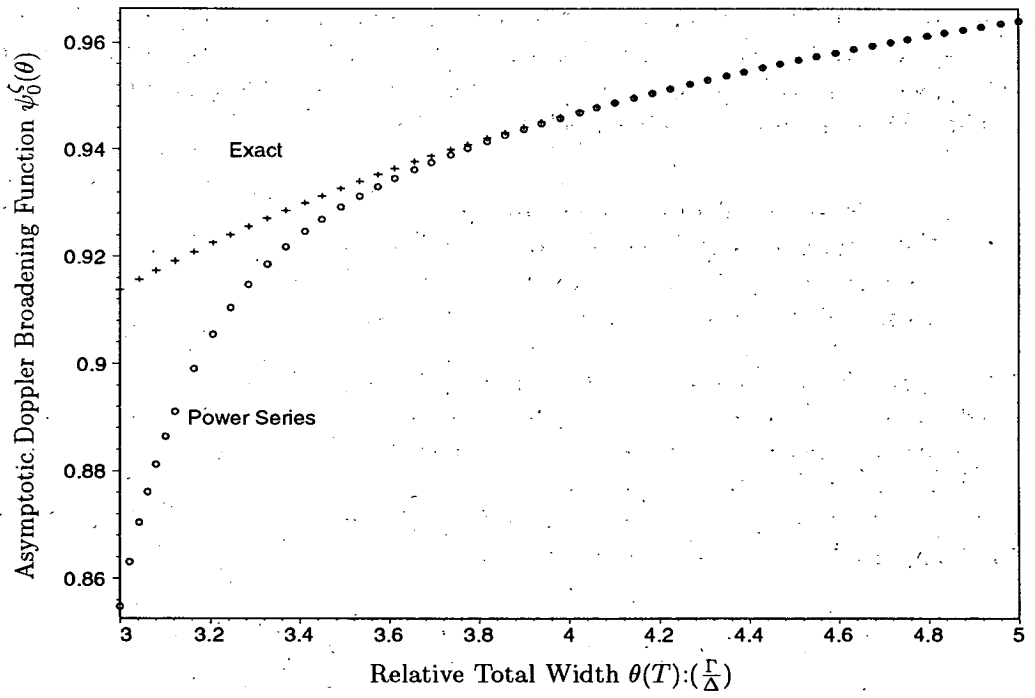

Figure 39: Asymptotic Doppler Broadening Function $\psi_0^\zeta\{\theta(T)\}$ at the resonance position based on the asymptotic expansion Eq. (87).

4.3 Resonance Integral and Resonance Self-Shielding Factor

The effective cross section Eq. (22) based on the narrow resonance (NR) approximation can be expressed in terms of the effective resonance integral J_{ik} and peak total cross section $\sigma_{0\,ik}$ as

$$\sigma_{eff\,xik} = \sigma_{0\,ik} \cdot \frac{\Gamma_{xik}}{\Delta u^k \cdot E_{ik}} \cdot \beta_{ik} J_{ik}(\beta, \zeta), \tag{88}$$

$$J_{ik} = \frac{1}{2} \cdot \int_{-\infty}^{+\infty} \frac{\psi_i}{\beta_{ik} + \psi_i + a_{pik} \cdot \chi_i + \sum_{j \neq i}^{I} (A_j \psi_j + B_j \chi_j)} dx, \tag{89}$$

$$\simeq \frac{1}{2} \cdot \int_{-\infty}^{+\infty} \frac{\psi_i}{\beta_{ik} + \psi_i + a_{pik} \cdot \chi_i} dx \quad \cdots \text{when interference megrected}, \tag{90}$$

$$\beta_{ik} = \frac{\sigma_{pi} + \sigma_{backi}}{\sigma_{0ik}}, \tag{91}$$

$$\sigma_{backi} = \frac{\sum_{j \neq i} N_j \sigma_{t,j}}{N^i}, \tag{92}$$

$$A_j = \frac{N_j \sigma_{0\,jk}}{N_i \sigma_{0\,ik}}, \tag{93}$$

$$B_j = a_{pjk} A_j, \tag{94}$$

where the summation with respect to suffix j in the denominator of integrand of Eq. (89) is over all resonant materials except a resonance of interest, and σ_{backi} is the potential scattering cross section per resonant absorber atom. It is assumed that the neutron energy E is close to the resonance energy E_{ik} because in the wing region far from the resonance position the Doppler broadening functions rapidly decrease and consequently minor contributions to the resonance integral. The other quantities are defined below,

$N_{i(j)}$	:	Atom density of $i(j)$-th isotope $(atom \cdot cm^{-3})$,
$\sigma_{0\,ki}$	:	Peak total cross section of i-th isotope and k-th resonance $(barn)$,
σ_{backi}	:	Potential scattering cross section per absorber atom $(barn)$,
σ_{pi}	:	Isotopic potential scattering cross section $(barn)$.

Usually, $\sigma_{back,i}$ is called as "σ_0" in Bondarenko type cross section set. In the present work the $\sigma_{0\,ik}$ is used for the peak total cross section and thus the $\sigma_{back,i}$ is for the potential scattering cross section per resonance absorber instead of ordinary "σ_0" to avoid confusion. As shown by Eq. (91), for infinitely diluted absorber the β-value tends to ∞ and then $\beta_{ik} \cdot J_{ik}$ of Eq. (90) becomes $\frac{\pi}{2}$, and consequently $\sigma_{eff\,xik}$ becomes $\frac{\pi}{2}\sigma_{0\,ki} \cdot \frac{\Gamma_{x\,ik}}{\Delta u^k E_{ik}}$. Therefore, total resonance integral I_x including $1/v$-term can be given by

$$I_x = 2g \cdot \sigma^{th} \cdot \sqrt{\frac{E_{th}}{E_c}} + \frac{\pi}{2} \cdot cnst \cdot \left[\frac{A_i + 1}{A_i}\right]^2 \sum_k \frac{\Gamma_{xik}}{E_{ik}} \cdot \frac{g\Gamma_{nik}}{\Gamma_{ik}} \tag{95}$$

where g is Westcott g factor, and E_{th} and E_c mean the thermal neutron energy and thermal cut-off energy, respectively, and σ^{th} is thermal cross sectin.

In this work, the J-function is approximated by Eq. (90) where interference effect is missed, since present work aims at the uncertainty evaluation by the sensitivity analysis defined by relative deviation of J-value where the interference effect is assumed to be the second order

correction term.

The resonance self-shielding factor $f(t,\sigma_0)$ can be defined by the ratio of the effective cross section of interest to that of infinitely diluted cross section, which is simply expressed by introducing H-function as shown below,

$$H_{xik}(T,\beta_{ik}) = \beta_{ik}J_{xik}(T,\beta_{ik}), \tag{96}$$

$$f_{xik}(T,\beta_{ik}) = \frac{2}{\pi}\cdot H_{xik}(T,\beta_{ik}), \tag{97}$$

where π came from the definite integration of the ψ function in the range from $[-\infty,+\infty]$ in case of infinitely diluted cross section and was introduced so that $f_{xik}(t,\beta_{ik})$ converges to unity as β-value tends to ∞.

By using the resonance self-shielding factor defined above, the resonance part defined in the Section 3 can be expressed in term of the total peak cross section σ_{0ik}^{Res} and resonance self-shielding factor f_{xi}^{k} as,

$$<\nu\Sigma_f\phi>^{Res}=\sum_i\sum_k\frac{\pi}{2}\cdot N_i^{Res}\phi_k\Delta V\cdot\nu_{ik}^{Res}\left(\frac{\sigma_{0ik}^{Res}}{E_{rik}}\right)\Gamma_{fik}^{Res}f_{xi}^{k}. \tag{98}$$

where N_i^{Res} and ΔV mean the atom density of resonant isotope denoted by i and volume element, respectively. While, for the non-resonant part, the multi-group reaction rates based on the effective cross sections are used;

$$<\nu\Sigma_f\phi>^{Non-Res}=\sum_i\sum_g N_i^{Non-Res}\phi_g\Delta u^g\Delta V\nu_{ig}^{Non-Res}\sigma_{fig}^{Non-Res}. \tag{99}$$

Consequently the total reaction rate including the non-resonance part can be expressed in terms of the peak total cross section, resonance width and f-factor as;

$$\begin{aligned}<\Sigma_f\phi>^{Tot} &= \sum_i\sum_g\Delta V\cdot\left\{\frac{\pi}{2}\sum_{k\in g}N_i^{Res}\phi_k\nu_{ik}^{Res}\left(\frac{\sigma_{0ik}^{Res}}{E_{rik}}\right)\Gamma_{fik}^{Res}f_{fi}^{k}\right.\\ &\qquad\left.+N_i^{Non-Res}\nu_{ig}^{Non-Res}\sigma_{fig}^{Non-Res}\phi^g\Delta u\ g\right\},\end{aligned} \tag{100}$$

$$\begin{aligned}<\Sigma_\gamma\phi>^{Tot} &= \sum_i\sum_g\Delta V\cdot\left\{\frac{\pi}{2}\sum_{k\in g}N_i^{Res}\phi_k\nu_{ik}^{Res}\left(\frac{\sigma_{0ik}^{Res}}{E_{rik}}\right)\Gamma_{\gamma ik}^{Res}f_{\gamma i}^{k}\right.\\ &\qquad\left.+N_i^{Non-Res}\phi_g\Delta u^g\nu_{ig}^{Non-Res}\sigma_{\gamma ig}^{Non-Res}\right\},\end{aligned} \tag{101}$$

where the non-resonance parts are assumed to be for infinitely dilution and estimated from a typical multi-group cross section set such as ABBN Cross Section Set.

5 Analytical Formula for Resonance Self-Shielding Factor

5.1 Power Series Expansion of Resonance Self-Shielding Function

The H-function defined by Eq. (96) is essentially the resonance integral function and is a functional function with respect to the Doppler broadening functions ψ and χ. Such a function

cannot be analytically integrated in general because these Doppler-broadening functions are transcendental functions. For a special case like extremely high or low temperature system, an analytical integration can be performed. However, actual reactor is not so in high or low temperature but in an intermediate temperature. Therefore, the ψ and χ functions have to be shown by an approximated expressions for analytical formulation. In order to obtain analytical expression of the resonance self-shielding factor and related sensitivity coefficients, the integrand of Eq. (90) has to be transformed to a series expansion in terms of ψ and χ functions.

Explicit form of H function is a functional function of ψ and χ functions as shown below,

$$H(\beta,\theta) = \frac{1}{2}\int_{-\infty}^{\infty}\frac{\beta\,\psi(x,\theta)}{\beta+\psi(x,\theta)+a_p\,\chi(x,\theta)}dx, \tag{102}$$

$$\simeq \frac{1}{2}\int_{-\infty}^{\infty}\frac{\beta\,\psi(x,\theta)}{\beta+\psi(x,\theta)}dx. \tag{103}$$

Possibility for the power series expansion of the fractional function $H(\psi,\chi)$ can be examined from the magnitude of the denominator of H-function. For simplicity, the integrand of H function is expressed by $Q(x,\beta,\theta)$ and its denominator by $D(x,\beta,\theta)$ as shown below,

$$Q(x,\beta,\theta) = \frac{\beta\,\psi(x,\theta)}{\beta+\psi(\theta;x)+a_p\,\chi(x,\theta)} = \frac{\beta\,\psi(x,\theta)}{D(x,\beta,\theta)}, \tag{104}$$

$$D(x,\beta,\theta) = \beta+\psi(x,\theta)+a_p\,\chi(x,\theta) \tag{105}$$

$$= (\beta+1)\cdot\left[1-\left\{\frac{1-[\psi(x,\theta)+a_p\,\chi(x,\theta)]}{\beta+1}\right\}\right]. \tag{106}$$

As expected from Eq. (104), the convergence criteria for the power series expansion of Q is the second term in [...] of Eq. (106) which is denoted by $E(x,\beta,\theta)$,

$$E(x,\beta,\theta) = \left\{\frac{1-[\psi(x,\theta)+a_p\,\chi(x,\theta)]}{\beta+1}\right\}. \tag{107}$$

The integrand function $Q(x,\beta,\theta)$ defined by Eq. (104) will be expanded in terms of the intermediate function $E(x,\beta,\theta)$. In prior to the expansion, the behavior of the $E(x,\beta,\theta,x)$ function in the practical ranges of variables β, θ and x is discussed to examine the convergence. As evident from the form of $E(x,\beta,\theta)$ the following relation exists for arbitrary positive β

$$E(x,\beta,\theta) = \frac{1-\psi(x,\theta)-a_p\chi(x,\theta)}{\beta+1} \le 1-\psi(x,\theta)-a_p\chi(x,\theta), \tag{108}$$

and the $E(x,\beta,\theta)$ has the following characteristics at special points of x for arbitrary positive β,

$$E(x,\beta,\theta) = \begin{cases} \frac{1}{\beta+1} & |x|\to\infty \qquad \text{(far from resonance position)}, \\ \frac{1-\psi(0,\theta)}{\beta+1} & \text{for } x=0 \qquad \text{(at resonance position)}. \end{cases}$$

As shown in **Fig. 40**, the magnitude of E-function is smaller than unity in the overall range of temperature T and neutron energy E even at the smaller β-value for $\sigma_{backi}=10$ barn which is nearly equal to the potential scattering cross section σ_{pi} of heavy (fuel) element. For an extremely large $\theta(\propto\frac{1}{\sqrt{t}})$, i.e., extremely low temperature, the $E(x,\beta,\theta)$-value along with the valley $x=0$ (at resonance position) tends to zero as indicated by natural line width for ψ

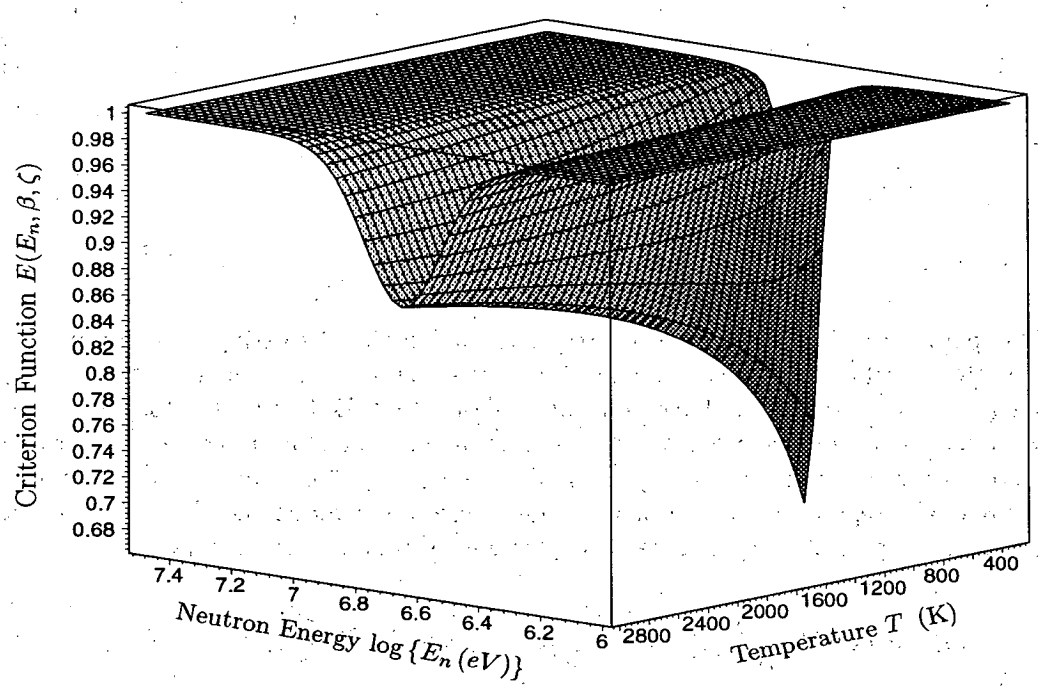

Figure 40: Criterion Function $E(E_n,\beta,\zeta)$ of Infinite Power Series Expansion of Functional Function $Q(\psi,\chi)$ for ^{238}U 6.67 eV Resonance. E_n means the neutron energy, and β and ζ are expressed in terms of neutron energy E_n and temperature T. The potential scattering cross section per resonant material is set to $\sigma_{backi} = 10$ barn.

function defined by Eq. (76);

$$\lim_{\theta\to\infty} E(0,\beta,\theta) = \frac{1-\lim_{\theta\to\infty}\{\psi(0,\theta)+a_p\chi(0,\theta)\}}{\beta+1} = \frac{1-\psi(0,\infty)}{\beta+1}$$

$$= \lim x \to 0\left[\frac{1}{\beta+1}\left\{1-\frac{1}{x^2+1}\right\}\right] \Longrightarrow \frac{1-1}{\beta+1} = 0 \qquad (109)$$

where the absolute temperature T is assumed to be 0. However, acceptable lower absolute temperature is restricted to 273 K of the room temperature. Considering the behavior around $x = 0$ in Fig. 40, the E-function at $\theta = 0(T \to \infty)$ is unity for overall x range. This special case cannot be expected physical point of view since $\theta = 0$ appears either at null resonance width $\Gamma_{ik} = 0$ or at an infinitely high temperature $(T \to \infty)$. Therefore, the E-function has a functional value less than unity and the series expansion is possible.

According to the above discussion, the integrand of H-function can be expanded to an infinite power series in terms of ψ and χ functions as shown below,

$$Q(x,\beta,\theta) = \frac{\beta}{\beta+1}\psi(x,\theta)\cdot\frac{1}{1-E(x,\beta,\theta)}, \qquad (110)$$

$$= \frac{\beta}{\beta+1}\psi(x,\theta)\cdot\sum_{n=0}^{\infty}\{E(x,\beta,\theta)\}^n, \qquad (111)$$

$$= \frac{\beta}{\beta+1}\sum_{n=0}^{\infty}\sum_{r=0}^{n}\sum_{s=0}^{n-r}(-1)^{n-r}\omega^n\binom{n}{r}\binom{n-r}{s}$$

$$\times {a_p}^{n-r-s} \cdot \psi^{s+1} \chi^{n-r-s} \tag{112}$$

with

$$\binom{n}{r} = {}_nC_r = \frac{n!}{(n-r)!r!}: \text{Binomial coefficients} \tag{113}$$

$$\omega = \frac{1}{\beta+1} \tag{114}$$

This power series can give an exact result for Q function by taking a higher order of n. However, the formula for analytical integration of the power series terms $\psi^i \cdot \chi^j$ $(i, j \geq 0)$ for an arbitrary i and j are not available. As will be shown from Eqs. (120) to (130), the terms at most $i+j \leq 3$ can be analytically integrated and dominant contributions come from these lower order terms since the ψ and χ function is smaller than unity. Therefore, in the present work, exact analytical integration is performed up to the third order terms and the remainder higher order terms are replaced by approximated expressions of ψ and χ functions, i.e.,

$$\begin{aligned} Q(x,\beta,\theta) &= \frac{\beta}{\beta+1}[(1+\omega+\omega^2)\psi - (\omega+2\omega^2)\psi^2 - (a_p\omega + 2a_p\omega^2)\psi\chi \\ &+ \omega^2\psi^3 + {a_p}^2\omega^2\psi\chi^2 + 2a_p\omega^2\psi^2\chi \\ &+ \sum_{n=3}^{\infty}\sum_{r=0}^{n}\sum_{s=0}^{n-r} f_{sum}^{n,r,s}(\psi,\chi)], \end{aligned} \tag{115}$$

where ω^n-terms in $\psi - \chi$ polynomials are truncated up to 3 and higher order terms of ω^n is included in power series. The power series expansion term $f_{sum}^{n,r,s}$ is defined as function of Doppler broadening functions ψ and χ as shown below,

$$f_{sum}^{n,r,s}(\psi,\chi) = (-1)^{n-r}\omega^n \binom{n}{r}\binom{n-r}{s} {a_p}^{n-r-s} \cdot \psi^{s+1}\chi^{n-r-s}. \tag{116}$$

An acceptable form for the higher order term in the series expansion can be set on the approximated high or low temperature model of Doppler broadening function as discussed in the case (a) or (b) of Section 4.2.4 depending on the temperature and/or total resonance width of interest. The lower temperature model in 4.2.4(b), namely "Natural Line Width", has no temperature dependence and thus temperature effects such as Doppler reactivity worth are missed. As shown in the high temperature model introduced in 4.2.4(a), the Doppler symmetric function ψ is non-vanishing function but the Doppler asymmetric function χ is automatically vanishing in the high temperature, and consequently the higher order terms in the power series expansion becomes as,

$$f_{sum}^{n,r} = (-1)^{n-r}\omega^n \binom{n}{r} \cdot \psi^{n-r+1}, \quad n \geq 3. \tag{117}$$

5.2 Resonance Self-Shielding Factor of Individual Resonance

The resonance self-shielding factor, namely "f-factor", for single level resonance can be obtained by integration of $Q(x,\beta,\theta)$ in the range [-∞, +∞] with respect to dimensionless energy x as,

$$f(\beta,\theta) = \frac{\beta}{\beta+1}\left[(1+\omega+\omega^2)\int_{-\infty}^{\infty}\psi(\theta;x)dx - (\omega+2\omega^2)\int_{-\infty}^{\infty}\psi(x,\theta)^2dx\right.$$

$$- (a_p\omega + 2a_p\omega^2)\int_{-\infty}^{\infty}\psi(x,\theta)\chi(x,\theta)dx + \omega^2\int_{-\infty}^{\infty}\psi(x;\theta)^3dx$$

$$+ {a_p}^2\omega^2\int_{-\infty}^{\infty}\psi(x,\theta)\chi(x,\theta)^2dx + 2a_p\omega^2\int_{-\infty}^{\infty}\psi(x,\theta)\chi(x,\theta)dx$$

$$+ \sum_{n=3}^{\infty}\sum_{r=0}^{n}\sum_{s=0}^{n-r} f_{sum}^{n,r,s}(x,\theta)\Bigg], \tag{118}$$

where the integrated power series expansion term $F_{sum}^{n,r,s}(\beta,\theta)$ is defined by

$$F_{sum}^{n,r,s}(\beta.\theta) = \int_{-\infty}^{\infty} f_{sum}^{n,r,s}(x,\beta,\theta)dx. \tag{119}$$

Analytical integration can be performed by introducing the approximated expressions of ψ and χ functions, i.e., the high temperature approximation Eq. (83) for narrow resonance width with small θ-value and the low temperature model Eqs. (76) and (79) for wide resonance width with large θ-value.

Integration of ψ and χ polynomials Eq. (116) with respect to dimensionless energy x can be analytically obtained from the following integration formula,

$$\int_{-\infty}^{\infty}\psi_{ik}dx_{ik} = \pi, \tag{120}$$

$$\int_{-\infty}^{\infty}\chi_{ik}dx_{ik} = 0, \tag{121}$$

$$\int_{-\infty}^{\infty}\psi_{ik}^2dx_{ik} = \frac{\pi}{2}\psi_{ik}(0,\sqrt{2}\theta_{ik}), \tag{122}$$

$$\int_{-\infty}^{\infty}\chi_{ik}^2dx_{ik} = 2\pi\psi_{ik}(0,\sqrt{2}\theta_{ik}), \tag{123}$$

$$\int_{-\infty}^{\infty}\psi_{ik}\chi_{il}dx_{ik} = \pi\frac{\Gamma_{il}}{\Gamma_{ik}+\Gamma_{il}}\chi_{ikl}, \tag{124}$$

$$\int_{-\infty}^{\infty}\psi_{ik}\psi_{il}dx_{ik} = \pi\frac{\Gamma_{il}}{\Gamma_{ik}+\Gamma_{il}}\psi_{ikl}, \tag{125}$$

$$\int_{-\infty}^{\infty}\psi_{ik}^2\psi_{il}dx_{ik} = \sqrt{\frac{\pi}{2}}\frac{\pi}{4}\theta_{ik}\frac{2\Gamma_{il}}{\Gamma_{ik}+\Gamma_{il}}(I_{1kl}+I_{2kl}), \tag{126}$$

$$\int_{-\infty}^{\infty}\chi_{ik}^2\psi_{il}dx_{ik} = \sqrt{\frac{\pi}{2}}\frac{\pi}{4}\theta_{ik}\frac{2\Gamma_{il}}{\Gamma_{ik}+\Gamma_{il}}(I_{1kl}-I_{2kl}), \tag{127}$$

$$\int_{-\infty}^{\infty}\chi_{ik}^{2n-1}\psi_{il}^m dx_{ik} = 0 \qquad (m,n >= 1,\ \text{m,n: integers}), \tag{128}$$

$$\psi_{ikl} = \psi_{ik}\left[2\frac{E_{0ik}-E_{0il}}{\Gamma_{ik}+\Gamma_{il}}, \frac{\Gamma_{ik}+\Gamma_{il}}{\sqrt{{\Delta_{ik}}^2+{\Delta_{il}}^2}},\right], \tag{129}$$

$$\chi_{ikl} = \chi_{ikl}\left[2\frac{E_{0ik}-E_{0il}}{\Gamma_{ik}+\Gamma_{il}}, \frac{\Gamma_{ik}+\Gamma_{il}}{\sqrt{{\Delta_{ik}}^2+{\Delta_{il}}^2}}\right]. \tag{130}$$

Doppler broadening function $\psi_{i\,kl}$ and $\chi_{i\,kl}$ are introduced by Hwang[14] for the resonance overlapping between the k- and l-th resonances. As the limiting case of $l \to k$, these functions tend to the ordinary Doppler broadening function introduced by Eqs. (27) and (28) where suffix kl is dropped for simplicity.

Besides, the following intermediate functions I_1 and I_2 are needed for Eqs. (126) and (127),

$$I_{1\,kl} = A_4 \left[A_5 \psi_{i\,kl} - A_7 \frac{\partial \chi_{i\,kl}}{\partial x_{kl}} - A_8 \frac{\partial^2 \chi_{i\,kl}}{\partial x_{kl}^2} + A_9 \frac{\partial^3 \chi_{i\,kl}}{\partial x_{kl}^3} \right], \tag{131}$$

$$I_{2\,kl} = \frac{2}{\sqrt{\pi}} A_3 \left[\frac{\partial \chi_{i\,kl}}{\partial x_{kl}} - \frac{2}{3} A_3^2 \frac{\partial^2 \chi_{i\,kl}}{\partial x_{kl}^2} \right]. \tag{132}$$

where[1] the coefficients A_i can be related to the rational function of $exp(t^2) \cdot erfc(t)$ as made in the MC^2-2 code of which formalism is basically used for present work. Its rational expression is

$$exp(t^2) \cdot erfc(t) \simeq \sum_{i=1}^{imax} \frac{a_i}{1+pt}, \tag{133}$$

which is based on the following expansion of error function;

$$erf(x) \simeq 1 - exp(-x^2) \cdot \sum_{i=1}^{imax} (a_i t^i) + \epsilon(x), \tag{134}$$

$$t = \frac{1}{1+px}, \tag{135}$$

and truncation error $|\epsilon(x)|$ is 2.5×10^{-5} for $imax = 3$ or 1.5×10^{-7} for $imax = 5$[15]. In

Table 1. Coefficients for the rational expression

$imax$	p	a_1	a_2	a_3	a_4	a_5
3	0.47047	0.3480242	-0.0958798	0.7478556		
5	0.3275911	0.254829592	-0.284496736	1.421413741	-1.453152027	1.061405429

present work the $imax = 3$ set of the coefficients is used.

As mentioned above, final expression of resonance properties such as resonance self-shielding factor can be described by the Doppler broadening function at a resonance energy, namely $\psi(0, \sqrt{2\theta})$, as expected from Eqs. (120) to (130). Therefore, only functional value at the resonance energy is used for the numerical analysis. The functional values of ψ is estimated from the numerical table prepared by MAPLE Release V[8] with the option "digits=18" based on the exact formula Eqs. (37) and (38). The highly accurate value by 18 digits is needed since the difference of the resonance self-shielding factors is essential for the sensitivity analysis of Doppler reactivity worth.

In the present work, an intermediate variable ζ is introduced as the result of the study on the power series expansion of the resonance self-shielding factor. The ζ variable is defined as

$$\zeta = \frac{1}{1 + \frac{p\theta(T)}{\sqrt{2}}}. \tag{136}$$

[1]The partial derivative inconsistencies found in the original formula used for MC^2-2 code are corrected.

For extremely high temperature the ζ tends to unity due to the vanishing of θ resulted from the extremity of the Doppler width Δ_{ik}-value and the θ-value vanishing. The θ and temperature T can be expressed by the ζ-variable as shown below;

$$\theta = \sqrt{2} \cdot \frac{(1-\zeta)}{p\zeta}, \tag{137}$$

$$T = \frac{A\,\Gamma^2}{2\,E_r\,\kappa_{Blz}} \cdot \left\{ \frac{p\zeta}{2(1-\zeta)} \right\}^2. \tag{138}$$

The consistency between newly introduced variable ζ and temperature T is shown in **Fig. 41** as a function of temperature. The linearity between the temperature T and temperature $T(\zeta)$ as a function of ζ is hold good in **Fig. 41**. It means that the auxiliary variable ζ defined by the relative resonance width θ to Doppler width can reveal the given temperature T.

The auxiliary functions $\zeta(\theta)$'s are shown in **Fig. 42** as functions of temperature for the

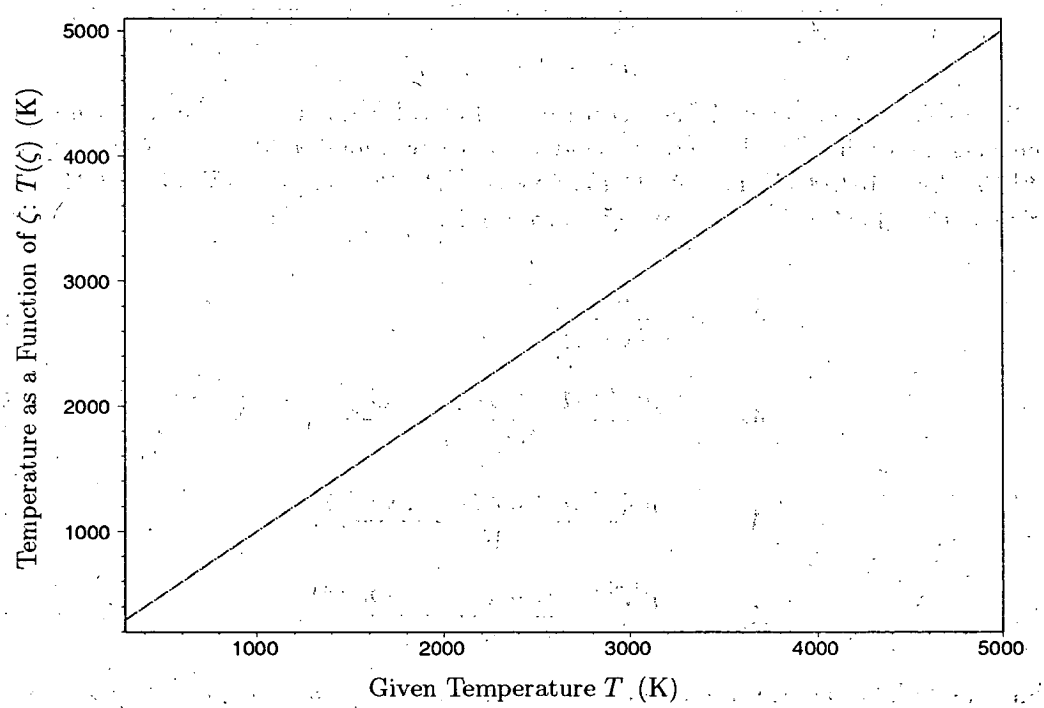

Figure 41: Temperature as Function of intermediate variable ζ defined by Eq. (138).

narrow resonance of ^{238}U with width $\Gamma_{ik} = 24.89$ meV at $Er = 6.67$ eV, the wide resonance of ^{239}Pu with $\Gamma_{ik} = 11.22$ eV at 214.65 eV and the first resonance of ^{240}Pu at 1.05 eV, respectively.

The coefficients A_i's introduced in Eqs. (131) and (132) for narrow resonances are shown as a function of the another coefficients a_i's for the rational approximation of $erf(x)$ as

$$A_3 = \frac{p\zeta}{4-4\zeta}, \tag{139}$$

$$A_4 = \zeta, \tag{140}$$

$$A_5 = a1 + a2\,\zeta + a3\,\zeta^2 \tag{141}$$

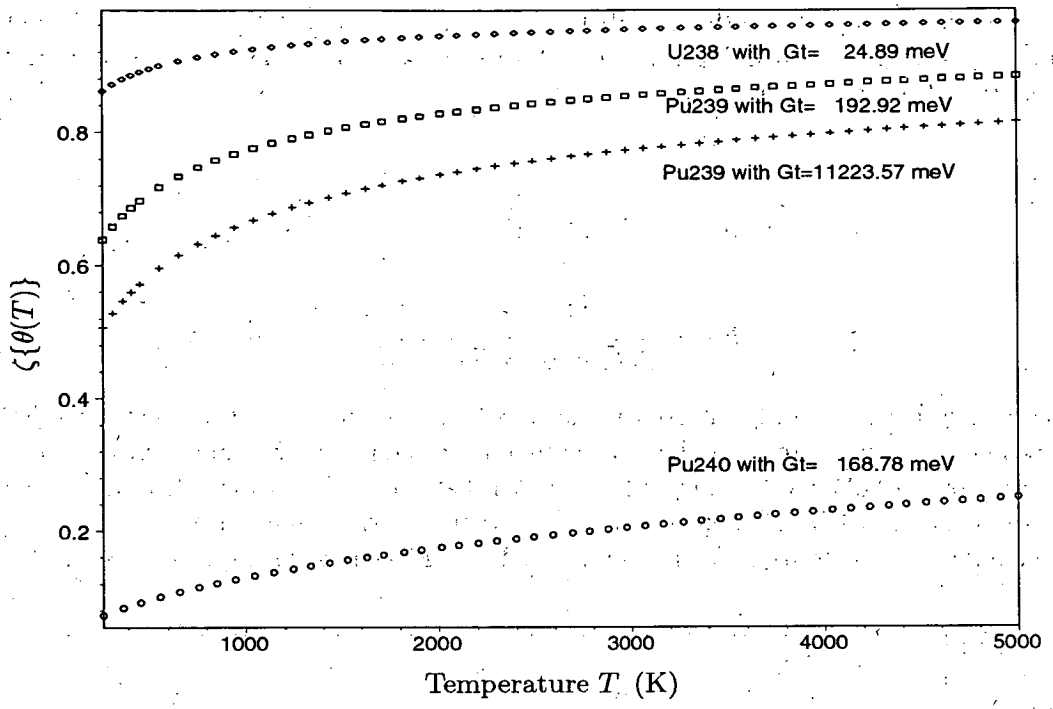

Figure 42: $\zeta(T)$'s as Functions of Temperature for Typical Resonances. The resonance data for four resonances are for the ^{238}U: Resonance energy $Er = 6.67$ eV, total width $\Gamma_t(i.e.,\ Gt) = 24.89$ meV, for the ^{239}Pu: $Er = 10.928$ eV, $\Gamma_t = 0.192$ eV, for the ^{239}Pu: $Er = 214.65$ eV, $\Gamma_t = 11.224$ eV, and for the ^{240}Pu: $Er = 1.057$ eV, $\Gamma_t = 0.1688$ eV, respectively.

$$A_6 = \frac{p^2\zeta}{4(1-\zeta)}, \tag{142}$$

$$A_7 = \frac{p^2\zeta^2\,(a1 + 2\,a2\,\zeta + 3\,a3\,\zeta^2)}{4(1-\zeta)}, \tag{143}$$

$$A_8 = \frac{p^4\zeta^4\,(a1 + 3\,a2\,\zeta + 6\,a3\,\zeta^4)}{16}, \tag{144}$$

$$A_9 = \frac{p^6\zeta^6\,(a1 + 4\,a2\,\zeta + 10\,a3\,\zeta^2)}{64}, \tag{145}$$

While, for wide resonances the A_i's are defined as an inverse of θ i.e. $(\theta^{-1} \propto \frac{p\zeta}{1-\zeta})$, as shown below,

$$A_3 = \frac{p\zeta}{4(1-\zeta)}, \tag{146}$$

$$A_4 = \frac{p\zeta}{\sqrt{\pi}\,(1-\zeta)}\left[1 - \frac{1}{2}\left\{1 - \frac{3\,p\zeta}{2(1-\zeta)}\right\}\left(\frac{p\zeta}{1-\zeta}\right)^2\right], \tag{147}$$

$$A_5 = 1, \tag{148}$$

$$A_6 = \frac{1}{4}\frac{p\zeta}{1-\zeta}, \tag{149}$$

$$A_7 = \frac{1}{4}\left(\frac{p\zeta}{1-\zeta}\right)^2, \tag{150}$$

$$A_8 = \frac{1}{16}\left(\frac{p\zeta}{1-\zeta}\right)^4, \tag{151}$$

$$A_9 = \frac{1}{64}\left(\frac{p\zeta}{1-\zeta}\right)^6. \tag{152}$$

By using these constants A's, the resonance self-shielding function $f(\beta,\zeta)$ can be shown as below,

$$\begin{aligned} f(\beta,\theta) &= \frac{\beta}{\beta+1}\left[(1+\omega+\omega^2)\pi-(\omega+2\omega^2)\frac{\pi}{2}\psi_0\right. \\ &+ \omega^2\sqrt{\frac{\pi}{2}}\frac{\pi}{4}\theta\cdot(I_1+I_2)+{a_p}^2\omega^2\sqrt{\frac{\pi}{2}}\frac{\pi}{4}\theta\cdot(I_1-I_2) \\ &+ \left.\sum_{n=3}^{\infty}\sum_{r=0}^{n}F_{sum}^{n,r}\right] \end{aligned} \tag{153}$$

$$\begin{aligned} &= \frac{\pi}{2}\frac{\beta}{\beta+1}\left[1+\omega+\{1-\frac{1}{4}\sqrt{\frac{\pi}{2}}\theta\cdot(I_c-I_{p2})-\sqrt{\frac{\pi}{2}}\theta\cdot(I_c+I_{p2})\,{a_p}^2\}\omega^2\right. \\ &- \frac{1}{2}\left\{\omega+2\omega^2-\frac{1}{2}\sqrt{\frac{\pi}{2}}\{(1+4{a_p}^2)I_{p1}-(1-4{a_p}^2)I_{p2}\}\theta\cdot\psi_0\right\} \\ &+ \left.\sum_{n=3}^{\infty}\sum_{r=0}^{n}F_{sum}^{n,r}\right], \end{aligned} \tag{154}$$

$$\psi(0,\theta) = \sqrt{\frac{\pi}{2}}\cdot\theta\cdot\exp\left(\frac{\theta^2}{2}\right)\cdot erfc\left(\frac{\theta}{\sqrt{2}}\right), \tag{155}$$

$$\psi_0 = \psi(0,\sqrt{2}\theta) = \sqrt{\pi}\cdot\theta\cdot\exp\left(\theta^2\right)\cdot erfc(\theta), \tag{156}$$

where ψ_0 means the ψ-value at the resonance energy $x=0$ and it is a function of only ζ-variable or temperature T, and the other intermediate functions such as $I_d(\zeta)$ are shown below. For instance, for the narrow resonance,

For Narrow Resonance

$$\begin{aligned} I_d(\zeta) &= \zeta(1-\zeta)^2\left\{\frac{a1+2\,a2\,\zeta+3\,a3\,\zeta^2}{4(1-\zeta)}\right. \\ &+ \left.\frac{p^2(1-\zeta)^2\zeta^2\,(a1+4\,a2\,\zeta+10\,a3\,\zeta^2)}{32}\right\}, \end{aligned} \tag{157}$$

$$I_{p1}(\zeta) = \zeta\left\{a1+a2\,\zeta+a3\,\zeta^2\right.$$

$$+ \frac{(1-\zeta)\,(a1+2\,a2\,\zeta+3\,a3\,\zeta^2)}{4}$$

$$+ \frac{p^2\,(1-\zeta)^2\,\zeta^2\,(a1+3\,a2\,\zeta+6\,a3\,\zeta^4)}{16}$$

$$+ \frac{3\,p^4\,(1-\zeta)^2\,\zeta^4\,(a1+4\,a2\,\zeta+10\,a3\,\zeta^2)}{128}\Bigg\}, \tag{158}$$

$$I_{p2}(\zeta) = \frac{1}{2\sqrt{\pi}} \cdot \frac{(1-\zeta)}{p\zeta}. \tag{159}$$

Although similar equations can be defined for wide resonance, these equations are missed here since they are temporally used to derive the final expression of the resonance self-shielding factor.

By substituting these auxiliary functions into Eq. (154), the final expression of the resonance self-shielding factor $f(\beta,\zeta)$ can be obtained as

$$f(\beta,\zeta) = \{1-\omega(\beta)\}\left[1+\omega(\beta)+\left(1-\frac{\sqrt{\pi}}{4}\frac{1-\zeta}{p\zeta}f_{z2}(\zeta)\right)\{\omega(\beta)\}^2\right.$$

$$\left.-\left\{\frac{1}{2}\omega(\beta)+\left(1-\frac{\sqrt{\pi}}{4}\frac{1-\zeta}{p\zeta}f_{z1}(\zeta)\right)\{\omega(\beta)\}^2\right\}\psi_0(\zeta)+F_{sum}(\beta)\right] \tag{160}$$

$$= \{1-\omega(\beta)\}\left\{1+\omega(\beta)-\frac{1}{2}\psi_0(\zeta)\omega(\beta)+\omega(\beta)^2\cdot g_z(\zeta)+F_{sum}(\beta)\right\}, \tag{161}$$

where

$$g_z(\zeta) = 1-\psi_0(\zeta)-\frac{\sqrt{\pi}}{4}\left(\frac{1-\zeta}{p\zeta}\right)\cdot\{f_{z2}(\zeta)-\psi_0(\zeta)\cdot f_{z1}(\zeta)\} \tag{162}$$

$$\psi_0(\zeta) = \sqrt{\pi}\cdot\left\{\frac{\sqrt{2}(1-\zeta)}{p\zeta}\right\}\cdot\exp\left[\left\{\frac{\sqrt{2}(1-\zeta)}{p\zeta}\right\}^2\right]\cdot erfc\left\{\frac{\sqrt{2}(1-\zeta)}{p\zeta}\right\}. \tag{163}$$

The intermediate functions $f_{z1}(\zeta)$ and $f_{z2}(\zeta)$ based on the I_{p1}, I_{p2} and I_c functions are defined for the narrow or wide resonance as shown below,

For Narrow Resonance

$$f_{z1}(\zeta) = \left(1+4.0a_p{}^2\right)\zeta\left\{a1+a2\,\zeta+a3\,\zeta^2\right.$$

$$+ \frac{(1-\zeta)\,(a1+2\,a2\,\zeta+3\,a3\,\zeta^2)}{4}$$

$$+ \frac{p^2\,(1-\zeta)^2\,\zeta^2\,(a1+3\,a2\,\zeta+6\,a3\,\zeta^4)}{16}$$

$$+ \left.\frac{3\,p^4\,(1-\zeta)^2\,\zeta^4\,(a1+4\,a2\,\zeta+10\,a3\,\zeta^2)}{128}\right\}$$

$$- \frac{1-4.0\,a_p^2}{2\sqrt{\pi}} \cdot \left(\frac{1-\zeta}{p\zeta}\right) \tag{164}$$

$$= (1+4.0\cdot a_p^2)\cdot\zeta\sum_{j=0}^{8} Cof^{(N)}(1,j)\cdot\zeta^j - \frac{1-4.0\cdot a_p^2}{2\sqrt{\pi}}\cdot\left(\frac{1-\zeta}{p\zeta}\right). \tag{165}$$

$$f_{z2}(\zeta) = \left(1+4.0{a_p}^2\right)(1-\zeta)^2\zeta\left\{\frac{a1+2\,a2\,\zeta+3\,a3\,\zeta^2}{4(1-\zeta)}\right.$$

$$\left. + \frac{p^2\zeta^2\left(a1+4\,a2\,\zeta+10\,a3\,\zeta^2\right)}{32}\right\} - \frac{1-4.0\,a_p^2}{2\sqrt{\pi}}\cdot\left(\frac{1-\zeta}{p\zeta}\right) \tag{166}$$

$$= (1+4.0\cdot a_p^2)\cdot\zeta\sum_{j=0}^{8} Cof^{(N)}(2,j)\cdot\zeta^j - \frac{1-4.0\cdot a_p^2}{2\sqrt{\pi}}\cdot\left(\frac{1-\zeta}{p\zeta}\right) \tag{167}$$

For Wide Resonance

$$f_{z1}(\zeta) = \frac{(1+4.0\,a_{pi}^2)}{\sqrt{\pi}}\frac{p\zeta}{1-\zeta}\left\{1-\frac{1}{2}\left(1-\frac{3}{2}\frac{p\zeta}{1-\zeta}\right)\left(\frac{p\zeta}{1-\zeta}\right)^2\right\}\left\{\frac{5}{4}+\frac{1}{16}\left(\frac{p\zeta}{1-\zeta}\right)^2\right.$$

$$\left. + \frac{3}{128}\cdot\left(\frac{p\zeta}{1-\zeta}\right)^4\right\} - \frac{1-4.0\,a_{pi}^2}{2\sqrt{\pi}}\cdot\left(\frac{1-\zeta}{p\zeta}\right) \tag{168}$$

$$= \frac{(1+4.0\cdot a_p^2)}{\sqrt{\pi}}\cdot\frac{p\zeta}{1-\zeta}\sum_{j=0}^{7} Cof^{(W)}(1,j)\cdot\left(\frac{p\zeta}{1-\zeta}\right)^j - \frac{1-4.0\cdot a_p^2}{2\sqrt{\pi}}\cdot\left(\frac{1-\zeta}{p\zeta}\right) \tag{169}$$

$$f_{z2}(\zeta) = \frac{(1+4.0\,a_{pi}^2)}{\sqrt{\pi}}\frac{p\zeta}{1-\zeta}\left\{1-\frac{1}{2}\left(1-\frac{3}{2}\frac{p\zeta}{1-\zeta}\right)\left(\frac{p\zeta}{1-\zeta}\right)^2\right\}\cdot\left\{\frac{1}{4}+\frac{1}{32}\left(\frac{p\zeta}{1-\zeta}\right)^4\right\}$$

$$- \frac{1-4.0\,a_{pi}^2}{2\sqrt{\pi}}\cdot\left(\frac{1-\zeta}{p\zeta}\right), \tag{170}$$

$$= \frac{(1+4.0\cdot a_p^2)}{\sqrt{\pi}}\cdot\frac{p\zeta}{1-\zeta}\sum_{j=0}^{5} Cof^{(W)}(2,j)\cdot\left(\frac{p\zeta}{1-\zeta}\right)^j - \frac{1-4.0\cdot a_p^2}{2\sqrt{\pi}}\cdot\left(\frac{1-\zeta}{p\zeta}\right) \tag{171}$$

with the coefficients $Cof^{(N,W)}$ given below

$$\omega(\beta) = \frac{1}{1+\beta} = \frac{1}{1+\frac{\sigma_{pi}+\sigma_{back\,i}}{\sigma_{0\,ik}}}. \tag{172}$$

The $\omega(\beta)$-value is vanishing when the β tends to ∞ indicating infinitely diluted mixture with $\sigma_{back\,i}=\infty$, while for dense mixture with $\frac{\sigma_{pi}+\sigma_{back\,i}}{\sigma_{0\,ik}} << 1$, i.e., $\sigma_{back\,i}\simeq 0$ the $\omega(\beta)$ becomes unity and then the f-factor proportional to $\{1-\omega(\beta)\}$ is vanishing.

The power series term $F_{sum}(\beta,\zeta)$ can be obtained by substituting the ψ-function based on high temperature approximation for narrow resonance or that based on low temperature approximation for wide resonance as shown below,

For High Temperature Approximation (Narrow Resonance)

Table 2. Coefficients for $f_{z1}(\zeta)$ and $f_{z2}(\zeta)$

Order j	Narrow Resonance		Wide Resonance	
	$Cof^{(N)}(1,j)$	$Cof^{(N)}(2,j)$	$Cof^{(W)}(1,j)$	$Cof^{(W)}(2,j)$
0	0.43503025	0.08700605	5/4	1/4
1	-0.23082575	-0.13494595	0	0
2	1.36150172	0.61123886	−9/16	−3/32
3	-0.57449992	-0.57317353	15/16	3/16
4	0.01317248	0.07678339	−1/128	−1/64
5	-0.00521879	-0.23246056	3/64	3/128
6	0.07194213	0.32339063	−3/256	0
7	-0.14176389	-0.20956762	9/512	0
8	0.07066175	0.05172871	0	0

$$F_{sum}(\beta,\zeta) = \sum_{n=3}^{N}\sum_{r=0}^{n} F_{sum}^{n,r}(\beta,\zeta), \tag{173}$$

where

$$F_{sum}^{n,r} = \{\omega(\beta)\}^n \frac{(-1)^{n-r}}{\sqrt{n-r+1}} \binom{n}{r} \left\{\sqrt{\frac{\pi}{2}}\left(\frac{1-\zeta}{p\zeta}\right)\right\}^{n-r}, \tag{174}$$

$$\binom{n}{r} = \frac{\Gamma(n+1)}{\Gamma(r+1)\,\Gamma(n-r+1)}. \tag{175}$$

Convergence of this power series $F_{sum}(\beta,\zeta)$ is shown in **Fig. 43** as a function of order nmax. Up to $nmax = 8$, the power series is conversed to about 90 % of $nmax = \infty$.

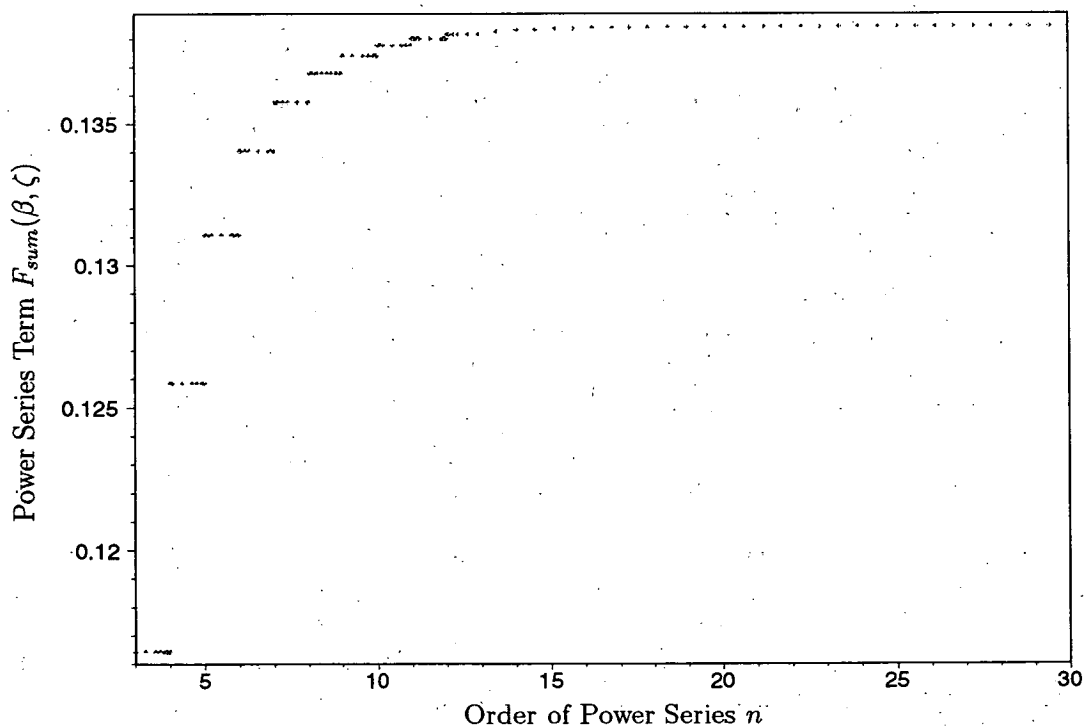

Figure 43: Converzence Criteria of the Power Series Term $F_{sum}(\beta,\zeta)$ of Eq. (173) as a function of the order $nmax$ at $\sigma_0 = 10^4$ barn and $T = 293$ k.

For Low Temperature Approximation (Wide Resonance)

$$F_{sum}^{n,r,s}(\beta) = (-1)^{n-r}\omega(\beta)^n \binom{n}{r}\binom{n-r}{s} \cdot a_{pi}^{n-r-s} 2^{n-r-s} \cdot \{1+(-1)^{n-r-s}\} \times \frac{1}{2} B\left(\frac{n-r-s+1}{2}, \frac{n-r+s+1}{2}\right), \quad (176)$$

where $B(x,y)$ is the Beta function.

The resonance self-shielding factor of the first resonance of ^{238}U existing at $E_r = 6.67$ eV is shown in **Fig. 44** as a function of the potential scattering cross section per resonant absorber σ_0 (barn), instead of $\sigma_{back\,i}$ for simplicity, and the temperature T (K). As a whole, the smooth trends are found since the present model neglects the interference terms between resonance of interest and those of the different resonant materials as evident from Eq. (90). The magnitude of the f-factor tends to unity as the potential scattering cross section σ_0 becomes infinity. In this ^{238}U case, around $\sigma_0 = 10^4$ (barn) the f-factor almost saturates. While, the f-factor tends to zero when σ_0 is getting small as expected from the definition of H-function giving the resonance self-shielding factor Eq. (97). For these extreme cases, the f-factors can be expressed by the following approximations.

For extremely large σ_0

$$f_{ik} = \frac{1}{\pi}\cdot\int_{-\infty}^{+\infty}\frac{\beta_{ik}\psi}{\beta_{ik}+\psi+a_{pik}\chi}dx = \frac{1}{\pi}\cdot\int_{-\infty}^{+\infty}\frac{\psi}{1+\frac{\psi+a_{pik}\chi}{\beta_{ik}}}dx$$

$$\simeq \frac{1}{\pi}\cdot\int_{-\infty}^{+\infty}\psi dx = 1. \quad (177)$$

For extremely small σ_0

$$f_{ik} = \frac{1}{\pi}\cdot\int_{-\infty}^{+\infty}\frac{\beta_{ik}\psi}{\beta_{ik}+\psi+a_{pik}\chi}dx \quad (178)$$

$$\simeq \frac{\beta_{ik}}{\pi}\cdot\int_{-\infty}^{+\infty}\frac{\psi}{\psi+a_{pik}\chi}dx$$

$$\propto \beta_{ik} \quad \to 0. \quad (179)$$

In order to examine such a special trend of the f-factor, the individual components of the f-factor are shown in **Fig. 45** for "Constant term", **Fig. 46** for "Non-ψ term", **Fig. 47** for "ψ-term" and **Fig. 48** for "Power Series Term" which are defined by

$$Constant-Term = 1-\omega(\beta),$$

$$Non-\psi-Term = \{1-\omega(\beta)\}\left[\omega(\beta,\zeta)+\left(1-\frac{\sqrt{\pi}}{4}\frac{1-\zeta}{p\zeta}f_{z2}(\zeta)\right)\{\omega(\beta)\}^2\right],$$

$$\psi\,Term = -\{1-\omega(\beta)\}\left[\left\{\frac{1}{2}\omega(\beta)+\left(1-\frac{\sqrt{\pi}}{4}\frac{1-\zeta}{p\zeta}f_{z1}(\zeta)\right)\{\omega(\beta)\}^2\right\}\psi_0(\zeta)\right],$$

$$Power\,Series\,Term = \{1-\omega(\beta)\}\left[F_{sum}(\beta)\right],$$

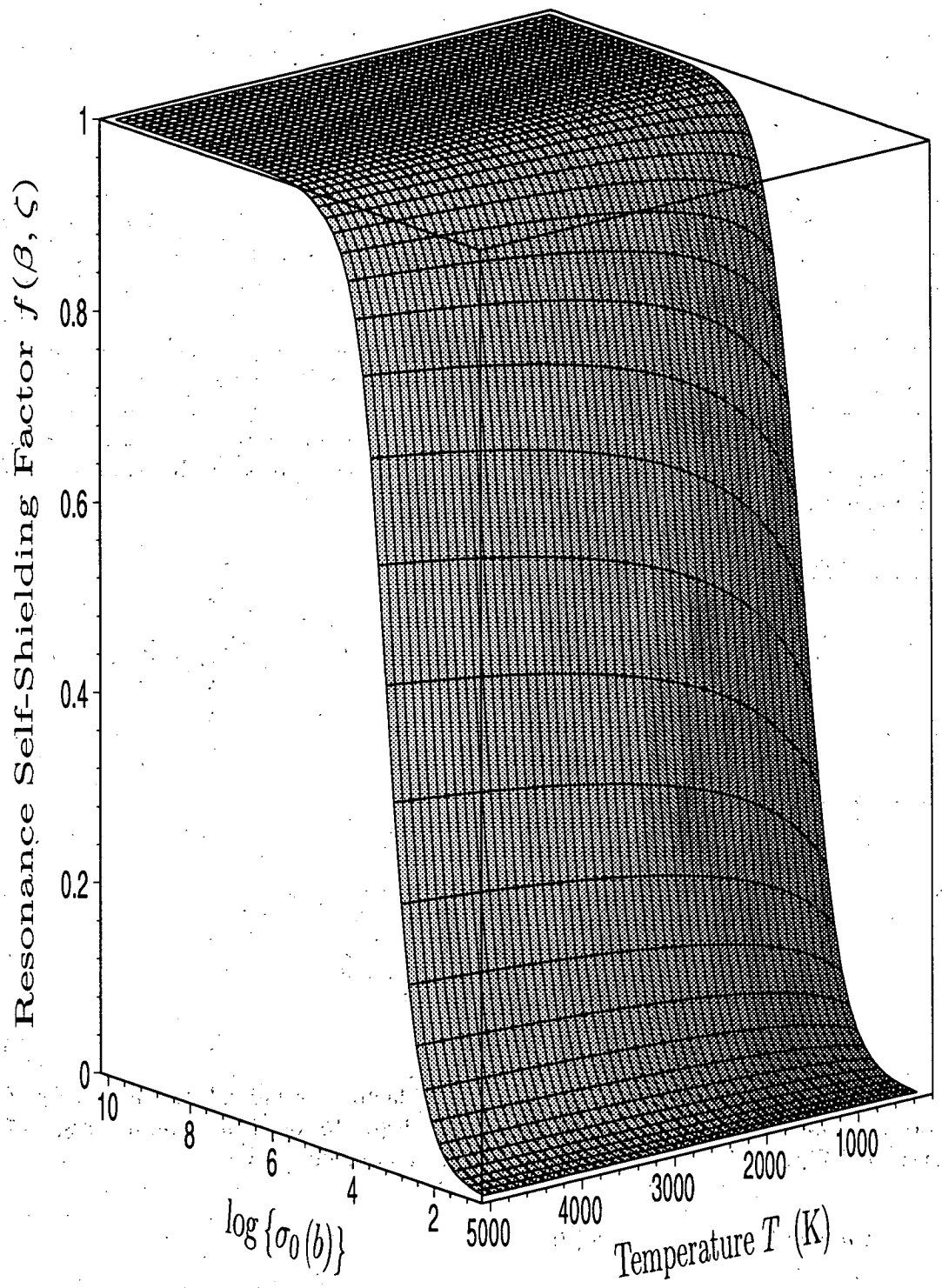

Figure 44: Resonance Self-Shielding Factor $f(\sigma_0, T)$ for ^{238}U 6.67 eV Resonance as an Example of Narrow Resonance.

then,

$$f(\beta,\zeta) = (Constant) + (Non\,\psi) + (\psi) + (Power\,Series). \tag{180}$$

The σ_0-dependence of f-factor is mainly expressed by the constant term and $Non-\psi-Term$, while temperature dependence is characterized by $\psi-Term$ in low temperature and by *Power Series Term* in high temperature which chancel one another.

The f_{z2}-terms with the coefficient function $\sqrt{\pi}(1-\zeta)/(4\cdot p\zeta)$ is a monotonously decreasing function like $1/\sqrt{T}$ as shown in **Fig. 49**, but the $f_{z1}(\zeta)$ term is monotonously increasing function whose magnitude is much smaller than F_{z2}'s. At least, the F_{z1}-term can be omitted for f-factor. Therefore, the resonance self-shielding factor can be approximately expressed as shown below,,

$$f^{App}(\beta,\zeta) = \{1-\omega(\beta)\}\left[1+\omega(\beta)+\{\omega(\beta)\}^2-\frac{1}{2}\left\{\omega(\beta)+2\,\{\omega(\beta)\}^2\right\}\psi_0(\zeta)\right] \tag{181}$$

where the F_{z2}-term was also missed because it is much smaller than unity. This simplified expression makes an important role for the wide resonance such as ^{239}Pu at $E_r = 214.56$ eV. The simplified formula can be obtained by setting $f_{z1} = f_{z2} = 0$ in Eq. (160). The relative error of this approximation is shown in **Fig. 50** as $\frac{f(Eq.181)-f(Eq.160)}{f(Eq.160)}$ in percentage where two resonance self-shielding factors (exact and approximated ones) are shown in the upper half of the figure.

As an example of the wide resonance, the resonance self-shielding factor (f-factor) of the ^{239}Pu resonance at the resonance energy $E_r = 214.65$ eV with $g\Gamma_n = 9.57$ meV, $\Gamma_\gamma = 42.00$ meV and $\Gamma_f = 11.17$ eV is shown in **Fig. 51** as function of the potential scattering cross section and temperature. The magnitude of the f-factor is localized in a limited range from 0.9 to 1.0, so-called "Frozen to the 1.0 Ceiling", and the temperature dependency is extremely small.

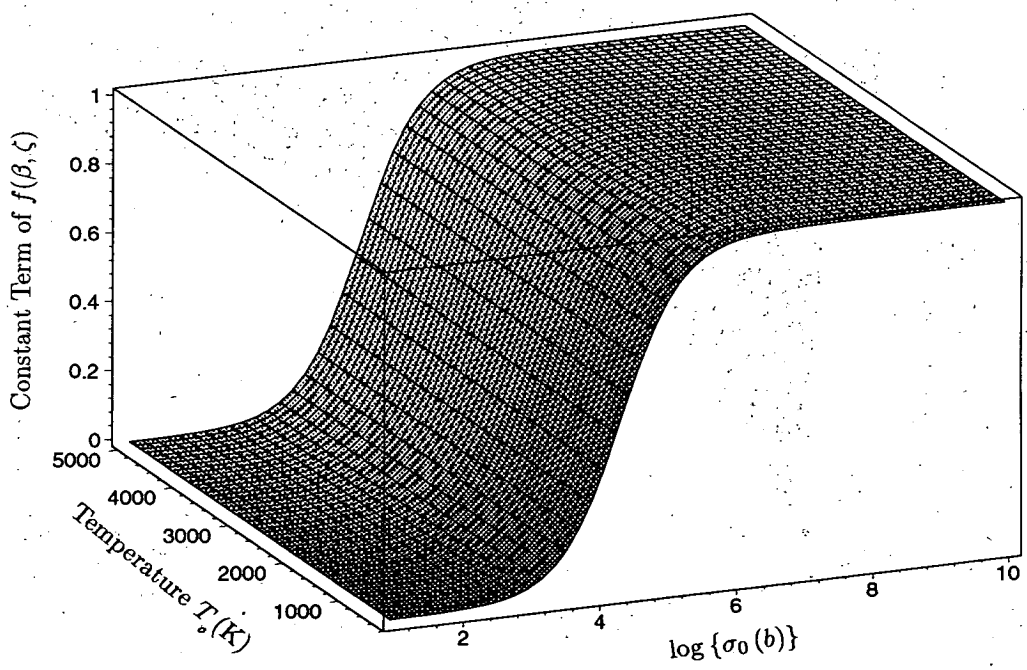

Figure 45: Constant - Term of Resonance Self-Shielding Factor Eq. (180) for ^{238}U 6.67 eV Resonance.

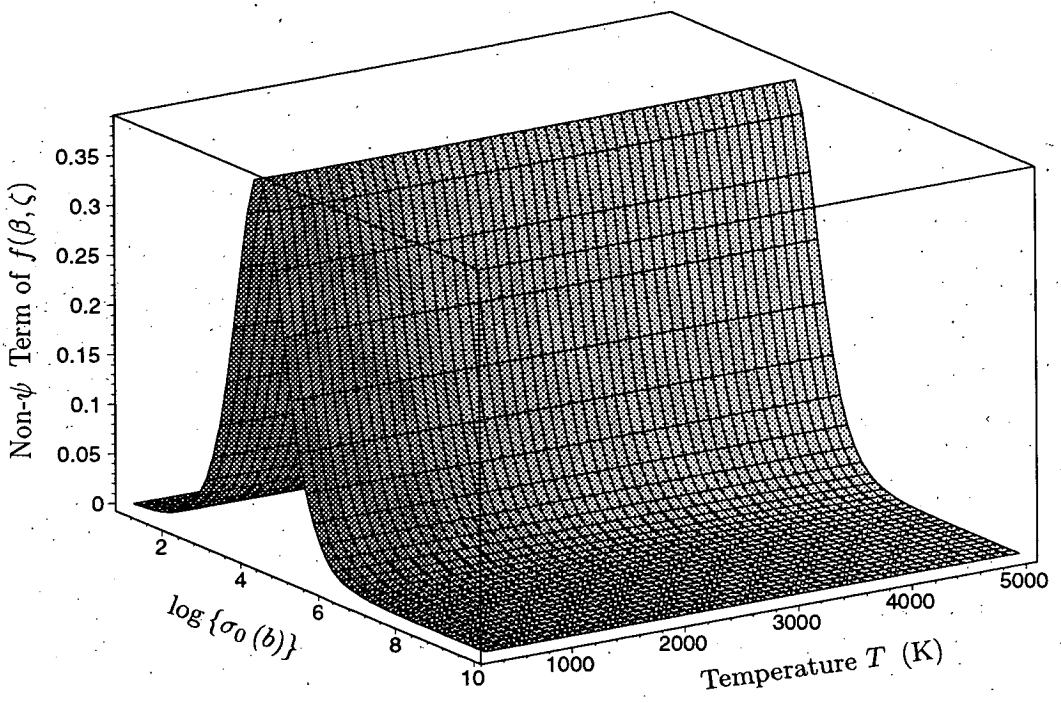

Figure 46: Non-ψ Term of Resonance Self-Shielding Factor Eq. (180) for ^{238}U 6.67 eV Resonance.

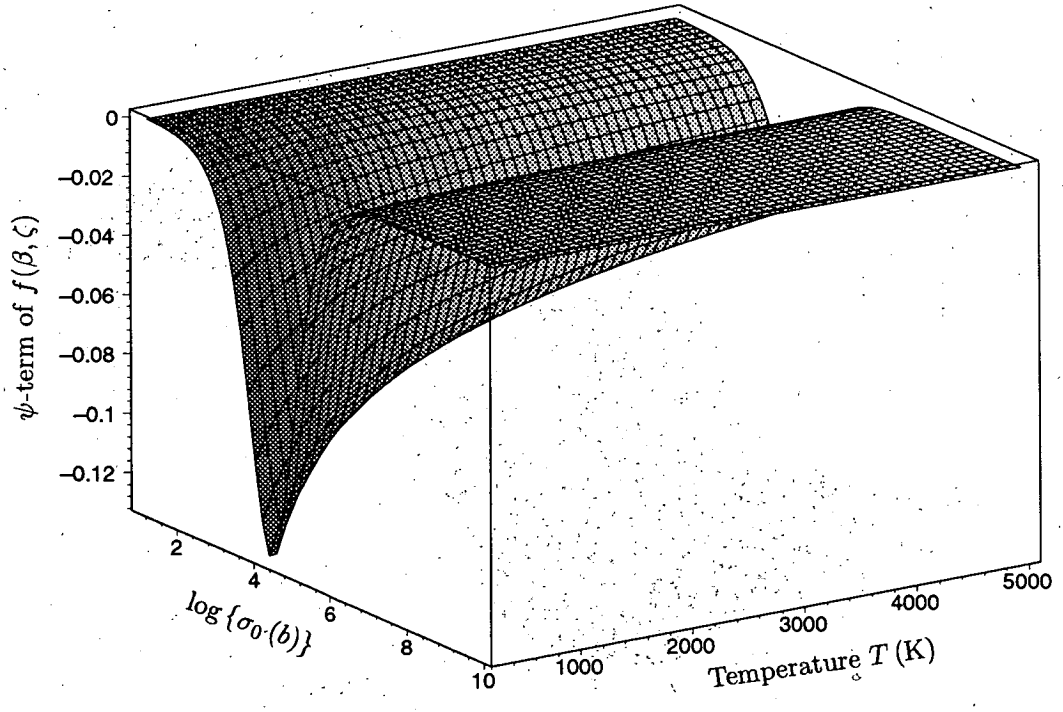

Figure 47: ψ Term of Resonance Self-Shielding Factor Eq. (180) for ^{238}U 6.67 eV Resonance.

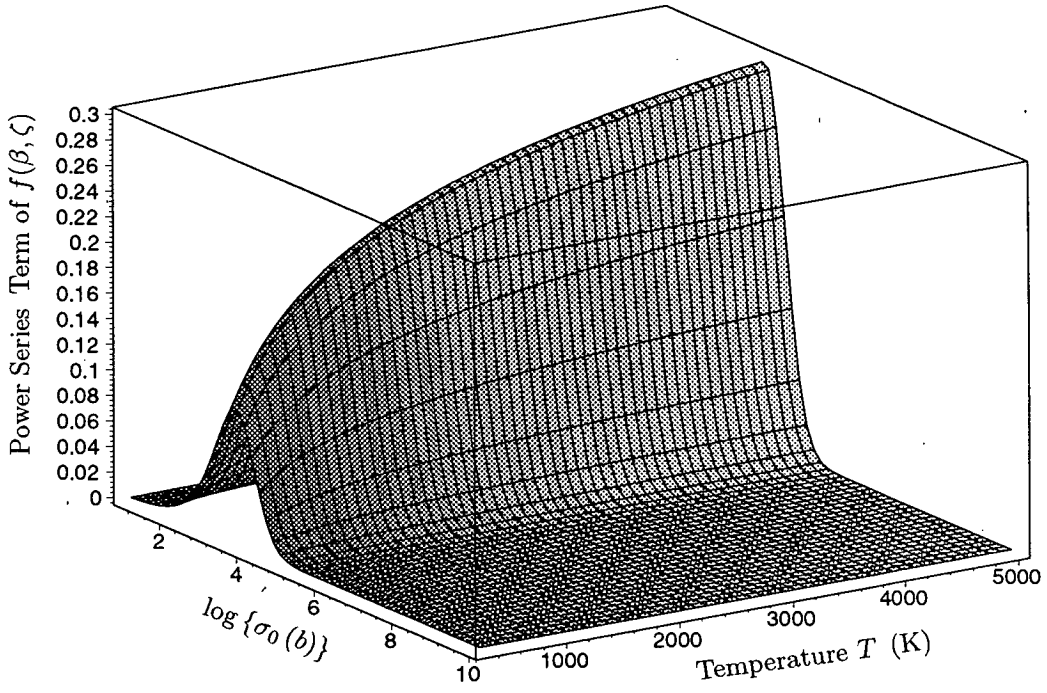

Figure 48: Power-Series Term of Resonance Self-Shielding Factor Eq. (180) for ^{238}U 6.67 eV Resonance.

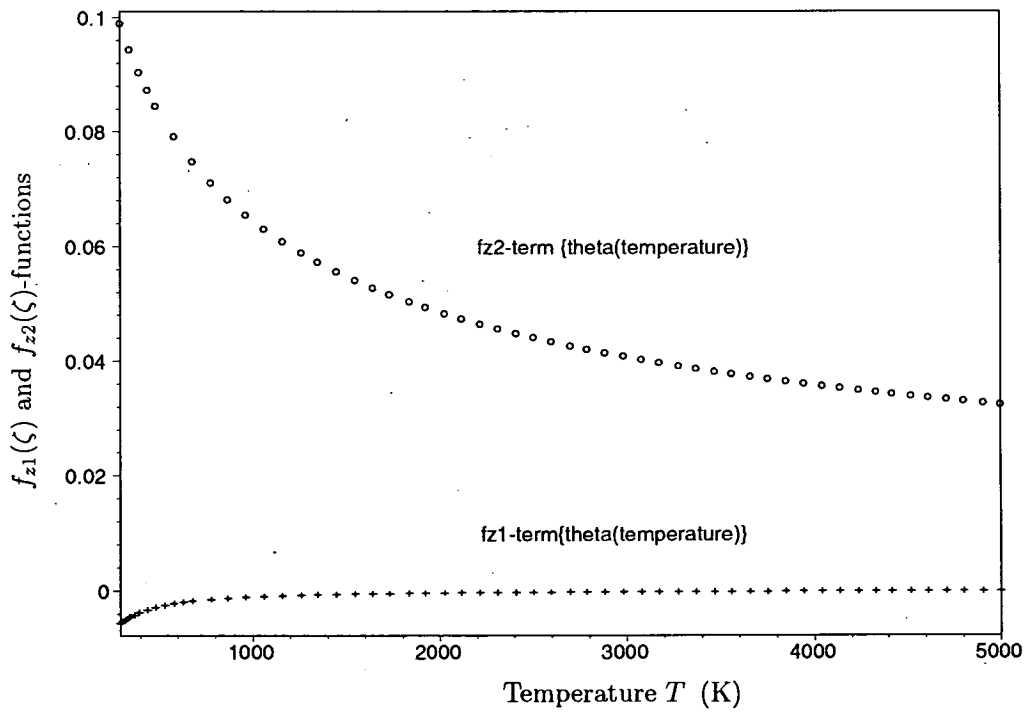

Figure 49: The $f_{z1}(\zeta)$ and $f_{z2}(\zeta)$-functions for Narrow Resonance like ^{238}U 6.67 eV Resonance as functions of Temperature T. The variable ζ is a function of temperature T.

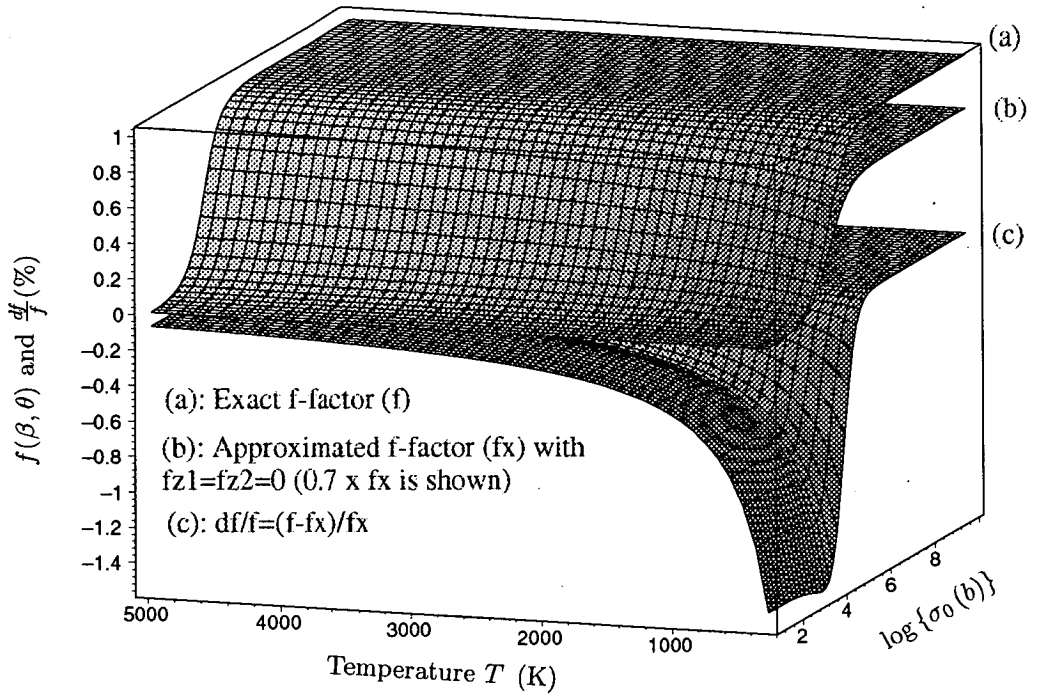

Figure 50: Comparison of Approximated f-factor $f_x(\beta,\zeta)$ with the Exact one $f(\beta,\zeta)$ for ^{238}U 6.67 eV Resonance. The approximation is made by setting $f_{z1} = f_{z2} = 0$ as shown by Eq. (181). In the upper half of the figure, two f-factors are shown and in the lower half the relative error defined by $\frac{f_x - f}{f}$ is shown in percent. The approximated f-factor denoted by fx is shown by $0.7 \times fx$ since two f-factors cannot be distinghed because of the small error.

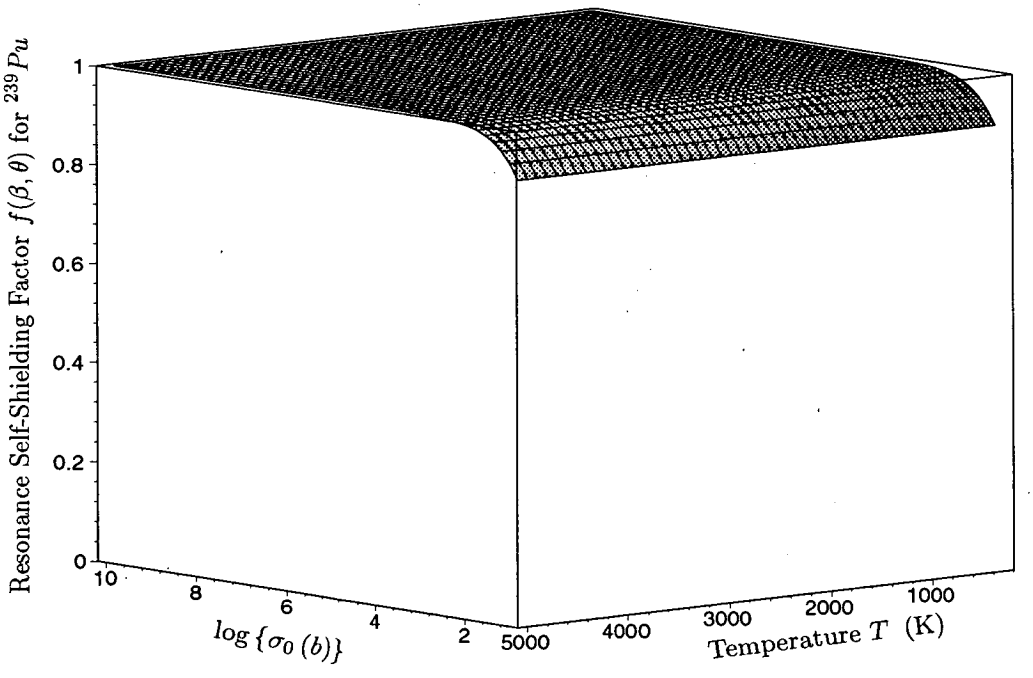

Figure 51: Resonance Self-Shielding factor $f(\beta,\theta)$ for ^{239}Pu 214.65 eV Resonance as an Example of Wide Resonance. The ^{239}Pu resonance has the following parameters; $\Gamma_n = 9.575$, $\Gamma_\gamma = 42.00$, $\Gamma_f = 11172$, and $\Gamma = 11223.57$ meVs, which is one of subthreshold fissions.

5.3 Partial Derivatives of Resonance Self-Shielding Factor

Partial derivatives of f-factor with respect to β and ζ providing the sensitivity coefficients are as follow,

$$\frac{\partial f}{\partial \beta} = \omega(\beta)^2 \cdot \left[\frac{1}{2}\cdot\psi_0(\zeta) - 2\cdot\left\{g_z(\zeta)+\frac{1}{2}\cdot\psi_0(\zeta)\right\}\omega(\beta) + 3g_z(\zeta)\omega(\beta)^2\right] + \frac{\partial}{\partial\beta}\{1-\omega(\beta)\}F_{sum}(\beta,\zeta) \quad (182)$$

with the partial derivatives of the series expansion term with respect to β as shown below.

Narrow Resonance Approximation

$$\frac{\partial}{\partial\beta}\{1-\omega(\beta)\}F_{sum}(\beta,\zeta) = \sum_{n=3}^{\infty}\sum_{m=0}^{n}\frac{\partial}{\partial\beta}\{1-\omega(\beta)\}F_{sum}^{n,m}(\beta,\zeta) \quad (183)$$

$$= -\sum_{n=3}^{\infty}\sum_{r=0}^{n}\omega(\beta)\{n-(n+1)\omega(\beta)\}\cdot F_{sum}^{n,m}(\beta,\zeta) \quad (184)$$

Wide Resonance Approximation

$$\frac{\partial}{\partial\beta}\{1-\omega(\beta)\}F_{sum}(\beta,\zeta) = -\sum_{n=3}^{\infty}\sum_{m=0}^{n}\sum_{l=0}^{m}\omega(\beta)\{n-(n+1)\omega(\beta)\}\cdot F_{sum}^{n,m,l}(\beta,\zeta) \quad (185)$$

The partial derivative $\frac{\partial f}{\partial\beta}$ for the first resonance at $E_r = 6.67$ eV of ^{238}U is shown in **Fig. 52** as function of potential scattering cross section σ_0 and temperature T, and that for the ^{239}Pu 214.56 eV resonance is shown in Fig. 53.

The partial derivatives $\frac{\partial f}{\partial\zeta}$ of f-factor with respect to ζ is given by

$$\frac{\partial f}{\partial\zeta} = \{1-\omega(\beta)\}\left[-\frac{1}{2}\frac{\partial\psi_0(\zeta)}{\partial\zeta}\cdot\omega(\beta)+\omega(\beta)^2\cdot\frac{\partial}{\partial\zeta}g_z(\zeta)+\frac{\partial F_{sum}}{\partial\zeta}\right] \quad (186)$$

where $\frac{\partial\psi_0(\zeta)}{\partial\zeta}$ can be given by

$$\frac{\partial\psi_0(\zeta)}{\partial\zeta} = \left\{\frac{2\sqrt{2}(1-\zeta)}{p\zeta}+\frac{p\zeta}{\sqrt{2}(1-\zeta)}\right\}\cdot\psi_0(\zeta)+4\frac{1-\zeta}{(p\zeta)^2} \quad (187)$$

and the partial derivative of $F_{sum}(\beta,\zeta)$ can be defined by the two different approximations, High and Low temperature Approximations, as

For High Temperature Approximation

$$\frac{\partial}{\partial\zeta}F_{sum}(\beta,\zeta) = \sum_{n=3}^{\infty}\sum_{m=0}^{n}\frac{\partial}{\partial\zeta}F_{sum}^{n,m}(\beta,\zeta), \quad (188)$$

$$\frac{\partial}{\partial\zeta}F_{sum}^{n,m}(\beta,\zeta) = -\frac{n-m}{\zeta(1-\zeta)}\cdot F_{sum}^{n,m}(\beta,\zeta) \quad (189)$$

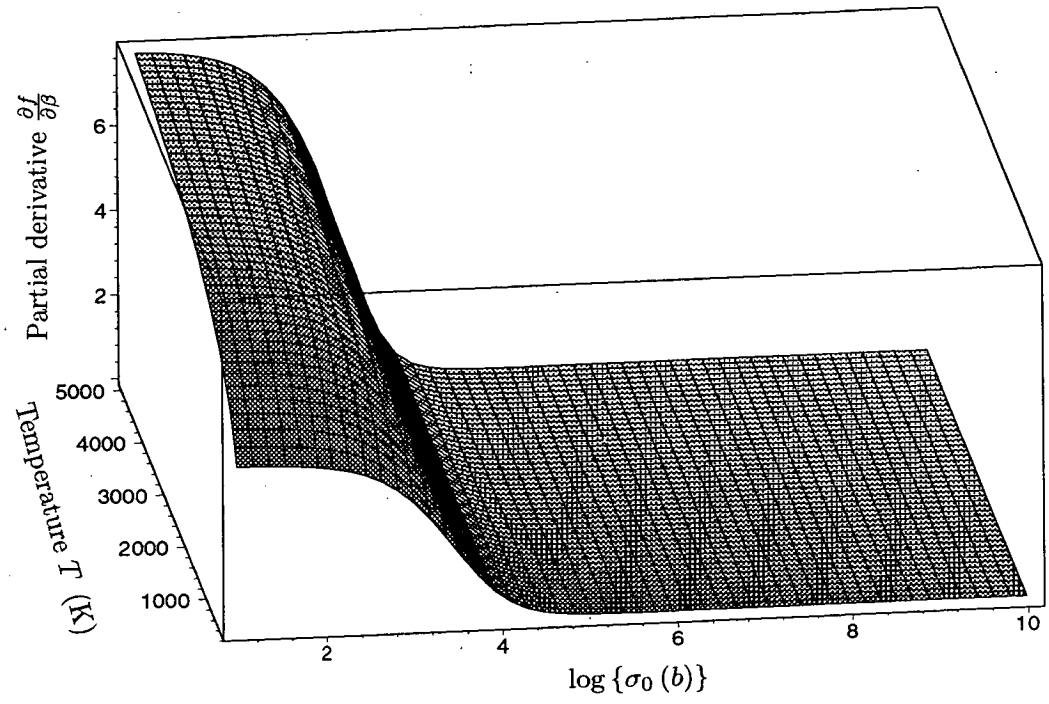

Figure 52: Partial derivative $\frac{\partial f}{\partial \beta}$ for the Resonance Self-shielding Factor of ^{238}U First Resonance at $E_r = 6.67$ eV with respect to Intermediate variable β.

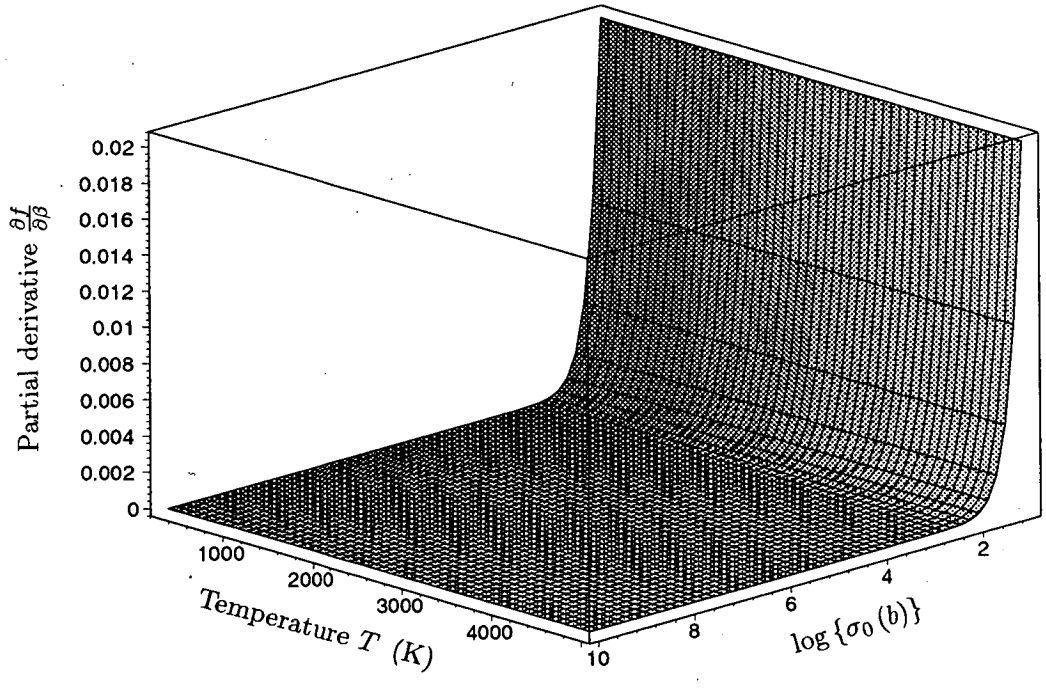

Figure 53: Partial derivative $\frac{\partial f}{\partial \beta}$ for the Resonance Self-shielding Factor of ^{239}Pu First Resonance at $E_r = 214.65$ eV with respect to Intermediate variable β.

For Low Temperature Approximation

$$\frac{\partial}{\partial\zeta}F_{sum}(\beta,\zeta) = \sum_{n=3}^{\infty}\sum_{m=0}^{n}\sum_{l=0}^{m}\frac{\partial}{\partial\zeta}F_{sum}^{n,m,l}(\beta,\zeta), \tag{190}$$

$$\frac{\partial}{\partial\zeta}F_{sum}^{n,m}(\beta,\zeta) = 0.0, \tag{191}$$

as expected from the $F_{sum}^{n,m}$ for the low temperature defined by Eq. (176), which is not a function of ζ as well as the temperature.

The partial derivatives of $(\frac{\partial f}{\partial\zeta})$'s are shown in Fig. 58 for the ^{238}U 6.67 eV resonance and in Fig. 59 for the ^{239}Pu 214.65 eV resonance. The former has a maximum value around $\sigma_0 \simeq 10^4$ barn, but the latter is monotonously increasing function of temperature in the smaller σ_0-region below 10^4 barn.

The Doppler broadening function and its derivatives with respect to ζ at a resonance position, namely $\psi_0(\zeta)$ and $\frac{\partial\psi_0(\zeta)}{\partial\zeta}$, are shown in **Figs. 54** and **55** for the narrow resonance of ^{238}U and in **Figs. 56** and **57** for the wide resonance of ^{239}Pu, respectively. As shown in the three-dimensional plot of ψ in **Fig. 26**, the $\psi_0(\zeta)$ is decreasing function with respect to the temperature, which means the change of the resonant total peak cross section shown in **Fig. 23**. The derivatives of $\psi_0(\zeta)$ for the 6.67 eV narrow resonance of ^{238}U is also monotonous decreasing function as shown in **Fig. 55**. While, the $\psi_0(\zeta)$ for the 214.65 eV wide resonance of ^{239}Pu are nearly linear function of temperature and its derivative $\frac{\partial\psi_0(\zeta)}{\partial\zeta}$ is nearly equal to zero as shown in **Fig. 57** and milder behavior than ^{238}U's.

The derivatives of the resonance self-shielding factors $\frac{\partial f(\beta,\zeta)}{\partial\zeta}$ are shown in **Fig. 58** for

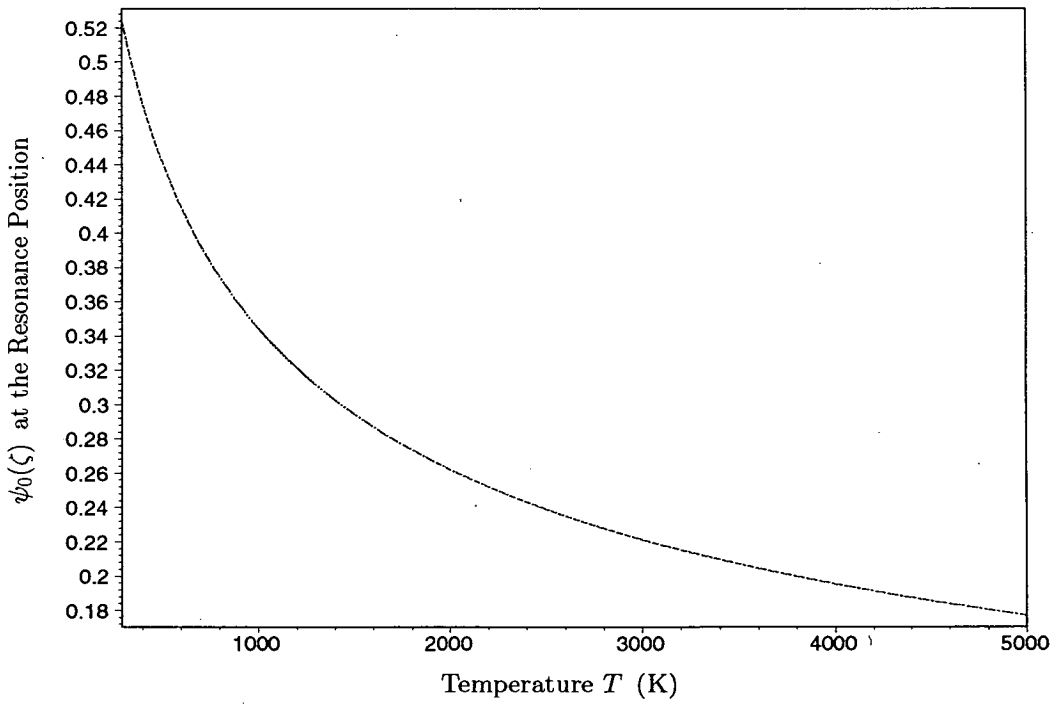

Figure 54: Symmetric Doppler Broadening Function $\psi_0(\zeta)$ at the Resonance Position of ^{238}U 6.67 eV Resonance as a Function of Temperature.

the narrow resonance of ^{238}U and **Fig. 59** for the wide resonance of ^{239}Pu, respectively.

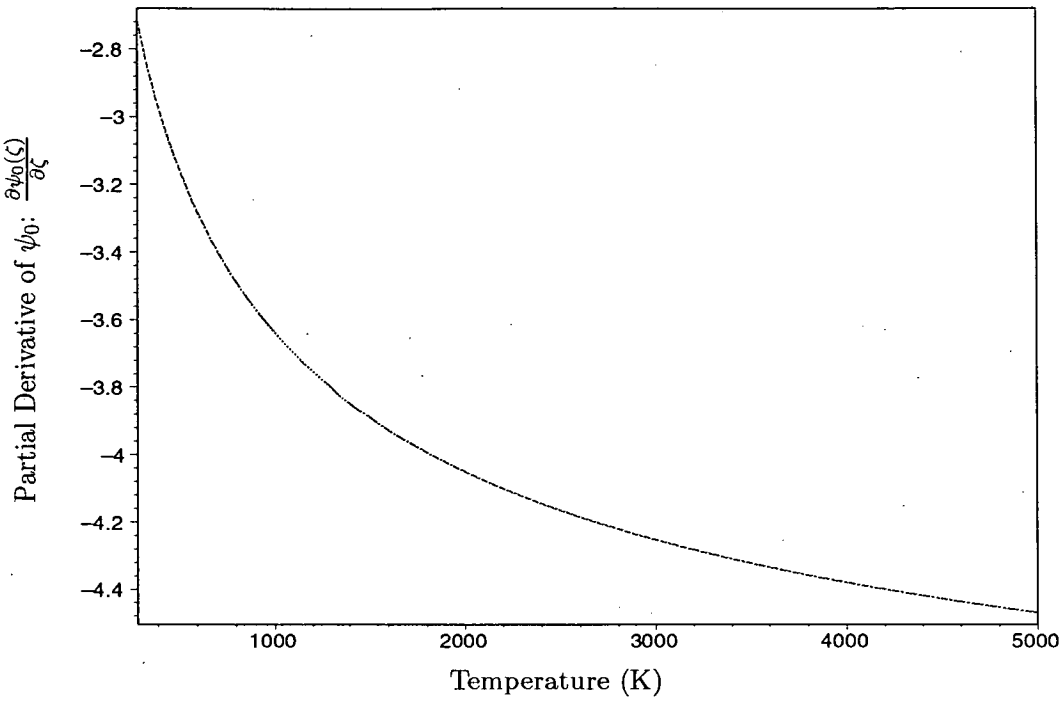

Figure 55: Partial Derivative of Symmetric Doppler Broadening Function $\frac{\partial\psi_0(\zeta)}{\partial\zeta}$ at the Resonance Position of ^{238}U 6.67 eV Resonance as a Function of Temperature.

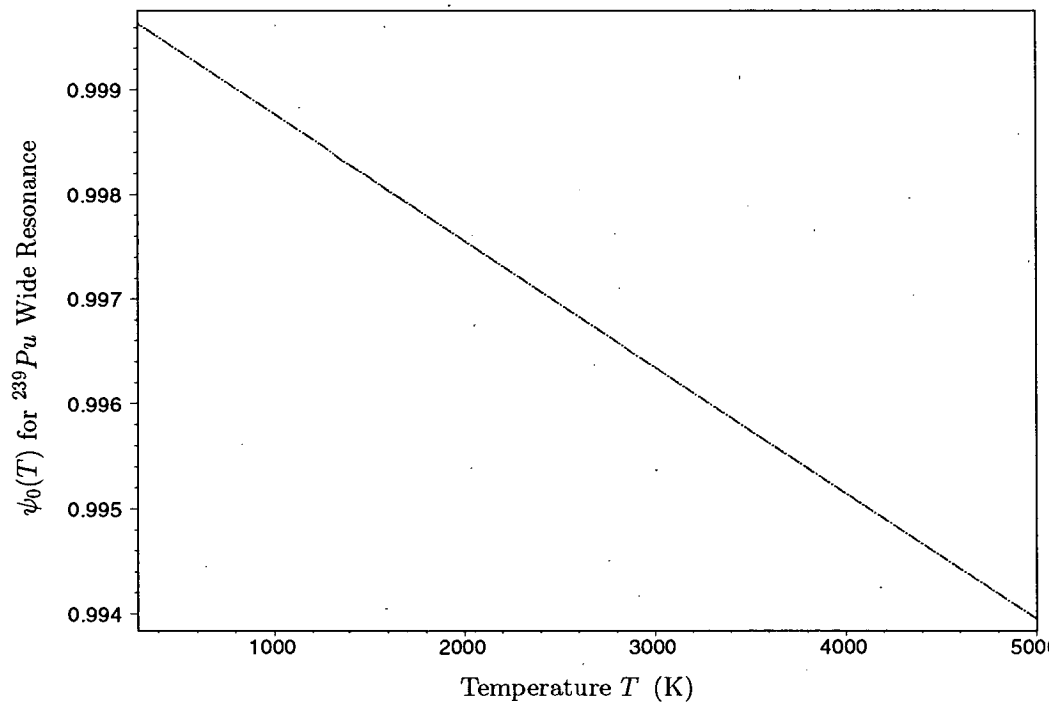

Figure 56: Symmetric Doppler Broadening Function $\psi_0(\zeta)$ at the Resonance Position of ^{239}Pu 214.65 eV Resonance as a Function of Temperature.

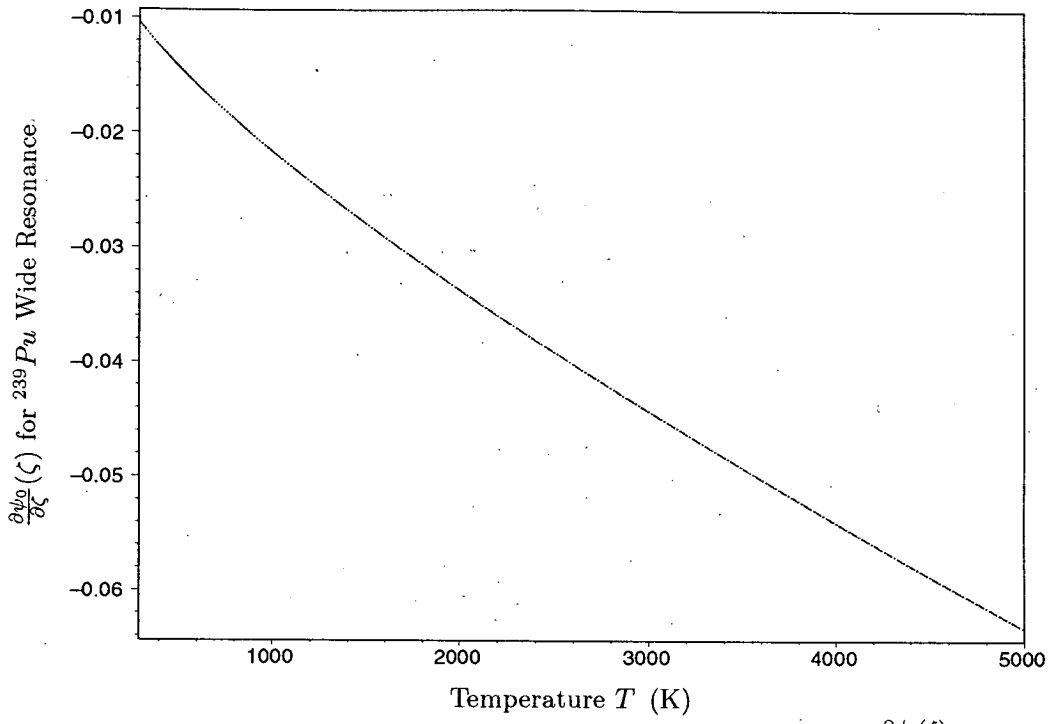

Figure 57: Partial Derivative of Symmetric Doppler Broadening Function $\frac{\partial\psi_0(\zeta)}{\partial\zeta}$ at the Resonance Position of ^{239}Pu 214.65 eV Resonance as a Function of Temperature.

As shown in **Fig. 44**, the temperature dependence of the f-factor for ^{238}U is an increasing function and tends to constant value in the high temperature region, and the σ_0 dependency of the derivative $\frac{\partial f}{\partial\zeta}$ has the maximum value around $\sigma_0 \simeq 1.0^4$ barn and is decreasing towards zero as shown in **Fig. 58**. The $\sigma_0 = 10^4$ barn is a turning point of the temperature dependence of f-factor as shown in **Fig. 44**. On the other hand, for the wide resonance of ^{239}Pu, the magnitude of $\frac{\partial f}{\partial\zeta}$ is extremely small, about one tens of ^{238}U's, and slightly increasing trend with temperature can be found but the turning point could not be found in this case.

Further derivatives with respect to temperature T or a resonance parameter Γ_{xl} of the reaction x of the l-th resonance can be obtained by

$$\frac{\partial f}{\partial\Gamma_{xl}} = \frac{\partial f}{\partial\beta}\cdot\frac{\partial\beta}{\partial\Gamma_{xl}}, \tag{192}$$

$$\frac{\partial f}{\partial t} = \frac{\partial f}{\partial\zeta}\cdot\frac{\partial\zeta}{\partial t}. \tag{193}$$

5.4 Multi-group Resonance Self-Shielding Factor

The effective cross section for the k-th resonance of an isotope i and reaction x is defined by the infinitely diluted cross section $\sigma_{\infty xik}$ multiplied by the resonance self-shielding factor f^k_{xi} as,

$$\sigma^k_{effxi} = \sigma^k_{\infty xi}\cdot f^k_{xi}. \tag{194}$$

The ultra-fine group effective cross section σ^k_{effix} can be obtained from the average cross

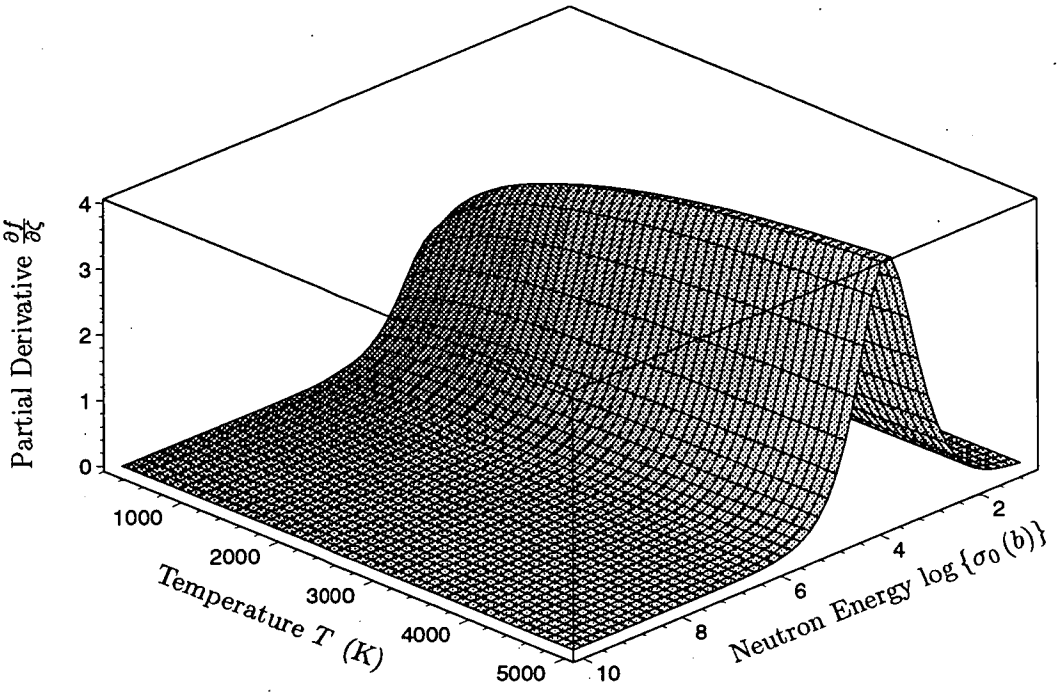

Figure 58: Partial Derivative $\frac{\partial f}{\partial \zeta}$ of Resonance Self-shielding Factor for ^{238}U 6.67 eV Resonance with respect to Intermediate variable ζ.

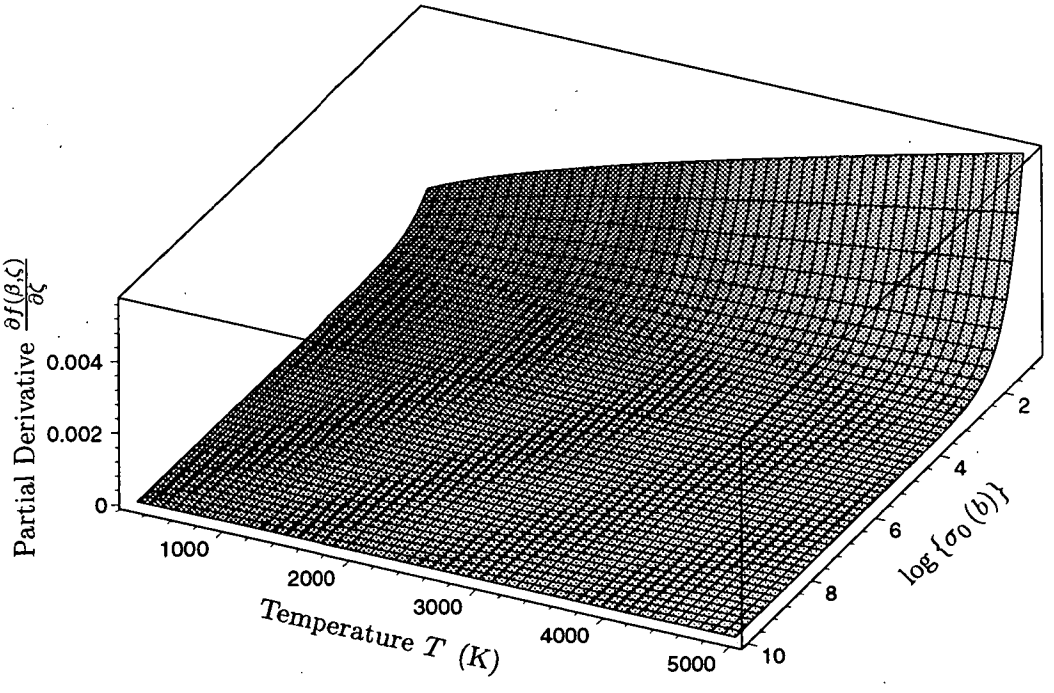

Figure 59: Partial Derivative $\frac{\partial f(\beta,\zeta)}{\partial \zeta}$ of resonance self-shielding factor for ^{239}Pu 214.65 eV Resonance as a Function of Temperature.

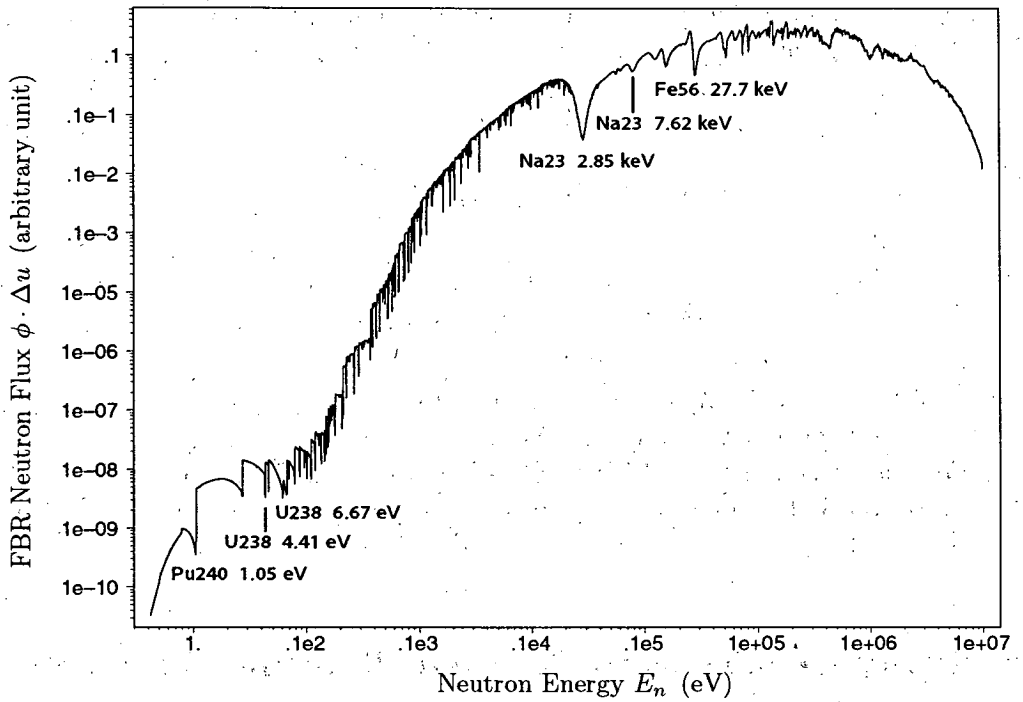

Figure 60: Neutron Spectrum of a Typical Large Fast Breeder Reactor based on MC^2-2 Ultra-fine Group Calculation. Typical resonance positions of fuel matrials (U238, Pu240, U235), coolant (Na23) and structural material (Fe56) are shown.

section of point-wise cross sections based on nuclear data with the weight of neutron flux in an ultra-fine group. As the reaction rate of the g (broad) group has to be equal to the sum of the contributions from ultra-fine groups, the following balance equation of reaction rates has to be satisfied.

$$\sum_{k\in g}^{g} \sigma^k_{eff\,xi} \cdot \phi^k \Delta u^k = \sigma^g_{eff,xi} \cdot \sum_{k\in g}^{g} \phi^k \Delta u^k. \tag{195}$$

The ultra-fine group neutron spectrum was obtained by using the MC^2-2 code with the lethargy width $\Delta u^k = \frac{1}{120}$. The neutron spectrum for typical large fast breeder reactor is shown in **Fig. 60** where flux dips due to resonance absorption and/or scattering can be found.

Even if taking about two thousands of energy groups such as 2024 in present case, individual resonance profile could not be faithfully revealed. The magnitude of reaction rates, however, are seemed to be reasonably evaluated since MC^2-2 code exactly evaluate isotopic and resonance-wise reaction rate by using the resonance integral J-function in cooperation with continuous slowing down theory coupled with the criticality search. In these processes, resonances of all constituent isotopes are taken into account. Therefore, a few thousand groups calculation can give consistent result with more finer group calculation so as to conserve the reaction rates as shown by Eq.(Eq:179).

Consequently, the effective cross section of a broad group can be obtained as the summation of the ultra-fine group contributions as shown below,

$$\sigma^g_{eff,xi} = \frac{\sum^g_{k\in g} \sigma^k_{\infty,xi} \cdot f^k_{xi} \cdot \phi^k \Delta u^k}{\sum^g_{k\in g} \phi^k \Delta u^k}, \tag{196}$$

where $k \in g$ means the ultra-fine group k falling into to the broad group g. While, the g group resonance self-shielding factor f_{xi}^g is summation of the ultra-fine group contributions with weight Λ_{xi}^k as,

$$f_{xi}^g = \sum_{k \in g}^{g} \lambda_{xi}^k \cdot f_{xi}^k, \tag{197}$$

$$\lambda_{xi}^k = \frac{\sigma_{\infty,xi}^k \cdot \phi^k \Delta u^k}{\sum_{l \in g}^{g} \sigma_{\infty,xi}^l \cdot \phi^l \Delta u^l}. \tag{198}$$

The ultra-fine group resonance self-shielding factor f_{xi}^k was provided by Eq. (160) as a function of temperature and the resonance parameters, and thus the effective cross section defined by Eq. (196) can be obtained if the ultra-fine group neutron spectrum is available. In the present work, the k-th resonance in a resonance sequence of all resonant materials belongs to an ultra-fine group.

6 Sensitivity Coefficient to Resolved Resonance Parameter

6.1 Sensitivity Coefficients of Resonance Self-Shielding Factor f_{xi}^k

6.1.1 Sensitivity Coefficients for Multi-variable Function

Sensitivity coefficient $S_{\Gamma_{pik}}^{f_{xi}^k}$ of the resonance self-shielding factor $f_{xi}^k(\beta, \zeta)$ against an arbitrary resonance parameter Γ_{pik} including resonance energy E_r is defined by

$$S_{\Gamma_{pik}}^{f_{xi}^k} = \frac{\Gamma_{pik}}{f_{xi}^k(\beta,\zeta)} \cdot \frac{\partial f_{xi}^k(\beta,\zeta)}{\partial \Gamma_{pik}}, \tag{199}$$

$$= \frac{\Gamma_{pik}}{H_{xik}(\beta,\zeta)} \cdot \frac{\partial H_{xik}(\beta,\zeta)}{\partial \Gamma_{pik}}, \tag{200}$$

The sensitivity coefficient of an arbitrary functional function $f[g\{h(x)\}]$ can be obtained by a successive product of the sensitivity coefficients for intermediate parameters as a result of following algebra,

$$\delta f(x) = \frac{\partial f(g)}{\partial g} \cdot \frac{\partial g(h)}{\partial h} \cdot \frac{\partial h(x)}{\partial x} \cdot \delta x, \tag{201}$$

$$= f(x) \cdot \frac{\delta x}{x} \cdot S_g^f(g) \cdot S_h^g(h) \cdot S_x^h(x). \tag{202}$$

Therefore, an effective sensitivity coefficient S_x^f of functional function $f(x)$ to the change of x can be expressed by

$$\frac{\frac{\delta f}{f}}{\frac{\delta x}{x}} \simeq \frac{x}{f} \cdot \left(\frac{\partial f}{\partial x}\right) = S_x^f = S_g^f(g) \cdot S_h^g(h) \cdot S_x^h(x). \tag{203}$$

In the present work the resonance self-shielding factor $f(\beta, \zeta)$ is a typical functional function of β and ζ which are also function of total resonance width Γ, resonance energy E_r and so on, i.e.,

$f[\beta\{\Gamma_{ik}\, g\Gamma_{n0i},\, E_r\},\, \zeta\{\theta(\Gamma_{ik},\, g\Gamma_{n0i}\, E_r)\}]$.

For a multi-dimensional function such as $f(\beta,\zeta)$, the sensitivity coefficient can be obtained as a linear combination of intermediate sensitivity coefficients as shown below,

$$S^{f^k_{xi}}_{\Gamma_{xik}} = S^{f^k_{xi}}_{\beta} \cdot S^{\beta}_{\Gamma_{xik}} + S^{f^k_{xi}}_{\zeta} \cdot S^{\zeta}_{\Gamma_{xik}} \tag{204}$$

This formula implies that the sensitivity coefficient $S^{f^k_{xi}}_{\Gamma_{xik}}$ of the resonance self-shielding factor f to an arbitrary resonance parameter Γ_{xik} can be expressed in terms of the sensitivity coefficients for intermediate variables β and θ. In general, as far as the sensitivity coefficient is defined by a dimensionless quantity $S = \frac{Y}{x} \cdot \frac{\partial Y}{\partial x}$, such a successive operation can be used even if a lot of intermediate variables are concerned.

The sensitivity coefficients of f-factor to individual resonance parameter are given by

$$S^f_{E_r} = \frac{1}{2} \cdot \left(2 \cdot S^f_\beta \cdot S^\beta_{E_r} - S^f_\zeta \cdot S^\zeta_{E_r}\right) \tag{205}$$

$$S^f_{\Gamma_n} = -\left\{\left(\frac{\Gamma_\gamma + \Gamma_f}{\Gamma}\right) \cdot S^f_\beta \cdot S^\beta_{\Gamma_n} - \left(\frac{\Gamma_n}{\Gamma}\right) \cdot S^f_\zeta \cdot S^\zeta_{\Gamma_n}\right\} \tag{206}$$

$$S^f_{\Gamma_\gamma} = -\frac{\Gamma_\gamma}{\Gamma} \cdot \left(S^f_\beta \cdot S^\beta_{\Gamma_\gamma} - S^f_\zeta \cdot S^\zeta_{\Gamma_\gamma}\right) \tag{207}$$

$$S^f_{\Gamma_f} = -\frac{\Gamma_f}{\Gamma} \cdot \left(S^f_\beta \cdot S^\beta_{\Gamma_f} - S^f_\zeta \cdot S^\zeta_{\Gamma_f}\right) \tag{208}$$

Explicit sensitivity coefficient of the resonance self-shielding factor to individual intermediate variable are as shown below

6.1.2 Sensitivity Coefficient of f-factor to β: S^f_β

The sensitivity coefficient of f-factor to $\beta(=\frac{\sigma_{pi}+\sigma_{back\,i}}{\sigma_{0ik}})$ can be shown by a fractional function as,

$$S^f_\beta(\beta,\zeta) = \frac{N^f_\beta(\beta,\zeta)}{D^f_\beta(\beta,\zeta)} \tag{209}$$

where the numerator and denominator functions are defined by

$$N^f_\beta(\beta,\zeta) = \omega(\beta)^2 \left[\frac{1}{2}\psi_0(\zeta) - 2\left\{g_z(\zeta) + \frac{1}{2}\psi_0(\zeta) - 1\right\}\omega(\beta) + 3g_z(\zeta)\omega(\beta)^2 \frac{\partial}{\partial\beta}\{1-\omega(\beta)\}F_{sum}(\beta,\zeta)\right], \tag{210}$$

$$D^f_\beta(\beta,\zeta) = 1 - \frac{1}{2}\psi_0(\zeta) + \{g_z(\zeta)\psi_0(\zeta) - 1\}\omega(\beta)^2 - g_z(\zeta)\omega(\beta)^3 - \{1-\omega(\beta)\}F_{sum}(\beta,\zeta), \tag{211}$$

and $\frac{\partial}{\partial\beta}\{1-\omega(\beta)\}F_{sum}(\beta,\zeta)$ was defined by Eq. (184) for narrow resonance and Eq. (185) for wide resonance respectively.

The sensitivity coefficient S^f_β for the first resonance of ^{238}U at $E_r = 6.67$ eV is shown in **Fig.**

61 which is vanishing in the region of σ_0 larger than 10^5 barn because of the saturation profile of the f-factor as shown in **Fig. 44**. The temperature dependence is monotonous decreasing function similar to $\frac{1}{\sqrt{T}}$.

As shown in **Fig. 44**, the f-factor smoothly trends to flattening in both $\sigma_0 \to 0$ and $\sigma_0 \to \infty$ where the gradients tend to zero's. For $\sigma_0 \to \infty$, the f-factor is unity and thus S^f_β is zero. However, for $\sigma_0 = 0$ the f-factor itself is vanishing and then $\frac{1}{f} \cdot \frac{\partial f}{\partial \beta}$ becomes unity.

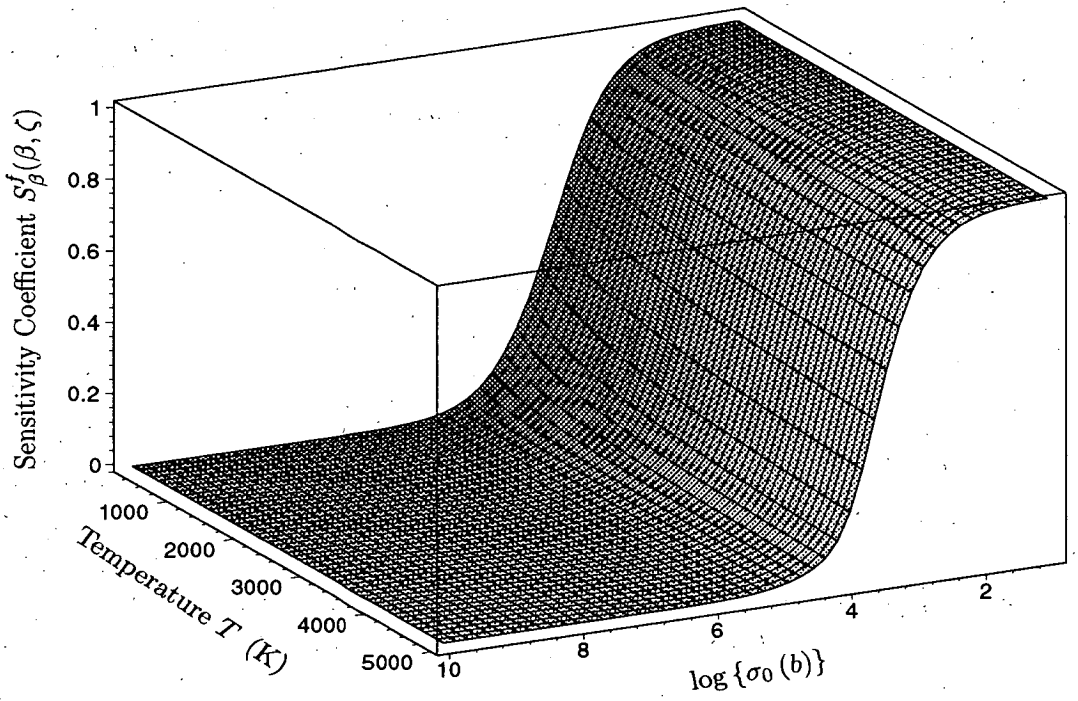

Figure 61: Sensitivity Coefficient $S^f_\beta(\beta,\zeta)$ of Resonance Self-Shielding Factor f to β for ^{238}U 6.67 eV Resonance as a Function of σ_0 and T.

6.1.3 Sensitivity Coefficient of f-factor to ζ: S^f_ζ

The sensitivity coefficient of the resonance self-shielding factor to the ζ is shown below.

$$S^f_\zeta(\beta,\zeta) = \zeta \cdot \{1-\omega(\beta)\} \cdot \frac{N^f_\beta(\beta,\zeta)}{D^f_\beta(\beta,\zeta)} \tag{212}$$

where

$$N^f_\zeta(\beta,\zeta) = -\frac{1}{2}\frac{\partial}{\partial\zeta}\psi_0(\zeta) - g_z(\zeta)\omega(\beta)^2 - \frac{\partial}{\partial\zeta}F_{sum}(\beta,\zeta), \tag{213}$$

$$D^f_\zeta(\beta,\zeta) = 1 - \frac{1}{2}\psi_0(\zeta) + \{g_z(\zeta)\psi_0(\zeta) - 1\}\,\omega(\beta)^2 - g_z(\zeta)\omega(\beta)^3 - \{1-\omega(\beta)\}\,F_{sum}(\beta,\zeta) \tag{214}$$

and $\frac{\partial F_{sum}}{\partial\zeta}(\beta,\zeta)$ was defined by Eqs. (188) and (190) for high and low temperature approximations, respectively.

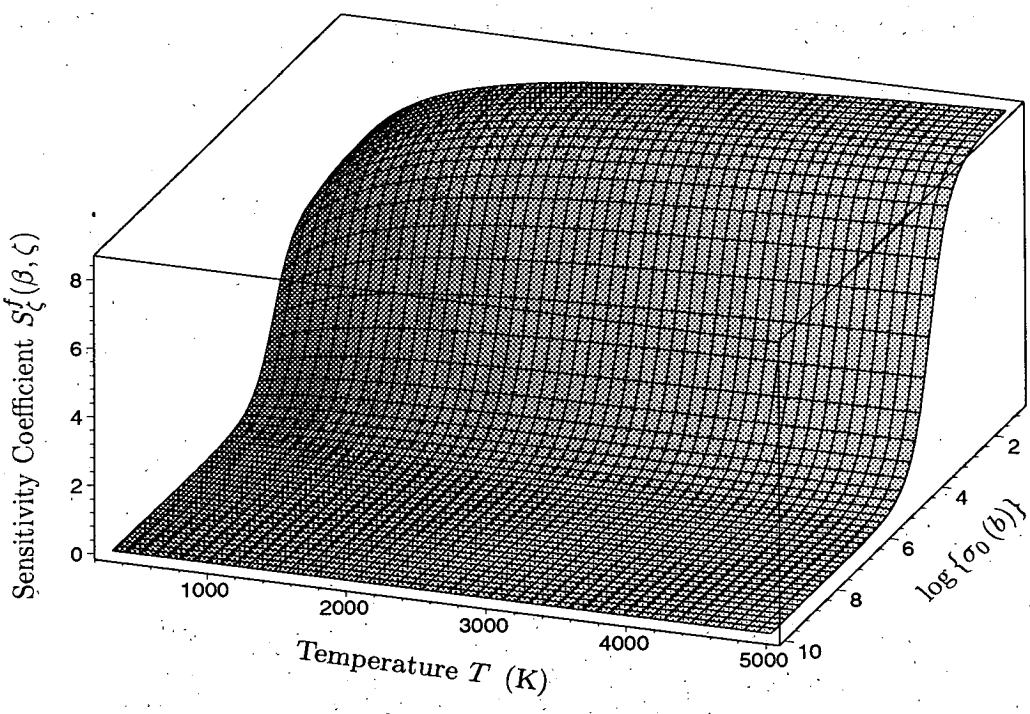

Figure 62: Sensitivity Coefficient $S_\zeta^f(\beta,\zeta)$ of Resonance Self-Shielding Factor f to ζ for ^{238}U 6.67 eV Resonance as a Function of σ_0 and T.

The sensitivity coefficient S_ζ^f for the first resonance at $E_r = 6.67$ eV of ^{238}U is shown in **Fig. 62** as function of potential scattering cross section and temperature. This sensitivity coefficient is essentially the temperature dependence of f-factor and monotonous increasing function overall range of potential cross section σ_0.

6.1.4 Sensitivity Coefficient of f-factor to θ: $S_\theta^f = S_\zeta^f \cdot S_\theta^\zeta$

The sensitivity coefficient of f-factor to $\theta(=\frac{\Gamma}{\Delta})$ can be obtained from the formula Eq. (203) for derivative of functional functions, i.e., $S_\zeta^f \cdot S_\theta^\zeta$, and can be expressed by the previous S_ζ^f multiplied by $(\zeta - 1)$ as

$$S_\theta^f(\beta,\zeta) = (\zeta - 1) \cdot S_\zeta^f. \tag{215}$$

The ζ-function is monotonous function of temperature T and less than unity as shown in **Fig. 42**. Therefore, the resultant S_θ^f for the first resonance at $Er = 6.67$ eV of ^{238}U is a negative and monotonously decreasing function with temperature as shown in **Fig. 63**.

6.1.5 Sensitivity Coefficient of f-factor to T: $S_T^f = S_\zeta^f \cdot S_\theta^\zeta \cdot S_T^\theta$

The sensitivity coefficient of f-factor to temperature T can be obtained as a triple product of partial sensitivity coefficients, $S_\zeta^f \cdot S_\theta^\zeta \cdot S_T^\theta$, and the resultant S_T^f is

$$S_T^f = -\frac{1}{2}(\zeta - 1) \cdot S_\zeta^f, \tag{216}$$

where the following partial sensitivity coefficients were used

$$S_\theta^\zeta = \zeta - 1, \qquad S_T^\theta = -\frac{1}{2}. \tag{217}$$

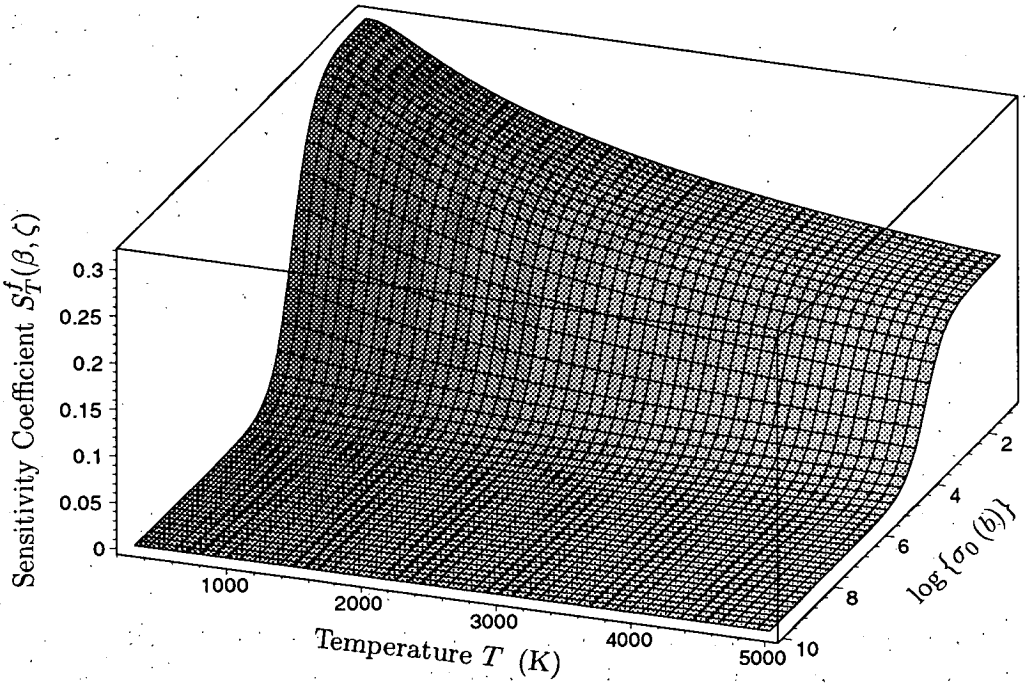

Figure 63: Sensitivity Coefficient $S_T^f(\beta,\zeta)$ for ^{238}U of Resonance Self-Shielding Factor f to Temperature T for ^{238}U 6.67 eV Resonance as a Function of σ_0 and T.

6.1.6 Sensitivity Coefficient of f-factor to Resolved Resonance Parameter

Finally, in order to obtain the sensitivity coefficients of f-factor to the resonance parameter, the sensitivity coefficients for intermediate parameters β and θ against the resonance parameters are needed. Resultant sensitivity coefficients are shown in Table 3.

Table 3. Sensitivity Coefficient of β and θ.

β Sensitivity	θ Sensitivity
$S^\beta_{E_{ik}} = 1$	$S^\theta_{E_{rik}} = -\frac{1}{2}$
$S^\beta_{\Gamma_{nik}} = -\left(1 - \frac{\Gamma_{nik}}{\Gamma_{ik}}\right)$	$S^\theta_{\Gamma_{nik}} = \frac{\Gamma_{nik}}{\Gamma_{ik}}$
$S^\beta_{\Gamma_{\gamma ik}} = \frac{\Gamma_{\gamma ik}}{\Gamma_{ik}}$	$S^\theta_{\Gamma_{\gamma ik}} = \frac{\Gamma_{\gamma ik}}{\Gamma_{ik}}$
$S^\beta_{\Gamma_{fik}} = \frac{\Gamma_{fik}}{\Gamma_{ik}}$,	$S^\theta_{\Gamma_f} = \frac{\Gamma_{fik}}{\Gamma_{ik}}$

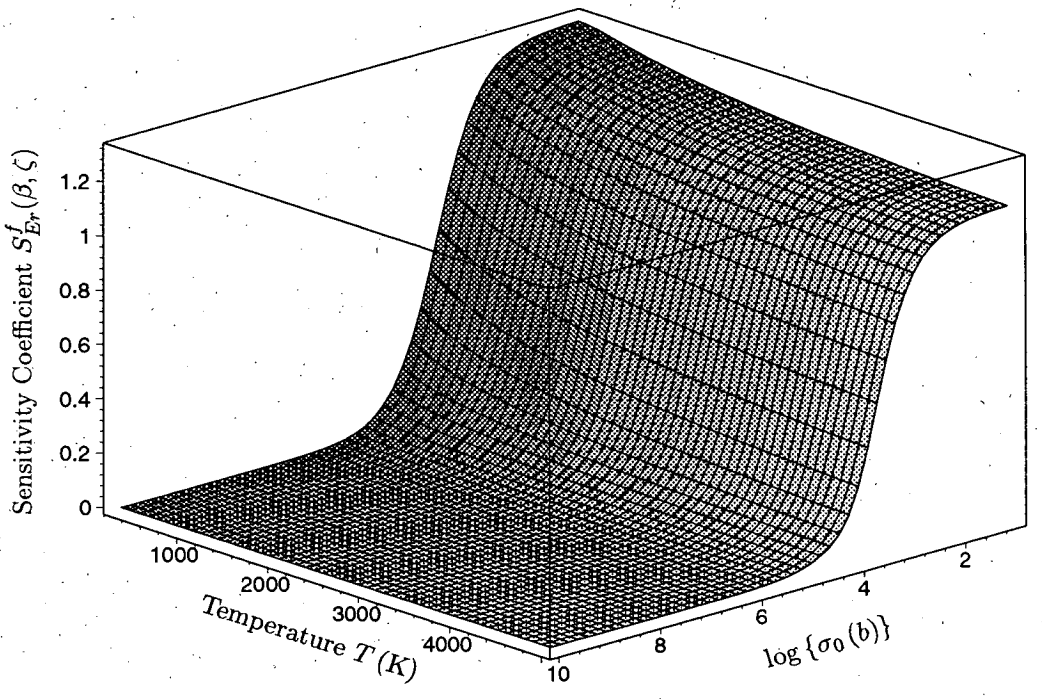

Figure 64: Sensitivity Coefficient $S^f_{Er}(\beta,\zeta)$ of f-factor to Resonance Energy Er for ^{238}U 6.67 eV Resonance as a Function of σ_0 and T.

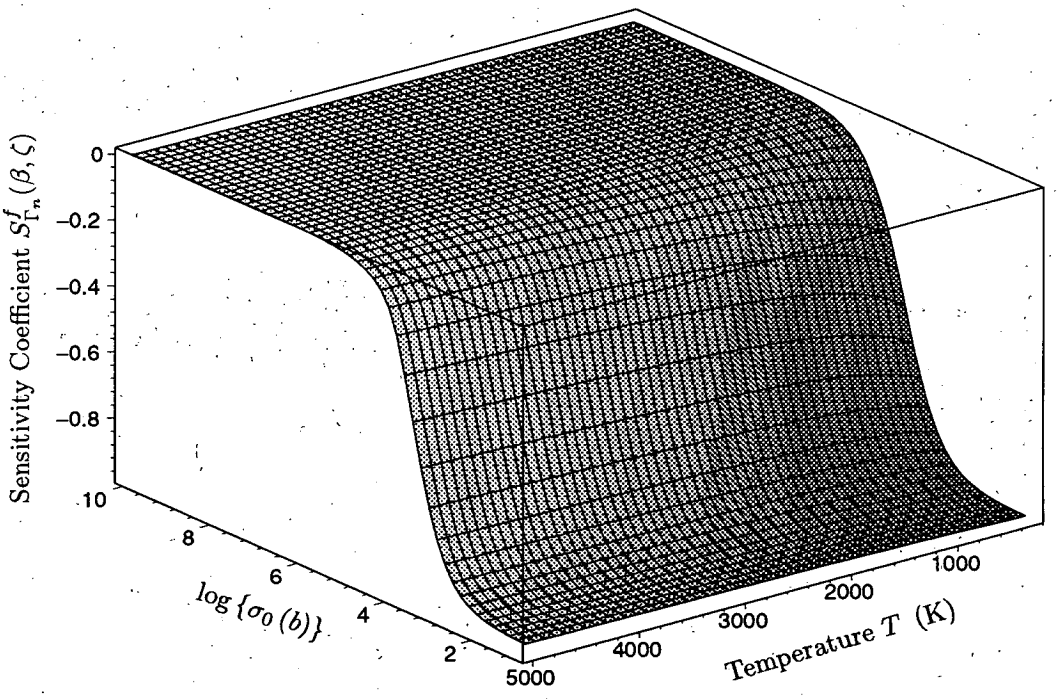

Figure 65: Sensitivity Coefficient $S^f_{\Gamma_n}(\beta,\zeta)$ of f-factor to Neutron Width Γ_n for ^{238}U 6.67 eV Resonance as a Function of σ_0 and T.

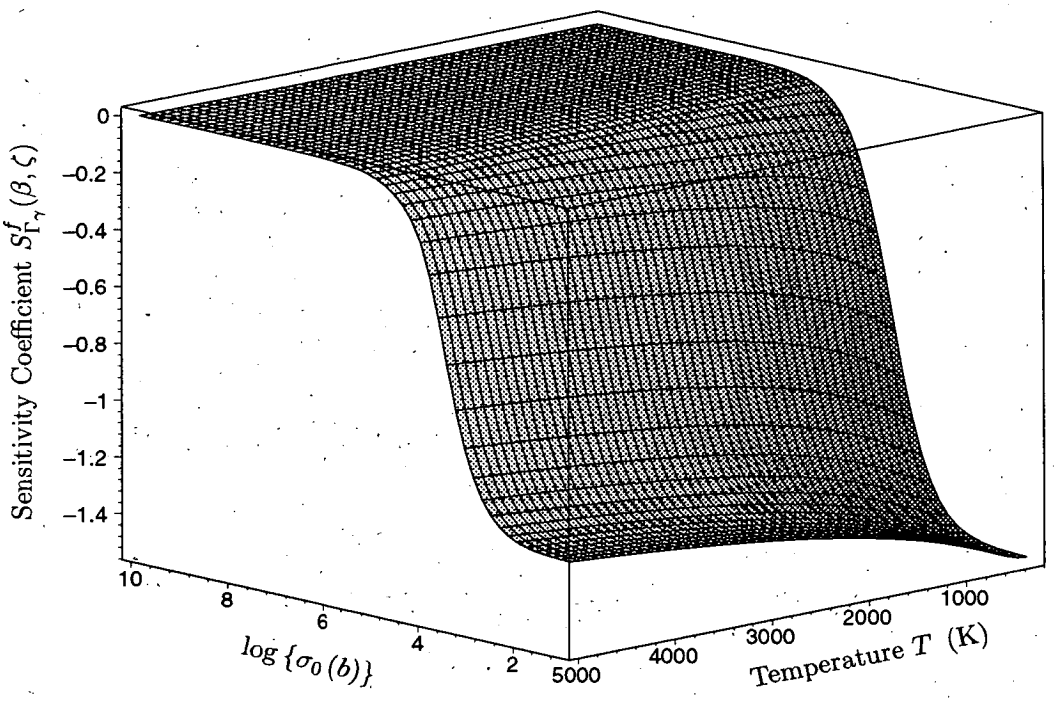

Figure 66: Sensitivity Coefficient $S^f_{\Gamma_\gamma}(\beta,\zeta)$ of f-factor to Radiation Width Γ_γ for ^{238}U 6.67 eV Resonance as a Function of σ_0 and T.

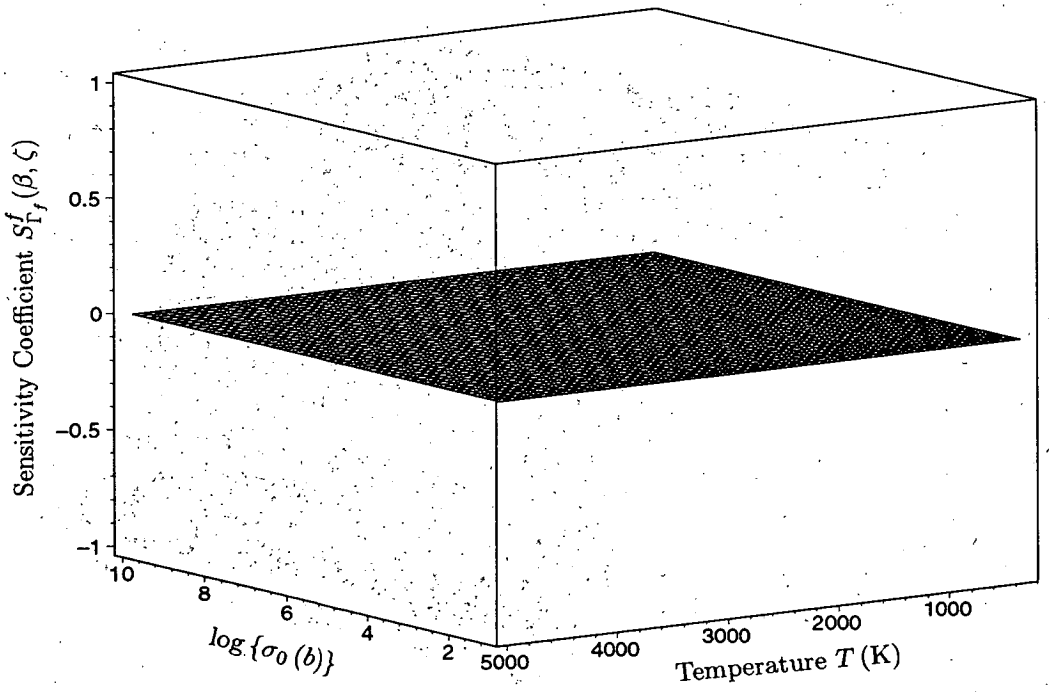

Figure 67: Sensitivity Coefficient $S^f_{\Gamma_f}(\beta,\zeta)$ of f-factor to Fission Width Γ_f for ^{238}U 6.67 eV Resonance as a Function of σ_0 and T.

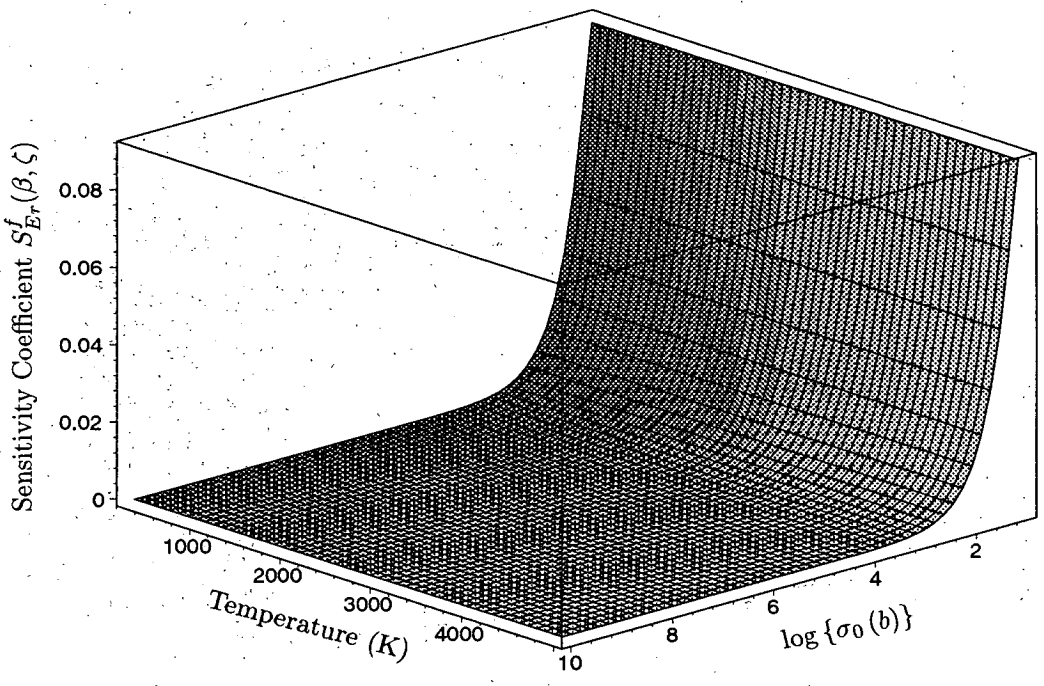

Figure 68: Sensitivity Coefficient $S^f_{Er}(\beta,\zeta)$ of f-factor to Resonance Energy Er for ^{239}Pu 214.65 eV Resonance as a Function of σ_0 and T.

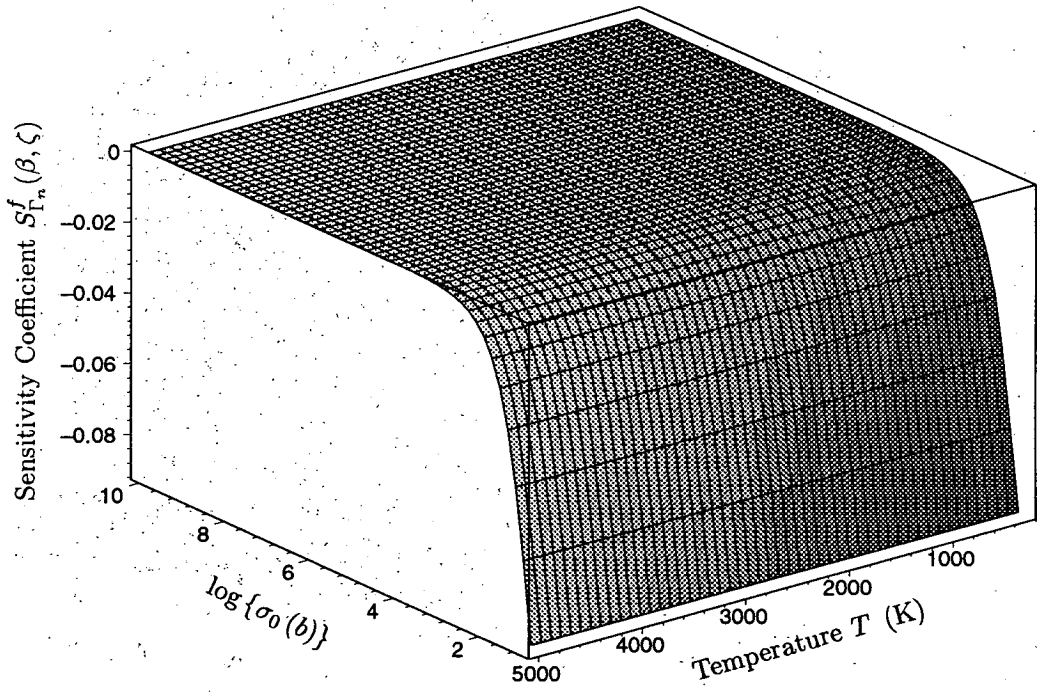

Figure 69: Sensitivity Coefficient $S^f_{\Gamma_n}(\beta,\zeta)$ of f-factor to Neutron Width Γ_n for ^{239}Pu 214.65 eV Resonance as a Function of σ_0 and T.

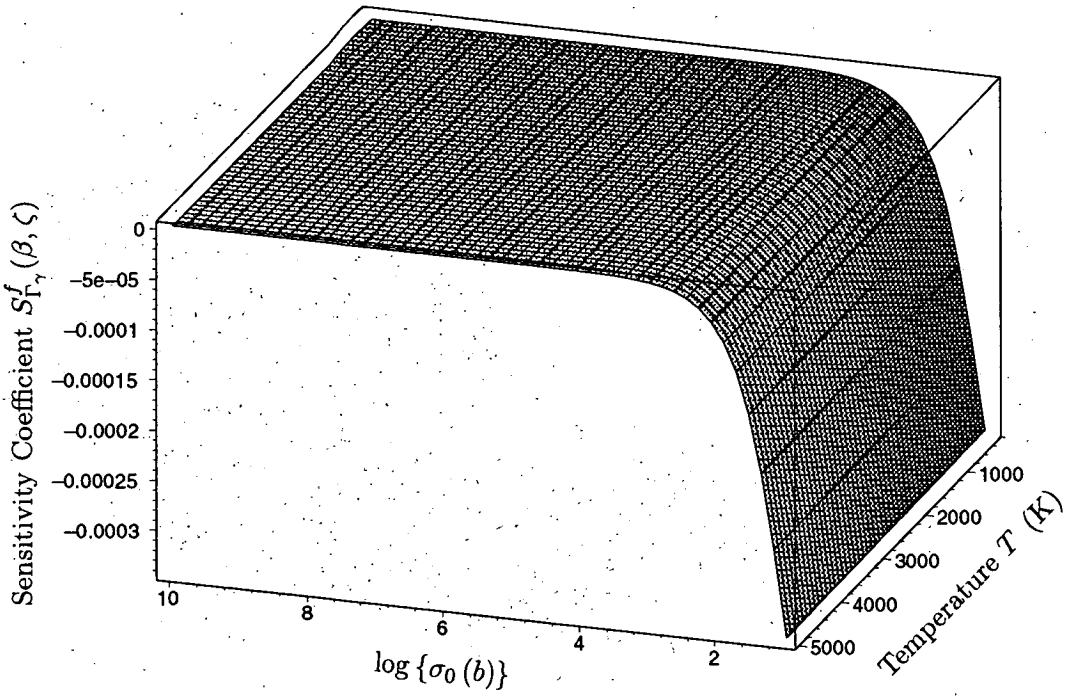

Figure 70: Sensitivity Coefficient $S^f_{\Gamma_\gamma}(\beta,\zeta)$ of f-factor to Radiation Width Γ_γ for ^{239}Pu 214.65 eV Resonance as a Function of σ_0 and T.

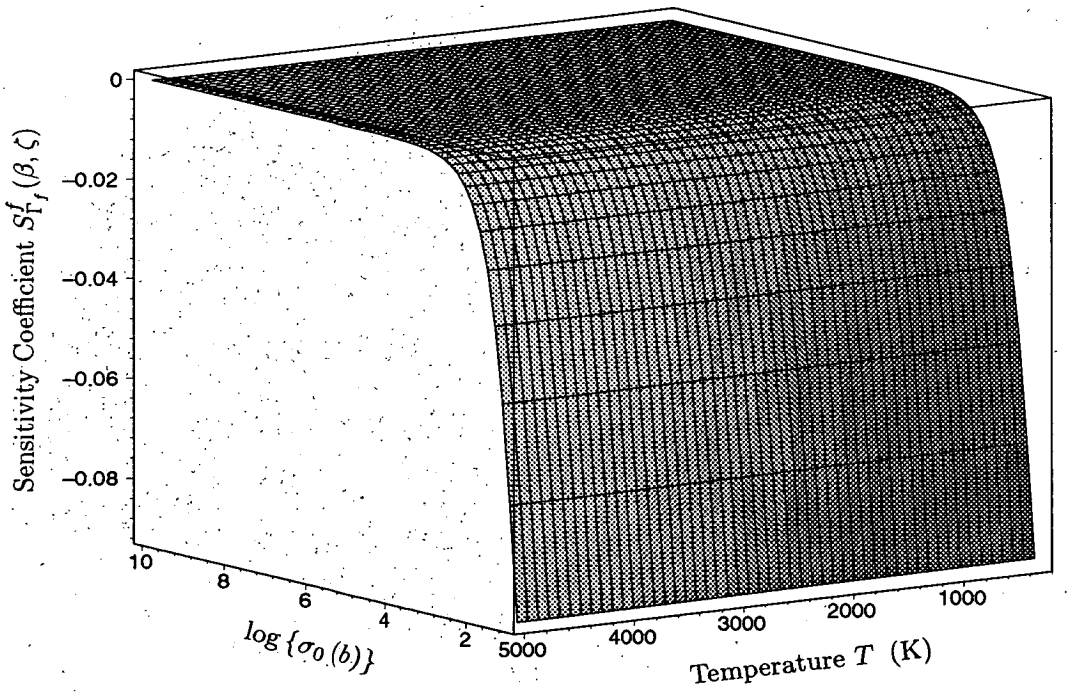

Figure 71: Sensitivity Coefficient $S^f_{\Gamma_f}(\beta,\zeta)$ of f-factor to Fission Width Γ_f for ^{239}Pu 214.65 eV Resonance as a Function of σ_0 and T.

The sensitivity coefficients of f-factor to individual resonance parameter are shown in Fig. 64 to 67 for the ^{238}U 6.67 eV resonance as a narrow resonance, and in Fig. 68 to 71 for the ^{239}Pu 214.65 eV resonance as a wide resonance, respectively. As long as these cases, the ^{239}Pu is less sensitive to resonance parameter as expected from the behaviors of resonance self-shielding factor on the $\sigma_0 - T$ plane as shown in Fig. 44 and 51.

Uncertainty of the resonance self-shielding factor $\frac{\delta f^k_{pik}}{f^k_{pik}}$ of a single resonance due to the uncertainty of the resonance parameter $\frac{\delta \Gamma_{pik}}{\Gamma_{pik}}$ can be estimated by,

$$\frac{\delta f^k_{pi}}{f^k_{pi}} = S^{f^k_{pi}}_{\Gamma_{pik}} \cdot \left(\frac{\delta \Gamma_{pik}}{\Gamma_{pik}}\right). \tag{218}$$

The effective cross section as well as the resonance self-shielding factor of a broad or ultra-fine group is a function of many sets of resonance parameters for many isotopes, and consequently the sensitivity coefficients is also a function of these many parameters. The uncertainty of the broad group resonance self-shielding factor for the reaction x, denoted by $\left(\frac{\delta f_x}{f_x}\right)^g$, can be obtained by the error propagation law with the broad group weighting function $w^{f,k}_{xi}$ as,

$$\left(\frac{\delta f_x}{f_x}\right)^g = \sqrt{\sum_k^{All\,k} \sum_p^{All\,p} \left\{ w^{f,k}_{xi} \cdot S^{f^k_{xi}}_{\Gamma_{pik}} \right\}^2 \cdot \left(\frac{\delta \Gamma_{pik}}{\Gamma_{pik}}\right)^2}. \tag{219}$$

where p: for resonance parameters to be changed, i.e., E_r, Γ_n, Γ_γ and Γ_f, while x: for reaction of interest, i.e., (n,γ) and (n,f)
The weighting function $w^{f_x,k}_{xi}$ can be obtained from the effective resonance self-shielding factor as shown below,

$$w^{f,k}_{xi} = \frac{\lambda^k_{xi} f^k_{xi}(\beta_0,\zeta_0)}{\sum \lambda^k_{xi} f^k_{xi}(\beta_0,\zeta_0)} \tag{220}$$

$$= \frac{\phi_{0k}\left(\frac{\sigma_{0ik}}{E_{rik}}\right)\Gamma_{xik} f^k_{xi}(\beta_0,\zeta_0)}{\sum_{ik}\left[\phi_{0k}\left(\frac{\sigma_{0ik}}{E_{rik}}\right)\Gamma_{xik} f^k_{xi}(\beta_0,\zeta_0)\right]} \tag{221}$$

and the reference point (β_0,ζ_0) can be set on the infinitely diluted system at room temperature for simplicity. The coefficients multiplied by $f(\beta_0,\zeta_0)$ in Eeq. (221) come from the infinitely diluted cross sections.

6.2 Sensitivity Coefficient of Effective Multiplication Factor k_{eff}

The effective multiplication factor k_{eff} defined by Eq. (3) can be explicitly described by the level-wise resonant cross sections multiplied by the f-factor and additional non-resonant cross sections as ;

$$k_{eff} = \frac{\sum_i \sum_k N^i \phi^k \nu^i_k \left(\frac{\sigma^i_{0k}}{E^i_{0k}}\right)\Gamma_{fik} \cdot f_{fik} + \Delta < \nu\Sigma_f\phi >}{\sum_i \sum_k N^i \phi^k \left(\frac{\sigma^i_{0k}}{E^i_{0k}}\right)(\Gamma_{fik}+\Gamma_{\gamma ik}) \cdot \frac{f^k_{ai}}{2} + \Delta < \Sigma_a\phi > + L}, \tag{222}$$

where

i : Isotope indicator,

k : Resonance indicator,

$\Delta(\nu\Sigma_f\phi)$: Non-resonant neutron production rate,

$\Delta(\Sigma_a\phi)$: Non-resonant absorption rate,

f_{fi}^k : Resonance self-shielding factor for fission reaction,

f_{ai}^k : Resonance self-shielding factor for absorption reaction $f_{fi}^k + f_{\gamma i}^k = 2 \cdot f_{fi}^k$.

As evident from the definition Eq. (96) with Eq. (90) of resonance self-shielding factor (f-factor) for an individual resonance in a ultra-fine group k, the fission and capture resonance self-shielding factors are equal to the one another, i.e., $f_{fik} = f_{\gamma ik}$ since the f-factor is a function of β as a function of only total peak cross section as shown by Eq. (91). Therefore, $f_{aik}/2$ in Eq. (222) is equal to f_{fik} or $f_{\gamma ik}$.

The change of k_{eff} due to the change of a resonance parameter $\delta\Gamma_{pik}$ is defined by;

$$\frac{\delta k_{eff}}{k_{eff}} = \sqrt{\sum_i \sum_p \sum_k \left[\left\{ S_{\Gamma_{pik}}^{keff} \right\}^2 \cdot \left(\frac{\delta\Gamma_{pik}}{\Gamma_{pik}} \right)^2 \right]}. \tag{223}$$

The $S_{\Gamma_{pik}}^{keff}$ is the sensitivity coefficient of the k_{eff} against a resonance parameter Γ_{pik} of a reaction $p(= E_r, \Gamma_n, \Gamma_\gamma$ and, Γ_f at k-th resonance position. Explicit forms of the sensitivity coefficients are given by,

$$S_{\bar{\nu}}^{k_{eff}} = \frac{\bar{\nu} < \Sigma_f\phi >}{\bar{\nu} < \Sigma_f\phi > + \Delta(\nu\Sigma_f\phi)}, \tag{224}$$

$$S_{Erik}^{k_{eff}} = -2 \left\{ (\bar{\nu} - k_{eff}) \Lambda_{fk}^i w_{fk}^i - k_{eff} \Lambda_{\gamma k}^i w_{\gamma k}^i \right\}, \tag{225}$$

$$S_{nik}^{k_{eff}} = \left\{ (\bar{\nu} - k_{eff}) \Lambda_{fk}^i w_{fk}^i - k_{eff} \Lambda_{\gamma k}^i w_{\gamma k}^i \right\} \cdot \left(1 - \frac{\Gamma_{nik}}{\Gamma_{ik}} \right), \tag{226}$$

$$S_{\gamma ik}^{k_{eff}} = -\left\{ (\bar{\nu} - k_{eff}) \Lambda_{fk}^i w_{fk}^i \frac{\Gamma_{\gamma ik}}{\Gamma_{ik}} - k_{eff} \Lambda_{\gamma k}^i w_{\gamma k}^i \cdot \left(1 - \frac{\Gamma_{\gamma ik}}{\Gamma_{ik}} \right) \right\}, \tag{227}$$

$$S_{fik}^{k_{eff}} = \left\{ (\bar{\nu} - k_{eff}) \Lambda_{fk}^i w_{fk}^i \left(1 - \frac{\Gamma_{fik}}{\Gamma_{ik}} \right) + k_{eff} \Lambda_{\gamma k}^i w_{\gamma k}^i \cdot \frac{\Gamma_{fik}}{\Gamma_{ik}} \right\}, \tag{228}$$

$$S_{\Gamma_{pik}}^{k_{eff}, f_{xi}^k} = \left\{ (\bar{\nu} - k_{eff}) \Lambda_{fk}^i w_{fk}^i - k_{eff} \Lambda_{\gamma k}^i w_{\gamma k}^i \right\} \cdot S_{\Gamma_{xik}}^{f_{xi}^k}, \tag{229}$$

$$S_{\Gamma_{pik}}^{k_{eff}, L} = \frac{\Gamma_{pik}}{\bar{\nu} < \Sigma_f\phi > + \Delta(\nu\Sigma_f\phi)} \frac{\partial}{\partial\Gamma_{pik}} \left\{ \Delta(\nu\Sigma_f\phi) - k_{eff}\Delta(\Sigma_a\phi) - k_{eff} L \right\}, \tag{230}$$

where $\Gamma_{pik} = E_{rik}$, Γ_{nik}, $\Gamma_{\gamma,ik}$, Γ_{fik}, and L: Leakage Term. and the weighting functions are;

$$\Lambda_{fk}^i = \frac{< \Sigma_f\phi >_k^i}{\bar{\nu} < \Sigma_f\phi > + \Delta(\nu\Sigma_f\phi)}, \tag{231}$$

$$\Lambda^i_{\gamma k} = \frac{< \Sigma_\gamma \phi >^i_k}{\bar{\nu} < \Sigma_f \phi > + \Delta(\nu \Sigma_f \phi)}, \tag{232}$$

$$w^i_{fk} = \frac{N^i \phi^k \left(\frac{\sigma^i_{0k}}{E^i_{0k}}\right) \Gamma_{fik} \cdot f^k_{fi}}{\sum_i \sum_k N^i \phi^k \left(\frac{\sigma^i_{0k}}{E^i_{0k}}\right) \Gamma_{fik} \cdot f^k_{fi}}, \tag{233}$$

$$w^i_{\gamma k} = \frac{N^i \phi^k \left(\frac{\sigma^i_{0k}}{E^i_{0k}}\right) \Gamma_{\gamma ik} \cdot f^k_{\gamma i}}{\sum_i \sum_k N^i \phi^k \left(\frac{\sigma^i_{0k}}{E^i_{0k}}\right) \Gamma_{\gamma ik} \cdot f^k_{\gamma i}}, \tag{234}$$

where the Λ^i_{fk} is for total fission reaction and $\Lambda^i_{\gamma k}$ that for total neutron capture reaction rates relative to the total neutron production rates in the overall energy range, and w^i_{fk} means the weighting function for ultra-fine group resonance fission reaction rate relative to total fission reaction rates in the resonance region of all isotopes, and $w^i_{\gamma k}$ that for total neutron capture rate of the k'th resonance relative to total neutron capture rates in the resonance region of all isotopes. The $S^{ffik}_{\Gamma_{xl}}$ and C^{ffik}_{xl} are sensitivity coefficient of f-factor to resonance parameter Γ_{xl} and coefficient for $S^{ffik}_{\Gamma_{xl}}$, and $< \Sigma_f \phi >^i_k$ and $< \Sigma_\gamma \phi >^i_k$ mean the fission and capture reaction rates of the k-th resonance of i-th isotope, respectively.

6.3 Sensitivity Coefficient of Temperature Coefficient α

The temperature coefficient α can be expressed as a superposition of isotopic temperature coefficient α_{ik} since the k_{eff} is defined by the ratio of neutron production rates to the absorption rates. The α-value is essentially equal to the change of resonance self-shielding factor due to the temperature change when geometric expansion effect is missed. The resultant expression for α is expressed by the temperature sensitivity coefficient of f-factor defined by Eq. (216) as shown below;

$$\alpha(\beta, \zeta) = T \cdot \frac{\partial k_{eff}}{\partial T} = \sum_i \sum_k w^\alpha_{ik} \cdot \alpha_{ik}, \tag{235}$$

$$\alpha_{ik}(\beta, \zeta) = \frac{\{(\bar{\nu} - k_{eff}) \Gamma_{fik} - k_{eff}\, \Gamma_{\gamma ik}\}}{\Gamma_{fik} + \Gamma_{\gamma ik}} \cdot \Big\{ S^f_T(\beta, \zeta) + S^{Ni}_T + S^\phi_T(\beta, \zeta) - k_{eff} \cdot \frac{< DB^2 \phi >}{< \nu \Sigma_f \phi >} S^{<DB^2>}_T \Big\} \tag{236}$$

$$\simeq \frac{\{(\bar{\nu} - k_{eff}) \Gamma_{fik} - k_{eff}\, \Gamma_{\gamma ik}\}}{\Gamma_{fik} + \Gamma_{\gamma ik}} \cdot S^f_T(\beta, \zeta). \tag{237}$$

The numerator $\{(\bar{\nu} - k_{eff}) \Gamma_{fik} - k_{eff}\, \Gamma_{\gamma ik}\}$ of Eq. (237) is proportional to the effective neutron production cross section and the denominator, $\Gamma_{fik} + \Gamma_{\gamma ik}$, is also proportional to the absorption cross section. Therefore, the first term in right-hand side of Eq. (237) means the infinite multiplication factor. The flux terms in both reaction rates are included in the weighting function w^α_{ik} defined by

$$w^\alpha_{ik} = \frac{N_i \phi_k \left(\frac{\sigma_{0ik}}{E_{rik}}\right) (\Gamma_{fik} + \Gamma_{\gamma ik})\, f_{ik}(\beta, \zeta_0)}{\sum_{ik} \left[N_i \phi_k \left(\frac{\sigma_{0ik}}{E_{rik}}\right) (\Gamma_{fik} + \Gamma_{\gamma ik})\, f_{ik}(\beta, \zeta_0) \right]}. \tag{238}$$

Temperature coefficient of the ^{238}U first resonance at $Er = 6.67$ eV is shown in **Fig. 72**. In this case, the Γ_{fik} is zero and the first term of Eq. (237) is $-k_{eff}\left(\frac{\Gamma_{\gamma ik}}{\Gamma_{fik}+\Gamma_{\gamma ik}}\right) < 0$. The α_{ik} is increasing function with temperature on σ_0-axes as expected from the temperature gradient of f-factor and the null α-value above $\sigma_0 > 10^6$ as shown in **Fig. 44**.

Uncertainty of the temperature coefficient $\alpha_{ik}(\beta,\zeta)$ due to the resonance parameters can be obtained by the error propagation law using the sensitivity coefficients as,

$$\frac{\delta\alpha_{ik}}{\alpha_{ik}} = \sqrt{\sum_i \sum_p \sum_k \left[\left\{w^{\alpha}_{ik}\cdot S^{\alpha}_{\Gamma_{pik}}\right\}^2 \cdot \left(\frac{\delta\Gamma_{pik}}{\Gamma_{pik}}\right)^2\right]}. \tag{239}$$

where the sensitivity coefficients for E_{rik}, Γ_{nik}, $\Gamma_{\gamma ik}$, and Γ_{fik} are shown below

$$S^{\alpha}_{E_{rik}} = \frac{\zeta}{2} + \frac{E_{rik}}{S^f_\zeta}\cdot\frac{\partial S^f_\zeta}{\partial E_{rik}} \tag{240}$$

$$S^{\alpha}_{\Gamma_{nik}} = -\zeta\cdot\frac{\Gamma_{nik}}{\Gamma_{ik}} + \frac{\Gamma_{nik}}{S^f_\zeta}\cdot\frac{\partial S^f_\zeta}{\partial\Gamma_{nik}} \tag{241}$$

$$S^{\alpha}_{\Gamma_{\gamma ik}} = -C_{\gamma ik} - \zeta\cdot\frac{\Gamma_{\gamma ik}}{\Gamma_{ik}} + \frac{\Gamma_{\gamma ik}}{S^f_\zeta}\cdot\frac{\partial S^f_\zeta}{\partial\Gamma_{\gamma ik}} \tag{242}$$

$$S^{\alpha}_{\Gamma_{fik}} = C_{fik} - \zeta\cdot\frac{\Gamma_{fik}}{\Gamma_{ik}} + \frac{\Gamma_{fik}}{S^f_\zeta}\cdot\frac{\partial S^f_\zeta}{\partial\Gamma_{fik}} \tag{243}$$

with

$$C_{\gamma ik} = \frac{(\bar{\nu}-k_{eff})\Gamma_{fik}}{(\bar{\nu}-k_{eff})\Gamma_{fik} - k_{eff}\,\Gamma_{\gamma ik}} = \frac{\Gamma_{fik}}{\Gamma_{fik}+\Gamma_{\gamma ik}} \tag{244}$$

$$C_{fik} = \frac{k_{eff}\Gamma_{\gamma ik}}{(\bar{\nu}-k_{eff})\Gamma_{fik} - k_{eff}\,\Gamma_{\gamma ik}} - \frac{\Gamma_{\gamma ik}}{\Gamma_{fik}+\Gamma_{\gamma ik}} \tag{245}$$

and the sensitivity coefficient S^f_ζ of the resonance self-shielding factor to ζ was given by Eq.(212).

6.4 Sensitivity Coefficient of Doppler Reactivity Worth ρ

6.4.1 Reference Case without Correlation between Two Temperature Systems

Doppler reactivity worth is the difference of reactivities between two different temperature systems, namely target and reference systems, and consequently perturbation of the reactivity worth due to the change of resonance parameter are expected in both systems. Even if the perturbations are simultaneously taken placed for both systems in phase, the resultant Doppler reactivity worth is reduced, but if out of phase it is enhanced. Therefore, the sensitivity coefficient can be defined for uncorrelated case when the reference system is fixed and only the target system is perturbed by the change of resonance parameters, and for correlated case between the reference and target temperature systems when the simultaneous changes of resonance parameters are taken placed.

The Doppler reactivity worth ρ_{ik} for a single resonance denoted by ik (i:isotope, k:resonance)

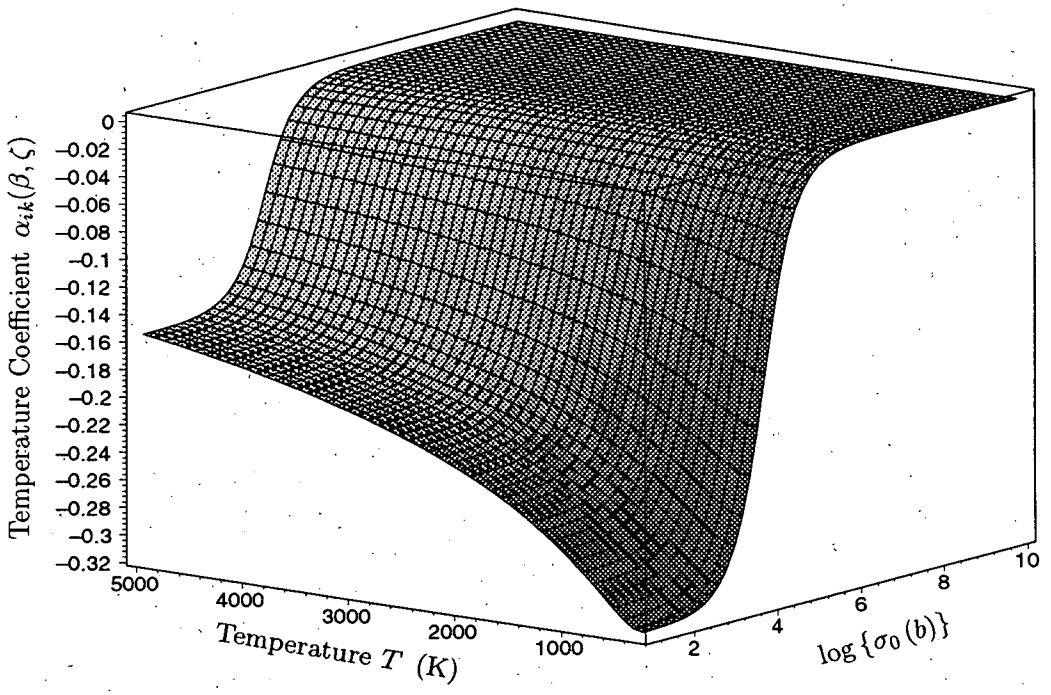

Figure 72: Temperature Coefficient $\alpha_{ik}(\beta,\zeta)$ defined by Eq.(237) of ^{238}U 6.67 eV resonance as a Function of σ_0 and T. This figure is the sign inverted **Fig. 63** since $\alpha_{ik} = \frac{\{(\bar{\nu}-k_{eff})\Gamma_{f\,ik}-k_{eff}\,\Gamma_{\gamma\,ik}\}}{\Gamma_{f\,ik}+\Gamma_{\gamma\,ik}} \times$ **Fig. 63** and the coefficient is -1 for the present ^{238}U 6.67 eV resonance with $\Gamma_{f\,ik} = 0$.

is defined by the direct k-difference as shown by Eq. (17), and the formula for its sensitivity coefficients to a generalized resonance parameter Γ_{pik} including the resonance energy E_r are derived from the sensitivity coefficients of k_{eff} as shown below,

$$\rho_{ik}(\beta,\zeta,\zeta_0) = w^{\rho}_{ki} \cdot \frac{(\bar{\nu}-k_{eff})\Gamma_{f\,ik} - k_{eff}\,\Gamma_{\gamma\,ik}}{\Gamma_{\gamma\,ik}+\Gamma_{f\,ik}} \cdot \frac{f_{ik}(\beta,\zeta) - f_{ik}(\beta,\zeta_0)}{f_{ik}(\beta,\zeta_0)}, \tag{246}$$

with

$$w^{\rho}_{ik} = \frac{N_i\,\phi_k\Delta u^k \left(\frac{\sigma_{0ik}}{E_{rik}}\right)\{(\bar{\nu}-k_{eff})\Gamma_{f\,ik} - k_{eff}\,\Gamma_{\gamma\,ik}\}\,\delta f_{ik}(\beta,\zeta,\zeta_0)}{\sum_{ik}\left[N_i\,\phi_k\Delta u^k \left(\frac{\sigma_{0ik}}{E_{rik}}\right)\{(\bar{\nu}-k_{eff})\Gamma_{f\,ik} - k_{eff}\,\Gamma_{\gamma\,ik}\}\,\delta f_{ik}(\beta,\zeta,\zeta_0)\right]}, \tag{247}$$

where w^{ρ}_{ki} is the weighting function for the k-th resonance contribution relative to total Doppler reactivity worth, and ζ_0 is the reference ζ-value corresponding to the reference temperature $T_0(= 273$ K). The $\bar{\nu}$ is the average neutron yield per fission.

The second term of Eq. (246) is essentially the infinite multiplication factor k_∞ and the third one means the temperature dependence of the effective cross section through the resonance self-shielding factor.

As a typical example, Doppler reactivity worth of the ^{238}U first resonance at $Er = 6.67$ eV is shown in **Fig. 73** as functions of the potential scattering cross section σ_0 and temperature T. The ρ-value at the reference temperature t_0 is vanishing and for larger σ_0 is also vanishing where temperature and σ_0 dependencies are diminished as evident from **Fig. 52**. Below $\sigma_0 \simeq 10^3$ barn, the Doppler reactivity worth ρ_{ik} is monotonously increasing function in absolute like $\rho_{ik} \propto \frac{\Delta f}{f} \propto -\left(\sqrt{\frac{T}{T_0}}-1\right)$ under the assumption $f(T) \propto \sqrt{T}$. It is noticed that the absolute ρ-value is significantly enhanced from $\sigma_0 \simeq 10^3$ and reach to maximum around $\sigma_0 \simeq 10^2$ while

above $\sigma_0 \geq 10^6$ it is completely vanishing.

The other example of Doppler reactivity worth of the wide resonance at $E_r = 214.65$ eV of the ^{239}Pu is shown in **Fig. 74** as functions of the potential scattering cross section σ_0 and temperature T. In this fissionable material, the second term corresponding to k_∞ of Eq. (246) is no longer negative, whose the neutron production term is emphasized and thus the positive ρ-value is given. The magnitude, however, is negligibly small as the result that its f-factor is almost flat along with temperature as shown in **Fig. 51**.

The sensitivity coefficient S^{ρ}_{xik} of the Doppler reactivity worth can be obtained from Eq.

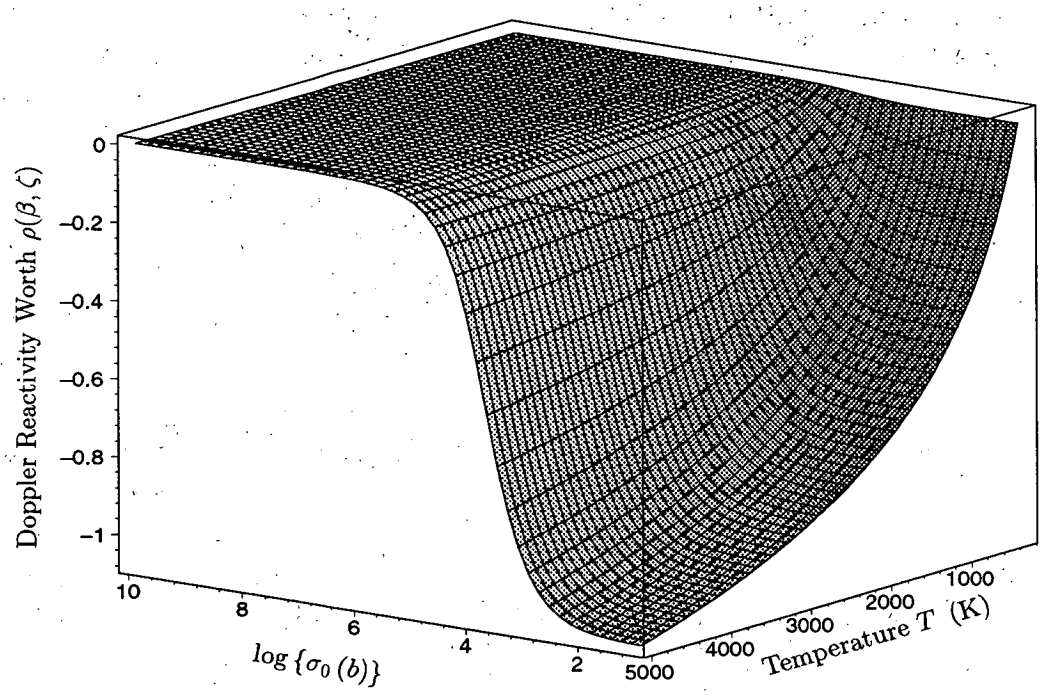

Figure 73: Doppler Reactivity Worth $\rho(\beta,\zeta)$ defined by Eq. (247) for ^{238}U 6.67 eV Resonance as Function of Potential Cross Section σ_0 and Temperature T.

(246). The resultant expressions for individual resonance parameter are shown below

$$S^{\rho}_{E_r}(\beta,\zeta,\zeta_0) = -\frac{3}{2} - F_\beta(\beta,\zeta,\zeta_0) + \frac{1}{2}F_\theta(\beta,\zeta,\zeta_0), \tag{248}$$

$$S^{\rho}_{\Gamma_n}(\beta,\zeta,\zeta_0) = \frac{\Gamma_n}{\Gamma} + \left(1 - \frac{\Gamma_n}{\Gamma}\right) F_\beta(\beta,\zeta,\zeta_0) - \frac{\Gamma_n}{\Gamma} F_\theta(\beta,\zeta,\zeta_0), \tag{249}$$

$$S^{\rho}_{\Gamma_\gamma}(\beta,\zeta,\zeta_0) = \frac{\Gamma_\gamma}{\Gamma}\left\{1 - \frac{k_{eff}\,\Gamma}{(\bar{\nu} - k_{eff})\Gamma_f - k_{eff}\,\Gamma_\gamma} - F_\beta(\beta,\zeta,\zeta_0) - F_\theta(\beta,\zeta,\zeta_0)\right\}, \tag{250}$$

$$S^{\rho}_{\Gamma_f}(\beta,\zeta,\zeta_0) = \frac{\Gamma_f}{\Gamma}\left\{1 + \frac{(\bar{\nu} - k_{eff})\Gamma}{(\bar{\nu} - k_{eff})\Gamma_f - k_{eff}\,\Gamma_\gamma} - F_\beta(\beta,\zeta,\zeta_0) - F_\theta(\beta,\zeta,\zeta_0)\right\}, \tag{251}$$

where for simplicity suffixes ik meaning the isotope and resonance are omitted and auxiliary functions are defined by

$$F_\beta(\beta,\zeta,\zeta_0) = 1 - \Theta_\beta(\beta,\zeta,\zeta_0), \tag{252}$$

$$\Theta_\beta(\beta,\zeta,\zeta_0) = \frac{f(\beta,\zeta)S^f_\beta(\beta,\zeta) - f(\beta,\zeta_0)S^f_\beta(\beta,\zeta_0)}{f(\beta,\zeta) - f(\beta,\zeta_0)}, \tag{253}$$

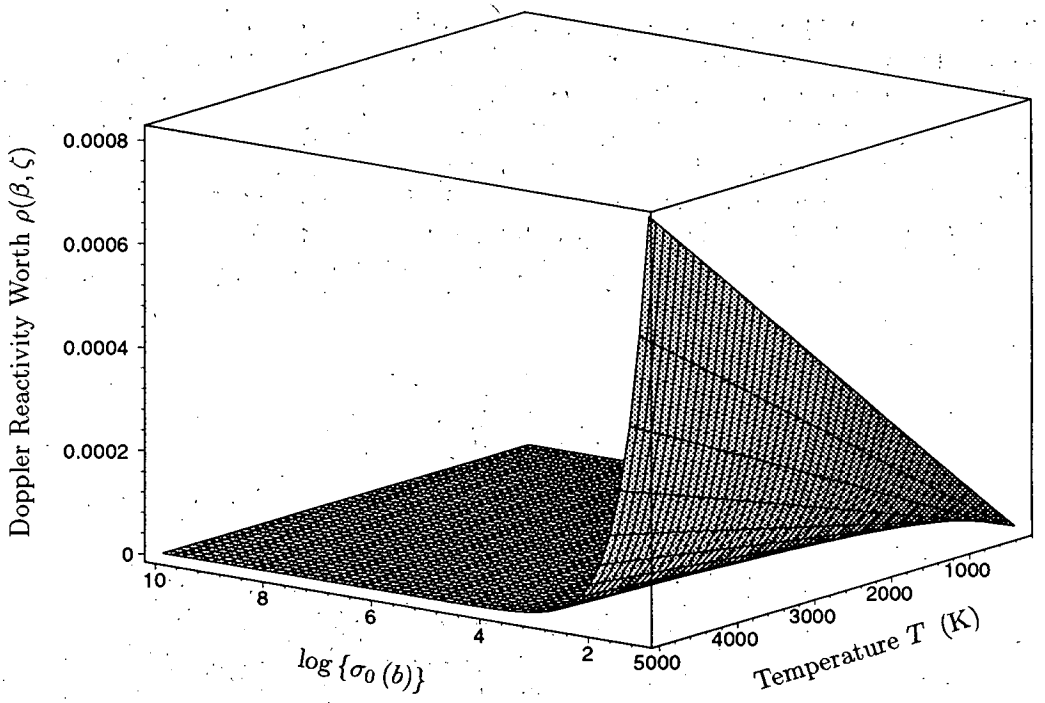

Figure 74: Doppler Reactivity Worth $\rho(\beta,\zeta)$ defined by Eq. (247) for ^{239}Pu 214.65 eV Resonance as Function of Potential Cross Section σ_0 and Temperature T.

$$F_\theta(\beta,\zeta,\zeta_0) = 1 - \Theta_\theta(\beta,\zeta,\zeta_0). \tag{254}$$

$$\Theta_\theta(\beta,\zeta,\zeta_0) = \frac{f(\beta,\zeta)S^f_\theta(\beta,\zeta) - f(\beta,\zeta_0)S^f_\theta(\beta,\zeta_0)}{f(\beta,\zeta) - f(\beta,\zeta_0)}. \tag{255}$$

where the β_θ and Θ_θ functions are introduced in order to define the sensitivity coefficients of Doppler reactivity worth through only the changes of resonance self-shielding factors as defined below.

The sensitivity coefficients defined by Eqs.(248) to (251) include the contributions from resonance self-shielding factors and the others as evident from the definition of the Doppler reactivity worth Eq.(246), i.e., the second term. Considering only the contributions from the resonance self-shielding factor, the Doppler reactivity sensitivity coefficients can be defined by;

$$S^{\rho,f}_{E_r}(\beta,\zeta,\zeta_0) = \Theta_\beta(\beta,\zeta,\zeta_0) - \frac{1}{2}\Theta_\theta(\beta,\zeta,\zeta_0), \tag{256}$$

$$S^{\rho,f}_{\Gamma_n}(\beta,\zeta,\zeta_0) = -\left(1 - \frac{\Gamma_n}{\Gamma}\right)\Theta_\beta(\beta,\zeta,\zeta_0) + \frac{\Gamma_n}{\Gamma}\Theta_\theta(\beta,\zeta,\zeta_0), \tag{257}$$

$$S^{\rho,f}_{\Gamma_\gamma}(\beta,\zeta,\zeta_0) = \frac{\Gamma_\gamma}{\Gamma}\{\Theta_\beta(\beta,\zeta,\zeta_0) + \Theta_\theta(\beta,\zeta,\zeta_0)\} \tag{258}$$

$$S^{\rho,f}_{\Gamma_f}(\beta,\zeta,\zeta_0) = \frac{\Gamma_f}{\Gamma}\{\Theta_\beta(\beta,\zeta,\zeta_0) + \Theta_\theta(\beta,\zeta,\zeta_0)\} \tag{259}$$

The functions $F_\beta(\beta,\zeta,\zeta_0)$ and $F_\theta(\beta,\zeta,\zeta_0)$ are shown in **Figs. 75** to **79** for the narrow resonance of ^{238}U, respectively and those of ^{239}Pu in **Figs. 81** to **85**. Alternative presentations are shown by multiplying the factor δf existing in the weighting function in order to show the effective contributions of the F_β and F_ζ to the sensitivity coefficients.

The F_β is essentially the weighted difference of the f-factors with the weights of β sensitivity

coefficients themselves S_β^f's as defined by Eq. (209) and its trend is similar to the $(1 - S_\beta^f)$. The same interpretation can be made for the $F_\theta(\beta, \zeta, \zeta_0)$. Less sensitive regions for both F_β and F_θ functions can be found in the β range greater than about 10^5 where the f-factor is flat. While, in the sensitive region below $\beta < 10^5$ barn, the temperature dependencies of F_β and F_θ are opposite, i.e., increasing and decreasing, respectively.

The Θ_β and Θ_ζ functions are shown in **Figs. 77** and **80** for ^{238}U 6.67 eV resonance and those for ^{239}Pu 214.56 eV resonance in **Figs. 83** and **86**, respectively. The $\Theta_{\beta/\theta}$ and $F_{\beta/\theta}$ are in the relation of $\Theta_{\beta/\theta} + F_{\beta/\theta} = 1$ as evident from their definitions Eqs.(252) and (254).

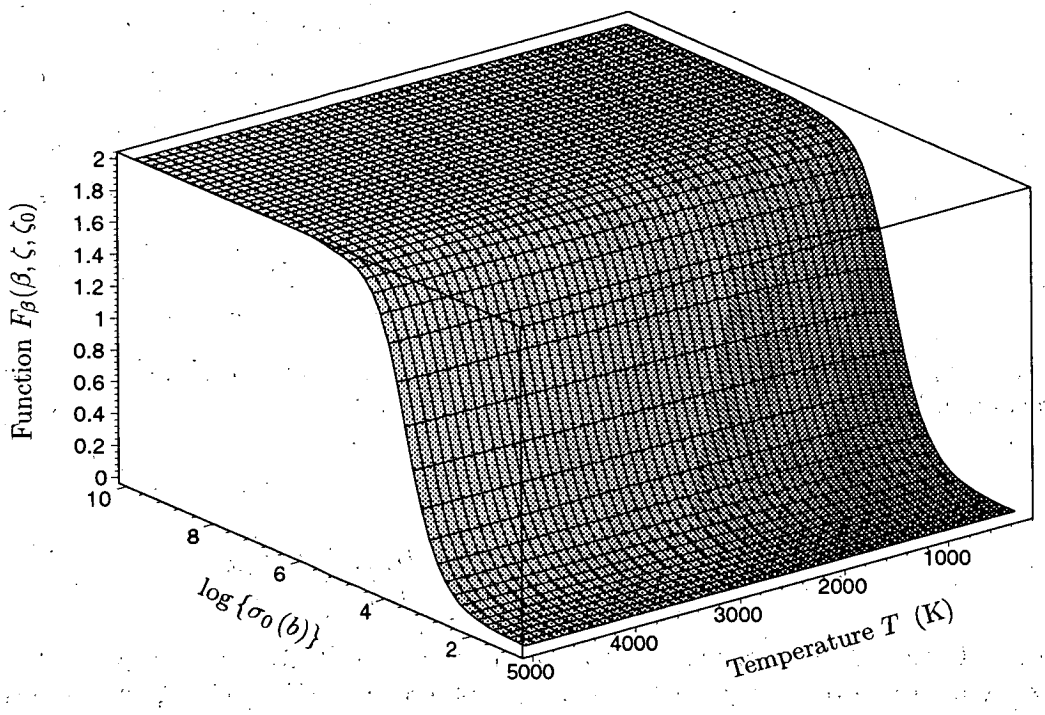

Figure 75: Function $F_\beta(\beta, \zeta, \zeta_0)$ for ^{238}U 6.67 eV Resonance as a Function of σ_0 and T.

Final sensitivity coefficients of the Doppler reactivity worth are shown in **Fig. 87** to **91** for narrow resonance of ^{238}U and those for wide resonance of ^{239}Pu in **Figs. 92** to **95**, respectively. General trends of each sensitivity coefficients are hardly interpreted since they are the second order change of f-factor in a sense of $\rho \propto \delta f(\beta, \zeta)$ and cancellation is made between $f(\beta, \zeta)$ and $f(\beta_0, \zeta_0)$ as well as among resonance parameters.

The uncertainty of the Doppler reactivity worth $\frac{\delta\rho}{\rho}$ can be estimated by the error propagation law as shown below,

$$\frac{\delta\rho}{\rho} = \sqrt{\sum_k^{All\,k} \sum_p^{All\,p} \left\{ S^\rho_{\Gamma_{pik}} \right\}^2 \cdot \left(\frac{\delta\Gamma_{pik}}{\Gamma_{pik}} \right)^2} \tag{260}$$

where Γ_{pik} : E_{rik}, Γ_{nik}, $\Gamma_{\gamma ik}$ and Γ_{fik}. The sensitivity coefficients $S^\rho_{\Gamma_{pik}}$'s were given by Eqs.(248) to (251). In this formula, the contributions from the second term based on the infinitely diluted cross section of Eq. (246) are taken into account. When the Doppler reactivity worth uncertainty due to the change of resonance self-shielding factor is needed, the sensitivity coefficients $S^\rho_{\Gamma_{pik}}$ should be replaced by $S^{\rho f}_{\Gamma_{pik}}$ defined by Eqs. (256) to (259).

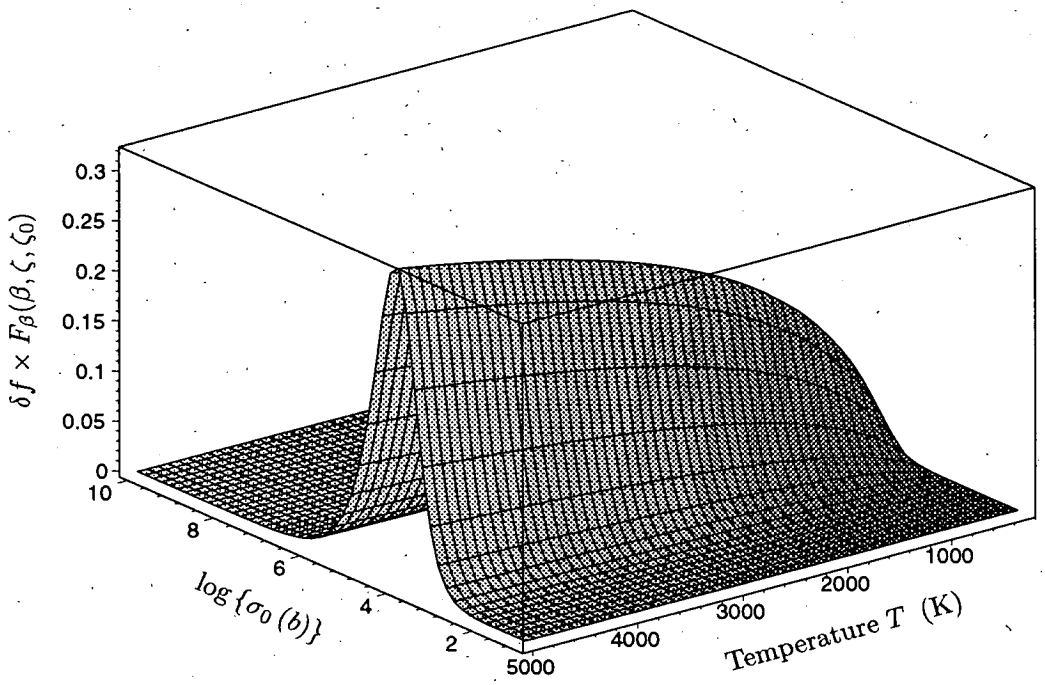

Figure 76: An Alternative Presentation of $F_\beta(\beta, \zeta, \zeta_0)$ shown in **Figure 75**b as $\delta f \cdot F_\beta$. The δf means the difference of f-factors at two different temperatures, i.e.,$\delta f = f(\beta, \zeta) - f(\beta, \zeta_0)$ which comes from the weighting function Eq. (247). This presentation implies the net contribution of F_β to the Doppler reactivity worth.

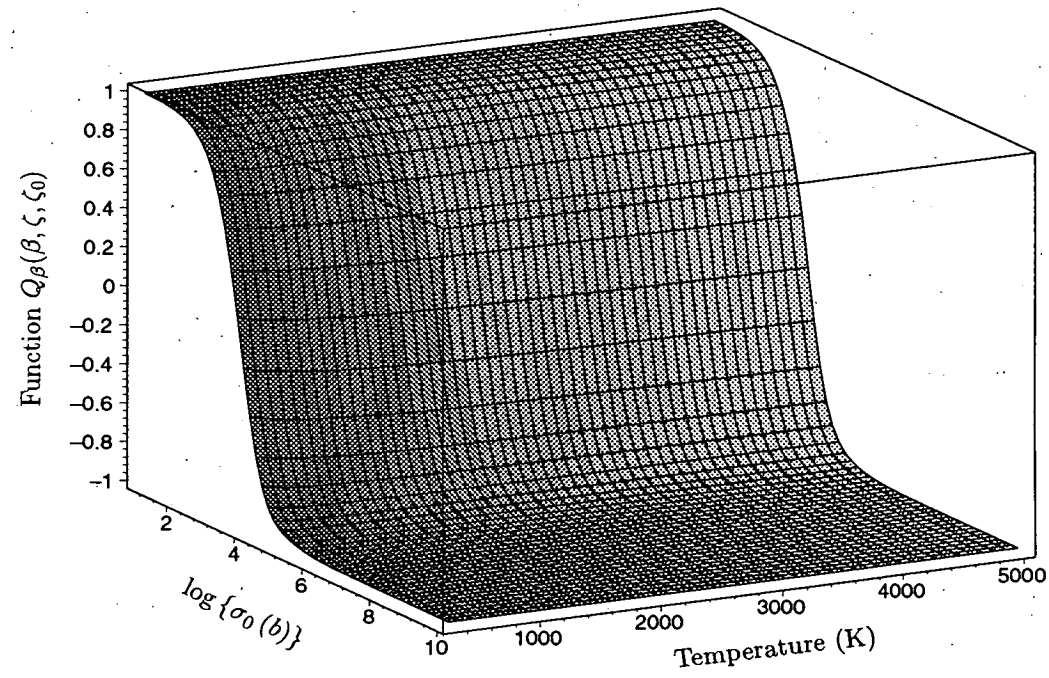

Figure 77: Function $Q_\beta(\beta, \zeta, \zeta_0)$ for ^{238}U 6.67 eV Resonance as a Function of σ_0 and T. Resonance part of F_β.

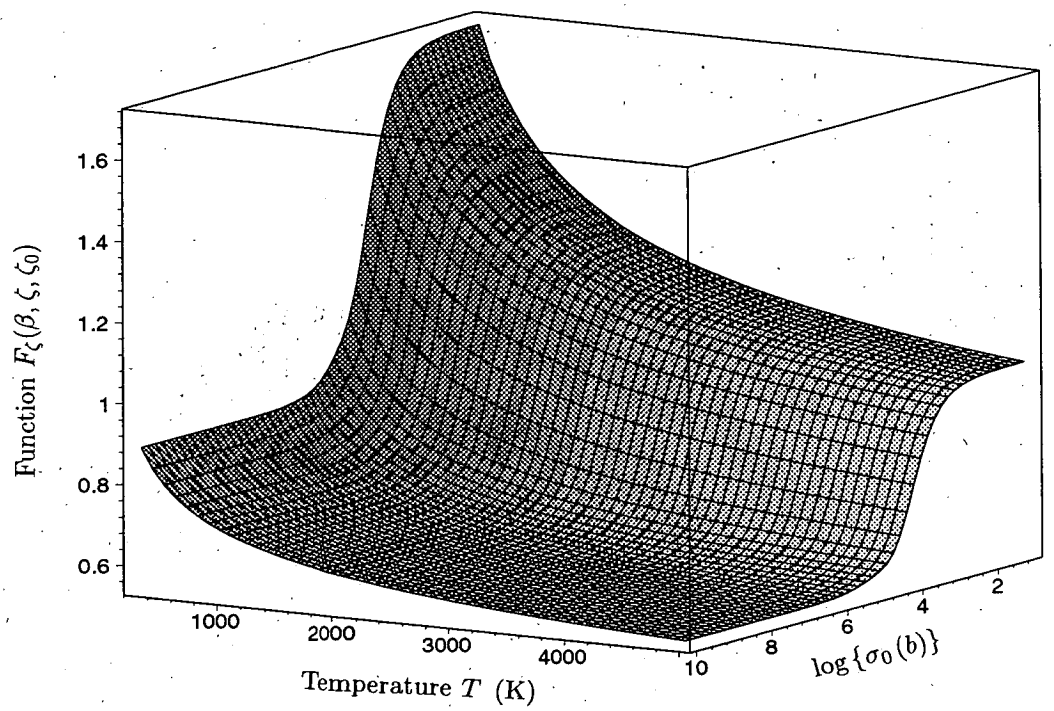

Figure 78: Function $F_\zeta(\beta, \zeta, \zeta_0)$ for ^{238}U 6.67 eV Resonance as a Function of σ_0 and T.

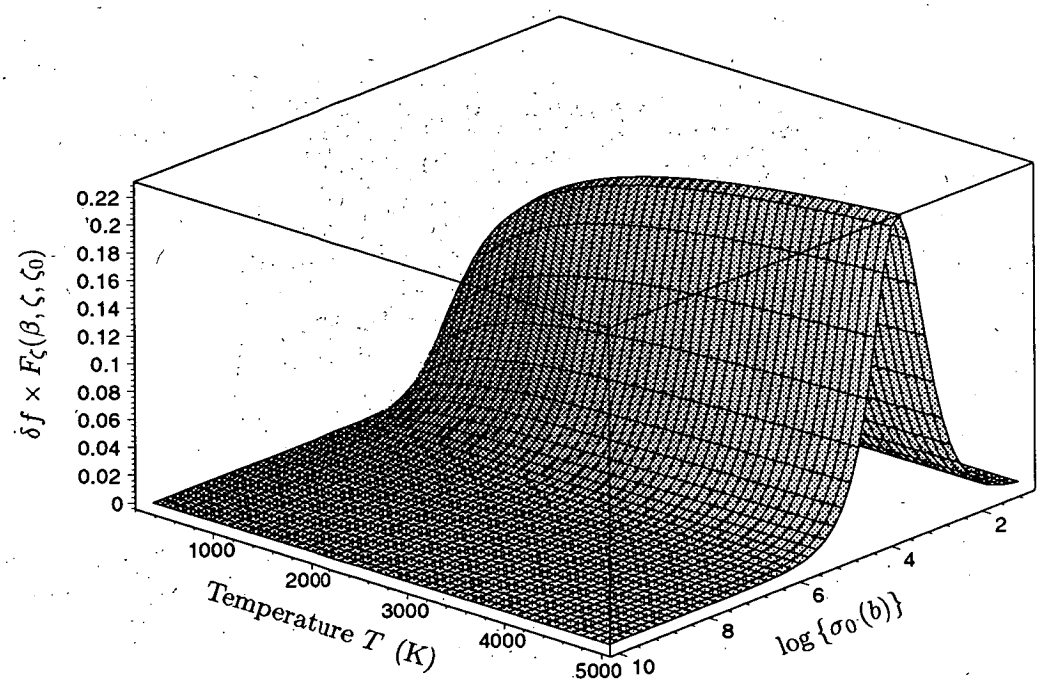

Figure 79: An Alternative Presentation of $F_\zeta(\beta, \zeta, \zeta_0)$ shown in **Figure 78** as $\delta f \cdot F_\zeta$.

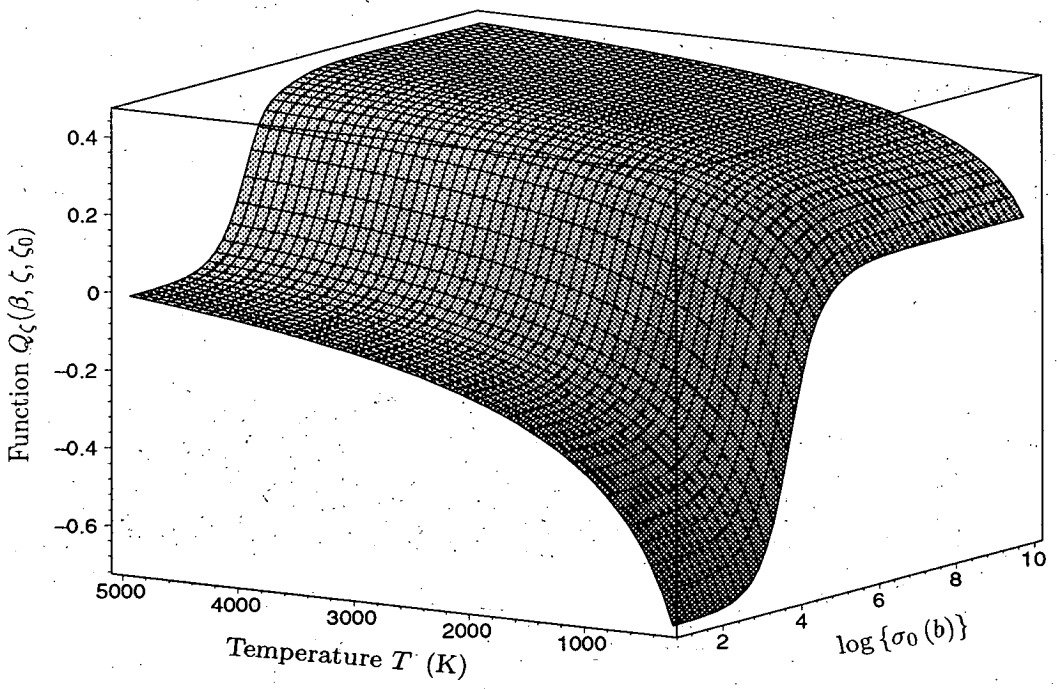

Figure 80: Function $Q_\zeta(\beta,\zeta,\zeta_0)$ for ^{238}U 6.67 eV Resonance as a Function of σ_0 and T. Resonance part of F_ζ.

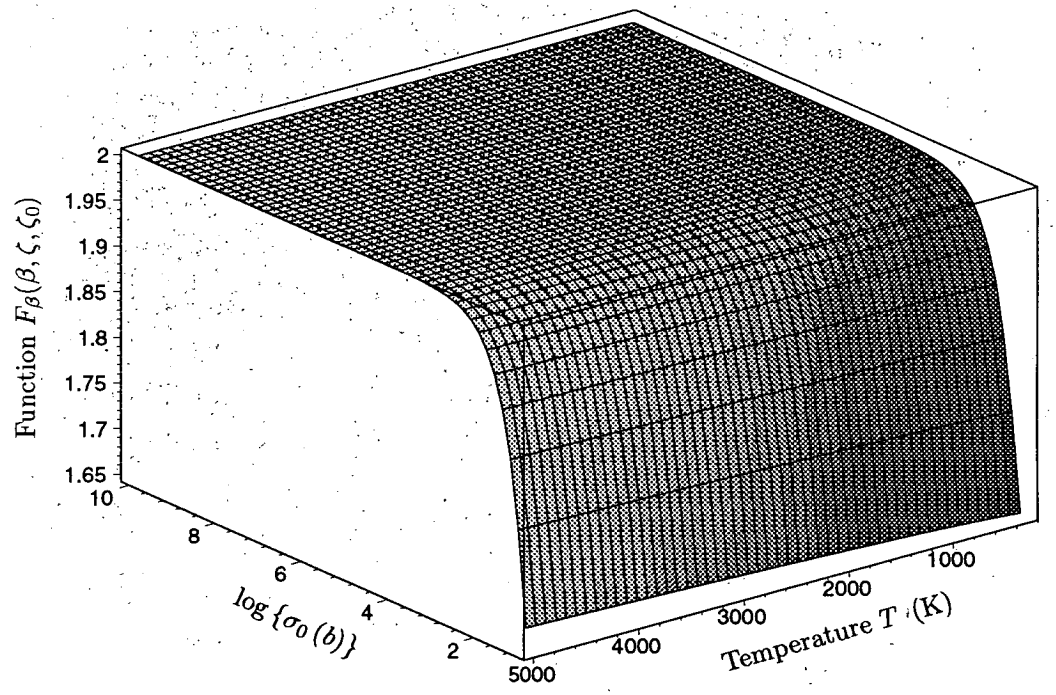

Figure 81: Function $F_\beta(\beta,\zeta,\zeta_0)$ for ^{239}Pu 214.65 eV Resonance as Function of σ_0 and T.

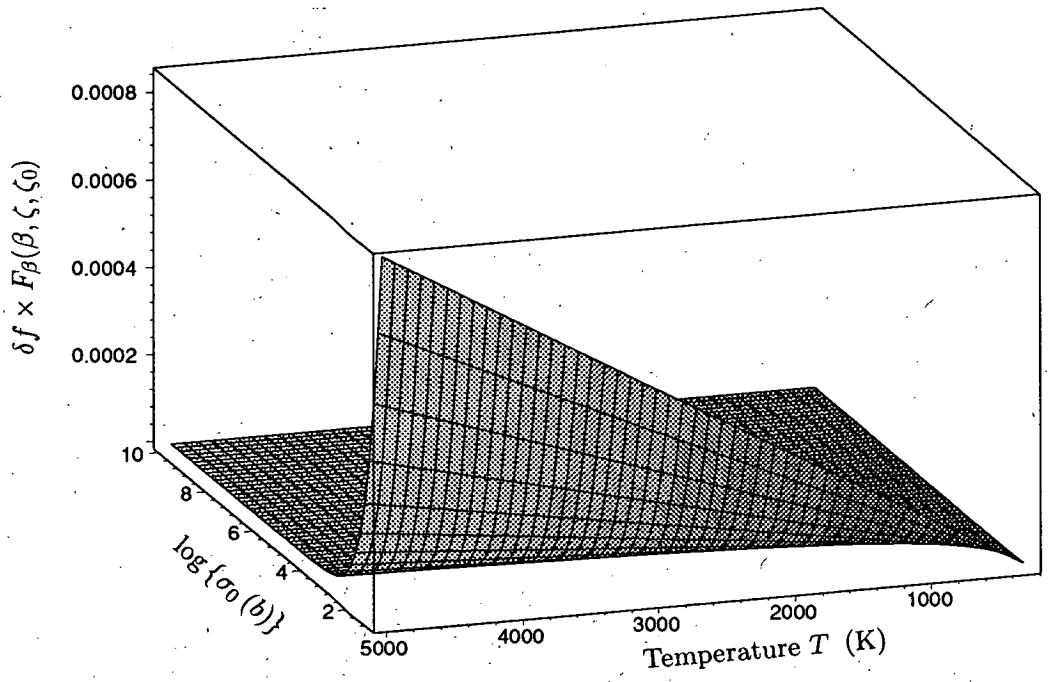

Figure 82: An Alternative Presentation of $F_\beta(\beta, \zeta, \zeta_0)$ shown in **Figure 81** as $\delta f \times Fbt$.

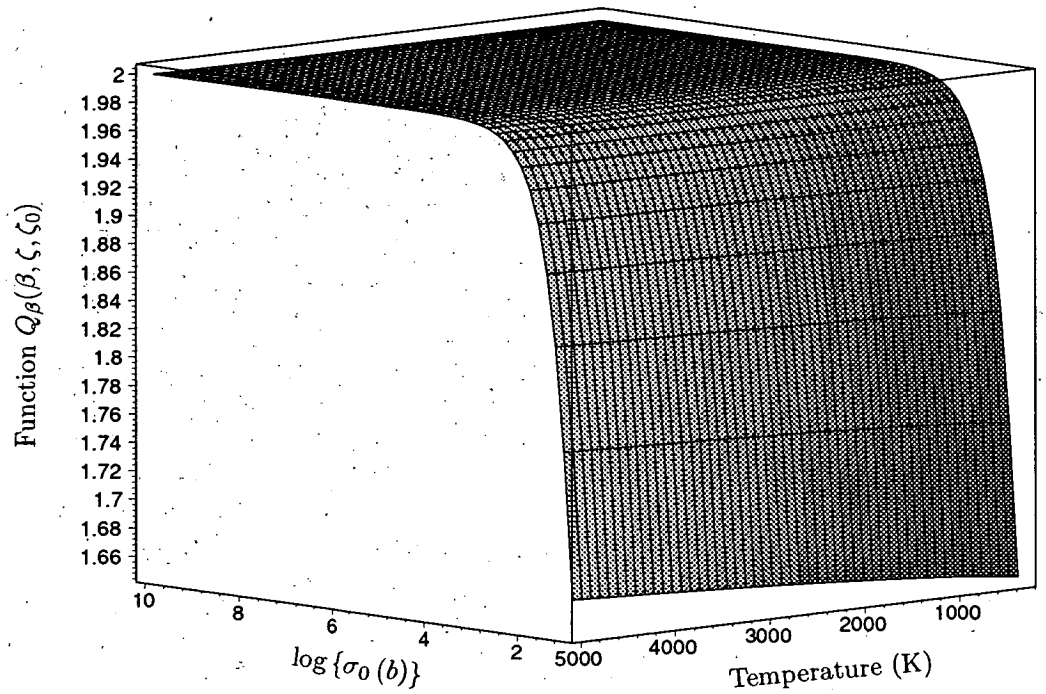

Figure 83: Function $Q_\beta(\beta, \zeta, \zeta_0)$ for ^{239}Pu 214.65 eV Resonance as Function of σ_0 and T. Resonance part of F_β.

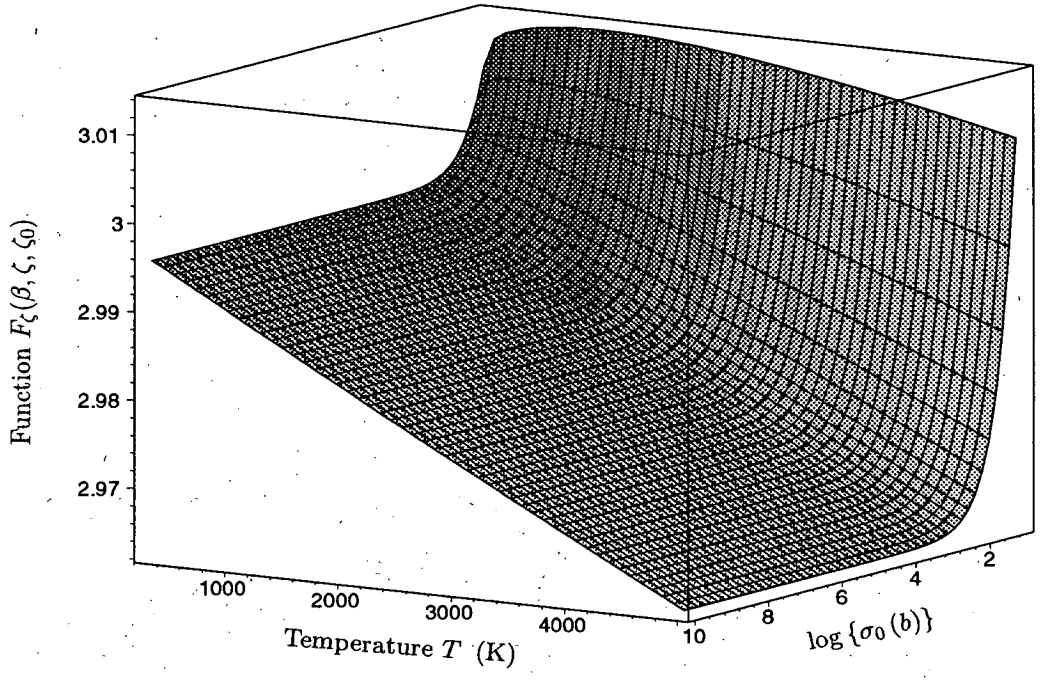

Figure 84: Function $F_\zeta(\beta,\zeta,\zeta_0)$ for ^{239}Pu 214.65 eV Resonance as a Function of σ_0 and T.

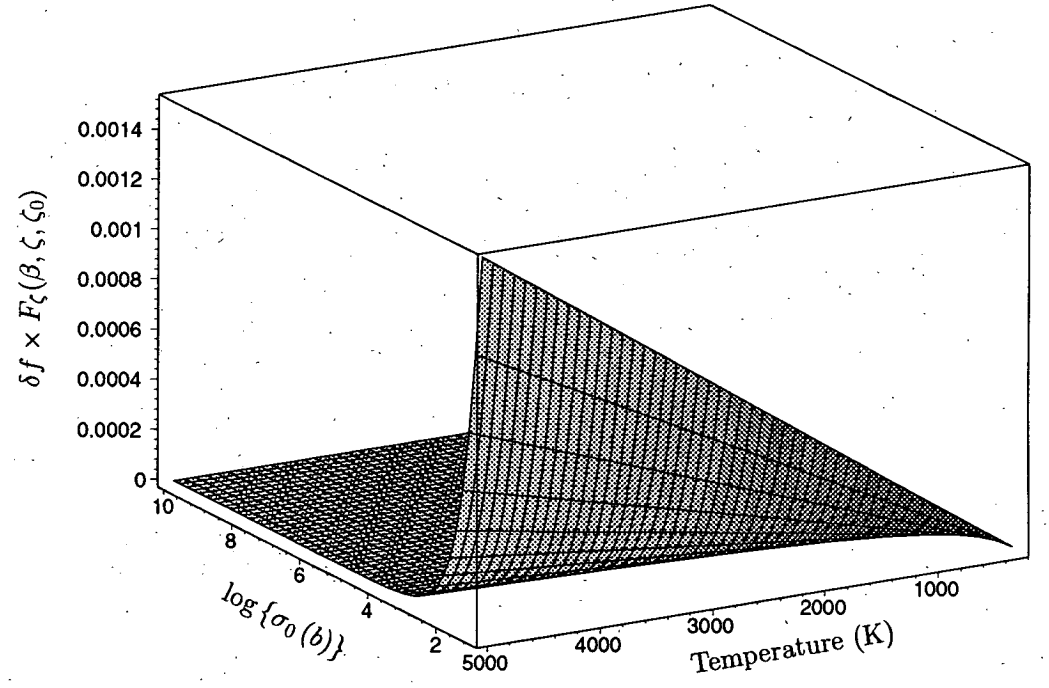

Figure 85: An Alternative Presentation of $F_\zeta(\beta,\zeta,\zeta_0)$ shown in **Figure 84** as $\delta f \cdot F_\zeta(\beta,\zeta,\zeta_0)$.

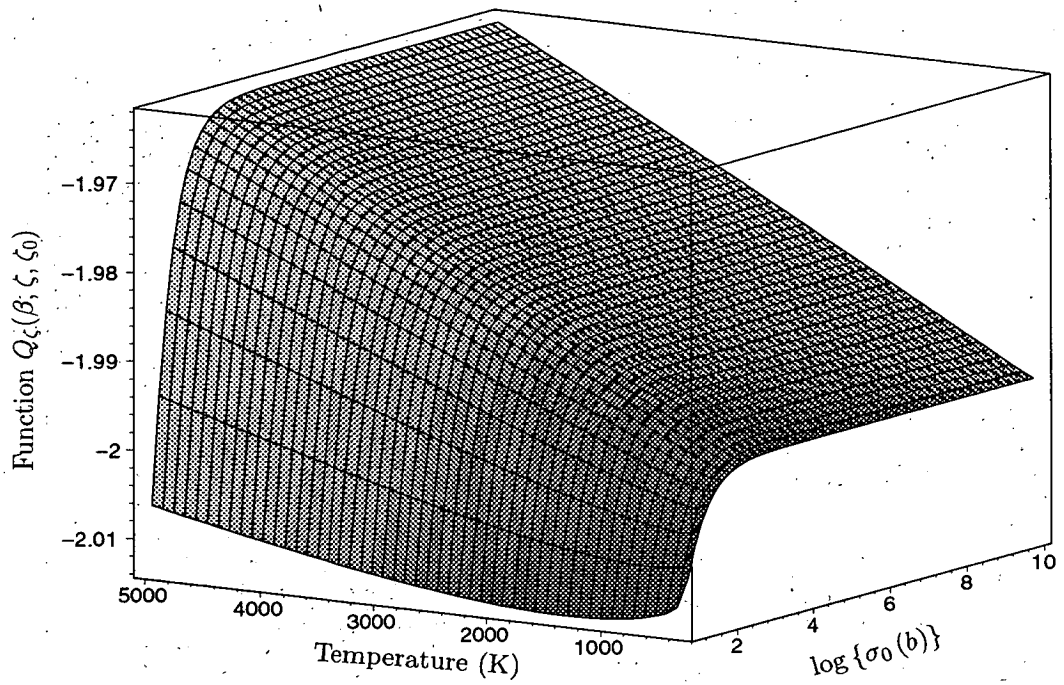

Figure 86: Function $Q_\zeta(\beta,\zeta,\zeta_0)$ for ^{239}Pu 214.65 eV Resonance as a Function of σ_0 and T. Resonance part of F_ζ.

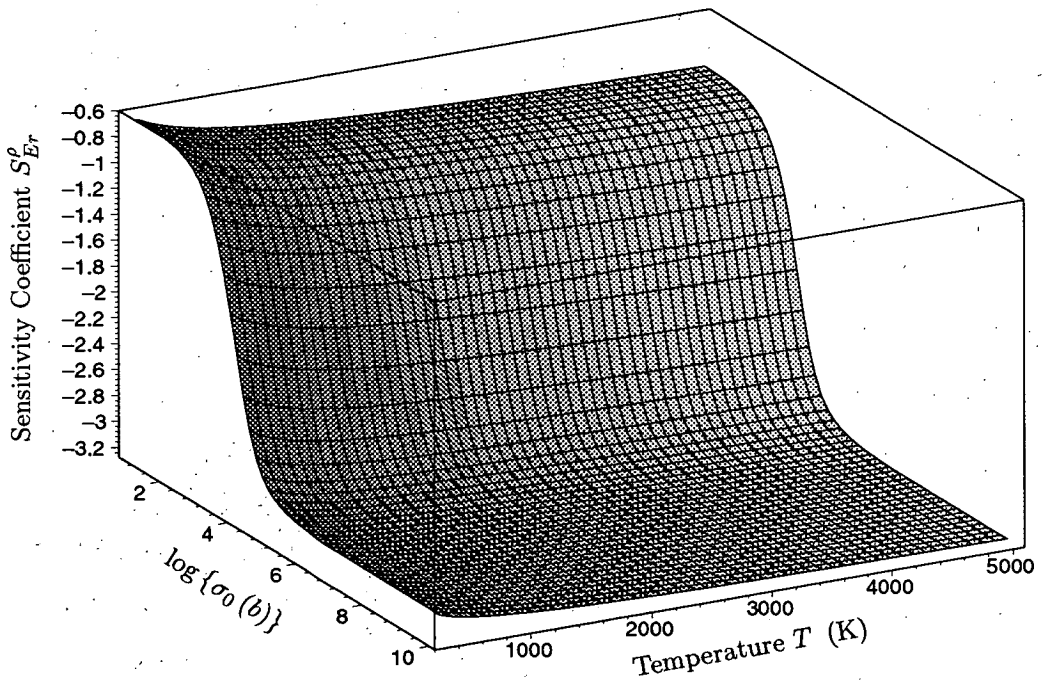

Figure 87: Sensitivity Coefficient S^ρ_{Er} of Doppler Reactivity Worth to Resonance Energy Er for ^{238}U 6.67 eV Resonance as Function of β and ζ.

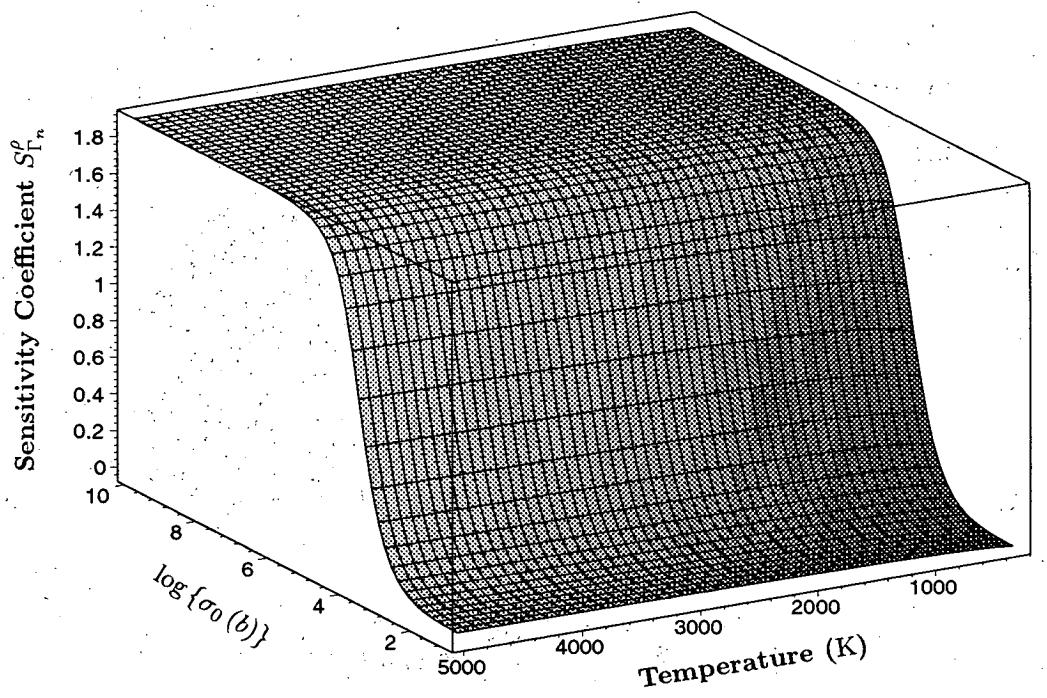

Figure 88: Sensitivity Coefficient $S^{\rho}_{\Gamma_n}$ of Doppler Reactivity Worth to Neutron Width Γ_n for ^{238}U 6.67 eV Resonance as Function of β and ζ.

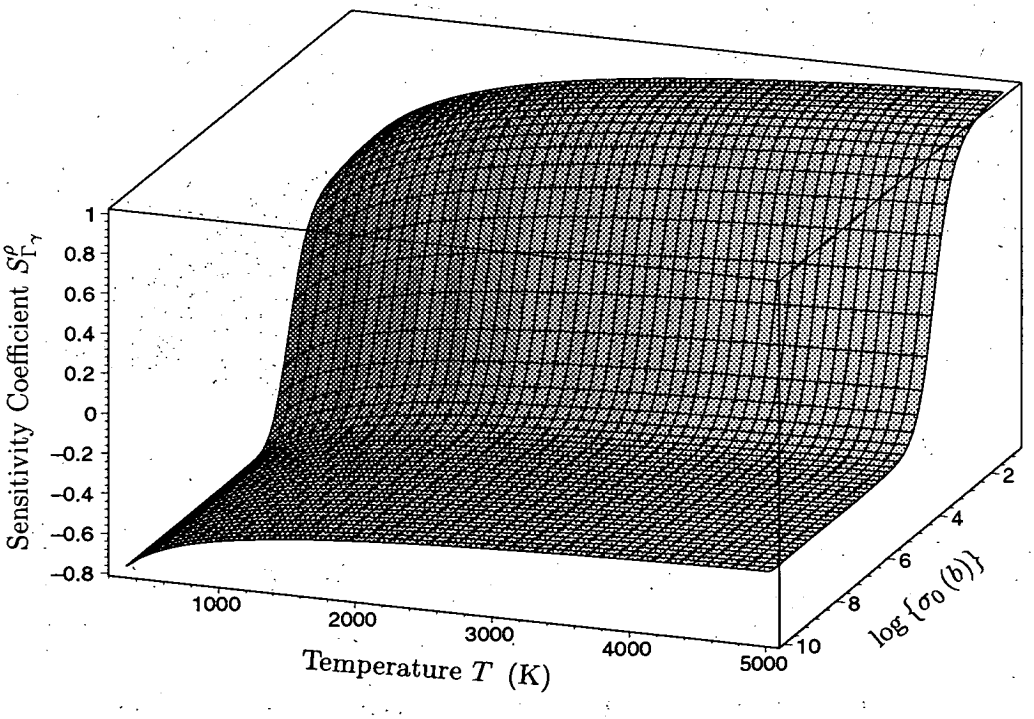

Figure 89: Sensitivity Coefficient $S^{\rho}_{\Gamma_\gamma}$ of Doppler Reactivity Worth to Radiation Width Γ_γ for ^{238}U 6.67 eV Resonance as Function of β and ζ.

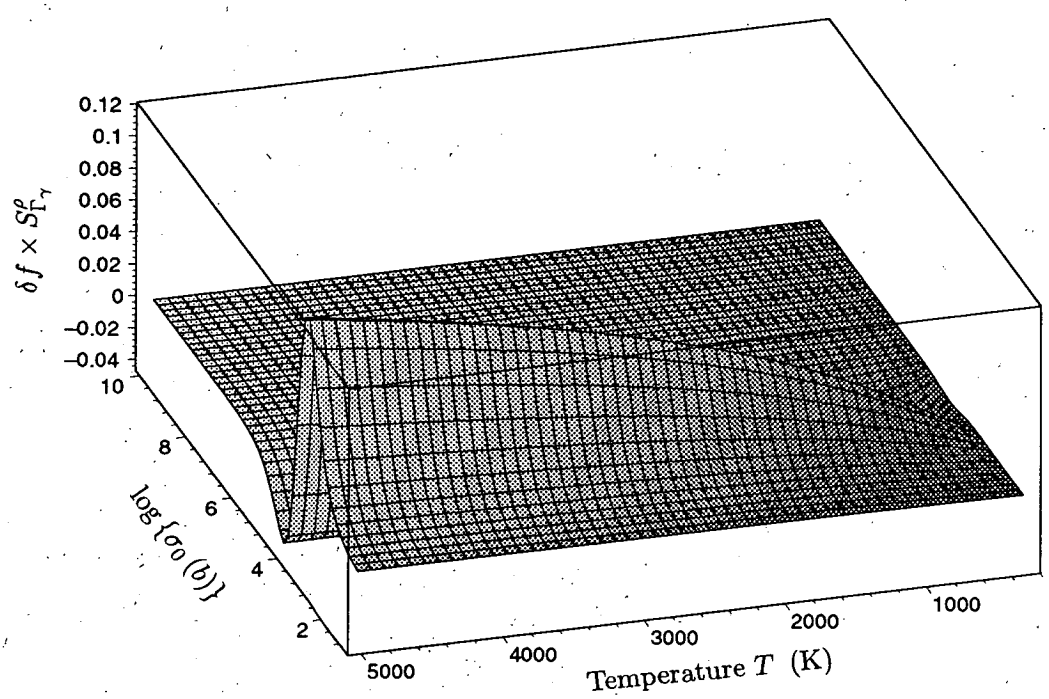

Figure 90: An Alternative Presentation of $S^{\rho}_{\Gamma_\gamma}$ as $\delta f \times S^{\rho}_{\Gamma_\gamma}$.

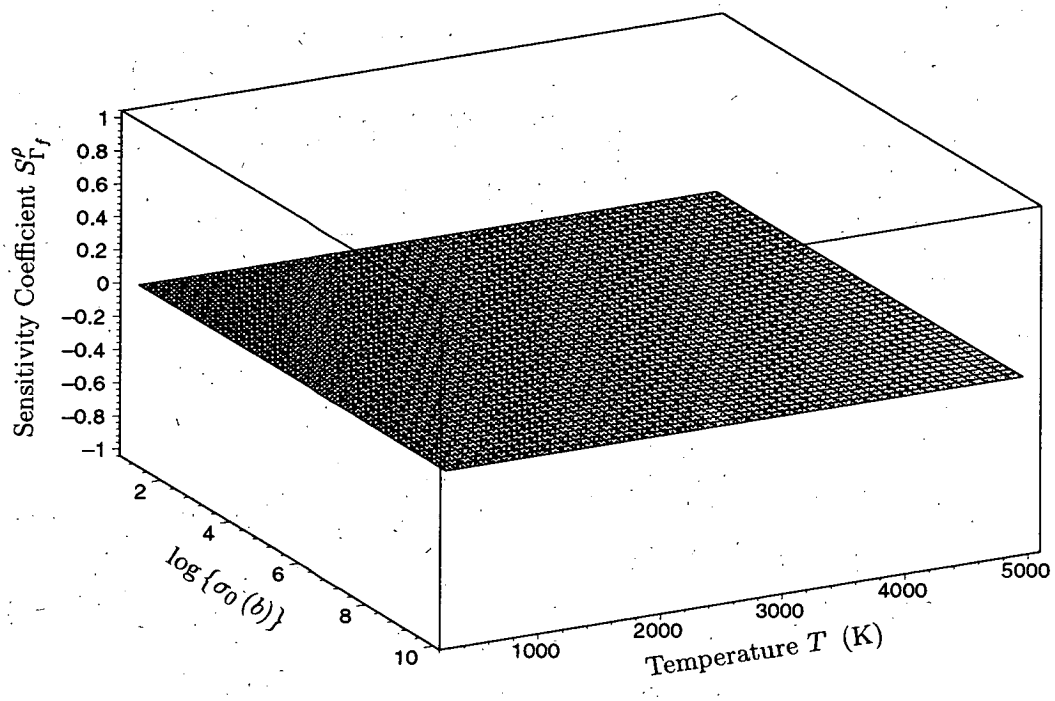

Figure 91: Sensitivity Coefficient $S^{\rho}_{\Gamma_f}$ of Doppler Reactivity Worth to Fission Width Γ_f for ^{238}U 6.67 eV Resonance as Function of β and ζ.

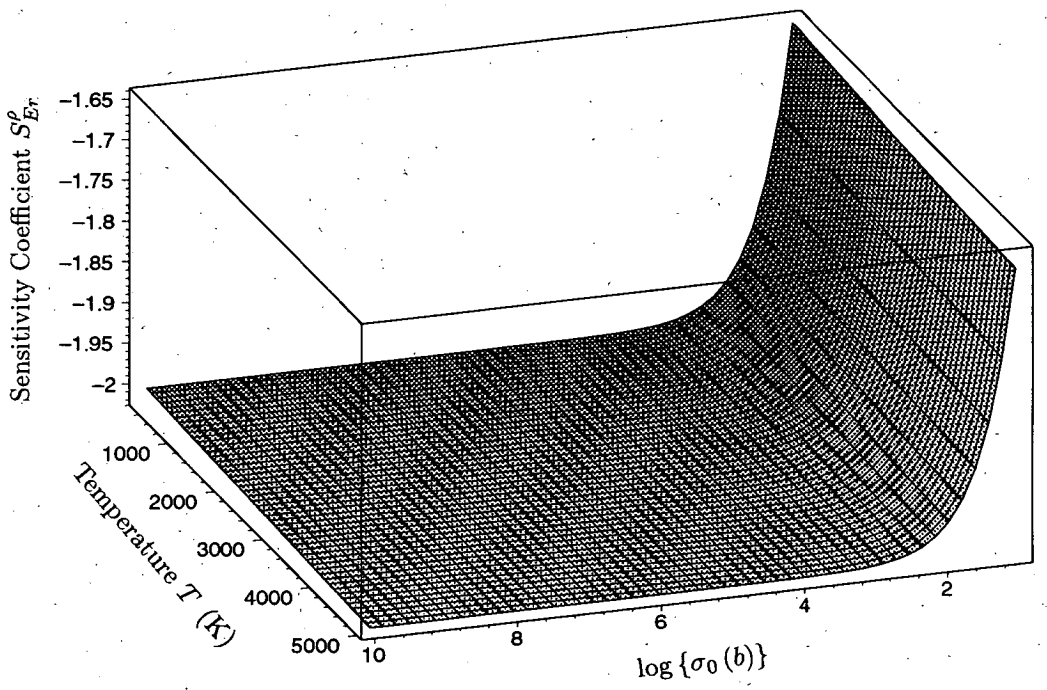

Figure 92: Sensitivity Coefficient S^{ρ}_{Er} of Doppler Reactivity Worth to Resonance Energy Er for ^{239}Pu 214.67 eV Resonance as Function of σ_0 and T.

6.4.2 Correlated Case between Two Temperature Systems

The sensitivity coefficients of Doppler reactivity worth in the reference case were shown by Eqs. (250) and (251). The β sensitivity coefficients $S^f_\beta(\beta,\zeta)$ and $S^f_\beta(\beta,\zeta_0)$ in the F_β function defined by Eq. (252) have the same signs and thus a cancellation between them is taken placed so as to reduce the net sensitivity coefficient. The same trend is also expected for F_θ function.

Statistically, the probability finding that a temperature system has a set of resonance parameters belonging to some statistical distribution may be independent on the other system, and consequently some correlation between both terms having ζ and ζ_0 in the numerator of Eqs. (252) and (254) may be expected.

Composite probability density function for a system to be in temperature T^s_i and to have resonance parameter Γ^s_{pi} in a system "s" can be expressed by;

$$Pr(T^s_i,\Gamma^s_{pi}) = \frac{1}{2\,\sigma_{T_i}\sigma_{p_i}\sqrt{1-\gamma^2_{T_i p_i}}}\cdot exp\left\{-\frac{1}{2}\cdot Q_{pr}(T^s_i,\Gamma^s_{pi})\right\}, \tag{261}$$

$$Q_{pr}(T^s_i,\Gamma^s_{pi}) = \frac{1}{1-\gamma_{Tipi}{}^2}\left\{\left(\frac{T^s_i-\overline{T^s_i}}{\sigma_{T_i}}\right)^2+\left(\frac{\Gamma^s_{pi}-\overline{\Gamma^s_{pi}}}{\sigma_{\Gamma^s_{pi}}}\right)^2 -2\gamma_{T_i p_i}\cdot\left(\frac{T^s_i-\overline{T^s_i}}{\sigma_{T^s_i}}\right)\left(\frac{\Gamma^s_{pi}-\overline{\Gamma^s_{pi}}}{\sigma_{\Gamma^s_{pi}}}\right)\right\}, \tag{262}$$

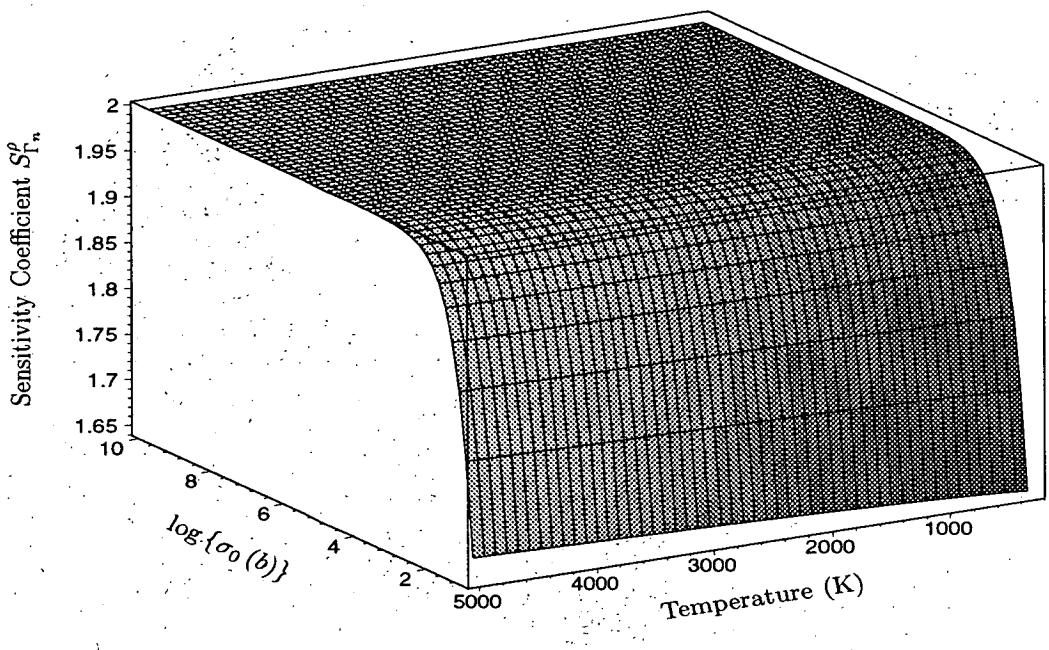

Figure 93: Sensitivity Coefficient $S^{\rho}_{\Gamma_n}$ of Doppler Reactivity Worth to Neutron Width Γ_n for ^{239}Pu 214.67 eV Resonance as Function of σ_0 and T.

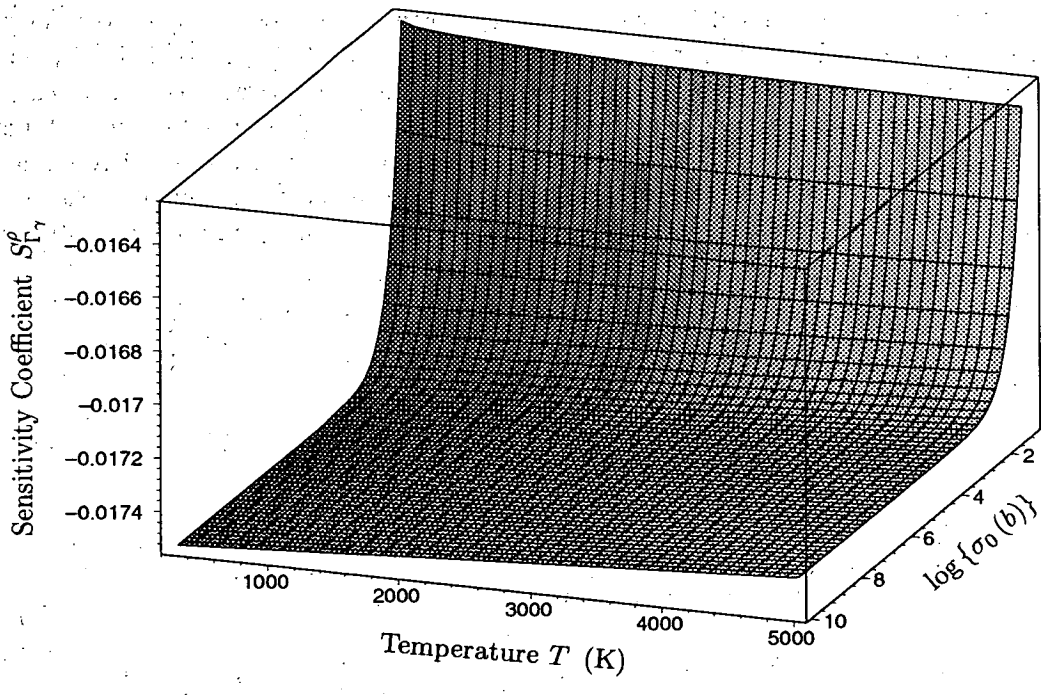

Figure 94: Sensitivity Coefficient $S^{\rho}_{\Gamma_\gamma}$ of Doppler Reactivity Worth to radiation Width Γ_γ for ^{239}Pu 214.67 eV Resonance as Function of σ_0 and T

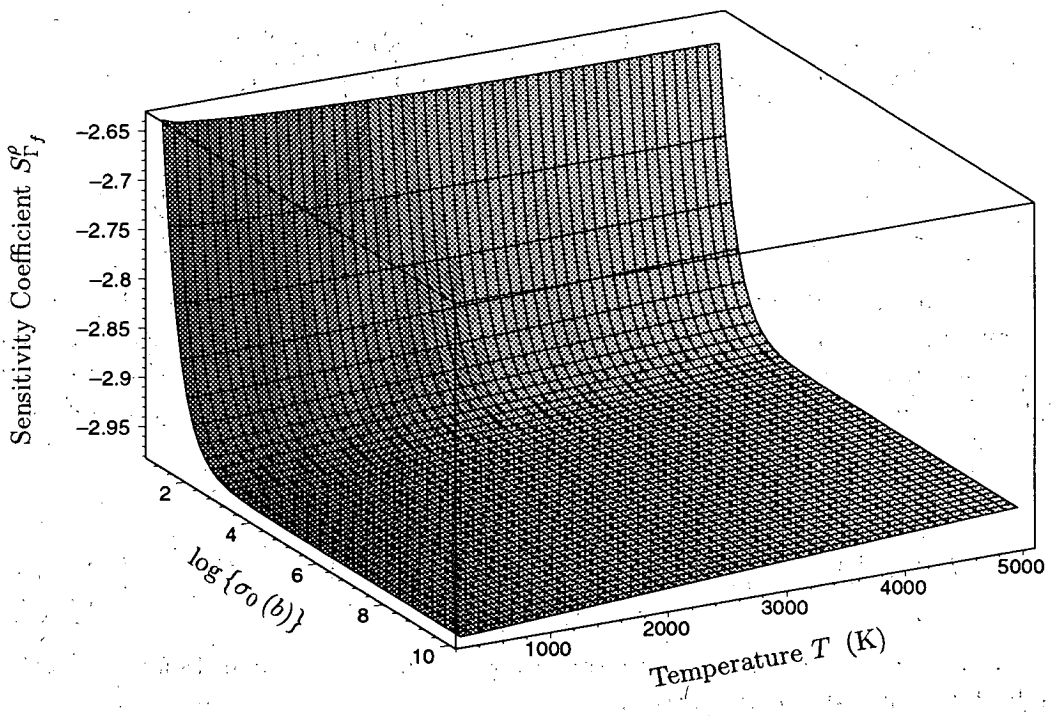

Figure 95: Sensitivity Coefficient $S^{\rho}_{\Gamma_f}$ of Doppler Reactivity Worth to Fission Width Γ_f for ^{239}Pu 214.67 eV Resonance as Function of σ_0 and T.

where

s : System indicator; $s = 0, 1$,

$\overline{T_i^s}$: Temperature expectation value,

$\overline{\Gamma_{pi}^s}$: Resonance parameter expectation value,

σ_{T_i} : Variance of T_i^s,

$\sigma_{\Gamma_{pi}^s}$: Variancee of Γ_{xi}^s.

γ_{Tipi} : Correlation coefficient between T_i^T and Γ_{pi}^r.

The "System" means a reactor core system which has a set of resonance parameters Γ_{pi}^s's at a definite temperature T_i^s under the same geometry and composition. For instance, consider the Doppler sample experiment, there exits a sample system having two temperatures $T_i^0 \pm \sigma_{T_i^0}$ and $T_i^1 \pm \sigma_{T_i^1}$, and two different sets of resonance parameters $\Gamma_{pi}^0 \pm \sigma_{\Gamma_{pi}^0}$ and $\Gamma_{pi}^1 \pm \sigma_{\Gamma_{pi}^1}$ where the $\sigma_{T_i^s}$, $(s = 0, 1)$ means the uncertainty of sample temperature and $\sigma_{\Gamma_{pi}^s}$ the uncertainty of resonance parameters in one standard deviations.

In general, the uncertainty of the temperature may be a few degrees and its effect to the Doppler reactivity may be negligibly small. While, the correlation between the temperature and resonance parameter can not be expected as long as the evaluated resonance parameters are used since the Doppler effect to the resonance cross section and/or resonance area had been removed by the experimenters and/or nuclear data evaluators.

The probability density function for two sets of resonance parameters can be expressed in the similar equation to Eq. (261) with the following argument Q_{pr}^{Γ};

$$Q^{\Gamma}_{pri} = \frac{1}{1-\gamma_{01pi}{}^2}\left\{\left(\frac{\Gamma^0_{pi}-\overline{\Gamma^0_{pi}}}{\sigma_{\gamma^0_{pi}}}\right)^2+\left(\frac{\Gamma^1_{pi}-\overline{\Gamma^1_{pi}}}{\sigma_{\Gamma^1_{pi}}}\right)^2 -2\gamma_{01pi}\cdot\left(\frac{\Gamma^0_{pi}-\overline{\Gamma^0_{pi}}}{\sigma_{\Gamma^0_{pi}}}\right)\left(\frac{\Gamma^1_{pi}-\overline{\Gamma^1_{pi}}}{\sigma_{\Gamma^{1s}_{pi}}}\right)\right\}. \quad (263)$$

The correlation factor denoted by γ_{01pi} between the resonance parameters Γ^0_{pi} for reference system and Γ^1_{pi} for perturbed system is vanishing in the sense that a choice of a resonance parameter in the reference system does not affect the perturbed system and vise versus, i.e., the error distributions in both systems are quite independent. Consequently, the probability density distribution function is

$$Pr(\Gamma^0_{pi},\Gamma^1_{pi}) = \frac{1}{2\pi\sigma^0_{pi}\sigma^1_{pi}}\cdot exp\left[-\frac{1}{2}\cdot\left\{\left(\frac{\Gamma^1_{pi}-\overline{\Gamma^1_{pi}}}{\sigma^1_{pi}}\right)^2+\left(\frac{\Gamma^0_{pi}-\overline{\Gamma^0_{pi}}}{\sigma^0_{pi}}\right)^2\right\}\right]. \quad (264)$$

Therefore, the probability finding the resonance parameters in the one standard deviation(1σ) in the both systems can be obtained by

$$Prob = \frac{1}{2\pi}\int_{-1}^{+1}\int_{-1}^{+1} exp\left[-\frac{1}{2}\left\{(x_0)^2+(x_1)^2\right\}\right]dx_0dx_1 \quad (265)$$

$$= \left[\frac{1}{2\pi}\int_{-1}^{+1} exp\left(-\frac{1}{2}\cdot x^2\right)dx\right]^2 = 0.46606 \quad (266)$$

In order to consider the correlation and to define an effective F_β as well as F_ζ functions, the correlation factor γ_{TT_0} is introduced as;

$$(f\cdot S-f_0S_0)^2_{eff} = (f\cdot S)^2+(f_0S_0)^2+2\cdot\gamma_{TT0}\cdot f\,f_0S\,S_0, \quad (267)$$

$$= (f\cdot S-f_0S_0)^2+2\cdot(1+\gamma_{TT0})\cdot f\,f_0S\,S_0, \quad (268)$$

where the left-handed term means the effective numerator in the correlated case and suffixes or superscripts are missed for simplicity. As evident from the above definition, the $\gamma_{TT_0}=-1$ is completely anti-correlation case as shown by Eq. (252) or (254). Contrarily, if $\gamma_{TT_0}=0$, $(f\cdot S-f_0S_0)^2_{eff}=(f\cdot S)^2+(f_0S_0)^2$ which implies completely random without correlation. Therefore, The possible range of γ_{TT_0} is from 0 to -1. A typical γ_{TT_0}-value is about -0.46 as shown by Eq. (266).

The *Fbt*-value is shown in **Fig. 96** as function of the potential scattering cross section and temperature under the assumption $\gamma_{TT_0}=-0.46$ and its alternative presentation with help of **Fig. 97** is shown in **Fig. 98**. Significantly rapid change of F_{bt}-value is found around the reference temperature $T_0=293$ (k) since the denominator of Eq. (252) is vanishing. Such a trend is unavoidable as far as the Doppler effect is based on the relative change of the resonance self-shielding factor. As shown in **Fig. 98**, this rapid change, however, is flattened by multiplying the difference term $\delta f_{ik}=f_{ik}(\beta,T)-f_{ik}(\beta,T_0)$ of the weighting function Eq. (247). A dip abound $\log(\sigma_0)=3$ comes from the second term of Eq. (268) for the interference between two temperature systems as evident from the comparison with **Fig. 76** without the interference

and the derivative of f-factor changes its sign around $\sigma_0 = 10^4$ as shown in **Fig. 58**. Similar behaviors are found in the **Fig. 98** concerning the β derivatives of f-factor. In the both wings of σ_0, the $\delta f \cdot F_\beta$ tends to zero because of $\frac{\partial f}{\partial \beta} = 0$ in the both sides of the turning point of f-factor as shown in **Fig. 52**.

The another intermediate function Fzt is shown in **Figs. 99** and **100**. In this case,

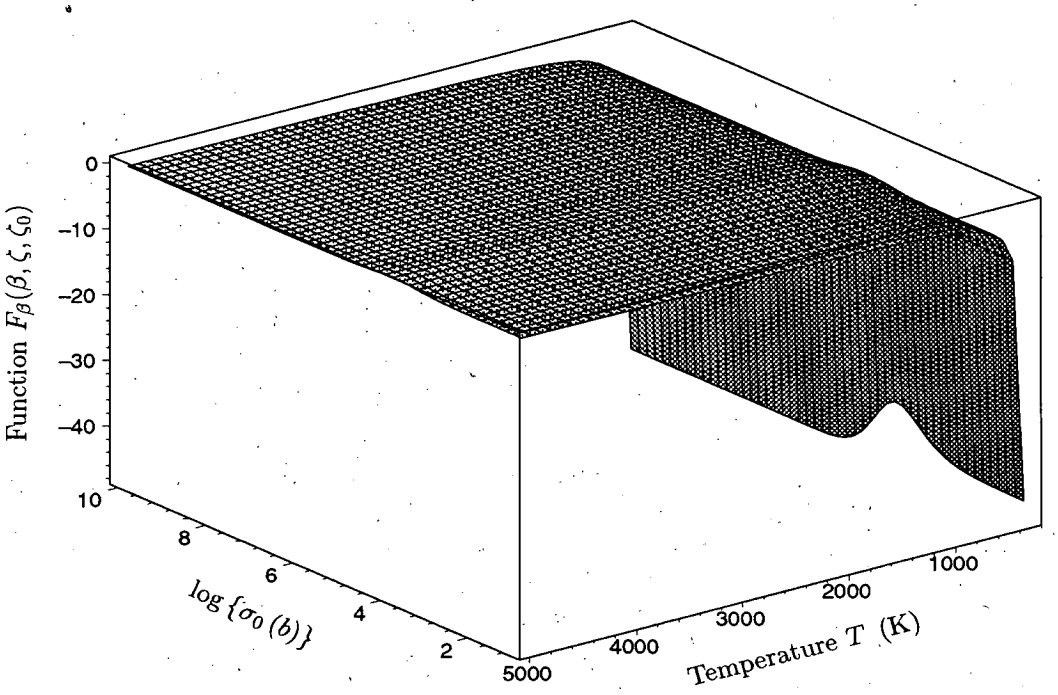

Figure 96: Intermediate Function $F_\beta(\beta,\zeta,\zeta_0)$ of ^{238}U 6.67 eV Resonance When Correlation between Two Temperature Systems.

the significant deep valley can be found in **Fig. 100** in comparison with **Fig. 79** without correlation where a hill was found around the turning point at $\sigma_0 \simeq 10^4$ barn.

By using these intermediate functions, the sensitivity coefficients of Doppler reactivity worth in case of correlating systems can be obtained as shown in **Figs. 87** to **107** for the ^{238}U 6.67 eV resonance with narrow resonance width. As shown in **Fig. 103** and **104**, the sensitivity coefficient of Doppler reactivity worth to neutron width has interesting behavior, i.e., negative sensitivity in low temperature region but positive in the relatively high temperature.

For the wide resonance of ^{239}Pu, the Fbt and Fzt functions become rapidly vanishing functions towards $\sigma_0 = \infty$ (b) as shown in **Figs. 108** to **111**. Their characteristic behaviors can be expected from the resonance self-shielding factor as shown in **Fig. 51**. Especially, the effective F_ζ-function has a interesting behavior as shown in **Fig. 111** but its magnitude is negligibly small.

Final sensitivity coefficients of the Doppler reactivity worth for wide resonance of ^{239}Pu 114.65 eV resonance are given by **Figs. 112** to **119**, respectively. In these sensitivity coefficients, the sensitive domain are restricted in the smaller β region less than about 10^5 barn.

The resonance energy sensitivity coefficient $S^\rho_{E_r}$ as shown in **Fig. 114** can be interpreted from its definition Eq. (248), i.e., its magnitude is determined by the first two terms in the right-hand side of Eq. (248) where F_β is greater F_ζ by about one order as shown in **Figs. 109**

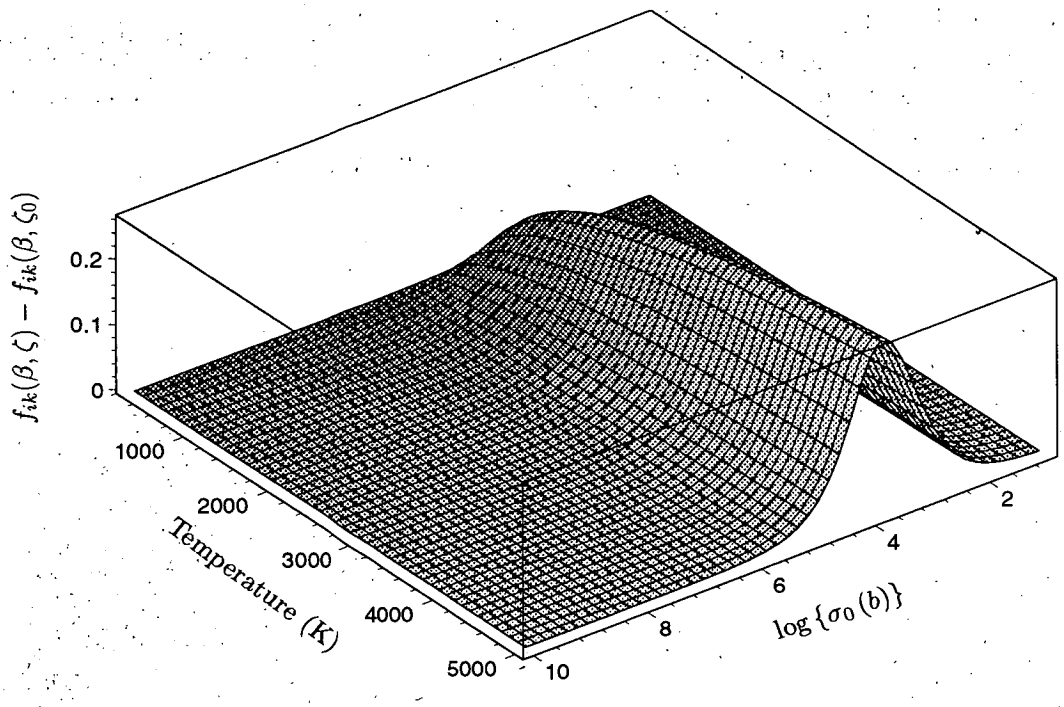

Figure 97: Difference of Resonance Self-shielding Factor $f_{ik}(\sigma_0, T) - f_{ik}(\sigma_0, T_0)$ for ^{238}U 6.67 eV Resonance.

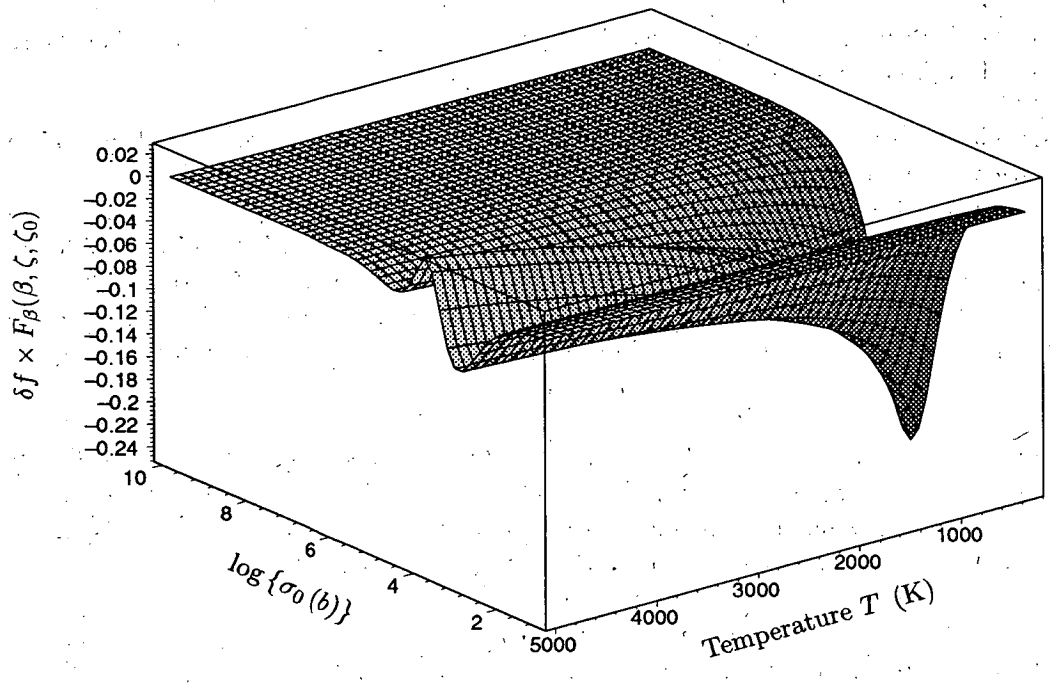

Figure 98: An Alternative Presentation of $F_\beta(\beta, \zeta, \zeta_0)$ shown in **Figure 96** as $\delta f \cdot F_\beta(\beta, \zeta, \zeta_0)$.

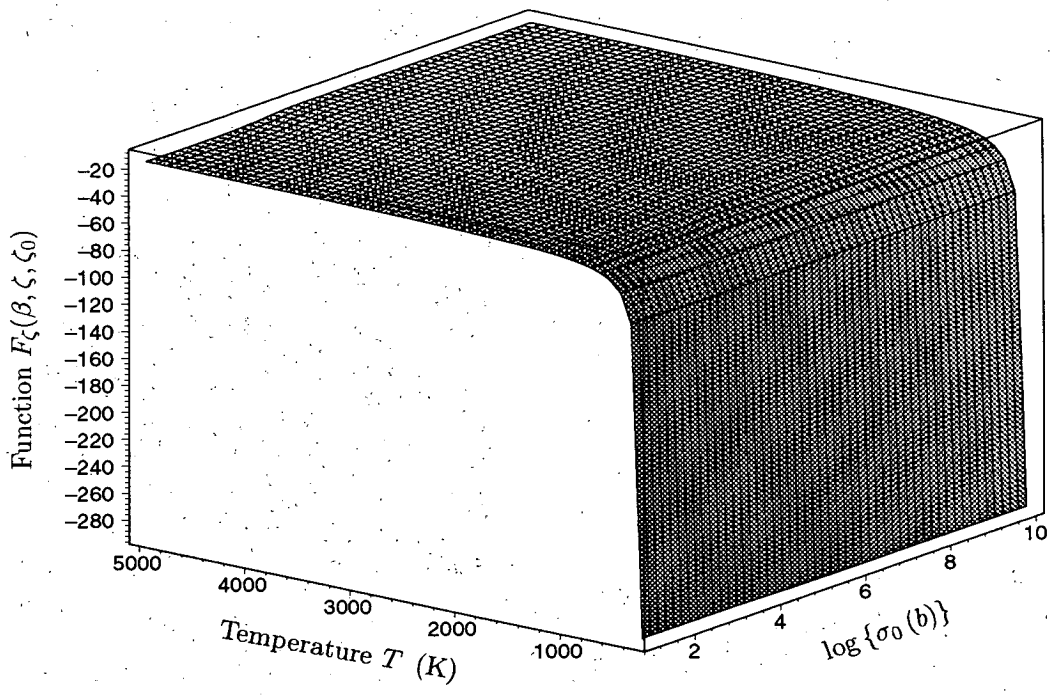

Figure 99: Intermediate Function $F_\zeta(\beta,\zeta,\zeta_0)$ of ^{238}U 6.67 eV Resonance When Correlation between Two Temperature Systems.

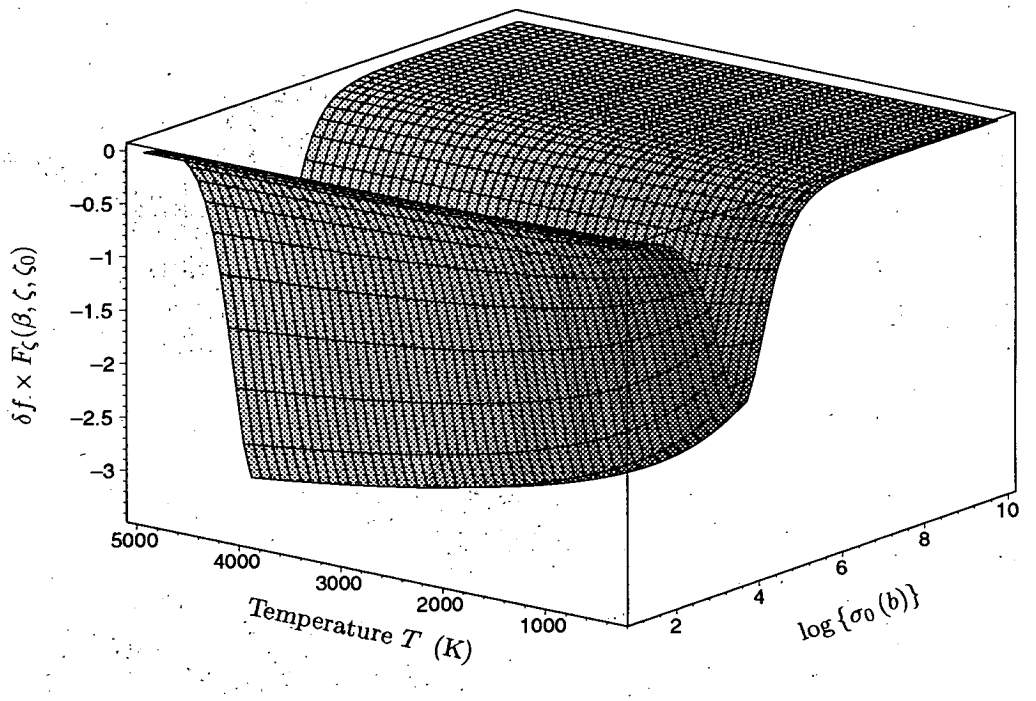

Figure 100: An Alternative Presentation of above $F_\zeta(\beta,\zeta,\zeta_0)$ shown in **Figure 99** as $\delta f \cdot F_\zeta(\beta,\zeta,\zeta_0)$.

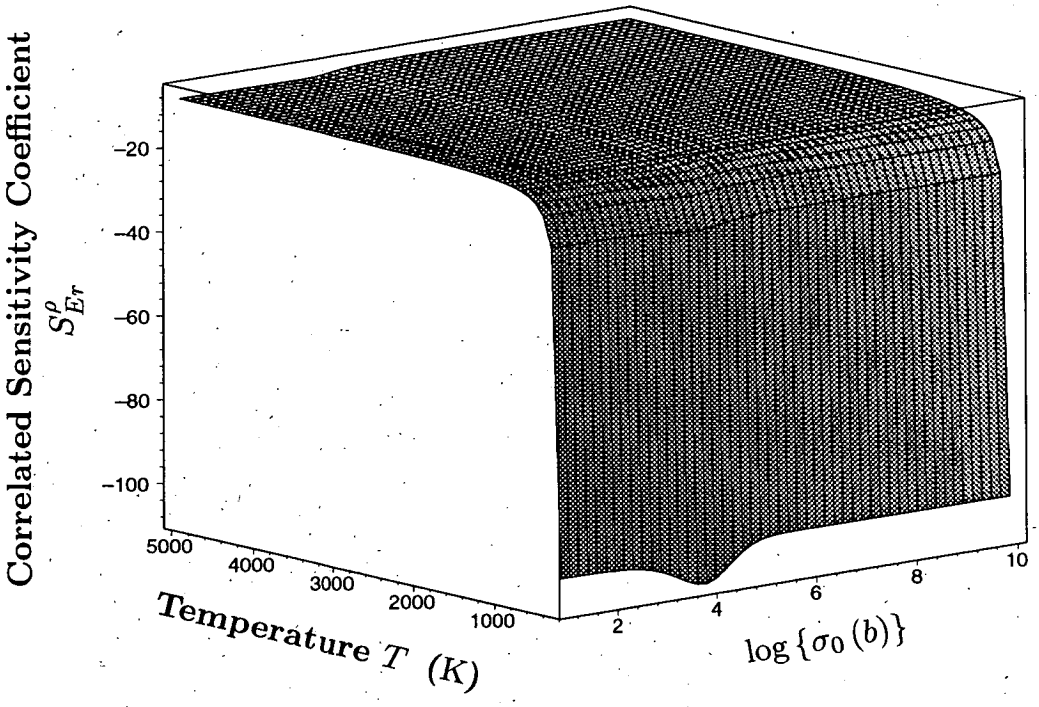

Figure 101: Correlated Sensitivity Coefficient S^{ρ}_{Er} for Doppler Reactivity Worth to Resonance Energy Er of ^{238}U 6.67 eV Resonance.

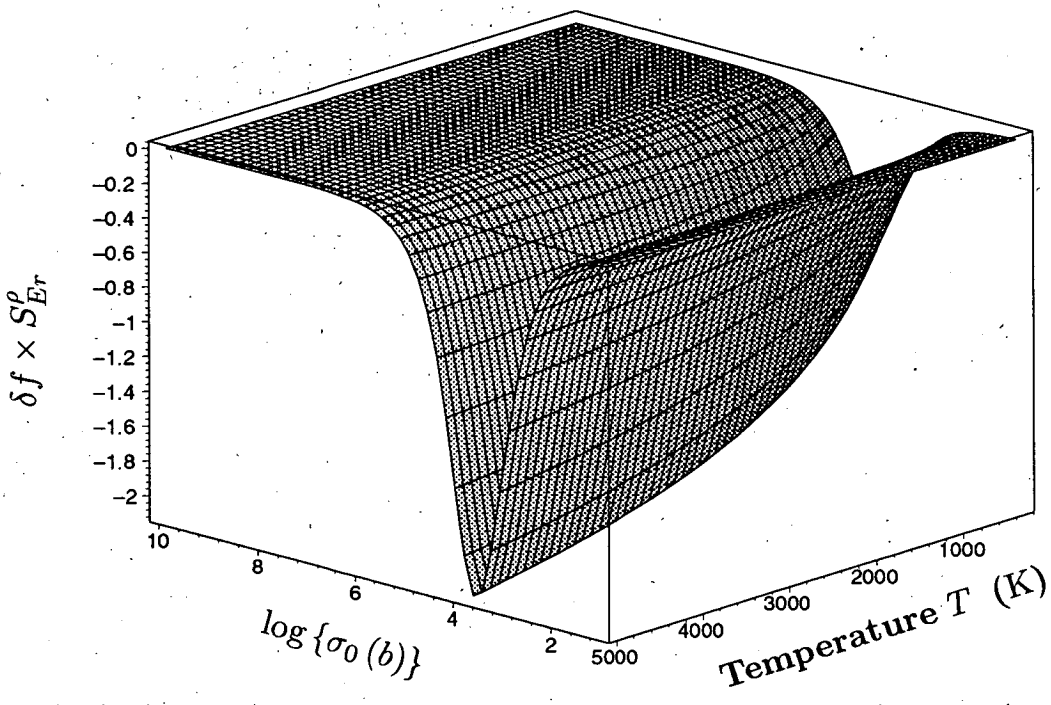

Figure 102: An Alternative Presentation of above S^{ρ}_{Er} as $\delta f \cdot S^{\rho}_{Er}$.

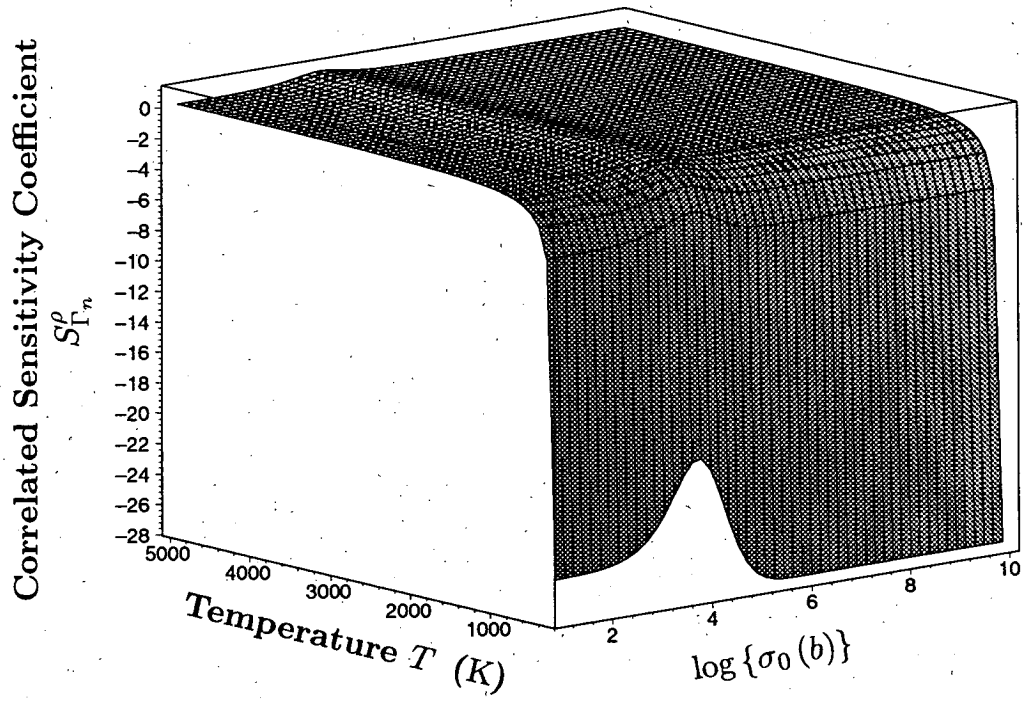

Figure 103: Correlated Sensitivity Coefficient $S^{\rho}_{\Gamma_n}$ for Doppler Reactivity Worth to Neutron Width Γ_n of ^{238}U 6.67 eV Resonance.

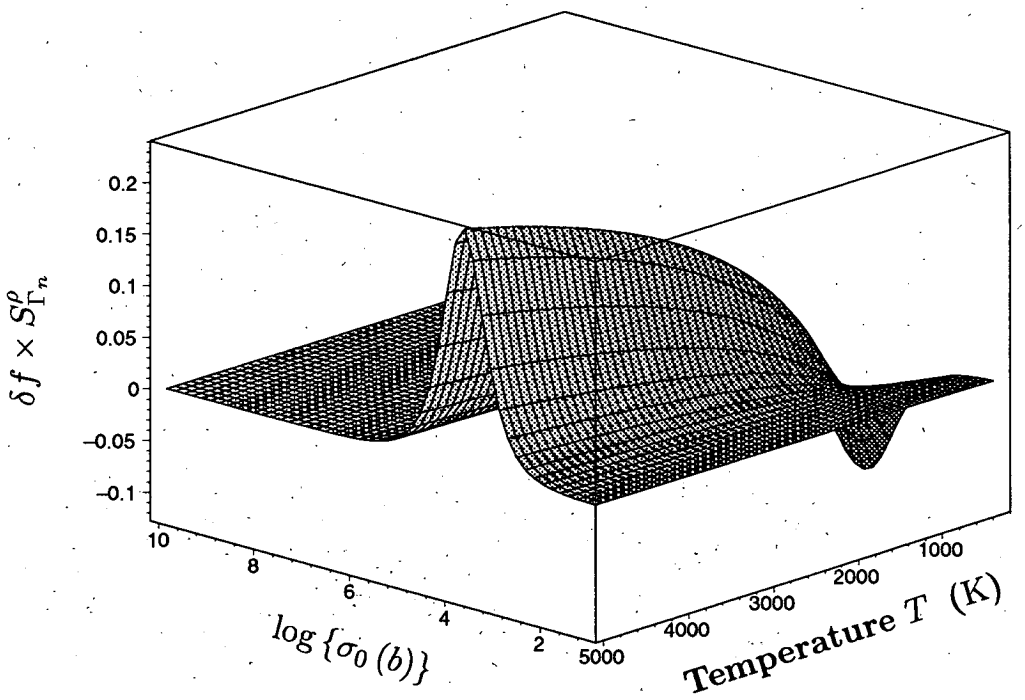

Figure 104: An Alternative Presentation of above $S^{\rho}_{\Gamma_n}$ as $\delta f \cdot S^{\rho}_{\Gamma_n}$.

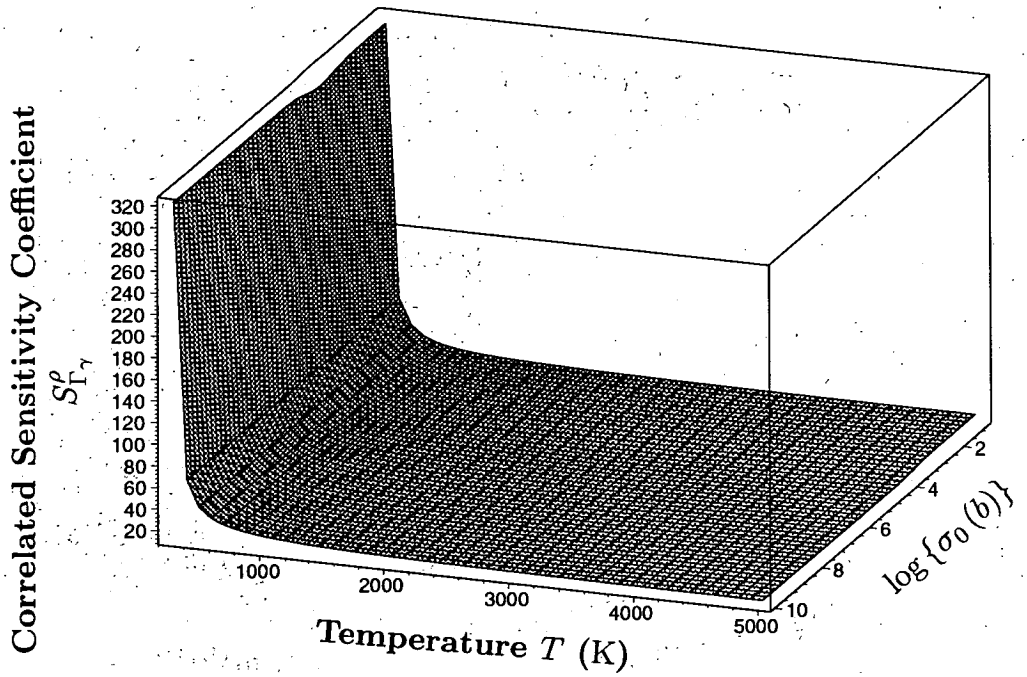

Figure 105: Correlated Sensitivity Coefficient $S^{\rho}_{\Gamma_\gamma}$ for Doppler Reactivity Worth to Radiation Width Γ_γ of ^{238}U 6.67 eV Resonance.

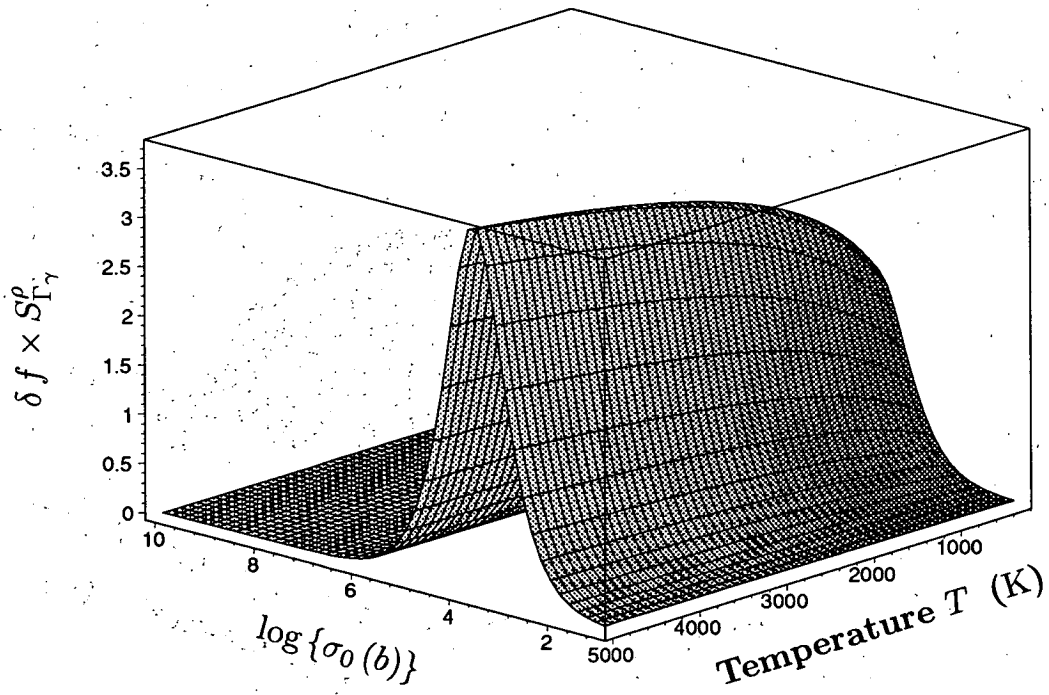

Figure 106: An Alternative Presentation of above $S^{\rho}_{\Gamma_\gamma}$ shown in **Figure 105** as $\delta f \cdot S^{\rho}_{\Gamma_\gamma}$.

and **111**. It implies that the energy dependence of Doppler reactivity worth is more sensitive to the potential scattering cross section than the Doppler width.

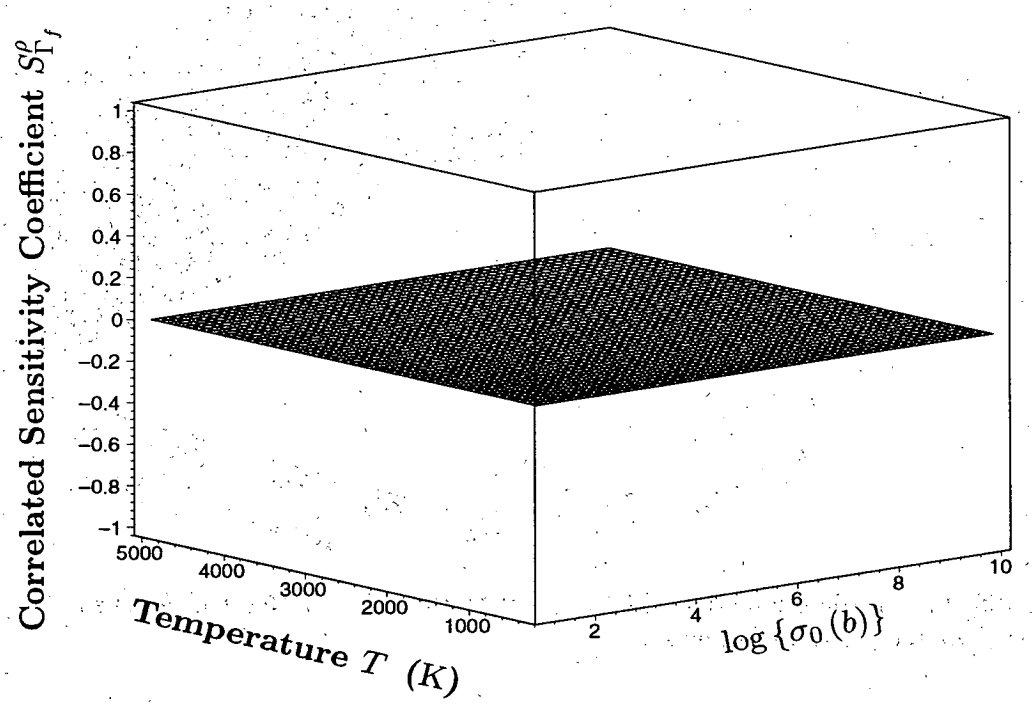

Figure 107: Correlated Sensitivity Coefficient $S^{\rho}_{\Gamma_f}$ for Doppler Reactivity Worth to Fission Width Γ_f of ^{238}U 6.67 eV Resonance.

7 Preliminary Result of Numerical Analysis

Doppler reactivity uncertainty for typical large fast breeder reactor due to the uncertainties of resolved resonance parameters is estimated for the numerical verification of the present method. Uncertainties of resonance parameters of the 1602 (s-wave=473, p-wave=1129) resonances of ^{238}U, 1015 (s-wave) resonances of ^{239}Pu, 205 (s-wave) resonances of ^{240}Pu and 127 (s-,p- and d-waves) of ^{56}Fe are given by T. Nakagawa and K. Shibata[6] of Japan Nuclear data Center in JAERI. As mentioned in Section 2, the uncertainties were estimated on the basis of Breit-Wigner Multi-Level Formula consistent with the original JENDL-3.2 evaluated nuclear data file[4] using Reich-Moore Formula. More detailed document on the uncertainty analysis will be described in the other report in near future.

Large sodium-cooled fast breeder reactor fueled by mixed oxide $PuO_2 - UO_2$ is considered, whose neutron spectrum was shown in **Fig. 60**. The two-region core is simplified to a single region by taking an average atom density and assumed to be homogeneous core.

Uncertainties of ^{238}U resonance self-shielding factor due to the uncertainties of resolved resonance parameter are evaluated and resultant uncertainties are shown in **Table 4** where the neutron energy group is the 70 group structure of JAERI-FAST-SET(JFS-J3). The $\left(\frac{\delta f}{f}\right)_{\Gamma}$ in the **Table 4** is the statistical sum of the uncertainty contributions from partial widths based on the error propagation law.

The uncertainty of ^{238}U resonance self-shielding factor is about a few percent except 45 and

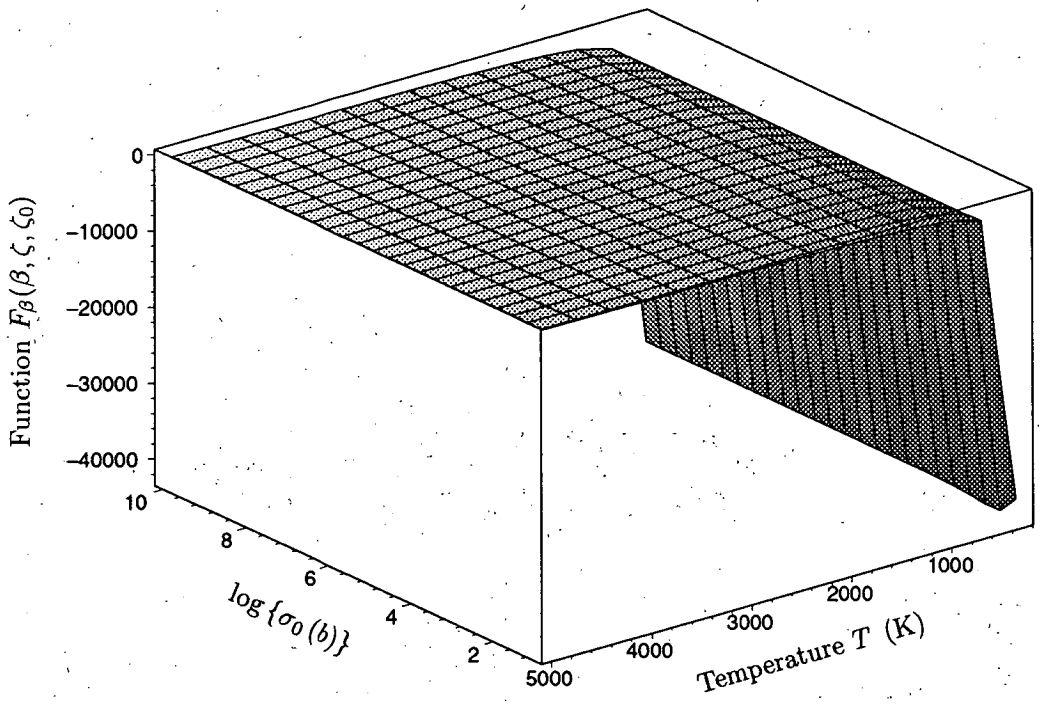

Figure 108: Intermediate Function $F_\beta(\beta,\zeta,\zeta_0)$ of ^{239}Pu 214.5 eV Resonance When Correlation between Two Temperature Systems.

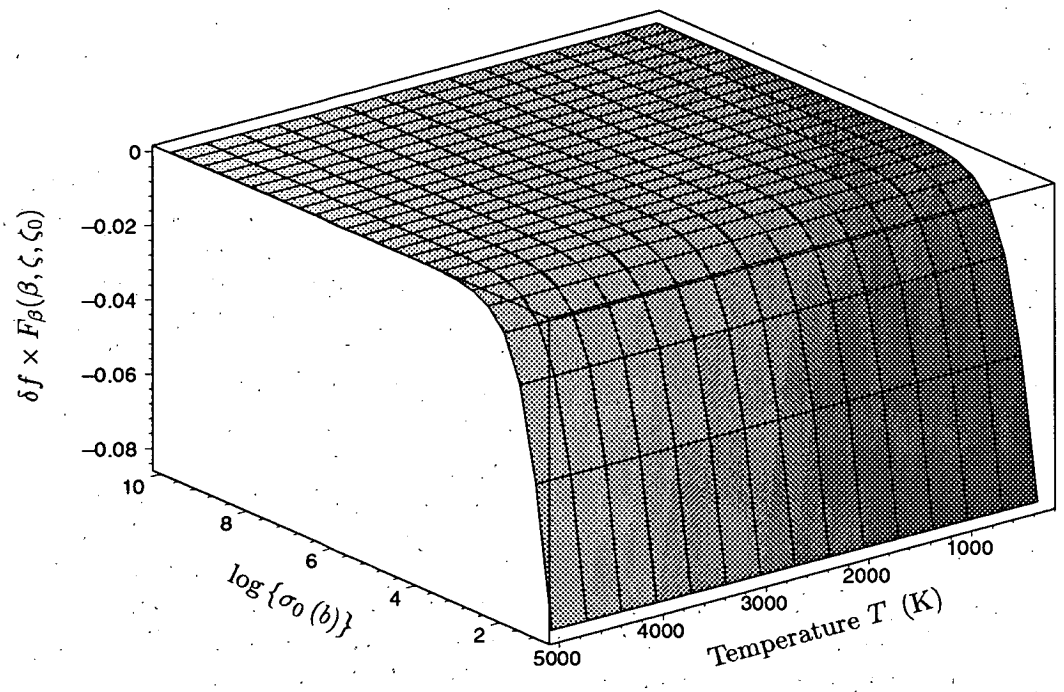

Figure 109: An Alternative Presentation of $F_\beta(\beta,\zeta,\zeta_0)$ shown in **Figure 108** as $\delta f \cdot F_\beta(\beta,\zeta,\zeta_0)$.

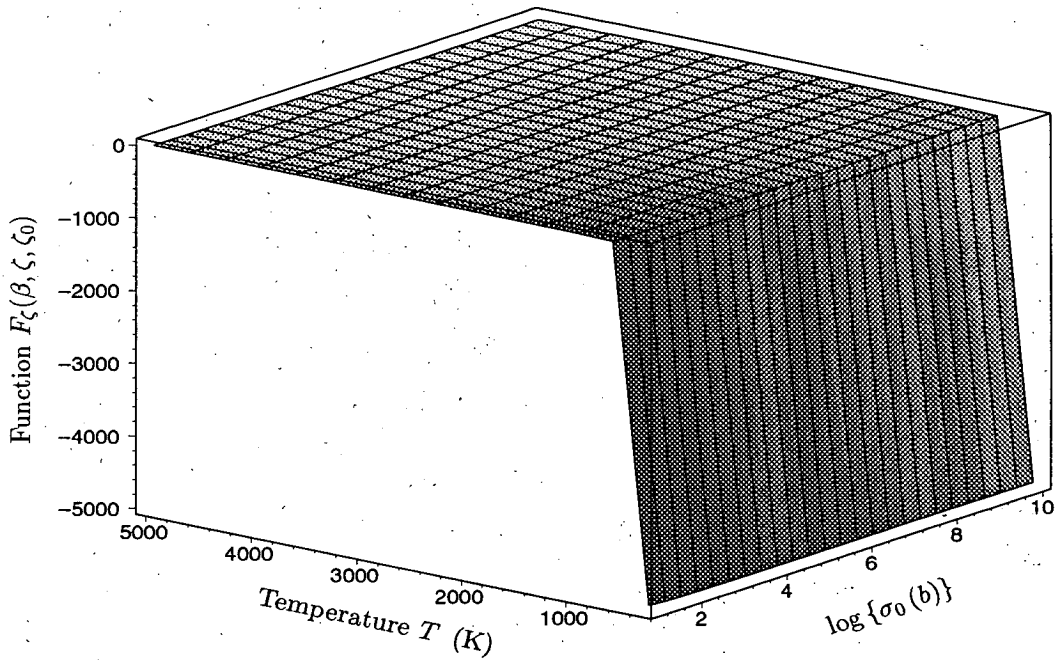

Figure 110: Intermediate Function $F_\zeta(\beta,\zeta,\zeta_0)$ of ^{239}Pu 214.5 eV Resonance When Correlation between Two Temperature Systems.

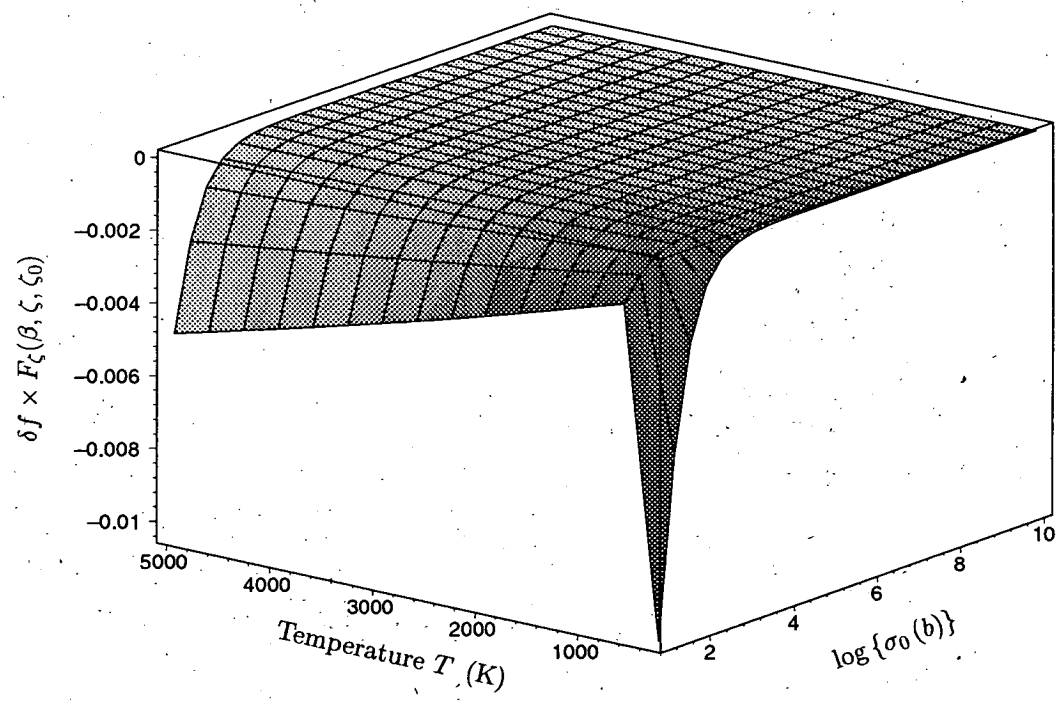

Figure 111: An Alternative Presentation of above $F_\zeta(\beta,\zeta,\zeta_0)$ shown in **Figure 110** as $\delta f \cdot F_\zeta(\beta,\zeta,\zeta_0)$.

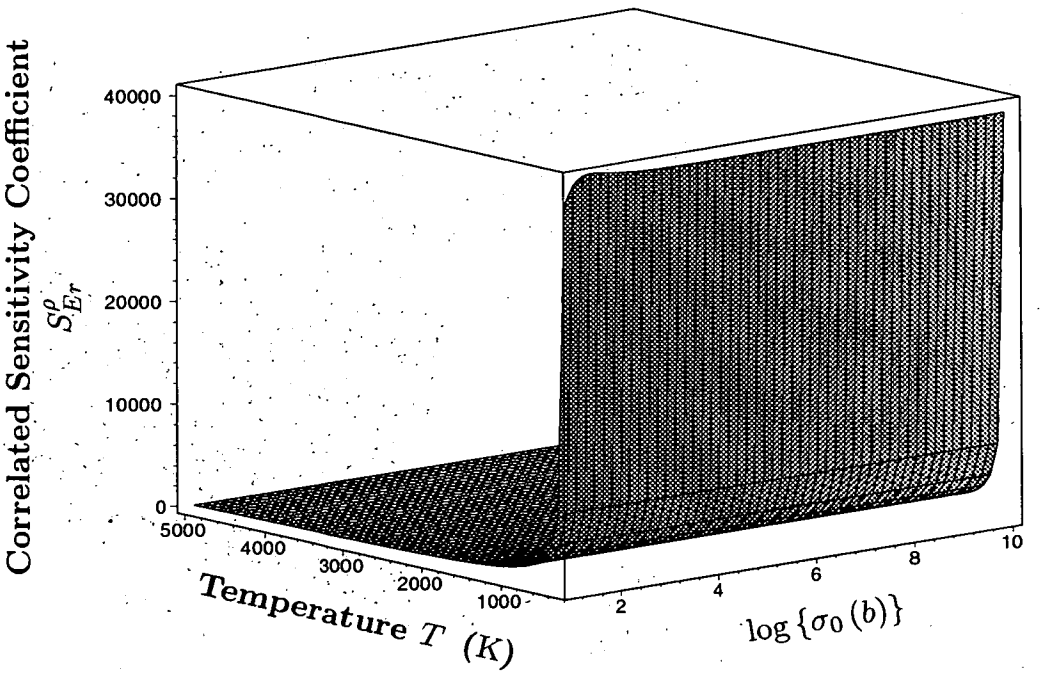

Figure 112: Correlated Sensitivity Coefficient S^{ρ}_{Er} for Doppler Reactivity Worth to Resonance Energy Er of ^{239}Pu 214.5 eV Resonance.

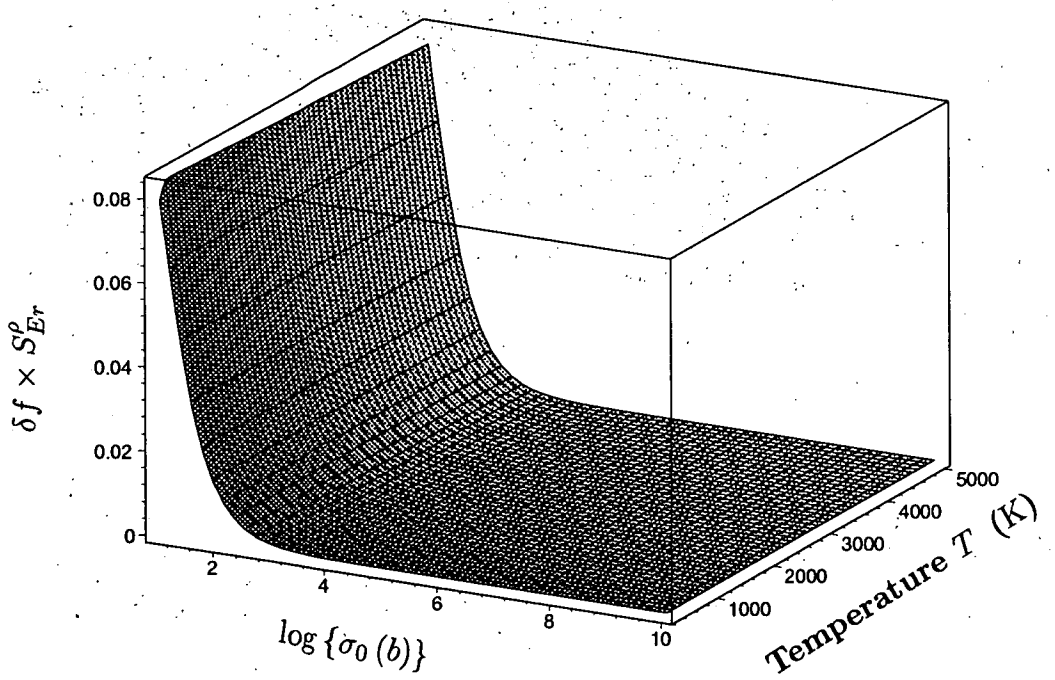

Figure 113: An Alternative Presentation of above S^{ρ}_{Er} shown in **Figure 112** as $\delta f \cdot S^{\rho}_{Er}$.

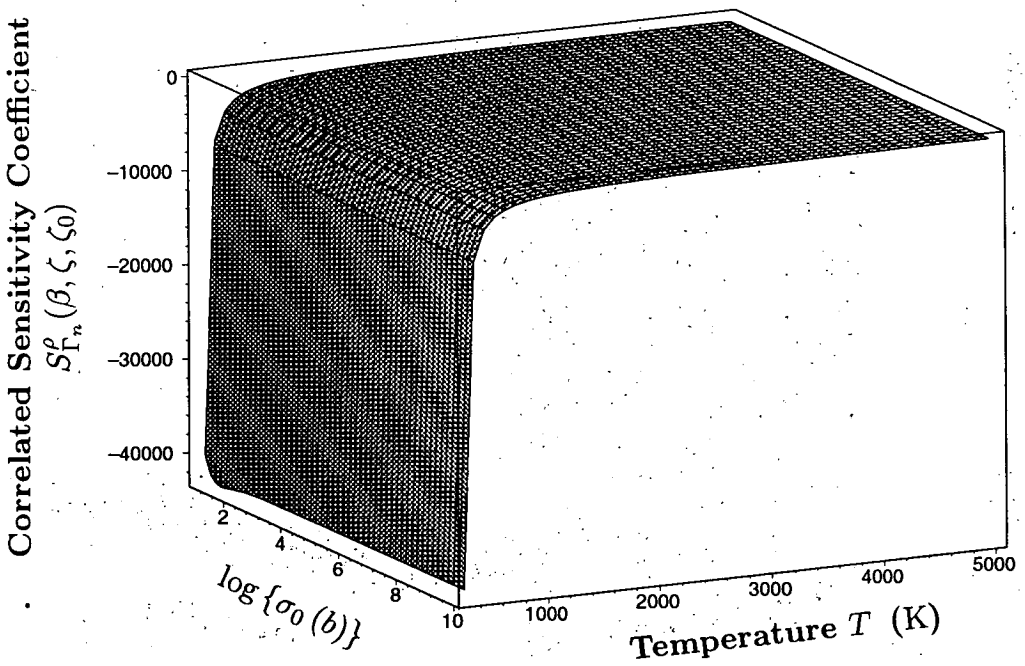

Figure 114: Correlated Sensitivity Coefficient $S^{\rho}_{\Gamma_n}(\beta,\zeta,\zeta_0)$ for Doppler Reactivity Worth to Neutron Width Γ_n of ^{239}Pu 214.65 eV Resonance.

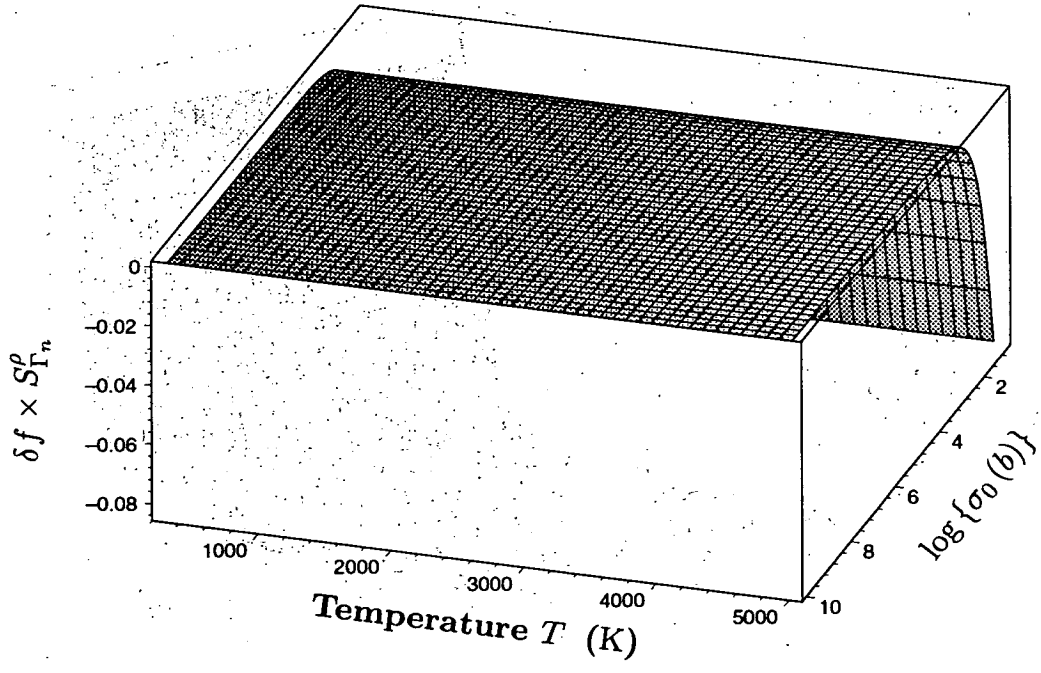

Figure 115: An Alternative Presentation of above $S^{\rho}_{\Gamma_n}$ shown in **Figure 114** as $\delta f \cdot S^{\rho}_{\Gamma_n}$.

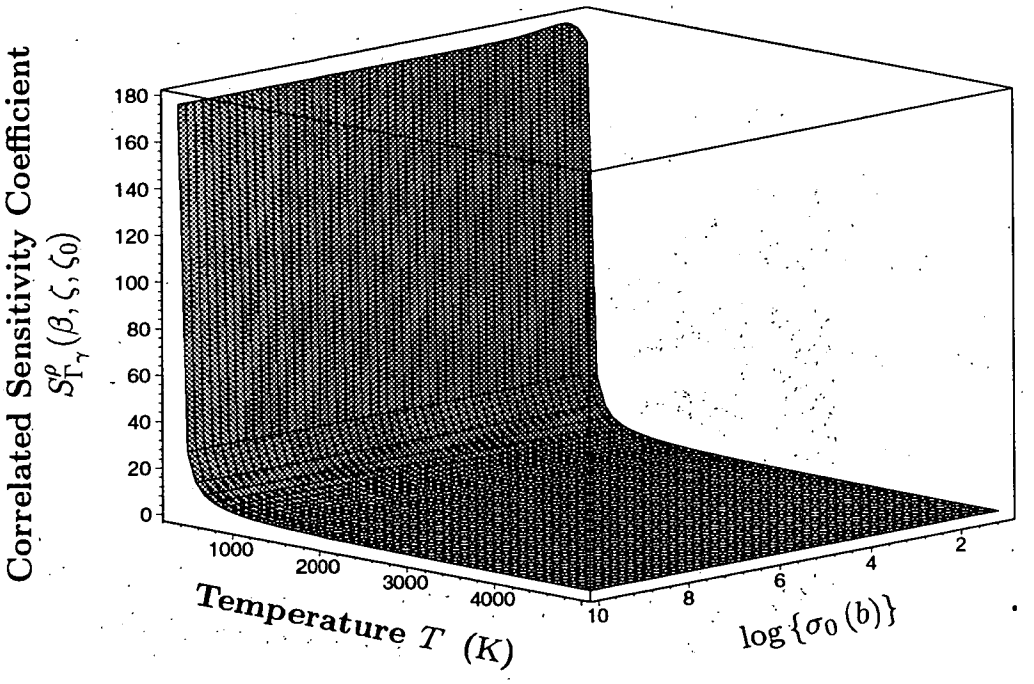

Figure 116: Correlated Sensitivity Coefficient $S^{\rho}_{\Gamma_\gamma}(\beta,\zeta,\zeta_0)$ for Doppler Reactivity Worth to Radiation Width Γ_γ of ^{239}Pu 214.65 eV Resonance.

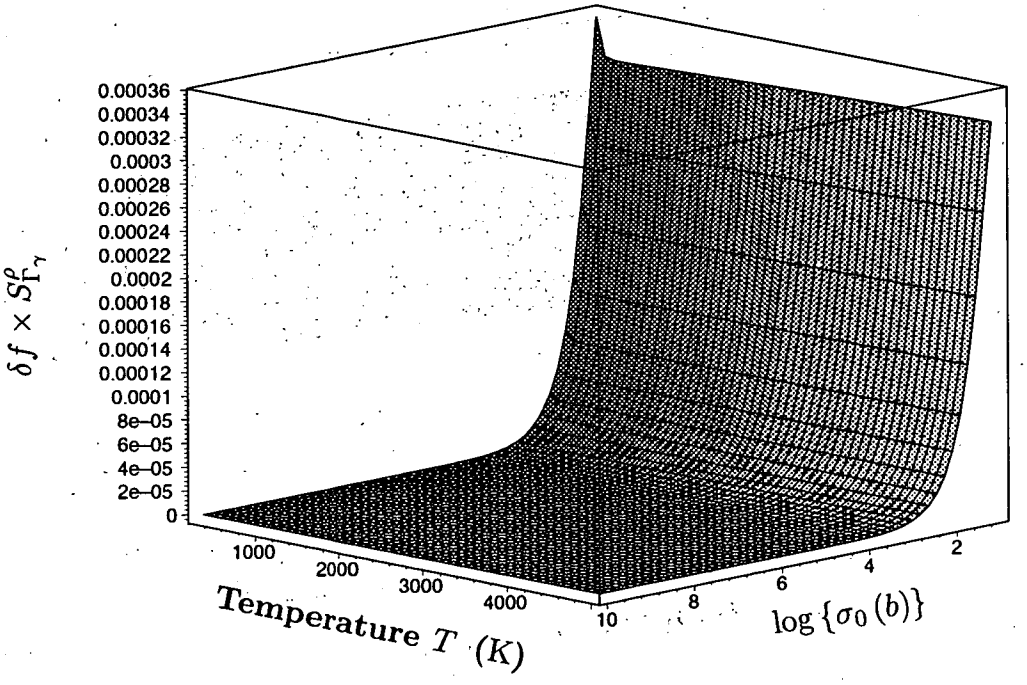

Figure 117: An Alternative Presentation of above $S^{\rho}_{\Gamma_\gamma}$ shown in **Figure 116** as $\delta f \cdot S^{\rho}_{\Gamma_\gamma}$.

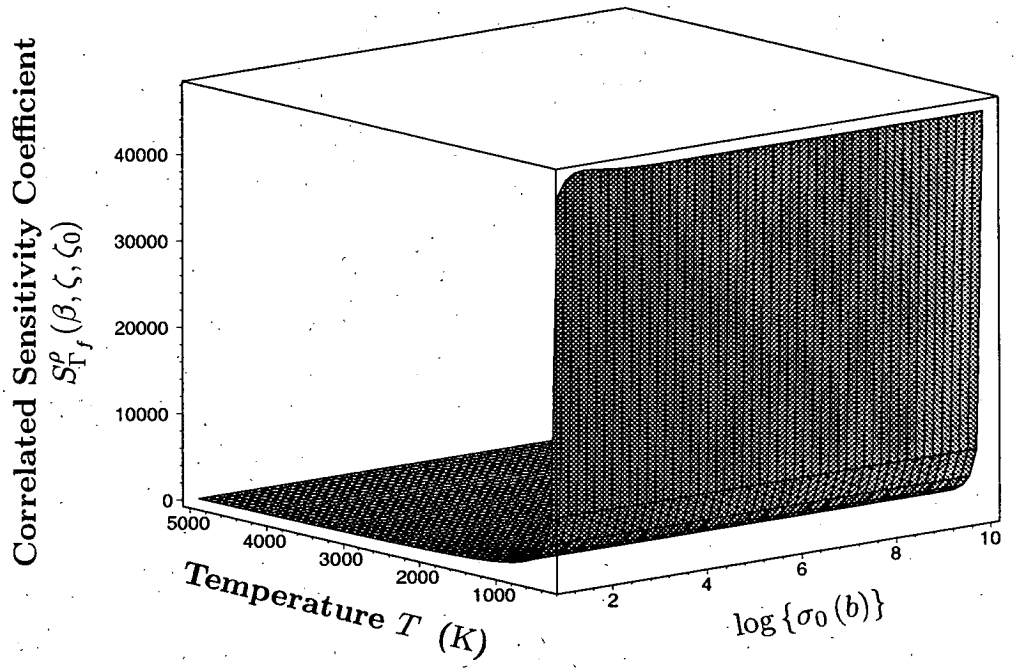

Figure 118: Correlated Sensitivity Coefficient $S^{\rho}_{\Gamma_{fission}}(\beta,\zeta,\zeta_0)$ for Doppler Reactivity Worth to Fission Width Γ_f of ^{239}Pu 214.65 eV Resonance.

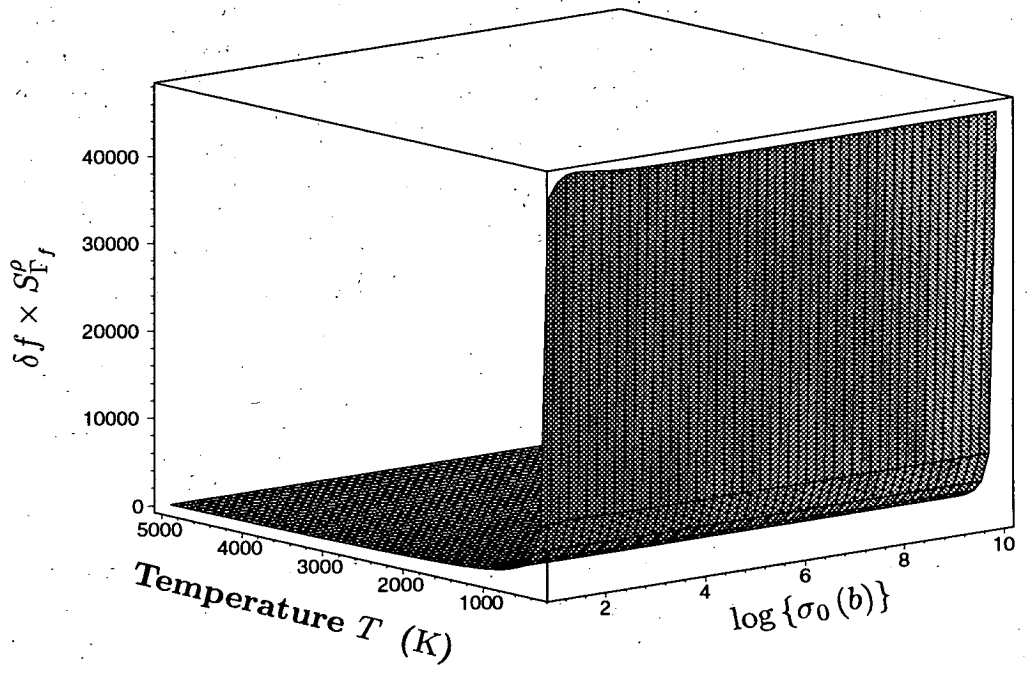

Figure 119: An Alternative Presentation of above $S^{\rho}_{\Gamma_f}$ shown in **Figure 118** as $\delta f \cdot S^{\rho}_{\Gamma_f}$.

Table 4 Uncertaity of ^{238}U Resonance Self-Shielding Factor for Neutron Capture Cross Section $\sigma_{n,\gamma}$ due to Uncertainty of Resonance Parameters at Room Temperature $T = 239^0$ K and $\sigma_0 = 37.0$ (barn).

Group	Upper Energy	$\left(\frac{\delta f}{f}\right)_{E_r}$	$\left(\frac{\delta f}{f}\right)_{\Gamma_n}$	$\left(\frac{\delta f}{f}\right)_{\Gamma_\gamma}$	$\left(\frac{\delta f}{f}\right)_{\Gamma_f}$	$\left(\frac{\delta f}{f}\right)_{\Gamma}$
28	11.7090 KeV	7.7442D-05	1.4244D-02	3.6049D-03	0.0	1.4693D-02
29	9.1188	4.8535D-05	9.7659D-03	2.5230D-03	0.0	1.0087D-02
30	7.1017	4.5776D-05	9.9927D-03	3.0268D-03	0.0	1.0441D-02
31	5.5308	4.5410D-05	8.9504D-03	3.4519D-03	0.0	9.5931D-03
32	4.3074	5.5019D-05	1.0910D-02	4.1993D-03	0.0	1.1691D-02
33	3.3546	4.0562D-05	9.7053D-03	5.0455D-03	0.0	1.0939D-02
34	2.6126	4.0520D-05	1.2261D-02	5.5380D-03	0.0	1.3453D-02
35	2.0347	5.1624D-05	1.2912D-02	6.6644D-03	0.0	1.4531D-02
36	1.5846	4.4436D-05	1.2006D-02	7.3594D-03	0.0	1.4082D-02
37	1.2341	5.2758D-05	1.5191D-02	7.0644D-03	0.0	1.6753D-02
38	961.1200 eV	8.8490D-05	2.0869D-02	8.9665D-03	0.0	2.2714D-02
39	748.5200	5.8584D-05	2.7365D-02	1.0788D-02	0.0	2.9415D-02
40	582.9500	1.3814D-04	2.9016D-02	1.1331D-02	0.0	3.1150D-02
41	454.0000	7.0428D-05	2.3704D-02	1.6745D-02	0.0	2.9022D-02
42	353.5800	9.5333D-05	4.4013D-02	4.2348D-02	0.0	6.1078D-02
43	275.3600	7.2140D-05	5.3218D-02	9.4965D-03	0.0	5.4059D-02
44	214.4500	7.7085D-05	5.3554D-02	3.7927D-03	0.0	5.3688D-02
45	167.0200	4.1371D-05	2.2803D-02	2.6665D-01	0.0	2.6762D-01
46	130.0700	1.3171D-04	4.1469D-02	1.4592D-02	0.0	4.3962D-02
47	101.3000	8.4537D-04	1.2997D-01	1.0381D-02	0.0	1.3039D-01
48	78.8930	1.7234D-04	3.2619D-02	2.0267D-03	0.0	3.2682D-02
49	61.4420	2.7565D-04	6.8508D-02	2.0435D-04	0.0	6.8509D-02
50	47.5810	4.1062D-04	8.8865D-02	3.1507D-04	0.0	8.8866D-02
51	37.2670	2.8743D-05	3.1535D-04	9.3484D-04	0.0	9.8701D-04
52	29.0230	6.0701D-04	9.1266D-02	2.2975D-04	0.0	9.1269D-02
53	22.6030	5.2088D-05	1.0628D-02	1.2398D-03	0.0	1.0700D-02
54	17.6030	0.0	0.0	0.0	0.0	0.0
55	13.7100	1.8083D-06	3.9327D-04	5.6009D-04	0.0	6.8437D-04
56	10.6770	5.0797D-06	1.1876D-03	2.7721D-03	0.0	3.0158D-03
57	8.3153	3.2437D-05	1.8905D-03	1.8915D-03	0.0	2.6745D-03
58	6.4760	0.0	0.0	0.0	0.0	0.0
59	5.0435	2.0813D-06	3.9660D-04	4.8468D-04	0.0	6.2626D-04

Table 5 Uncertainties of Resonance Self-Shielding Factors and Errors of Resolved Resonance Parameters.

Group	Group-wise Uncertainty / Resonance Parameter Error	El - EH (eV) / Res. Posit. Er (eV)	$\left(\frac{\delta f}{f}\right)_{Er}$ $\left(\frac{\delta E_r}{E_r}\right)$	$\left(\frac{\delta f}{f}\right)_{\Gamma_n}$ $\left(\frac{\delta \Gamma_n}{\Gamma_n}\right)$	$\left(\frac{\delta f}{f}\right)_{\Gamma_\gamma}$ $\left(\frac{\delta \Gamma_\gamma}{\Gamma_\gamma}\right)$	$\left(\frac{\delta f}{f}\right)_{\Gamma}$
45	Group-wise	167.02 - 130.07	4.14D-05	2.28D-02	2.67D-01	2.68D-01
	Resonance-1[†)]	133.24	3.75D-04	2.50D-01	4.35D-02	
	Resonance-2	135.95	1.00D-03	1.50D-01	4.35D-02	
	Resonance-3	145.66	6.87D-05	4.96D-02	4.48D-01	
	Resonance-4	152.42	1.31D-04	5.45D-02	4.35D-01	
	Resonance-5	158.94	1.89D-04	1.66D-01	4.35D-01	
	Resonance-6	164.50	9.97D-04	1.50D-01	4.35D-01	
	Resonance-7	165.29	6.05D-05	2.23D-03	1.14D-01	
46	Group-wise	130.07 - 101.30	1.32D-04	4.15D-02	1.46D-02	4.40D-02
	Resonance-1	102.56	9.75D-05	2.51D-03	8.33D-03	
	Resonance-2	111.15	3.60D-04	3.65D-03	1.13D-02	
	Resonance-3	116.90	8.55D-05	9.14D-03	4.07D-02	
	Resonance-4	119.28	9.98D-04	1.50D-01	4.35D-02	
	Resonance-5	124.99	2.40D-04	1.00D-01	4.35D-02	
47	Group-wise	101.30 - 78.89	8.45D-04	1.30D-01	1.04D-02	1.31D-01
	Resonance-1	80.75	2.48D-05	1.18D-02	2.47D-02	
	Resonance-2	83.06	1.00D-03	1.50D-01	4.35D-02	
	Resonance-3	83.70	1.08D-04	6.60D-02	4.35D-02	
	Resonance-4	89.22	1.00D-03	1.50D-01	4.35D-02	
	Resonance-5	83.08	2.15D-04	1.00D-01	4.35D-02	
	Resonance-5	98.00	1.00D-03	1.50D-01	4.35D-02	
	Resonance-7	102.56	9.75D-05	2.51D-03	8.33D-03	
	...					
	...					
57	Group-wise	8.51 - 6.48	3.25D-05	1.89D-03	1.89D-03	2.67D-03
	Resonance	6.67	3.00D-04	1.54D-03	1.83D-03	

[†)]: All resonances in the energy group of interest are shoewn

Table 6.1 Uncertainty of ^{238}U Doppler Reactivity Worth (%) with Correlation between Two Temperature Points.

σ_0(b) (barn)	Temperature (k)						
	239	644	794	935.4	1087	2000	5000
2.000D+01	0.0	1.456D+01	1.365D+01	1.392D+01	1.484D+01	1.565D+02	6.183D-01
3.700D+01[*)]	0.0	7.238D+00	6.217D+00	5.752D+00	5.472D+00	6.206D+00	1.074D+00
6.858D+01[•)]	0.0	5.001D+00	4.173D+00	3.754D+00	3.471D+00	3.050D+00	1.690D+00
1.000D+02	0.0	4.375D+00	3.620D+00	3.231D+00	2.965D+00	2.450D+00	1.896D+00
1.000D+03	0.0	2.634D+00	2.179D+00	1.940D+00	1.776D+00	1.392D+00	1.153D+00
1.000D+04	0.0	1.837D+00	1.557D+00	1.411D+00	1.311D+00	1.077D+00	9.339D-01
1.000D+06	0.0	1.268D+00	1.094D+00	1.009D+00	9.468D-01	8.024D-01	7.138D-01

[*)]: estimated by cell calculation code SLAROM.
[•)]: estimated by the criticality serach for two region homogeneous cell model described by resonance parameters as shown in section 3.

Table 6.2 Uncertainty of ^{239}Pu Doppler Reactivity Worth (%) with Correlation between Two Temperature Points.

σ_0(b) (barn)	Temperature (k)						
	239	644	794	935.4	1087	2000	5000
2.000D+01	0.0	1.243D+00	1.166D+00	1.189D+00	1.268D+00	1.342D+01	5.353D-02
3.700D+01	0.0	3.228D-01	2.767D-01	2.557D-01	2.429D-01	2.745D-01	4.745D-02
6.858D+01	0.0	9.806D-02	8.151D-02	7.311D-02	6.741D-02	5.866D-02	3.218D-02
1.000D+02	0.0	5.021D-02	4.134D-02	3.676D-02	3.362D-02	2.743D-02	2.094D-02
1.000D+03	0.0	2.293D-03	1.862D-03	1.635D-03	1.478D-03	1.107D-03	8.699D-04
1.000D+04	0.0	6.295D-04	5.122D-04	4.504D-04	4.077D-04	3.054D-04	2.397D-04
1.000D+06	0.0	4.457D-04	3.616D-04	3.191D-04	2.882D-04	2.141D-04	1.657D-04

47 groups. As evident from **Table 5**, significant large uncertainties in these two groups are due to the larger uncertainties of resonance parameters themselves. For instance, 26.8 %(2.68$D-01$ in absolute) uncertainty of the resonance self-shielding factor $\left(\frac{\delta f}{f}\right)_\Gamma$ came from the uncertainties of radiation widths for the 3rd to 6th resonance as shown in this **Table 5** as well as **Fig. 6**. The larger uncertainty of 13.1% in the 47 group is due to the larger uncertainties of neutron widths.

Resultant uncertainties of Doppler reactivity worths are shown in **Tables 6.1** to **6.3** as

Table 6.3 Uncertainty of ^{240}Pu Doppler Reactivity Worth (%) with Correlation between Two Temperature Points.

σ_0(b) (barn)	Temperature (k)						
	239	644	794	935.4	1087	2000	5000
2.000D+01	0.0	6.988D-02	6.753D-02	7.032D-02	7.635D-02	8.558D-01	3.600D-03
3.700D+01	0.0	4.565D-02	4.028D-02	3.800D-02	3.674D-02	4.398D-02	8.031D-03
6.858D+01	0.0	3.551D-02	3.036D-02	2.778D-02	2.605D-02	2.397D-02	1.388D-02
1.000D+02	0.0	3.106D-02	2.628D-02	2.383D-02	2.215D-02	1.908D-02	1.535D-02
1.000D+03	0.0	5.913D-03	4.985D-03	4.496D-03	4.157D-03	3.354D-03	2.838D-03
1.000D+04	0.0	1.385D-03	1.189D-03	1.087D-03	1.017D-03	8.529D-04	7.510D-04
1.000D+06	0.0	9.800D-04	8.390D-04	7.700D-04	7.193D-04	5.987D-04	5.208D-04

a function of potential scattering cross section and temperature, where the reference one T_0 is fixed at the room temperature(293 K). The $\sigma_0 = 37$ (b) or $\sigma_0 = 65.58$ (b) is for the fast breeder reactor of interest. The former one is obtained by cell calculation code SLAROM taking into account heterogeneity but the latter one is estimated by the neutron balance at critical core after criticality search as shown in Section 3.

As evident from the **Table 6**, the uncertainty is enhanced around the reference temperature due to the denominator of intermediate functions F_{bt} and F_{zt}, and at the larger σ_0 the uncertainty is tends to vanishing. For the σ_0 smaller than about 20 (b), however, the uncertainty is rapidly magnified since the resonance self-shielding factor is nearly flat as shown in **Fig. 44** and the temperature dependence $f(\sigma_0, T) - f(\sigma_0, T_0)$ is also vanishing as indicated by Eq. (246) implying null reactivity. The uncertainty of ρ can be described by the fractional change of f-factor due to resonance parameters to the temperature change of f-factor, i.e., $\frac{\delta\rho}{\rho} \propto \frac{\delta(f-f_0)}{f-f_0}$. Therefore, in general the Doppler reactivity uncertainty is significantly enhanced in the such a low σ_0 region.

8 Conclusion

In order to evaluate the uncertainties of nuclear performance parameters due to the uncertainties of resolved resonance parameters, an analytical method for the sensitivity analyses of effective multiplication factor k_{eff}, temperature coefficient α and Doppler reactivity worth ρ to the resolved resonance parameters has been developed. The following facts were obtained in this work.

1) Resonance integral as a functional function of Doppler broadening function ψ and χ could be expanded to a power series as function of ψ and χ, and up to the third order term of $\psi^i\chi^j$ (i,j:integers) could be analytically integrated and the remainders greater than 3, i.e. $(i+j)>3$, were integrated as the power series.
2) By introducing an intermediate variable ζ together with the conventional β variable, the resonance self-shielding factor $f(\beta,\zeta)$ could be expressed by a simple analytical function such as

$$f(\beta,\zeta) = \frac{\beta}{1+\beta}\cdot\{1+G(\beta,\zeta)\}$$

$$\beta = \frac{\sigma_p}{\sigma_0}, \quad \zeta = \frac{1}{1+\frac{p}{\sqrt{2}}\cdot\theta(t)}, \quad \theta(t) = \frac{\Gamma}{\Delta(t)}$$

where $G(\beta,\zeta)$: modulation function, $p=0.4707$, Γ: total width, σ_p: potential scattering cross section per resonance material, σ_0: peak total cross section, Δ: Doppler width and T: temperature.
3) The sensitivity coefficients of the f-factor to the variables β and ζ were provided as the basic quantities for the sensitivity analyses. Then, the final sensitivity coefficients for functional function were expressed as a successive operations from outer variable to the inner one such as $S_x^f = S_z^f \cdot S_y^f$ for $f[z\{y(x)\}]$ as the result of algebra.
4) Doppler reactivity worth ρ was expressed as a weighted sum of all resonance contributions. The resonance contribution from each level could be shown as a function of resonance parameters and the level-wise resonance self-shielding factor.
5) Preliminary analysis was made for a typical sodium-cooled fast breeder reactor and the uncertainties of the Doppler reactivity worth due to the uncertainties of the resolved resonance parameters were obtained. The main contributor was the ^{238}U having about 80% of the total Doppler reactivity worth, and the others ^{239}Pu and ^{240}Pu had nearly equal and small contributions. For the temperature increment from the room temperature of 239 K to 644 K, the uncertainty of the ^{238}U Doppler reactivity worth due to those of resolved resonance parameters was about 4.6 to 6.8 % depending on the magnitude of σ_0-value.
6) Uncertainties of Doppler reactivity worth due to errors of unresolved resonance parameters were out of present scope.

Acknowledgements

The authors would like to thank Dr. H. Takano of JAERI for his reviewing the present work and helpful comments.

References

[1] Shirakata, K., Ishikawa, M., Ikegami, T., Sanda, T., Kaneko, K., Kawashima, M., Kaise, Y., Shirakawa, M. and Hibi, K., "Development of Concept and Neutronic Calculation Method for Large LMFBR Core", Proc. Int. Conf. on Fast Reactors and Related Fuel Cycles (FR'91), kyoto, Vol. 1, p.3.5-1, (oct. 1991).

[2] Nagata, T., Hayashi, H., Moriyama, M., Nakaoji, M., Wakabayashi, T., Maeda, K. and Yamashita, Y.,"Design Study on Large Scale Fast Breeder Reactor", PNC Technical Review No. 82, p.19, (Feb. 1992)

[3] Ishikawa, M., Hoshi, T., Sanda, T., Ikegami, T. and Kawakita, T., "Improvement of Nuclear Design Method for Larger LMFBR Cores Using the Cross-Section Adjustment", Proc. Int. Conf. on Mathematical Methods and Supercomputing in Nuclear Applications (M&C+SNA'93), Karlsruhe, Vol. 1, p. 593 (April 1993)

[4] Nakagawa, T., et.al., J. Nucl. Sci. Technol., 32[12], 1259(1995)

[5] Rose, P. F., (ed.), BNL-NCS-17541 4th edition, "ENDF/B-VI Summary Documentation", ENDF-201 (1991)

[6] Nakagawa, T. and Shibata, K., "Uncertainty of Resolved Resonance Parameters of ^{56}Fe, ^{239}Pu, ^{240}Pu and ^{238}U", JAERI-Research, 97-035(1997).

[7] Char, B.W., Geddes, K.O., Gonnet, G.H., Leong, B.L., Monagan, M.B. and Watt, S. M. ,"First Leaves: A Tutorial Introduction to Maple V", Springer-Verlag, (1992)

[8] Monagan, M.B., Geddes, K.O., Heal, K.M., Laban, G. and Vorkoetter, S.M., "Maple V Programming Guid", Springer-Verlag, (1998)

[9] Migneco, E. and Theobald, J. P., "Resonance Grouping Structure in Neutron Induced Subthreshold Fission of ^{240}Pu", Nucl. Phys. **A112** (1968) 603

[10] Abramowitz, M. and Stegun, I. A., *Handbook of Mathematical Functions*, DOVER PUBLICATIONS, INC., NEW YORK, (1970), p.299, Formula No. 7.1.29

[11] ibid, 8, p.298, Formula No. 7.1.15

[12] MacFarlane, R. E. and Muir, D.W., *NJOY Nuclear Data Processing System Version 91*, PSR-368, NJOY97.0, Oak Ridge National Laboratory, RSICC Peripheral Shielding Routine Collection. (May,1998)

[13] Henryson, H., et.al., "MC^2-2: A Code to Calculate Fast Neutron Spectra and Multigroup Cross Section", ANL-8144 (1976)

[14] Hwang, R.N.,"Efficient Methods for the Treatment of Resonance Cross Sections", Nucl. Sci. Eng., **52**, 157-175, (1973)

[15] ibid, 8, p.299, Formula No. 7.1.26

国際単位系 (SI) と換算表

表 1　SI基本単位および補助単位

量	名称	記号
長さ	メートル	m
質量	キログラム	kg
時間	秒	s
電流	アンペア	A
熱力学温度	ケルビン	K
物質量	モル	mol
光度	カンデラ	cd
平面角	ラジアン	rad
立体角	ステラジアン	sr

表 2　SIと併用される単位

名称	記号
分，時，日	min，h，d
度，分，秒	°，′，″
リットル	l，L
トン	t
電子ボルト	eV
原子質量単位	u

1 eV = 1.60218 × 10^{-19} J

1 u = 1.66054 × 10^{-27} kg

表 5　SI接頭語

倍数	接頭語	記号
10^{18}	エクサ	E
10^{15}	ペタ	P
10^{12}	テラ	T
10^{9}	ギガ	G
10^{6}	メガ	M
10^{3}	キロ	k
10^{2}	ヘクト	h
10^{1}	デカ	da
10^{-1}	デシ	d
10^{-2}	センチ	c
10^{-3}	ミリ	m
10^{-6}	マイクロ	μ
10^{-9}	ナノ	n
10^{-12}	ピコ	p
10^{-15}	フェムト	f
10^{-18}	アト	a

表 3　固有の名称をもつSI組立単位

量	名称	記号	他のSI単位による表現
周波数	ヘルツ	Hz	s^{-1}
力	ニュートン	N	$m \cdot kg/s^2$
圧力，応力	パスカル	Pa	N/m^2
エネルギー，仕事，熱量	ジュール	J	N·m
工率，放射束	ワット	W	J/s
電気量，電荷	クーロン	C	A·s
電位，電圧，起電力	ボルト	V	W/A
静電容量	ファラド	F	C/V
電気抵抗	オーム	Ω	V/A
コンダクタンス	ジーメンス	S	A/V
磁束	ウェーバ	Wb	V·s
磁束密度	テスラ	T	Wb/m^2
インダクタンス	ヘンリー	H	Wb/A
セルシウス温度	セルシウス度	℃	
光束	ルーメン	lm	cd·sr
照度	ルクス	lx	lm/m^2
放射能	ベクレル	Bq	s^{-1}
吸収線量	グレイ	Gy	J/kg
線量当量	シーベルト	Sv	J/kg

表 4　SIと共に暫定的に維持される単位

名称	記号
オングストローム	Å
バーン	b
バール	bar
ガル	Gal
キュリー	Ci
レントゲン	R
ラド	rad
レム	rem

1 Å = 0.1 nm = 10^{-10} m

1 b = 100 fm^2 = 10^{-28} m^2

1 bar = 0.1 MPa = 10^5 Pa

1 Gal = 1 cm/s^2 = 10^{-2} m/s^2

1 Ci = 3.7 × 10^{10} Bq

1 R = 2.58 × 10^{-4} C/kg

1 rad = 1 cGy = 10^{-2} Gy

1 rem = 1 cSv = 10^{-2} Sv

(注)

1. 表1－5は「国際単位系」第5版，国際度量衡局 1985年刊行による。ただし，1 eVおよび1 uの値はCODATAの1986年推奨値によった。
2. 表4には海里，ノット，アール，ヘクタールも含まれているが日常の単位なのでここでは省略した。
3. barは，JISでは流体の圧力を表わす場合に限り表2のカテゴリーに分類されている。
4. EC閣僚理事会指令ではbar，barnおよび「血圧の単位」mmHgを表2のカテゴリーに入れている。

換算表

力

N(=10^5 dyn)	kgf	lbf
1	0.101972	0.224809
9.80665	1	2.20462
4.44822	0.453592	1

粘度　1 Pa·s(N·s/m^2) = 10 P(ポアズ)(g/(cm·s))

動粘度　1 m^2/s = 10^4 St(ストークス)(cm^2/s)

圧力

MPa(=10 bar)	kgf/cm^2	atm	mmHg(Torr)	lbf/in^2(psi)
1	10.1972	9.86923	7.50062×10^3	145.038
0.0980665	1	0.967841	735.559	14.2233
0.101325	1.03323	1	760	14.6959
1.33322×10^{-4}	1.35951×10^{-3}	1.31579×10^{-3}	1	1.93368×10^{-2}
6.89476×10^{-3}	7.03070×10^{-2}	6.80460×10^{-2}	51.7149	1

エネルギー・仕事・熱量

J(=10^7 erg)	kgf·m	kW·h	cal(計量法)	Btu	ft·lbf	eV
1	0.101972	2.77778×10^{-7}	0.238889	9.47813×10^{-4}	0.737562	6.24150×10^{18}
9.80665	1	2.72407×10^{-6}	2.34270	9.29487×10^{-3}	7.23301	6.12082×10^{19}
3.6×10^6	3.67098×10^5	1	8.59999×10^5	3412.13	2.65522×10^6	2.24694×10^{25}
4.18605	0.426858	1.16279×10^{-6}	1	3.96759×10^{-3}	3.08747	2.61272×10^{19}
1055.06	107.586	2.93072×10^{-4}	252.042	1	778.172	6.58515×10^{21}
1.35582	0.138255	3.76616×10^{-7}	0.323890	1.28506×10^{-3}	1	8.46233×10^{18}
1.60218×10^{-19}	1.63377×10^{-20}	4.45050×10^{-26}	3.82743×10^{-20}	1.51857×10^{-22}	1.18171×10^{-19}	1

1 cal = 4.18605 J(計量法)

= 4.184 J (熱化学)

= 4.1855 J (15 °C)

= 4.1868 J(国際蒸気表)

仕事率　1 PS(仏馬力)

= 75 kgf·m/s

= 735.499 W

放射能

Bq	Ci
1	2.70270×10^{-11}
3.7×10^{10}	1

吸収線量

Gy	rad
1	100
0.01	1

照射線量

C/kg	R
1	3876
2.58×10^{-4}	1

線量当量

Sv	rem
1	100
0.01	1

(86年12月26日現在)

Criticality and Doppler Reactivity Worth Uncertainty due to Resolved Resonance Parameter Errors –Formula for Sensitivity Analysis–